Functional Investigation of Dual αvβ3 and αIIbβ3 Integrin Inhibition in Haematological and Solid Tumour Models

Amal Abdallah Mahammad ELSHARIF

Submitted for the Degree of

Doctor of Philosophy

Institute of Cancer Therapeutics

Faculty of Life Sciences

University of Bradford

2018

Abstract

Amal Abdallah Mahammad Elsharif

Title: Functional investigation of dual αvβ3 and αIIbβ3 integrin inhibition in haematological and solid tumour models.

Keywords: RGD binding integrins, K562, adhesion, metastasis, integrin antagonists.

Invasion and metastasis of cancer is the leading cause of increased mortality. In addition, haematological malignancies (leukaemia and lymphoma) are a significant cause of morbidity and mortality in both children and adults. Therefore, new treatments which will inhibit cancer progression are required. Integrin adhesion receptors, particularly the RGD-binding integrin subfamily comprising αvβ3, αvβ5, αvβ6, αvβ8, αIIbβ3, α5β1, α8β1 and αvβ1 are related to progress and spread of cancer and poor prognosis. Because of the importance of integrin biology in the regulation of cancer dissemination, the integrin receptors are being utilised as targets to regulate cancer progression. The goal of this study was to develop a dual αvβ3/ αIIbβ3 expressing model for testing integrin antagonists. Expression of αv, αIIb, and β3 integrin subunits was characterised using immunofluorescence and flow cytometry in a panel of cell lines. After characterising the expression of αv, αIIb and β3 integrin subunits in inducible and natural expression models (K562 and MCF-7 cells respectively), functional tests for cellular adhesion, detachment and migration were determined. Phorbol 12-myristate 13-acetate (PMA)-treated K562 cells showed increased adhesion on fibrinogen compared to untreated cells. Adhesion of cancer cells (K562 ± PMA and MCF-7) to

fibrinogen was inhibited and detachment was induced by the known β3 antagonists, cRGDfV and GR104453.

Migration of cancer cells (K562 without PMA and MCF-7) was inhibited by combination of the known β3 antagonists. A panel of 12 novel small molecules developed in the ICT was investigated for cytotoxicity and activity in the validated function assays. ICT9055 was the most potent antagonist in inhibition of cell adhesion, migration, and inducing cell detachment. The data presented in this thesis had selected models and assays for evaluating small molecule integrin antagonists and identified ICT9055 as a promising molecule to develop for further preclinical evaluation.

Acknowledgement and dedication

Foremost I should express my deepest gratitude and thanks to Allah for his magnificent help in accomplishing this research work. I am grateful for the favour which God has bestowed upon me.

I would like to express my sincerest gratitude to my supervisors Dr. Helen Sheldrake, Dr. Steve Shnyder and Prof. Laurence Patterson for their advice, guidance and insightful comments in all the time of my research. I would like to thank The Libyan Embassy and my University, Omer Al Mukhtar/Faculty of Medical Technology/Derna-Libya for providing me with sponsorship.

Thanks to all colleagues, friends, and staff at the ICT, Hanadi, Ghasaq, Rima, Dany, Mariaanghela, Haneen, Azeza, Monika, Marcella, Anjania, Gary and Patricia who supported me during lab work. I would like to thank Dr. Mark Sutherland for teaching me the integrin adhesion assay and Dr. Simon Allison for teaching me flow cytometry.

My special thanks to my husband Mohsen Elhasade who has been always supporting and caring about me all over the time and for my children, Mohab, Monya and Munes. I am deeply thankful for my beloved Mum Azza Kriksh, without her continuous support and encouragement I would never have been able to achieve my goals and for my lovely brothers and sisters.

Last but not least, this thesis is dedicated to the memory of my late dad, Prof Abdallah Elsharif who was a great inspiration to me and a constant source of encouragement and support for me to continue my schooling.

Table of Contents

List of Figures

List of Tables

List of Abbreviations

ABC	Avidin Biotin Complex
AMD	Age- Macular Degeneration
AML	Acute Myeloid Leukaemia
ANG1	Angiopoietin-1
ANG2	Angiopoietin-2
ALL	Acute Lymphocytic Leukaemia
APES	3-Aminopropyltriethoxysilane
ATCC	American Type Culture Collection
BAX	Bcl-2-Associated X protein
BSA	Bovine Serum Albumin
BSP	Bone Sialoprotein
βTD	β-Tail Domain
CAMs	Cell Adhesion Molecules
CAM	Chick Chorioallantoic Membrane
Cas	Crk-associated substrate
cRGD	Cyclic Arginyl-Glycyl-Aspartic Acid
cRGDfV	Arg-Gly-Asp-Phe-Val
CCL2	Chemokine Ligand 2
CLL	Chronic Lymphocytic Leukaemia
CML	Chronic Myelogenous Leukaemia
COX-2	Cyclooxygenase-2
DAB	3, 3 Diaminobenzidine
DAPI	4, 6-Diamidino-2-phenylindole

DPX	Distyrene, tricresyl phosphate and xylene
DMSO	Dimethyl sulfoxide
DOCK180	Dedicator of Cytokinesis 1
ECM	Extracellular Matrix
EDTA	Ethylene diamine tetra acetic acid
EREG:	Epidermal Growth Factor Receptor
ERK	Extracellular Signal-Regulated Kinase Extracellular
ERKs	Signal–Regulated Kinases
FACS:	Fluorescence-Activated Cell Sorting
FAK:	Focal Adhesion Kinase
FBS	Foetal Bovine Serum
Fg	Fibrinogen
FGF	Fibroblast Growth Factor
FITC	Fluorescein Isothiocyanate
GFR	Growth Factor Receptor
GTPase	Enzyme binds to Guanosine Triphosphate
GIT	G-protein-coupled receptor Kinase-Interacting Protein
ICT	Institute of Cancer Therapeutics
I-EGF	Integrin Epidermal Growth Factor Domains
IGFR-1	Insulin-like Growth Factor Receptor-1
IL-8	Interleukin 8
ILK	Integrin Linked Kinase
ITGB3	Integrin β3
JNK	Janus Kinase
MAP	Mitogen-Activated Protein Knase
MGMT	Methylguanine-DNA Methyltransferase

MMP	Matrix Metalloproteinase
MTT	3-(4, 5-Dimethylthiazole-2-y1)-2, 5-diphenyl Tetrazolium Bromide
mTOR	Mammalian Target of Rapamycin
Mrna	Messenger RNA
LAP-TGF-β	Latency-Associated Protein -Transforming Growth Factor Beta
NGS	Normal Goat Serum
NF-kB	Nuclear Factor Kappa-light chain enhancer of activated B cells
OPN	Osteopontin
PI3K/PKB/AKT	Phosphotidylinositide 3-Kinase/protein Kinase B
PAb	Primary Ab
PAR1	Proteinase-Activated Receptor 1
PBS	Phosphate-Buffered Saline
PBST	Phosphate Buffer Saline TWEEN 2
PDGF	Platelet-Derived Growth Factor
PDGFR	Platelet-Derived Growth Factor Receptor
PLGF	Placental derived Growth Factor
PMA	Phorbol 12-myristate 13-acetate
PFA	Paraformaldehyde
PI3K	PAK Interactive Exchange Factor
PIX	Phosphatidylinositol-3 Kinase
PKC	Protein Kinase C
PSA	Prostate-Specific Antigen
PSI	Plexin Semaphorin and Integrin Domain

RGD	Arginine-Glycine-Aspartic acid
ROCK:	Rho-associated Protein Kinase
RPMI:	Roswell Park Memorial Institute
RT-PCR:	Polymerase Chain Reaction
RT	Room temperature
SD	Standard Deviation
SDF-1	Stromal Cell-Derived Factor-1
shRNAs	Short hairpin RNA or small hairpin RNA
SLN	Solid Lipid Nanoparticles
Syk	Spleen Tyrosine Kinase
TBS	Tris Buffered Saline
TCIPA	Tumour cell Induced Platelet Aggregation
TGFα/β	Transforming Growth Factor-conversion Factor increasing α/β
TK	Tyrosine Kinase
TMD	Transmembrane Domain
TNF	Tumour Necrosis Factor
TGF-α	Transforming Growth Factor α
TORC	Mammalian Target of Rapamycin Complex
TRITC	Tetramethylrhodamin isothiocyanate
MAPK	Mitogen-Activated Protein Kinase
mTOR	Mammalian Target of Rapamycin
MLL:	Mixed-Lineage Leukaemia
NKC	Natural Killer Cell
nM	Nanomolar
µg	Microgram

µL	Microli
µM	Micromolar
uPAR	urokinase- Plasminogen Receptor
VEGF	Vascular Endothelial Growth Factor
VEGFR2	Vascular Endothelial Growth Factor receptor 2
vWF:	von Willebrand factor

Publications early for this work.

1. Conference abstracts:

A Elsharif, H Sheldrake, SD Shnyder and LH Patterson (2017). New models for investigating novel integrin antagonists. Tumour Microenvironment – Basic Science to Novel Therapies. June 14 th -16 th 2017, Nottingham Conference Centre, Nottingham, UK. Abstract 93.

A Elsharif, H Sheldrake, SD Shnyder and LH Patterson (2017). New models for investigating novel integrin antagonists. University of Bradford Faculty of Life Sciences Research and Development Open Day. 6 th June 2017, Bradford, UK.

A Elsharif, H Sheldrake, SD Shnyder and LH Patterson (2016). New models for investigating novel integrin antagonists. The European Association for Cancer Research's biennial Congress. 9 th-12 th July 2016. Manchester UK. Abstract 294.

A Elsharif, H Sheldrake, SD Shnyder and LH Patterson (2016). Investigation of the expression and the function of β3 integrin in new models University of Bradford Faculty of Life Sciences Research and Development Open Day 31st May 2016 Bradford, UK.

Chapter 1: Introduction

1.1 Metastasis

Cancer metastasis is the transition of tumour cells from a primary host site to another site. This transition is comparatively common, either as polyclonal metastasis or as monoclonal metastasis (Gundem et al., 2015). The invasion of tumour and progress to metastasis are the signatures of malignancy that lead to the death of most cancer patients (Hanahan and Weinberg, 2011). As will be discussed below, the metastases produced by carcinomas are the result of a complex process of cellular biological events collectively called the invasion-metastasis cascade (Figure 1) (Huang et al., 2011; Valastyan and Weinberg, 2011).

1.1.1 Events of the invasion–metastasis cascade

Typically, the metastatic cascade involves tumour growth, lymphangiogenesis and angiogenesis, entrance of malignant cells into the circulation by intravasation, anchorage and/or attachment in the target organ, and infestation of the target organ by proliferation and extravasation within the parenchyma of the organ (Valastyan and Weinberg, 2011). These multiple steps depend on the loss of cell adhesion, which leads to the detachment of the cell from the primary tumour, and consequently the capability of the cell to achieve a motile phenotype by changes in cell interactions with extracellular matrix (Martin et al., 2013), and re-adhesion at the target site. Some cancer cells are able to form specific adhesive interactions in certain tissues that favour their trapping. For instance, the expression of αv integrin in circulating tumour cells causes

adherence within the hepatic micro-vessels. In contrast, migration of attached cells into the parenchyma of liver is not influenced by inhibiting αv-integrin. These data support the hypothesis that particular interactions between host organs and circulating tumour cells are required for the arrest of organ-specific tumour cells (Enns et al., 2005). Since cell-cell interactions enabling adhesion of tumour cells in the vasculature of specific organs are crucial stages in the metastatic cascade, blocking of these interactions represents a potentially valuable target for reduction of metastasis (Bendas and Borsig, 2012; Witz, 2008).

Moreover, the ubiquitous existence of integrins on tumour cells, stromal cells, vasculature, and blood components suggest that integrins may be involved in many steps of the metastatic cascade. As most human tumours originate from epithelial cells, integrins expressed on epithelial cells are normally present also in tumour cells (Bendas and Borsig, 2012).

Figure 1: The invasion–metastasis cascade.

Tumour cells leave their primary sites of growth, intravasate (following local invasion), need to survive in the circulation, arrest at a distant organ site, extravasate (translocate systemically), and adapt to survive in distant tissues (micro-metastasis formation, metastatic colonisation). Adapted from (Valastyan and Weinberg, 2011).

1.1.1.1 Invasion from the primary tumour site (local invasion)

Carcinoma cells need first to penetrate the basement membrane in order to invade the stroma (Bissell and Hines, 2011). Invasion involve the secretion of proteolytic enzymes to damage the extracellular matrix and the basement membrane and the suppression/expression of proteins participating in the control of cell movement and migration (Brooks, 1996). Additionally, the basement membrane also participates in transducing signal events into carcinoma cells through pathways originated by integrin-mediated cell-matrix adhesions which are the interaction of a cell with the extracellular matrix, resulting in changes in proliferation, cell polarity, survival, and invasiveness (Bissell and Hines, 2011). Most types of carcinomas have the ability to invade as coherent multicellular units at a cellular level by a process of collective invasion. Individual tumour cells can invade through two distinctive processes: the protease, stress-fibre, and integrin-independent, Rho-associated protein kinase (ROCK) dependent “amoeboid invasion” programme; or the protease, stress-fibre, and integrin-dependent “mesenchymal invasion” programme (Ganguly et al., 2013). Indeed, distinctive expression of molecules that allow either amoeboid or mesenchymal invasion can be shown in signs of local invasion obtained from mammary cancer models (Wang et al., 2004). Tumour cells are able to switch between these different invasion strategies in response to changes in microenvironmental conditions. This has led to the suggestion that strong suppression of single cell invasion needs associated inhibition of the amoeboid and mesenchymal invasion programmes (Friedl and Wolf, 2003).

1.1.1.2 Intravasation

To intravasate, invading carcinoma cells must first enter into lymphatic or blood vessels derived from the tumour neovasculature or located next to the tumour (Reymond et al., 2013). Whereas lymphatic spread of cancer cells is usually investigated in human tumours and represents a significant prognostic marker for cancer progression, spread through the haematogenous circulation represents the main mechanism by which metastatic cancer cells disseminate (Gupta and Massague, 2006). Intravasation is facilitated by molecular alterations that enhance the ability of cancer cells to pass barriers of endothelial cell that form the micro-vessels walls (Sonoshita et al., 2011). The mechanisms of intravasation are likely to be strongly impacted by the structural characteristics of tumour associated blood vessels through the mechanisms shown in Figure 2, many of which converge on the actions of vascular endothelial growth factor (VEGF). Cancer cells develop and form new blood vessels in their local microenvironment by the process of neoangiogenesis (Carmeliet and Jain, 2011).

Figure 2: Mechanisms of tumour angiogenesis.

Angiogenic factors such as VEGF, vascular endothelial growth factor; PDGF, platelet-derived growth factor and FGF, fibroblast growth factor are secreted from the tumour and surrounding cells to regulate and enhance main stages in angiogenesis. Endostatin directly interacts with VEGFR-2 to inhibit VEGF and bFGF, binding, and inhibits integrin function and MMP-2 activity in endothelial cells. Angiopoietin (Ang-1) and Ang-2, angiostatin and platelets factor 4 are also involved. Adapted from (Zhao and Adjei, 2015).

1.1.1.3 Cancer cells in the circulation

After cancer cells have intravasated into the blood vessels, they can spread via the arterial and venous systems. Recent diagnostic tools for circulating tumour cells such as the herringbone-chip and microfluidic mixing device have facilitated detection and characterisation of circulating tumour cells in the bloodstream of cancer patients (Stott et al., 2010). Circulating tumour cells apparently represent cancer cells that are *en route* between primary cancer cells and dissemination sites and consequently might represent “metastatic intermediates”. In order to reach distant organ sites, circulating tumour cells in the bloodstream must survive a variation of stresses. For instance, they must be able to survive loss of the integrin-dependent adhesion to the ECM that is typically important for cell survival; epithelial cells normally undergo programmed cell death in the absence of such anchorage (Guo and Giancotti, 2004).

In addition to stresses forced by matrix separation, tumour cells in the bloodstream must survive hemodynamic shear forces, and evade cells of the innate immune system, particularly NK cells (natural killer cells). Cancer cells appear to evade both of these threats via exploiting a mechanism of normal blood coagulation (Joyce and Pollard, 2009); triggering platelet aggregation to form a tumour cell-platelet complex. Consequently, platelet-coated tumour cells have more ability to continue in the circulation until they arrest at distant sites, an event whose probability may be further increased because of the larger effective diameter of these micro-emboli (Valastyan and Weinberg, 2011).

1.1.1.4 Extravasation

Cancer cells in the blood stream may begin growth and form a microcolony that ultimately breaches the walls of surrounding vessels and extravasates into the tissue parenchyma (Al-Mehdi et al., 2000). Otherwise, tumour cells may pass from the lumina of vessels into the tissue parenchyma by crossing pericyte layers and the endothelial cells that separate the lumina of vessels from the stromal microenvironment (Wyckoff et al., 2007).

Primary tumours are able to secrete factors that disrupt these microenvironments and enhance vascular hyperpermeability in order to conquer physical barriers to extravasation that work in tissues with low microvascular permeability (Padua et al., 2008). For instance, the secreted protein angiopoietin-like-4, in addition to the pleiotropically acting factors such as EREG, COX-2, MMP-1, and MMP-2, perturb pulmonary vascular endothelial cells junctions in order to promote the extravasation of breast cancer cells in the lungs (Gupta et al., 2007). In addition, MMP-3, MMP-10, angiopoietin-2, VEGF and placental growth factor secreted by different types of primary tumours are able to induce pulmonary hyperpermeability prior to the arrival of cancer cells in the lungs, thereby facilitating the subsequent extravasation of cancer cells in the bloodstream (Hiratsuka et al., 2011; Huang et al., 2009; Weis et al., 2004). Lastly, inflammation monocytes recruited to pulmonary metastases by CCL2-dependent mechanisms induce the extravasation of breast cancer cells in the lungs by releasing VEGF (Qian et al., 2011).

1.1.1.5 Micro-metastasis formation

Extravasated cancer cells need to survive in the foreign microenvironment that they encounter in distant tissues. The micro-environment of the metastatic site typically varies significantly from that in the existing site of primary tumour formation. These micro-environmental variations may include the ECM components, stromal cells, cytokines and growth factors, in addition to hematopoietic progenitor cells that adapt to the local microenvironments by producing MMP-9. Activation of MMP-9 at the new locus of metastasis may lead to stimulation of many integrins, as well as the release of molecules such as the chemoattractant stromal cell-derived factor-1 (SDF-1), that have been isolated in the ECM (Psaila and Lyden, 2009). Significantly, it is believed that all of these events occur prior to tumour cells arriving in metastatic sites. In order to survive in these foreign locations and produce small micro-metastases, it has become clear that tumour cells organise complex mechanisms to adapt distant microenvironments (Zhang et al., 2009).

1.1.1.6 Metastatic colonisation

Most of the disseminated tumour cells persist as micro-colonies over periods of weeks or months. The metastatic tumour cells could proliferate continually. Due to the counterbalancing effects of a high apoptotic rate, a net increase in their overall number may not occur, however. The underlying mechanisms of high tumour cell attrition rate remain unclear. A failure of the spreading tumour cells to trigger formation of new blood vessels is suggested as one explanation for this phenomenon, however (Chambers et al., 2002).

Furthermore, the capacity of spreading tumour cells to escape and to start effective proliferation may rely on cell non-autonomous mechanisms which are required to switch foreign microenvironments into most hospitable niches. For instance, the outgrowth of tumour cells may rely on the activation and mobilisation into the bone marrow-derived cell circulation and the sequential recruitment of these cells to a metastatic site. In some conditions, these processes might be activated by systemic signals secreted by cancer cells, such as SDF-1 (Hiratsuka et al., 2011; McAllister et al., 2008).

Investigating blood samples of cancer patients has shown the number of cancer cells (circulating tumour cells) far exceeds the number of overt metastatic lesions that develop. Tumour cells that survive after infiltrating certain organs, known as disseminated tumour cells, can be found in the bone marrow of tumour patients for a long time and yet only almost half of these patients progress overt metastasis. These clinical observation indicate that metastatic colonisation is a very ineffective process in which the majority of cells die and only small numbers survive and form macro-metastases (Massague and Obenauf, 2016).

Findings using experimental mouse models are in agreement with clinical data. For instance, intravenous injection of cancer cells in mouse models leads to the death of the majority of cells within two days after they are filtered by the lungs (Wong et al., 2001), also happens when arterially injected cancer cells reach the liver and brain (Minn et al., 2005).

1.2 Basic processes of leukaemia

Leukaemia is an uncontrolled proliferation of white blood cells leading to increased numbers in the bone marrow and blood. Leukaemias are categorised as acute or chronic, and on cell type, such as myelogenous or lymphocytic. The key classes of leukaemia are acute myeloid leukaemia (AML), chronic myeloid leukaemia (CML), acute lymphoblastic leukaemia (ALL), and chronic lymphocytic leukaemia (CLL) (Ball and Kagan, 2007).

The process of leukaemia transformation is based not only on increased proliferation but also, at least to some extent, on decreased apoptosis. Dysregulation of the processes controlling programmed cell death lead to prolong the life span of cells, leading to spread of leukaemia cells (Schnerch et al., 2012).

Moreover, the formation of new blood vessels and angiogenic factors are involved in the dissemination of some leukaemias. Increased vascularity has been reported in paediatric ALL (Perez-Atayde et al., 1997), AML (Hussong et al., 2000) and myelodysplastic syndrome (MDS). VEGF expression is a prognostic factor in AML (Aguayo et al., 1999). This suggests that angiogenic factors might have a direct impact on vascularity of bone marrow as well as on leukaemia cells (Aguayo et al., 2000).

Spreading in ALL involves migration of leukaemia cells within the bone marrow microenvironment and into the peripheral circulation. This migration is promoted at least partly because of VEGF/placental-derived growth factor (PDGF) stimulation of leukaemia cells within the bone marrow (Fragoso et al., 2006). Also, PLGF or VEGF stimulation of AML cell lines leads to an increase in cell migration over non-stimulated cells (Casalou et al., 2007). The

microenvironment through stromal cells, growth factors, and cytokines providing a permissive environment is also involved in initiation of leukaemia, development and metastasis, whereas leukaemia cells impact on stromal cells through secreted factors and cell–cell interactions (Ayala et al., 2009). The stromal cells also regulate migration and leukaemia blast cell (immature white blood cells) growth. The influence of stromal cells on leukaemia blasts, differing to the other, seems to be recapping normal physiological cell to cell adhesion through adhesive receptors such as integrins in normal hematopoietic progenitors. Stromal ligands such as fibronectin interact with leukaemic blast integrins (Bendall et al., 1994; Bradstock and Gottlieb, 1995) and the adhesive interaction is required for leukaemic blast proliferation and survival. In leukaemic blasts and stromal cells, reciprocal activation of ILK/Akt pathway seems to be important for this adhesion-driven AML blast survival (Ayala et al., 2009).

Leukaemia cells have an inherent mobility to move throughout the circulation, suggesting that no mutations are necessary for anchorage independent growth. Trendowski argues that leukaemia is inherently metastatic, endowed with the deadly phenotype of malignant cells simply because of their cell of origin. If leukaemia cells were inherently metastatic, they should have distinctive migratory patterns as found in other cancers. For example, in several tumour conditions, it seems that leukaemia cells behave similarly to cancers arising from other tissues such as the skin, breast, and other muscles (Trendowski, 2015).

Blocking the interactions of stromal cells or stroma-derived growth factors with leukaemic cells represent some of the main processes that should be targeted as a promising strategy to treat leukaemia. Inhibition of proangiogenic

pathways and developed of integrin inhibitors are among the most interesting areas for cancer therapy (Aguayo et al., 2000).

1.3 Integrins

Integrins are family I transmembrane heterodimeric glycoprotein receptors that are present in organisms ranging from echinoderms to corals, sponges, nematodes and mammals. They serve as the major metazoan receptors for cell adhesion and are associated with the extracellular and intracellular environments (Zent, 2010). Integrins mediate cell to cell, cell to ECM, and cell to pathogen interactions. They transfer bidirectional signals across the plasma membrane and regulate multiple biological functions, including cell differentiation, cell migration and wound healing (Luo and Springer, 2006). A characteristic of integrins is the individual family members' ability to bind multiple ligands. The major extracellular ligands of integrins include a large number of ECM proteins such as bone matrix proteins, fibronectins, collagens, fibrinogen, thrombospondins, laminins, von Willebrand factor (VWF) and vitronectin, reflecting the primary role of integrins in the adhesion of cells to extracellular matrices (Plow et al., 2000).

Structurally, integrins are non-covalent heterodimers containing an α and a β glycoprotein subunit (Figure 3) (Arnaout et al., 2005; Hynes, 2002b; Sheldrake and Patterson, 2009). There are 8 β and 18 α subunits which combine to form 24 human αβ integrin dimers (Figure 4) (Chen et al., 2012; Humphries, 2000; Hynes, 1992; Sheldrake and Patterson, 2009). Both subunits comprise a single transmembrane domain, short intracellular domains (except for β4 with long cytoplasmic domain) and a multi-domain extracellular portion (large extracellular

domain) (Humphries, 2000; Shimaoka et al., 2002). Each α and β integrin subunit has a large N-terminal globular domain (Liddington, 2014).

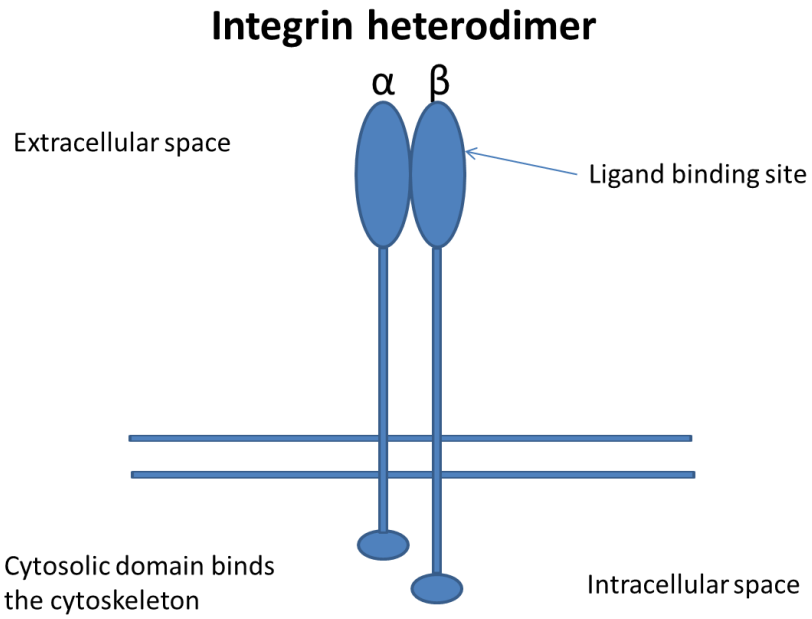

Figure 3: Basic integrin structure

Each integrin has one α chain and one β chain spanning the membrane into both the extracellular space and intracellular space, where a short cytosolic domain binds the cytoskeleton through effector proteins. Both α and β integrin subunits contribute to the distinct ligand-binding site which recognises the extracellular matrix.

Figure 4: The integrin family of matrix receptors that form 24 human αβ integrin dimers.

The integrin family can be considered in several subfamilies including RGD binding integrins (red) which recognise the tripeptide sequences arginine-glycine-aspartate existing in several ECM proteins, the collagen receptors (dark blue), laminin binding integrins (light blue) and leukocyte-integrins (green). Some integrin subunits have an inserted I-domain (underline) (Sheldrake and Patterson, 2014).

These integrins are divided into subfamilies (Figure 4) dependent on the identity of subunits and bound ligands. The 24 recognised integrin heterodimers are characterised as arginine–glycine–aspartate acid binding (RGD), leukocyte adhesion integrins, collagen-binding and laminin-binding integrins (Goodman and Picard, 2012).

The RGD-recognising integrins consist of 8 types (Table 1), which recognise the common sequence of RGD tripeptide at a binding site formed at the α and β subunit headpiece junction (Plow et al., 2000). This family of 8 integrins includes two β1 integrins (α5, α8), αIIbβ3 and five αv integrins (Humphries et al., 2006). Specifically the αv subunit pairs with β1, 3, 5, 6, and 8. The β3 integrin subunit is able to associate with not only αv but also the αIIb subunit (CD41) (Wilder, 2002). While some integrin pairs preferentially bind a single ligand, others recognise a number of ligands; for example, αvβ3 binds vitronectin, VWF, fibronectin, tenascin, fibrillin, osteopontin (OPN), fibrinogen, and thrombospondin (Calderwood, 1999; Weis and Cheresh, 2011). These integrins can readily differentiate between different RGD-containing ECM proteins and respond variously to the interaction with each one of them despite their obvious similarity (Kapp et al., 2017).

Integrins modulate signal transduction pathways that control cellular and biological functions including migration, cell adhesion, cell differentiation, proliferation and apoptosis (Zent, 2010). Also, integrins link the ECM to the actin cytoskeleton and transfer mechanical force and biochemical signals via the plasma membrane. This allows cells to produce traction through migration and uses tension through matrix remodelling. Linkages with the cytoskeleton

also permit integrins to regulate gene expression and cell shape, and mediate cell adhesion (Calderwood, 1999).

Table 1 : Ligands and functions of the RGD-recognising integrin subfamily (Sutherland et al., 2012).

Integrin	Ligands/ recognition sequences	Main function
α5β1	Fibronectin, Osteopontin	Angiogenesis
α8β1	Fibronectin, Vitronectin, Nephronectin	Development of lung and kidney Differentiation and function of hair cells
αIIβ3	Fibronectin, Fibrinogen, Von Willebrand factor, Vitronectin	Platelet aggregation
αvβ3	Fibronectin, Vitronectin, Fibrinogen, Von Willebrand factor, Bone sialoprotein, Osteopontin, LAP-TGF-β	Resorption of bone Angiogenesis
αvβ5	Vitronectin, Fibronectin, Bone Sialoprotein,	Angiogenesis
αvβ6	Fibronectin, Vitronectin, Osteopontin, LAP-TGF-β	Activation of TGF-β Fibrosis
αvβ8	Vitronectin, LAP-TGF-β	Activation of TGF-β, Brain development Angiogenesis
αvβ1	Fibronectin, Fibrinogen, Vitronectin, Osteopontin, LAP-TGF-β	Fibrosis

1.3.1 Activation of integrin and ligand binding

Both subunits αIIb and αv do not have an I domain. The I domain is responsible for ligand binding if present. If it is not present, ligand binding occurs on the I-like domain in the β subunit and the β-propeller headpiece of the α-subunit, and is supported by interactions between binding site residues, the ligand and one or more divalent cations bound in the integrin subunits (Figure 5) (Takagi, 2007; Xiong, 2002; Zhang and Chen, 2012).

Figure 5 : Characteristics of the RGD binding site.

The α subunit links the basic chain of arginine side via interactions with different subunit specific acidic residues. Ligand binding to the β subunit is basically through an electrostatic interaction between a positively charged metal ion (usually Mg^{2+}) conncected with the integrin subunit and a carboxylate group on the ligand (Sheldrake and Patterson, 2014).

A specific characteristic of integrins is their increasing ligand binding through affinity maturation which progresses from low affinity (inactive) to a high affinity (active) state (Figure 6) and which can be induced by high affinity ligands or by inside-out signalling (intracellular signalling events). Ligand binding enhances allosteric alterations in the receptor conformation, resulting in the activation of intracellular signalling pathways, including PI3K-PKB-mTOR, Ras-MAPK and small GTPases such as Rho, Rac pathways (outside-in signalling) (Alghisi et al., 2009; Hynes, 2002b). Integrin activation involves binding the cytoplasmic tail to talin. Talin is a high molecular weight cytoskeletal protein capable of linking integrins (Burridge and Connell, 1983). This leads the headpiece of the extracellular domain to extend to a vertical position above the cell surface, exposing the ligand binding site. This, in turn, permits the instigation of several signalling pathways (inside-out and outside-in signalling pathways) by enlisting intracellular molecules to bind to the cytoplasmic tail (Kim et al., 2011).

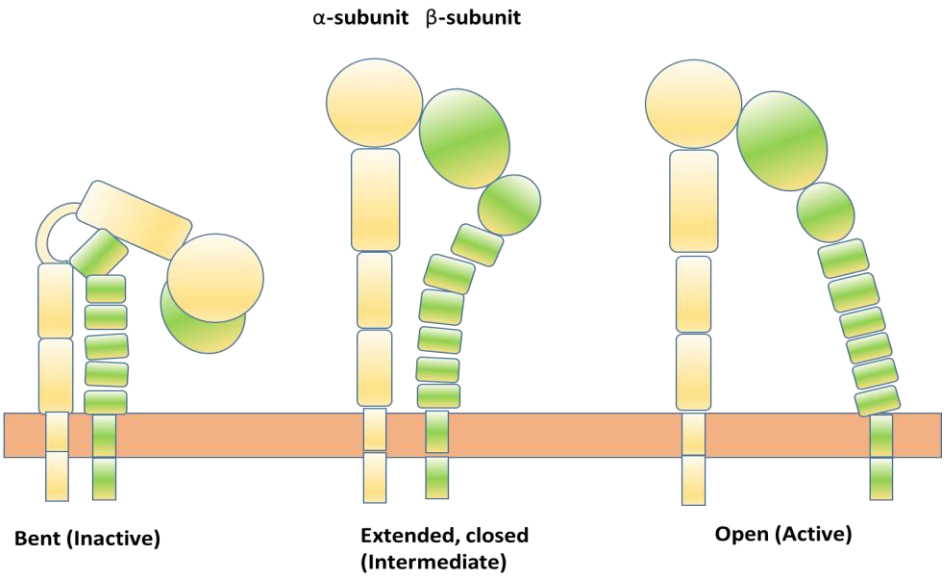

Figure 6: The conformational changes of integrin activation states.

The various conformations of an integrin are linked with distinct affinities: low affinity shows the bent conformation, and intermediate affinity and high affinity show the two extended conformations. Intracellular signalling activation increases ligand binding by inducing a transition between these affinity states, known as affinity regulation.

Figure 7 shows bidirectional signalling utilizing integrin αIIbβ3 as an example. αIIbβ3 has already been recognised as a target for antithrombotic therapy (Bakewell et al., 2003; Cohen et al., 2000; Goodman et al., 2012). Defects in structure or expression of αIIbβ3 lead to a variety of bleeding diseases identified as Glanzmann's thrombaesthenia (Tomiyama, 2000).

Figure 7: Bidirectional signalling of αIIbβ3 integrin.

αIIbβ3 equilibrates between activated and resting states; the activated state in stimulated platelets and the resting state is dominant in unstimulated platelets. (A) Inside-out signalling; agonist-dependent intracellular signals enhance the interaction of main regulatory ligands (talin) with integrin cytoplasmic tails (in this example the β3 tail). This results in conformational transitions in the extracellular domain that lead to high affinity for adhesive ligands (fibrinogen). (B) Outside-in signaling; binding of extracellular ligand, initially reversible, becomes increasingly irreversible and induces clustering of integrin and further conformational alterations.This results in the activation of enzymes, effectors and adaptors to form integrin-based signaling complexes. Adapted from (Shattil and Newman, 2004).

Integrins rely on intracellular effector proteins to transduce signals because they lack catalytic activity (Figure 8). Focal adhesion kinase (FAK) is a non-receptor tyrosine kinase (TK), which begins to be activated upon integrin-extracellular matrix interactions and integrin clustering. FAK reacts with several signalling proteins, including Cas, paxillin, phosphoinositide 3-kinase (PI3-K) and Src kinases (Mitra and Schlaepfer, 2006; Tilghman and Parsons, 2008). Through Src, integrin signalling is able to be FAK independent as Src also associates directly with β3, and β3 integrin clustering enhances activation of Src and auto-phosphorylation (Arias-Salgado, 2003; Taherian et al., 2011) (Taherian et al., 2011).

Figure 8: Integrin mediated signalling pathways. The composition of the ECM, its mechanical properties, and the environment of growth factors regulate the outside-in signalling by integrins in interacting with growth factor receptors. Growth factor signalling co-operates with integrin-mediated signalling on different levels: by regulating the affinity of the integrin for ECM ligands (I), by regulating the activity of integrin-intracellular effector proteins such as FAK, PI3K, and Src (II), and by regulating the downstream effectors activity such as, Akt, JNK, ERK and Rho GTPases (III). The essential signalling module downstream from integrins is the Src/FAK complex, which stimulates ERK and JNK and ERK to regulate proliferation, differentiation and cell survival. Also, through activation of Crk/Dock180 or alternatively PIX/GIT pathways, the Src/FAK complex regulates activity of Rho GTPase, leading to cytoskeletal reorganization and regulation of adhesion, migration and polarity. Integrins also activate PI3K, which in collaboration with integrin linked kinase (ILK) and mTOR, controls cell survival by Akt. Cross-talk between the several pathways. Adapted from (Legate et al., 2009).

Specific integrin signals allow tumour cells to detach from neighbouring cells, proliferate and survive in distant microenvironments during progression from the growth of the tumour to metastasis. There is further evidence that certain integrins bind to receptor tyrosine kinases to activate signalling pathways that are required for tumour invasion and metastasis (Guo and Giancotti, 2004). For example, αvβ3 integrin connects with IGFR-1 (insulin-like growth factor receptor), PDGFR (platelet-derived growth factor receptor) (Borges et al., 2000; Schneller et al., 1997), and VEGFR2 (vascular endothelial growth factor receptor-2) (Soldi et al., 1999). These connections suggest that the signalling relationship between integrins and receptor tyrosine kinases may be due to receptor co-clustering upon cell attachment or stimulation of growth factor ligand production. Growth factor stimulation of RTKs or ECM-integrin interactions promotes an increase in receptor tyrosine kinases and the local concentration of integrins at focal adhesions. This cross-talk can occur at the main edges of tumour cells, although it can even occur directly through changes of the intracellular localisation of integrins (Lipscomb and Mercurio, 2005).

1.3.2 Integrins in angiogenesis

Angiogenesis is the growth of new blood vessels that occurs in normal development and some pathophysiological conditions. Angiogenesis is the process of sprouting, cell migration, division and endothelial cell assembly from pre-existing vessels (Carmeliet and Jain, 2000; Fouad and Aanei, 2017). Therefore, angiogenesis has many roles in normal physiology involving in embryogenesis, wound healing, the female reproductive cycle and bone formation (Carmeliet, 2003). Moreover, angiogenesis has an important function

in the development of tumours. Primary cancer cells are supplied by nutrient and oxygen taken from adjacent vascular tissues, and the supply of local blood becomes insufficient when these cells proliferate, resulting in a nutrient-deprived tumour environment and inadequate oxygen supply. Angiogenesis in tumours can occur by recruitment of rare and circulating bone marrow-derived endothelial progenitor cells (Avraamides et al., 2008).

Angiogenesis supports tumour invasion, survival and metastasis. Endothelial cells that are in the microenvironment of the tumour are in an inactive state but when tumour cells begin producing pro-angiogenic factors this can result in an angiogenic switch (Bergers and Benjamin, 2003). Some endothelial integrins (αvβ3,αvβ5, αIIbβ3and α5β1) are involved in angiogenesis (Avraamides et al., 2008) and will be discussed in this section.

αvβ3 is one of the most investigated integrins because of its function in regulation of angiogenesis (Nussenbaum and Herman, 2010). It is expressed on angiogenic endothelial cells at high levels in remodelling and pathological tissues, while inactive endothelial cells express αvβ3 at low levels (Weis and Cheresh 2011). Through the function of pro-angiogenic and anti-angiogenic molecules, the interaction between the ECM and αvβ3 has the ability to control angiogenesis (Atkinson et al., 2014). The pro-angiogenic function for αvβ3 is supported by its cooperation with vascular endothelial growth factor receptor 2 (VEGFR2) in endothelial cells that enhance angiogenesis. Also, its function during angiogenesis is to activate MMP-2 at the migration tip of endothelial cells to disrupt elements of the ECM and facilitate cell infiltration and migration. These roles support αvβ3 as an essential tumour angiogenic promotor (Brooks et al., 1994; Brooks et al., 1995). Therefore, αvβ3 integrin has been considered

an attractive antiangiogenic target for the development of small molecule antagonists. β3 integrin subunit blocking utilising antibodies, signalling-defective mutants or RGD peptide antagonists lead to a reduction in tumour progression and angiogenesis (Brooks et al., 1994; Mahabeleshwar et al., 2006).

The expression of αvβ3 is also associated with tumour angiogenesis and the metastasis of cancer cells (Shan et al., 2015) such as the MDA-MB-435 human breast cancer cell line, where αvβ3-mediated interactions with platelets support the arrest of cancer cells within the bloodstream and results in haematogenous metastasis (Felding-Habermann et al., 2001). In addition, the interaction between αIIbβ3 on platelets and αvβ3 on endothelial cells through fibrinogen, acting as bridges among the cells, induces angiogenesis and inflammation (Katrancha and Gonzalez, 2014).

αvβ5 is needed for transforming growth factor α (TGF-α) or vascular endothelial growth factor (VEGF) prompted angiogenesis. Anti-αvβ3 antibodies inhibited angiogenesis promoted by basic fibroblast growth factor (bFGF), whereas anti αvβ5 antibodies inhibited angiogenesis promoted by VEGF in both the chick chorioallantoic membrane (CAM) and the rabbit corneal eye pocket assay (Friedlander et al., 1995). Angiogenic assays indicate that αvβ5 is required for VEGF and TGF-α mediated angiogenesis *in vivo,* whereas TNF-α and bFGF depend on αvβ3 to initiate angiogenesis. The pathway of VEGF/αvβ5 signalling is dependent on protein kinase C and Src kinase (Eliceiri et al., 2002).

α5β1 is abundantly expressed on the vasculature of human tumours while it is poorly expressed on inactive endothelial cells. The expression of α5β1 is induced by several angiogenic factors such as TNF-α, FGF and IL-8 (Kim et al., 2000). Notably, novel non-peptide antagonists of α5β1 had little effect on

angiogenesis induced by VEGF but inhibited angiogenesis induced by fibronectin in both murine and chick embryo models and led to regression of human tumour models *in vivo*. Therefore, integrin α5β1 and fibronectin, like integrin αvβ3, are involved in a pathway of angiogenesis that is distinct from VEGF-mediated angiogenesis (Kim et al., 2000).

The expression of RGD binding integrins is shown to correlate with cancer metastasis and poor prognosis (Nieberler et al., 2017; Pontes-Junior et al., 2010; Sutherland et al., 2012; Zheng et al., 1999). αvβ3, αIIbβ3 and α5β1 integrins are among the most prominent integrins in cancer progression and widely expressed in metastases in both haematological malignancies and solid tumours.

1.3.3 RGD binding integrins in haematological malignancies

1.3.3.1 αvβ3 in haematological malignancies

Interaction of the bone marrow microenvironment with immature haematopoietic cells is significant for several processes, including differentiation and proliferation of haematopoietic progenitor cells, mobilisation of progenitors in blood cell donors, and persistence of residual disease in leukaemia which is related to defensive effects of the bone marrow on leukaemia blasts during chemotherapy (Roselova et al., 2017). For example, acute myeloid leukaemia cells are dependent on integrins and chemokine receptors for marrow homing and migration (Bönig and Kim, 2015).

ECM signalling of integrins is important for the viability of cancer cells of the hematopoietic origin (Hehlgans et al., 2007).

Furthermore, adhesion within the marrow microenvironment leads to chemotherapy resistance in acute myeloid leukaemia and other hematologic malignancies by interfering with apoptosis or activating survival pathways (Becker and Appelbaum, 2015). Yi et al (2016) established that the expression level of integrin β3 is crucial for osteopontin-enhanced chemotherapy insensitivity in acute myeloid leukaemia cells. Miller et al.(2013) also found that loss of integrin β3 weakens leukaemia cell homing and prompts differentiation of myeloid cells via spleen tyrosine kinase (SYK), thereby inhibiting integrin β3–SYK signalling that might repress leukaemia growth with reduced toxicity. Therefore, RGD-binding integrins, particularly β3, represent potential therapeutic targets in leukaemia cells.

Lymphoma cells express αvβ3 integrin (Goodman and Picard, 2012). Lymphoid tumour cells (CEM T-cell lymphoblastic leukaemia, Burkitt's lymphoma, and U266 multiple myeloma) have been shown to interact with the ECM components vitronectin and fibronectin via αvβ3 integrin. This adhesion was inhibited by a neutralising monoclonal anti-αvβ3 integrin antibody. Vitronectin and fibronectin promote the formation of activated Src/FAK complex and activation of ERK-2 by engaging αvβ3 integrin. Engagement of αvβ3 integrin also may be of importance in the spread of human lymphoid tumours by modulating cell adhesion, proliferation, and interacting with the extracellular matrix components. The interaction of vitronectin and fibronectin allows cells to attach to the substratum and increases their proliferation and protease secretion (Vacca et al., 2001).

Although there are variable levels of integrin expression between different cases of chronic lymphocytic leukaemia, the integrin is still able to mediate change functional cellular responses to adhesion *in vitro* (Vincent et al., 1996).

ITGB3 (integrin β3 gene) was identified as an essential gene for human leukaemia cells in xenotransplantation studies and murine leukaemia cells *in vivo*. Knockdown of integrin β3 impaired homing of primary leukaemia cell, induced differentiation via the intracellular kinase Syk and downregulated leukaemia stem cell transcriptional programmes. In contrast, loss of integrin β3 in normal hematopoietic cells did not impair progenitor or stem cell differentiation or function in the primary transplant. In this context of malignant cells, using an integrin β3 knockout mouse model, β3 integrin is not necessary for normal haematopoiesis but is essential for leukaemogenesis such as mixed lineage leukaemia, demonstrating the importance of the integrin β3 signalling pathway as a promising target in acute myeloid leukaemia. Systemically, the data provided by Miller et al. indicate a significant role of β3 gene in both leukemic cells and interaction with stromal cells (Miller et al., 2013).

In addition, β3 integrin is required for mixed-lineage leukaemia cells (MLL-AF9) in mouse cells; mice transplanted bone marrow not encoding β3 survived longer than those transplanted with encoding β3 cells, showing the importance of the β3 gene in mediating leukaemic proliferation (Feliciano, 2013; Zeisig and So, 2013). AML cells such as transformed cells (MLL-AF9) interact with the microenvironment of bone marrow, most probably in the endosteal region (Ishikawa et al., 2007). This interaction is considered to be important for cell survival and impacted on the lineage fate of MLL-AF9 leukaemia (Wei et al., 2008).

A large set of integrin-associated proteins is required for the assembly of adhesion complexes by different cells types, including the leukaemia cell line, K562 (Horton et al., 2015; Roselova et al., 2017). K562 is a useful model to study the differentiation of blood cells induced by phorbol myristate acetate (PMA) (Huang et al., 2014). The expression of β3 integrin is controlled at the level of transcription, as confirmed by its response to phorbol ester treatment. High levels of β3 mRNA have been demonstrated by northern blot analysis and high expression of β3 was also shown in cell-free translation of mRNA from K562 cells stimulated with PMA (Huo et al., 2006).

Al-Asadi et al., (2017) found that the expression of αv and β3 subunits was significantly upregulated in dormant leukaemia-initiating cells and increased adhesion to vitronectin. Quantitative PCR confirmed adhesion-related protein upregulation (Al-Asadi et al., 2017).

αvβ3 is important for chemosensitivity and disease development in human AML cells. The interactome of the integrin consists of several intracellular mediators, including the Syk kinase, β-catenin, and a large number of HoxA genes and the FGF2 receptor that work together for downstream signalling of β3 integrins. Thus, inhibition of Syk as well as blocking of β3 by a specific antibody may be a potential strategy for inhibition of AML-supporting signalling circuits (Becker et al., 2015; Becker and Appelbaum, 2015; Tavernier-Tardy et al., 2009).

1.3.3.2 αIIbβ3 in haematological malignancies

αIIbβ3 (gpIIbIIIa) binds fibrinogen and regulates the accumulation of platelets into thromboses (Coller and Shattil, 2008). αIIbβ3 is the main membrane protein on the platelet surface (Quinn et al., 2003) and its primary adhesion receptor of blood platelet (Lau et al., 2009). Fibrinogen has six potential linking sites for αIIbβ3. Platelets binding fibrinogen leads to a crosslink between platelets which causes platelets aggregation as a central response for thrombosis and haemostasis (Katrancha and Gonzalez, 2014).

Plasma fibrinogen levels have a prognostic effect with an adverse outcome in acute myeloid leukaemia patients (AML) at the time of diagnosis without increased early mortality. Both solid-phase and soluble fibrinogen promote Syk signalling in human megakaryoblastic cell lines (Berger et al., 2017).

Thrombopoietin enhances the adhesion of leukemic cells to fibrinogen and the activation of αIIb integrin is thereby increased (Tohyama et al., 1998). Recognition of the RGD sequence on the fibrinogen ligand leads to increased binding. The impact is only seen with αIIbβ3, but not with αvβ3 integrins, and signalling through PI3K is significant for high integrin expression/binding. The level of β3 integrin expression per AML cell is comparable with the expression in endothelial carcinoma cells (Johansen et al., 2018; Zhai et al., 2015).

Chronic myelogenic leukemic cells such as K562 undergo megakaryocytic differentiation in response to PMA induction. Megakaryocytic cell surface markers CD41 and CD61 (αIIb and β3) are often utilised as differentiation markers of the megakaryocyte cell lineage expressed in K562 cells treated with PMA (Shelly et al., 2000). PMA-stimulated K562 cell adhesion mediated by β-

integrin agonists was partially inhibited by the selective αIIbβ3 antagonist (tirofiban) and α5β1 integrin agonists. These findings demonstrated that both α5β1 and αIIbβ3 integrins may participate in mediating cell K562 cell adhesion (Galletti et al., 2014). So far, no further published studies revealed the expression and suggested a role of αIIbβ3 in haematological malignancies.

1.3.3.3 α5β1 in haematological malignancies

α5β1 is a specific receptor for fibronectin. Both α5β1 and fibronectin play a significant role in the development of the vascular system during embryogenesis (Li et al., 2009; Serini et al., 2006). Expression of α5β1 integrin is upregulated in endothelial cells within new blood vessels and also on the surface of tumour cells. α5β1 integrin ligation stimulates cell growth and migration during Akt and MAPK activation mediated signalling pathways (Millard et al., 2011).

α5β1 is one of the integrins constitutively expressed in malignant T lymphocytes (Bachsais et al., 2016). Integrins expressed in lymphocytes participate in mediating interactions with ECM proteins during the transmigration process (Jin and Varner, 2004). For example, blocking of α5 with anti-α5 mAb represses the activity of pro-MMP-9 appreciably, showing the significant role of α5β1 integrin in the fibronectin-induced MMP activity and expression which promotes K562 cell migration (Dutta et al., 2010).

Integrins and tyrosine kinases contribute to mediating signals for cell survival and suppressing programmed cell death in acute lymphoblastic leukaemia bearing the Philadelphia chromosome (Ph+ leukaemia). An α5 inhibitory antibody prevented adhesion of Ph+ leukaemia cells to fibronectin and acted

synergistically with the BCR-ABL fusion protein inhibitor imatinib to enhance apoptosis. In immune-deficient mice, the α5 inhibitory antibody delayed and impaired the engraftment of Ph+ leukaemia cells (Hu and Slayton, 2014).

1.3.4 RGD binding integrins in solid tumours

1.3.4.1 αvβ3 in solid tumours

Different types of tumours express αvβ3 integrin including prostate cancer, breast cancer, melanoma, pancreatic cancer, ovarian cancer, pancreatic cancer, cervical cancer and glioblastoma (Desgrosellier and Cheresh, 2010). αvβ3 plays a vital role in multiple cellular processes that result in the development of cancer including tumour growth, malignant transformation, invasion and metastasis (Byzova et al., 2000; Enns et al., 2005). Furthermore, previous studies have demonstrated that there is a positive relationship between the expression of the αv subunit on tumours and their ability to migrate and adhere (Li et al., 2009). αvβ3 is implicated in regulating cancer cell survival and programmed cell death. αvβ3 signalling suppresses the expression of the pro-apoptotic protein Bax by p53 downregulation and regulates the expression and activity of bcl-2. αvβ3 integrin raises the BaX:bcl-2 ratio, which results in an increase in cancer cell survival by inhibiting the mitochondrial pathway of apoptosis that comprises caspase activation and the release of cytochrome c (Martin and Vuori, 2004).

In addition, tumour progression is induced by αvβ3 integrin through the activation of Src, which results in activation of the focal adhesion kinase FAK-independent survival pathway and induction of tumour growth (Albelda et al., 1990; Gruber et al., 2005).

High expression of αvβ3 permits cancer cells to link to ECM proteins such as fibrinogen, fibronectin vitronectin, osteopontin and von Willebrand factor which are present in the microenvironment of the tumour. These adherent interactions supply cell survival signals for invading endothelial cells (Davis, 1992; Desgrosellier and Cheresh, 2010).

αvβ3 is expressed in activated macrophages, cytokine-stimulated endothelial cells, leukocytes, osteoclasts, and certain invasive cancers, although it is not typically expressed in normal epithelial cells (Cooper et al., 2002; Suyin et al., 2013). αvβ3 is implicated in different cellular activities including cell adhesion, angiogenesis, and migration on components of extracellular matrices (Cooper et al., 2002). αvβ3 is significant in vascular angiogenesis in the early stages (Brooks et al., 1994), and in osteoclast-mediated resorption of bone which is mediated by αvβ3-expressing osteoclast attachment to the surface of the bone (Ross et al., 1993; Teti et al., 2002).

In different cancer types (breast cancer, prostate cancer, and melanoma), the αvβ3 and αvβ5 integrins are extensively expressed (Schittenhelm et al., 2013). The matching ligands exert a significant role in regulating the sprouting ability of endothelial cells through angiogenesis, and localisation of inflammatory cells recruited to the invasive tumour cells or wound repair sites (Weis and Cheresh, 2011).

In human breast cancer cells, αvβ3 mediates cell adhesion to vitronectin which is crucial for supplying strong binding to the underlying ECM and the necessary cytoskeletal rearrangements (Hamidi et al., 2016; Nieberler et al., 2017). Zhao et al., (2007) found that αvβ3 integrin overexpression in breast cancer cells such as MDA-MB-231 associated with increased incidence of bone metastasis

in vivo. αvβ3 expression was higher in tissue with metastatic tumours than in primary tissue. Tumour cell expression of αvβ3 stimulates osteoclast-mediated bone resorption and bone destruction once infiltrated into the bone marrow. A selective αvβ3 non-peptide antagonist not only blocks bone colonisation by αvβ3-expressing cancer cells, but also inhibits osteoclast-mediated bone resorption in animal models of bone metastasis (Zhao et al., 2007).

In a mouse model, transfection of cells from bone metastasis with αvβ3 or utilising MDA-MB-231 breast cancer cells leads to an elevated number and areas of osteolytic bone metastases associated with active αvβ3 expression on the cell surface. The anti-αvβ3 antibody LM609 inhibited tumour cell adhesion and invasion to cortical bone (Pecheur et al., 2002) and inhibited the metastasis of breast cancer cells (Felding-Habermann et al., 2001).

Other studies showed that MDA-MB-435 and 21NT human breast cancer cells both responded to exogenous or endogenous osteopontin with highly migratory and invasive characterisation *in vitro*, showing that osteopontin could contribute functionally to the malignant behaviour of breast cancer (Tuck et al., 1999; Tuck et al., 2000; Tuck et al., 2001). These effects can be inhibited functionally in MDA-MB-435 cells with αvβ3 antibodies but not with antibodies raised to αvβ1 or αvβ5. In contrast to this, antibodies to αvβ3 had no effect in 21NT cells, but migration and invasion were inhibited by anti αvβ1 or αvβ5 antibodies (Tuck et al., 2000). Both MDA-MB-435 and 21 NT cells expressed αvβ1 and αvβ5 integrins but only MDA-MB-435 cells have high levels of αvβ3. These data demonstrate that different levels of integrin expression may control how cells respond to a ligand in the tumour microenvironment. Additionally, 21NT cells stably transfected with osteopontin and β3 and injected in nude mice,

expression of αvβ3 alone is insufficient to induce colonisation in the mammary fat pad *in vivo*. The injected mice showed increased tumour take, a reduced tumour doubling time, and a reduced tumour latency period relative to controls (Furger et al., 2003).

It is likely that αvβ3 may have various roles at different stages of metastatic progression. Activated αvβ3 expressed in breast cancer cells increases migration and metastasis to the lung following intravenous injection of cancer cells in mice (Felding-Habermann, 2001; Felding-Habermann et al., 2002; Felding-Habermann et al., 2001). Enhanced metastasis of breast tumour cells was suggested to be mediated through aggregation of tumour-induced platelets and their capture in blood vessels. These events are blocked by antibodies targeting human αvβ3 on tumour cells or αIIbβ3 on platelets (Felding-Habermann et al., 2001).

Additionally, prostate adenocarcinomas isolated from bone metastases express αvβ3 receptors, which regulate adhesion to and migration by bone ECM proteins including osteopontin and vitronectin (Zheng et al., 2000). The αv subunit mediates prostate epithelial cell interactions with osteopontin, which stimulates cell proliferation and subpopulation growth (Elgavish et al., 1998). It has also been shown that bone sialoprotein promotes integrin-mediated migration, increases expression of MMPs, and upregulates integrin survival signalling pathways in prostate cancer cells (Gordon et al., 2009).

αvβ3 is expressed in the active conformation on prostate cancer cells and comparing matched samples of bone metastasis with primary tumour showed that integrin activation is elevated in bone metastases in comparison to the primary tumour (Marthick and Dickinson, 2012; Maruyama et al., 2002). The

subunits αv and β3 are found at all stages of prostate cancer; however, the αvβ3 heterodimer is associated with increased metastatic potential in cell lines (Edlund et al., 2001). Prostate cancer cells began to express integrin β3 upon oncogenic transformation, which is further increased in metastatic prostate cancer, leading to induced tumour metastasis and invasion. Notably, overexpression of αvβ3 in prostate cancer cells is associated with increased bone metastasis (McCabe et al., 2007). Overexpression of αvβ3 has been identified as a significant factor for prostate cancer progression and metastasis because it was expressed by tumour associated blood vessels. Therefore, αvβ3 integrin could be involved in prostate cancer metastasis even though no significant expression was found in prostate cancer cells (Heß et al., 2014).

The progression of malignant melanoma is also related to the expression of αvβ3 integrin (Pickarski et al., 2015). *In vivo* and *in vitro* studies in melanoma cells overexpressing αvβ3 showed that it can increase metastasis by enhancing adhesion to vitronectin (Li et al., 2001). Overexpression of αvβ3 is inversely related to the survival of melanoma patients (Trikha et al., 2002b). The expression of β3 integrin was not detected in benign melanocytes but only detected in metastatic melanoma cells. These data showed that the expression of β3 integrin might be a biomarker for the aggressive phase of melanoma (Albelda, 1990). Mouse models showed reduced metastasis of haematogenous B16 murine melanoma cells to the lung on blocking αv (Lonsdorf et al., 2012) or αvβ3 integrin (Ramos et al., 2008). Also, no alterations in the proliferation rate were shown in siRNA-transfected B16 cells; however, they had weak ability to connect to fibronectin. Furthermore, suppression of integrin β3 expression led to almost complete impairment of the capacity of B16 cells to migrate through matrigel and metastasise. Mice inoculated to form B16 metastasis in the lung

showed decreased number of colonies compared the control group (Nasulewicz-Goldeman et al., 2012).

1.3.4.2 αIIbβ3 integrin in solid tumours

αIIbβ3 integrin is not only expressed on the surface of platelets but is also on cancer cells (Millard et al., 2011). αIIbβ3 is aberrantly expressed in breast (Kononczuk et al., 2015), melanoma and prostate cancers and is related to increased tumour growth, metastasis, and recurrence (Trikha et al., 2002a). It also been established that the capability of breast cancer cells to aggregate platelets is associated with metastatic potential of the tumours, and blockade of tumour cell induced platelet aggregation (TCIPA) is related to the suppression of metastasis *in vivo* (Oleksowicz et al., 1995).

Prostate cancer cells, particularly those grown orthotopically, express αIIbβ3. αIIbβ3 expression is localised in focal contacts on the cells of prostate carcinoma. αIIbβ3 expression plays a partial role in the invasion of prostate tumour cells through a reconstituted basement membrane; αIIbβ3 antibodies inhibited cell invasion by approximately 40%, and the invasion of prostate tumour cells specifically requires the active αIIbβ3 integrin conformation (Trikha et al., 1996).

Association analysis between cancer integrin expression and biochemical recurrence probability following the surgical removal of localised prostate cancers found αIIbβ3 integrin expression in recurrent prostate tumours to be stronger than in non-recurrent tumours and was marginally significant for recurrence (Pontes-Junior et al., 2010). Moreover, the existence of αIIbβ3 on the surface of DU-145 prostate cells is related to high tumourigenicity,

development of lymph node metastases and local invasion. PC-3 cells, which have intracellular localisation of αIIbβ3, were less invasive. For example, PC-3 cells injected into mice led to the development of intraprostatic tumours while DU-145 cells injected in mice caused tumours that were able to metastasise to new sites, notably lymph nodes (Trikha et al., 1998).

Expression of αIIbβ3 was found to be high in later stages of melanoma but low in early stages, in contrast to the expression of αvβ3 integrin which was high in early stages of melanoma. Using isogenic cell lines, the importance of αIIbβ3 integrin in human melanoma cell growth was demonstrated. No differences were shown in the growth between mock-transfected cells and αIIbβ3 expressing cells *in vitro*, but, αIIbβ3 expressing cells expanded into larger tumours concomitant with a decrease their rate of programmed cell death *in vivo* (Trikha et al., 2002a). αIIbβ3 expressing cells in the exponential growth stage upregulate expression of basic fibroblast growth factor, thus providing an angiogenic growth factor for melanoma cells and stimulating tumour growth (Dome et al., 2005).

The interaction between tumour cells and platelets is related to increased metastases. Through the bridge of fibrinogen, the interaction of cancer cells with platelet αIIbβ3 and endothelial cells αvβ3 facilitated tumour cell metastasis (Bakewell et al., 2003; Gay and Felding-Habermann, 2011) In the presence of fibrinogen, the adhesion of melanoma cells to αIIbβ3 integrin-expressing Chinese Hamster Ovary (CHO) cells was increased. Inhibition of αIIbβ3 or αvβ3 on melanoma cells led to a significant reduction in adhesion of melanoma cells to other αIIbβ3 integrin expressing melanoma cells (Schwarz et al., 2006).

Exposure of B16 melanoma cells to RGD peptide significantly decreased the platelet-mediated adhesion of fluorescently-labelled melanoma cells to endothelial cell monolayers under flow conditions, compared with untreated B16 melanoma cells or a control peptide. Additionally, depletion of platelets caused a significant reduction in adhesion of melanoma cells to the injured vascular wall *in vivo* (Lonsdorf et al., 2012). Therefore, inhibition of αIIbβ3 integrin may be a therapeutic strategy against tumour metastasis by disrupting the engagement between platelet αIIbβ3 and tumour cells (Bakewell et al., 2003).

1.3.4.3 α5β1 integrin in solid tumours

α5β1 integrin controls fibronectin matrix assembly that leads to the stability and organisation of the ECM. Cellular α5β1 expression is associated with the capability of prostate cancer cells to accumulate a fibronectin matrix forming cohesive aggregates. Fibronectin matrix assembly and high α5β1 levels are inversely related to invasiveness; absence of integrin α5β1 allows detaching of cells, resulting in metastasis and intravasation (Jia et al., 2012). α5 is highly expressed in oesophageal squamous cell carcinoma (SCC) patient samples compared to normal oesophageal epithelial cell lines. α5 expression is significantly associated with tumour size, lymph node metastasis, and poor overall survival of oesophageal SCC patients (Xie et al., 2016). Inhibiting α5β1 integrin leads to a decrease in the dynamics of cell shape changes and cell spreading in the early stage of adhesion, and a decrease in the number of adherent cells. Re-organization of cytoskeletal proteins is also weaker than in control cells. In the spreading and adhesion of prostate cancer cells, α5β1 interacted with fibronectin, whereas inhibition of αvβ3 did not affect spreading

on, and adhesion to fibronectin (Stachurska et al., 2012). It has previously been observed that integrins α5β1 and αvβ3 support fibronectin-dependent platelet adhesion and promote formation of filopodia but, in contrast to αIIbβ3, are unable to induce formation of lamellipodia. These data highlight a possible role for fibronectin in supporting thrombus adhesion in cancer (McCarty et al., 2004).

Fibroblasts display continued migration on fibronectin coated substrates, as a role of fibronectin surface density. Characterisation of fibroblast dynamics and adhesion identified alterations in focal adhesion dynamics, adhesion plaque formation, cytoskeleton organisation, and intracellular signalling between fibronectin and vitronectin. Inhibition of α5β1 and αvβ3 showed that αvβ3-mediated reduction of the directional persistence of cell migration involved changed α5β1 trafficking rather than remodelling of actin cytoskeleton and adhesion structures. The results demonstrated that fibroblasts show increased directional persistence in migration on fibronectin but not vitronectin coated substrates. Hence the engagement of both integrins α5β1 and αvβ3 is essential for directional continuation in fibroblast migration on fibronectin but not on vitronectin (Missirlis et al., 2016).

1.4 Integrins as therapeutic targets

Integrins are widely recognized as targets for antitumor therapy (Ray et al., 2014; Sheldrake and Patterson, 2014). Integrin antagonists are generally designed to inhibit the interaction between integrins and their associated extracellular ligands. Some of the integrin antagonists are still under undergoing research in preclinical or clinical trials and some have reached the pharmaceutical market. Extensive details regarding integrin antagonists have

been reviewed (Cox et al., 2010; Galletti et al., 2014; Millard et al., 2011; Stupp et al., 2014).

Given the importance of αvβ3/αvβ5, αIIbβ3 and α5β1 integrins in the progression of a number of cancers, there is significant therapeutic potential for development of integrin antagonists.

1.4.1 αvβ3/αvβ5 integrin antagonists

A large number of non-peptidic and peptidic antagonist ligands for the αvβ3 receptor have been developed which are mostly associated with the minimal recognition motif RGD (Morgan et al., 2009). Pharmacological inhibitors of αvβ3 repress the development of new blood vessels in many models (Al-Husein et al., 2012; Kumar, 2003b), and antagonists of αvβ3 such as antibodies (MEDI-522), small molecules and peptides (cilengitide) have been investigated as antiangiogenic agents (Alghisi et al., 2009; Stupp et al., 2014), albeit without clinical success.

Cilengitide, an RGD cyclic peptide antagonising αvβ3 and αvβ5 entered into clinical trials in patients with recurrent glioblastoma. The phase I and phase II clinical trials showed responses that provided evidence for drug targeting to tumours, and evidence of dose-dependent effects (Reardon et al., 2008). However, the phase III trial in glioblastoma patients with a methylated MGMT promoter investigating cilengitide combined with standard chemo-radiotherapy showed no clinical response due to failure in meeting the primary endpoint for prolonging overall survival (Stupp et al., 2014). Becker et al.,(2015) demonstrated that the failure of cilengitide was because of its distribution from plasma to other body fluids, and was excreted by the kidney. The short half-life

of cilengitide also means tumours are not exposed to curative concentrations for much of the time and might unfortunately enhance tumour growth.

Normalization of blood vessels is a strategy to promote the antitumor impacts of chemotherapies, but this depends on dose and exposure time and is therefore difficult to achieve clinically. Wong et al.(2015) demonstrated that combining a low dose of cilengitide with a chemotherapy drug (gemcitabine) decreased tumour growth, and metastasis, and increased overall survival. This has been interpreted as the αvβ3/αvβ5 integrin inhibitor enhancing chemotherapy efficiency through vascular promotion by increased tumour blood flow and vascular leakiness, and tumour blood vessel density, resulting in increased chemotherapy delivery whilst also reducing tumour hypoxia.

Furthermore, Zhao et al. found also that combining cilengitide nanotherapy with ultrasound-targeted microbubble destruction could potentially be used in glioblastoma to overcome clinical issues such as fast blood clearance (including high kidney and liver uptake) and poor blood-brain barrier penetration. Cilengitide nanotherapy showed significant apoptotic and cytotoxic impacts in C6 glioblastoma cells. A bio-distribution study in a rat glioblastoma model showed build-up of high cilengitide level in tumours exposed to combined therapy. The tumour cilengitide level in rats was elevated over three-fold, renal clearance significantly reduced and tumour retention of cilengitide prolonged when compared with free cilengitide with or without ultrasound-targeted microbubble destruction (Zhao et al., 2016).

A recent study demonstrated that colony formation of epithelial cells on laminin was significantly decreased by single agent cilengitide and cetuximab an EGF-R

inhibitor, or cilengitide with cetuximab combined. Cytokine measurements also showed significant decreases in monocyte chemo-attractant protein 1, interleukin-6 and vascular endothelial growth factor. The largest decreases in colony formation of epithelial cells and release of monocyte chemoattractant protein 1 and vascular endothelial growth factor was observed by combining cilengitide and cetuximab. Efficacy of the combined drugs surpassed that of the individually applied agents, but the combination was not synergistic. Cetuximab could not significantly enhance the effects of cilengitide. In contrast, interleukin-6 (IL-6) release was significantly blocked by cetuximab but not by cilengitide, whereas their combination strongly decreased IL-6 release (Wichmann et al., 2017).

A range of αvβ3 inhibitory antibodies have been under investigation, such as LM609, CNTO95, MEDI-522, DI17E6, and c7E3 (Liu et al., 2008). DI17E6 is a humanised monoclonal antibody specific for the αv subunit (Wirth et al., 2014). DI17E6 was selected for clinical trial because in preclinical studies it induced detachment and blocked adhesion of prostate cancer cells to different extracellular matrix proteins and cells found in the bone microenvironment without effect on cell cycle or activity of caspase 3, and 7 or cell viability. In addition, DI7E6 inhibited invasion and migration of prostate cancer cells as well as reduced phosphorylation of downstream targets FAK, ERK and Akt. These results demonstrated that blocking of αv with DI17E6 prevents several pro-metastatic phenotypes of prostate cancer cells. In a phase 1 study in patients with progressive metastatic prostate cancer after chemotherapy it decreased PSA values in 2 patients (Jiang et al., 2017).

MEDI-522 (Etaracizumab) is a humanised monoclonal antibody specific for αvβ3 integrin. A phase I dose escalation trial in 25 patients with diverse metastatic solid tumours (prostate, colorectal, breast, melanoma, ocular melanoma, non-small cell lung cancer, sarcoma, and renal cancers) showed some evidence that treatment with MEDI-522 decreased the size of tumours as estimated by imaging with dynamic computer tomography. Treatment with MEDI-522 (Etaracizumab) was without severe toxicity, and no maximum tolerated dose or dose limiting toxicities were observed. Three patients with metastatic renal cell cancer had prolonged stable disease (McNeel et al., 2005). However, further investigations in patients with metastatic melanoma (phase 2) using Etaracizumab alone or in combination with dacarbazine show that both treatments failed to improve overall survival (Hersey et al., 2010).

There are many small molecule integrin antagonists such as GLPG0187 that was developed as a pan-antagonist for RGD-integrin receptors, targeting αvβ1, αvβ3, αvβ5, αvβ6, and α5β1 with nanomolar affinity. GLPG0187 inhibited of osteoclast-mediated bone resorption, angiogenesis, and the formation of new bone metastasis and the progression of bone metastasis during cancer treatment (van der Horst et al., 2011). GLPG0187 decreased cell number and reduced proliferation and migration in PC-3 prostate cancer cells implanted within the metatarsal *in vivo* but did not affect cell survival *in vitro* (Reeves et al., 2015). The effect of GLPG0187 was also investigated in breast carcinoma progression. It showed a reduction of tumour invasion in a zebrafish embryo model, inhibition of the progression of bone metastases in a mouse model, and maximum activity when in combination with paclitaxel (Li et al., 2015). GLPG0187 was withdrawn from development following a phase I clinical trial, having shown no response even with continuous dosing (Cirkel et al., 2016).

MK-0429 is a specific oral αvβ3 inhibitor. MK-0429 was shown to be selective for αvβ3 vs α5β1 or αIIbβ3 by measuring adhesion of transfected HEK293 cells and has been shown to reduce the development of B16F10 melanoma lung metastases following tail vein injection. This suggests αvβ3 is more important than α5β1 or αIIbβ3 in the growth and colonisation of B16F10 melanoma cells in the lungs, although the expression levels of αvβ3 appear to be lower than those of αvβ5 in these cells (Pickarski et al., 2015). MK-0429 has been used in clinical trials for prostate cancer and significantly reduces the bone resorption marker urinary N-telopeptide but did not reduce PSA levels (Rosenthal et al., 2010).

1.4.2 αIIbβ3 antagonists

The platelet αIIbβ3 integrin was the first integrin to be effectively targeted therapeutically. In the 1990s, three inhibitors of αIIbβ3 integrins were approved for use in heart disease: Abciximab (antibody), Eptifibatide (cyclic peptide) and Tirofiban (small molecule inhibitor), all of which are intravenously administered; decreasing the risk of ischaemic events in those undergoing percutaneous coronary intervention and patients with acute coronary syndromes (Cox et al., 2010). These three αIIbβ3 antagonists are quite discrete in design from one another, and all three are mechanistically distinct from other platelet inhibitors such as P2Y12 inhibitors or aspirin (Bledzka et al., 2013).

Both Abciximab and c have been investigated in programmed cell death in breast cancer cells such as MCF-7. Eptifibatide produced a stronger pro-apoptotic effect in MCF-7 cells than abciximab and could therefore be

considered as a novel candidate for anticancer therapy (Kononczuk et al., 2015).

Abciximab and related murine antibodies have dual β3 antagonist activity and are effective in blocking angiogenesis and tumour growth through targeting of the interaction of tumour cells with endothelial cells and platelets. This is in addition to the immediate impact of abciximab on tumour size and growth. However, the associated bleeding and immunogenicity of abciximab suggests that there is a need for additional development of a non-immunogenic small molecule as a more attractive clinical candidate for long term anticancer therapy (Trikha et al., 2002a).

1.4.3 α5β1 integrin antagonists

α5β1 is currently being targeted both for cancer therapy and retinal neovascularisation in age-related macular degeneration (AMD). An example α5β1 antagonist is Volociximab, a chimeric human-mouse monoclonal antibody with high affinity for the α5β1 integrin (Ramakrishnan et al., 2006). Volociximab has been well tolerated in Phase I trials without severe side effects (Ricart et al., 2008). In preclinical studies using a rabbit VX2 carcinoma model, Volociximab was effective in inhibiting tumours growing intramuscularly or subcutaneously and this effect was shown to be related to reduced blood vessel density within these tumours (Bhaskar et al., 2008). However, despite being safe, Volociximab was not effective in ovarian cancer (Bell-McGuinn et al., 2011), but did show some evidence of clinical activity in non-small cell lung cancer in combination with paclitaxel and carboplatin (Besse et al., 2013).

1.5 Aims and objectives

Targeted drugs for cancer therapy which will control the process of tumour progression and metastasis are required. The RGD-binding integrin subfamily including αvβ3, αvβ5, αIIbβ3 and α5β1 plays an important role in these processes and as has been described previously there is a need to develop new small molecule antagonists. The hypothesis underlying this work is that dual β3 integrin antagonists will have an enhanced effect on cancer progression and metastasis through targeting tumour cell interaction with αvβ3 on endothelial cells and αIIbβ3 on platelets resulting in inhibition of both angiogenesis and metastasis. The overarching aim in this work is that of characterising a dual β3-expressing model cell system which will be used to identify dual hit β3 integrin antagonists.

These aims will be addressed by the following means:

- Evaluation of the expression of αIIb, αv, α5, β3 and β5 integrin subunits in a panel of human tumour cell lines to use in cell-based assays to investigate the effects of β3 integrin antagonists.
- Evaluation of the effect of phorbol 12-myristate 13-acetate (a protein kinase C stimulator) on the expression of the αIIb integrin subunit in K562 cells.
- Development and validation of cell-based adhesion, detachment and migration assays to investigate the effect of β3 inhibition on cellular function in dual β3 expressing models.
- Evaluation of the effect of ICT compounds in the developed models to characterise and identify new integrin antagonists.

Chapter 2: Characterisation of αIIb, αv, α5, β3 and β5 integrin subunit expression in a panel of human cancer cell lines

2.1 Introduction

Integrin adhesion receptors, particularly the RGD-binding integrin subfamily are related to the spread of cancer and poor prognosis. Dual β3 antagonists are expected to have a direct anti-proliferative effect on dual β3 expressing models and inhibit angiogenesis and metastasis through targeting cancer cell interactions with platelet αIIbβ3 and endothelial cell αvβ3 integrin. The expression of αvβ3, αIIbβ3 and α5β1 is widely demonstrated in literature in many human tumour cell lines and tissues (see Chapter 1). The expression of integrins in many studies to date is not the same *in vivo* as *in vitro* (Goodman and Picard, 2012; Stachurska et al., 2012; Taylor et al., 2012; Terry et al., 2014).

Most cancer cells can express αvβ3 in different states of activation, and cells from metastatic lesions express the integrin in the high affinity/constitutively activated form (Felding-Habermann, 2001), targeting of the activated conformer of αvβ3 inhibited metastasis from the blood stream (Weber et al., 2016). Therefore, αvβ3 is considered to be important as a cancer drug target for its high expression in endothelial cells and many tumours in addition to its vital role in enhancing metastasis (Kumar, 2003a; Liu et al., 2008). Furthermore, αvβ3 may also become a valuable tumour marker to identify specific cells, which distinguish between healthy and tumour patients.

αIIbβ3 integrin is expressed mainly on platelets and its presence has also been detected on some tumour cells (Kononczuk et al., 2015; Millard et al., 2011; Trikha et al., 1998). For example, the expression of αIIbβ3 integrin in prostate cancer cells is involved in the process of tumour cell invasion (Gay and Felding-Habermann, 2011).

This section has been designed to characterise the expression of integrins in a panel of cancer cell lines (leukaemia cells; K562, prostate cells; LNCap, DU145, and PC-3, breast cells; MCF-7, melanoma; M14, MeWo, and UACC-62 and colon cells; HT-29), to determine the models to be utilised in screening novel integrin antagonists.

2.2 Aim and objectives

The aim of the work described in this chapter was to investigate a panel of cancer cell lines that may be used for screening novel integrin antagonists. This was achieved by the following means:

- Measuring growth rates of designated cell lines to optimise their seeding density for subsequent experiments.

- Characterising the expression of αv, αIIb, α5, β3 and β5 integrin subunits in a panel of cell lines using immunofluorescence and flow cytometry.

- Confirming the expression of αIIb and β3 in 3D cell culture for a selected model.

2.3 Materials and methods

2.3.1 Materials

All reagents such as media and their supplements, if not specified otherwise, were obtained from Sigma-Aldrich (Poole, U.K.). Primary antibodies and secondary antibodies were utilized to identify the expression of αIIb, αv, α5, β3, and β5 as shown in Table 2. The washing solution used was phosphate-buffered saline (PBS); pH 7.4 at 37 ºC. The blocking reagent used in all antibody dilutions was bovine serum albumin (BSA). Normal goat serum was obtained from Vector Laboratories Ltd (Peterborough, U.K.). VECTASHIELD® Mounting Media with DAPI (4', 6-diamidino-2-phenylindole) and Vectastain Avidin Biotin Complex (ABC) were obtained from Vector Laboratories Ltd (Peterborough, U.K.). 3, 3-diaminobenzidine tetra- hydrochloride (DAB) chromogen was from Sigma-Aldrich, Poole, U.K. Anti-αvβ5 adhirons C3 and A8 were generated and provided by Dr. Darren Tomlinson, University of Leeds.

2.3.2 Cancer cell lines and cell culture

The panel of cancer cell lines that were cultured were: K562 derived from chronic myelogenous leukaemia (CML); LNCap, a human prostate carcinoma derived from lymph node; DU-145, human prostate adenocarcinoma derived from dural metastasis; PC-3, human prostate adenocarcinoma derived from grade IV cancer metastasized to bone; MCF-7, breast adenocarcinoma derived from a metastatic site pleural effusion; HT-29, human colorectal adenocarcinoma derived from colon cancer; M14, MeWo, UACC-62, human melanoma derived from human skin tissue. All cell lines were obtained from the American Type Culture Collection (ATCC).

Primary antibodies	Type	Company	Secondary antibody	Company
Anti-β3 (B-7)	Monoclonal mouse antibody	Santa Cruz Biotechnology(Santa Cruz, USA)	Goat Anti-Mouse IgG H&L (Alexa Fluor® 488)	Abcam (Cambridge, U.K.)
Anti-α5 (C-9)	Monoclonal mouse antibody	Santa Cruz Biotechnology	Goat Anti-Mouse IgG H&L (Alexa Fluor® 488)	Abcam (Cambridge, U.K.)
Anti-αv (Q-20)	Polyclonal rabbit antibody	Santa Cruz Biotechnology (Santa Cruz, USA)	Donkey Anti-Rabbit IgG H&L (Alexa Fluor® 488)	Abcam (Cambridge, U.K.)
Anti-αIIb (EPR4330)	Monoclonal rabbit antibody	Abcam (Cambridge, U.K.)	Donkey Anti-Rabbit IgG (H&L) Antibody, Alexa Fluor® 546	Molecular Probes (Invitrogen**,** USA)
Anti-αIIb (C-20)	Polyclonal goat antibody	Santa Cruz Biotechnology (Santa Cruz, USA)	Donkey Anti-Goat IgG H&L(Alexa Fluor® 790)	Abcam (Cambridge, U.K.)
Anti-β5 (ab15459)	Polyclonal rabbit antibody	Abcam (Cambridge, U.K.)	Donkey Anti-Rabbit IgG H+L (Alexa Fluor® 488)	Abcam (Cambridge, U.K.)

Table 2: Primary antibodies (PAbs) and secondary antibodies (2Abs) used in immunofluorescence studies and flow cytometry.

2.3.3 Methods

2.3.3.1 Cell maintenance

To prepare one 500-ml portion of basic media (RPMI Medium 1640 I X), the RPMI medium was supplemented with 10% foetal bovine serum (FBS) (50 ml) 200 mM L-glutamine (5 ml) and 100 mM sodium pyruvate (5 ml). The RPMI medium was used for all cell lines except MCF-7, which was used with complete Dulbecco's Modified Eagle Medium (DMEM).

The cells were grown and maintained at 37 ºC, 5% humidity in an incubator. Cells were allowed to reach 70 - 80% confluence. Following this, the suspension cells (non-adherent cells) were removed directly and placed into a sterile tube. The cells were centrifuged at 1000 rpm for 5 minutes. Adherent cells were passaged by discarding the medium and washing the flask contents with 5 - 10 ml of PBS, depending on the size of the flask, before trypsinisation using 1 - 2 ml of a 0.25% trypsin/EDTA solution, and incubating for 2–5 minutes at 37 ºC. When cells were released in the flask, 10 ml of the complete medium was added to inhibit the trypsin/EDTA action. Then the trypsinised cells were placed into the sterile tube and centrifuged at 1000 rpm for 5 minutes (Heraeus Megafuge 1.0 centrifuge, DJB Labcare Ltd., U.K.). The cell pellet was re-suspended in the required volume of fresh media that was dependent upon the required split ratio. A portion of this was transferred into the new flasks.

To count cells, a Neubauer haemocytometer (7201004, VWR International Ltd. Poole, U.K.) was used. 10 µl of cell suspension pipetted on the edge of the coverslip allowed cells to be drawn under the coverslip to cover the counting grid. The cells were counted using an inverted microscope (Olympus, CK2, X20

objective lens magnification). The number of cells on the counting grid was multiplied by 1 X 10^4 to give the number of cells per ml.

2.3.3.2 Cell lines growth curve

Growth curves were characterised to assess whether cells utilised in experiments were within the log phase (exponential growth phase).

2.3.3.3 Growth curve for K562 cells growing in suspension culture

When cell lines reached 70 – 80% of confluency, cell suspension were poured into 20 ml tubes and centrifuged for 5 minutes at 1000 rpm. The supernatant was removed, and 10 ml of fresh medium was added to re-suspend cells by vortex shaking. 10 µl of suspension cells was placed in the chamber of the haemocytometer to count the number of cells for different concentrations: 1 $X10^4$, 2 $X10^4$, 5 $X10^4$ and 1 $X10^5$ cell/ml. Five flasks (T25) each containing 10 ml were prepared on days 1, 2, 3, 4, and 7. Every day, the flask was counted for each cell concentration, and the growth curves plotted. The growth curves of cells were measured in triplicate.

2.3.3.4. Growth curve by MTT assay

The number of proliferating cells was determined by MTT (3-(4, 5-Dimethylthiazol-2-yl)-2, 5-DiphenyltetrazoliumBromide) conversion to formazan, which indicates metabolic activity and consequently, cell viability. Briefly, cells

were counted as described above. 200 µl/well of cells was seeded at different concentrations: $1X10^2$, 5 $X10^2$, 1 $X10^3$, 5 $X10^3$,1 $X10^4$, 5 $X10^4$, 1 $X10^5$, 2 $X10^5$ cells/ml into five 96 well plates and were permitted to adhere (in case of adherent cells) to the bottom of the plate by incubating at 37 ºC for 24 hours. Every day, cell proliferation was measured by adding 20 µl of filter sterilised MTT per well (5 mg/ml in distilled water filtered through a 0.2 µm filter and stored for a maximum of 4 – 6 weeks at 4 ºC) and incubated 4 hours with MTT. Following this, the media was gently removed with a validate pipette, and 150 µl of DMSO was added and mixed with the blue formazan crystals to dissolve them. Finally, the absorbance of formazan solution was read spectrophotometrically at 540 nm. The mean absorbance was calculated and plotted versus time (days). This experiment was repeated three times.

2.3.3.5 Immunofluorescence/Immunocytochemistry

2.3.3.5.1 General protocol for αv, αIIb, α5, β3 and β5 antibody labelling

Dilution of 1 to 10 ml of poly-L-lysine solution (0.1 %) in distilled water was prepared and 300 µL (enough to cover the surface of the coverslip) was added onto autoclaved coverslips. The coverslips were incubated for 25 minutes. The poly-L-lysine solution was aspirated from the coverslips and allowed to air dry for 25 minutes. Coated coverslips were used either immediately or stored in a dark and dry place for up to one week before use.

Cell suspension were prepared and counted 5 $X10^5$ cells/ml were seeded on poly-L-lysine coated coverslips in 6-well plates and were incubated in 5% CO_2 at 37 ºC overnight.

The supernatant was removed from each well and the coverslips were rinsed with 1 ml of PBS. Cells were then fixed with 1 ml of fixative solutions 4% paraformaldehyde (PFA) for 5 – 15 minutes at room temperature, 100% methanol for 10 –15 minutes at -20 ºC, or 100% acetone for 5 seconds at room temperature. The plates were then left to dry and were used immediately or stored at -20 ºC until used. The cells were rinsed with 1 ml PBS to rehydrate them and were blocked by adding 300 µl of blocking solutions 5% BSA/PBS or 10% normal goat serum for one hour at room temperature.

The blocking solution was aspirated and 100 µl of the selected diluted primary antibody was added and incubated at 4 ºC overnight or for one hour at room temperature (this depends on the type of antibody, Table 3). The primary antibody was omitted for negative controls. Cells were washed three times for 5 to 10 minutes with PBS and then 100 µl of the diluted secondary antibody (concentration of secondary antibody depends on primary antibody, Table 3) was added and incubated for one hour in a dark place at room temperature. The cells were washed with PBS for 3 X 5 minutes. The PBS was then removed and the coverslips were mounted on each slide with a drop of mounting medium with DAPI stain and the slides were left for at least one hour at 4 ºC to be examined by immunofluorescence microscopy.

2.3.3.5.2 Preparation of adherent cells

A suspension of adherent cells was prepared and counted. 3 X 10^5 cells/ml were seeded immediately on coverslips in 6-well plates without a coating agent. The plates were incubated at 37 ºC overnight until cells were seen adhering to

coverslips. They were then labelled with antibodies or anti-αvβ5 adhiron as described in Table 3.

Table 3: Optimised concentrations of antibodies used for immunofluorescence.

	Anti-αv (Q-20)	Anti-β3 (B7)	Anti-β5 (C-9)	Anti-α5	Anti-αIIb (EPR4330)	Anti-αIIb (C-20)	Anti-αvβ5 (adhiron A8)	Anti-αv β5 (adhiron C3)
Cell seeding concentration	$5x10^5$ Cell/ml for all experiments							
Fixation	4% PFA	4% PFA	100%Acetone	4% PFA	4% PFA	4% PFA	4% PFA	4% PFA
Blocking	5% BSA/PBS	5% BSA/PBS	5% BSA/PBS	5% BSA/PBS & 10% normal goat serum	5% BSA/PBS	5% BSA/PBS	1.5% normal goat serum /PBS	1.5% normal goat serum /PBS
Dilution of primary Abs	1:50	1:50	1:200	1:100	1:50	1:50	1:50 &1:200 (anti-HIS)	1:100 &1:200 (anti-HIS)
Incubation of primary Abs	Overnight at 4 °C	Overnight at 4 °C	1 hour at room temperature	Overnight at 4 °C	Overnight at 4 °C	Overnight at 4 °C	1 hour at room temperature for each Ab without washing	1 hour at room temperatur e for each Ab without washing
Dilution of secondary Abs	1:200	1:50	1:200	1:200	1:200	1:200	1:200	1:200
Incubation of secondary Abs	One hour in a dark place at room temperature							

2.3.3.6 Flow cytometry

2.3.3.6.1 General protocol for indirect flow cytometry procedure

Indirect labelling requires two incubation steps: first with primary antibody then with a suitable secondary antibody. The secondary antibodies had fluorescent dyes (FITC, TRITC) and were used to detect integrin expression by the FACS machine (FACSCalibur^{TM}, Becton Dickinson).

2.3.3.6.2 General procedure for integrin subunit labelling by FACS analysis

Cells were harvested and washed with PBS and the cell number determined. 1ml of cell suspension (approximately $5X10^5$ cells/ml) was added to each FACS tube and spun down for 5 min at 1000 rpm, following which the supernatant was removed and 100 µl of 4% PFA was added. The solution was kept for 5 –10 minutes at room temperature. Fixed cells were obtained after the supernatant was removed. Dilution of primary antibodies was made in 1% BSA/PBS. 100µl of diluted primary antibodies were added to each tube according to their optimal concentrations in Table 3 and incubated for 30 – 60 minutes at 4°C in the dark. The cells were centrifuged with cold PBS three times at 1000 rpm for 5 minutes.

A fluorochrome-labelled secondary antibody was diluted (1:500) in 1% BSA/PBS. 100 µl of diluted secondary antibodies was added to each tube and incubated for at least 20 – 30 minutes at 4°C in the dark. The cells were centrifuged again with cold PBS three times at 1000 rpm for 5 minutes, and then 1 ml of 1% BSA/PBS was added to the cell suspension and the

suspension cells were immediately stored at 4°C in the dark until their analysis. For analysis on FACSCalibur^{TM}, cells were distinguished from debris by forward scatter and side scatter parameters. Positive and negative antibody staining was measured by log fluorescence in the FL1 channel as secondary antibodies were used conjugated to FITC.

2.3.3.6.3 Data analysis

Data analyses were performed using Cell Quest software and calculated their mean by Excel software.

2.3.3.7 MCF-7 spheroid preparation

100 µl/well of MCF-7 cells was seeded at 5X10^4 cell/ml into non-treated 96 well plates. The 96 well plates were centrifuged for 20 minutes/1000 rpm to aggregate the cells then incubated at 37°C. Media was refreshed every 2 - 3 days. The diameter of spheroids was measured using calibrated graticule fixed to the light microscope at X10 objective lens.

2.3.3.6.4 Preparation of methylcellulose

Methylcellulose (6 g) in 500 ml glass bottle was autoclaved then mixed with 250 ml medium preheated to 60°C for 30 min. After that, 250 ml medium was added and stirred for 30 - 45 minutes at RT. The solution was left in the fridge for 1 - 2 h at 4°C to ensure complete solubilization then centrifuged for 2 hours then divided in 50 ml tubes and kept at 4°C.

2.3.3.6.5 Fixation and paraffin embedding of spheroids

Spheroids were collected using a micropipette into 20 ml universal tube and they were left to settle as sediment. Media was removed, and PBS added for washing. The cell pellets were then fixed with 2 ml Bouin's solution (composed of 70% acetic acid, 5% picric acid and 25% formaldehyde in an aqueous solution) for 75-100 minutes at room temperature.

Bouin's solution was drained off, and spheroids were washed with 70% ethanol 3 times until the solution became colourless as much as possible (removing yellow colour of Bouin's solution) and then left in 70% ethanol at room temperature until the embedding processing.

Spheroids were then immersed in 90% ethanol/water for 1hr., followed by two changes of absolute (100%) ethanol after 30 minutes for each change and replaced with 100% xylene twice for 30 minutes. Afterwards, spheroids were transferred for embedding moulds with a small amount of xylene, then covered with liguid paraffin and left in an oven at 68 °C for 30 min. The paraffin/xylene mixture was removed, and the melted paraffin was added and left again in the oven for 5 minutes. This step was repeated two times. In the final stage spheroids were centered in the middle of the mould covered with fresh paraffin. Transfer moulds were stood on a cold plate for 2 - 3 hours then stored in the freezer at -20 °C.

2.3.3.6.6 Immunohistochemistry

2.3.3.6.6.1 APES coating slides

Slides coated with 4% 3-aminopropyltriethoxysilane (APES) in acetone before using for paraffin-embedded (PE) spheroids sections. The slides were sequentially immersed in 100% acetone and 4% APES, then washed in running tap water twice for 2 minutes each.

2.3.3.6.6.2 Paraffin-embedded spheroids

Sections (5 µm thick) of paraffin embedded spheroid blocks were cut using a microtome and mounted on super frost plus slides (BDH, Poole, UK). The slides were dried on a hot plate at 40°C for 2 - 3 hrs. Then the sections were subjected to H&E staining and immuno-detection.

2.3.3.6.6.3 H&E staining for Formalin Fixed Paraffin Embedding (FFPE) sections

Sections on APES slides were dewaxed by incubating for 5 min in 100% xylene (two times) and 50% xylene-ethanol and then rehydrated by incubating consecutively for 5 min in absolute ethanol (twice), 90% ethanol and finally 70% ethanol. Slides were stained first with Harris haematoxylin for 10 minutes followed by washing in running tap water, and then incubated in acid alcohol (0.5% HCl in 70% ethanol) for 5 seconds. Then excess haematoxylin was removed from the cells leaving the nuclei, but not cytoplasm strongly stained red. Again, the slides were briefly washed in tap water. Excess stain was removed from the section by washing with tap water for 5 minutes and

immersing in Scott's Tap Water (sodium bicarbonate 2 g. magnesium sulphate 20 g. dissolved in deionised water 1 litre) for 2 min to allow the colour to develop.

Sections were counterstained in 1% aqueous eosin for 1 - 2 minutes followed by washing briefly in tap water, then drained for 1 minute to let excess water runoff. Finally, sections were dehydrated by incubating for 3 minutes each in the following sequence of solution: 100% ethanol (twice), 50% xylene/ethanol (one time), and 100% xylene for 2 minutes. Slides were then immersed in clean xylene for 5 minutes. Finally, slides were mounted using DPX medium (distyrene-plasticiser-xylene) (VWR International Ltd. Poole, UK), a coverslip was applied, and the sections were left to dry.

2.3.3.6.6.4 Immuno-detection of αIIb and β3 integrin subunits expression in MCF-7 spheroids

Sections were deparaffinised and dehydrated by sequential immersion in xylene, 50% (xylene/ethanol), 100% ethanol two times, 90% ethanol, 70% ethanol and distilled water for 5 minutes for each step.

2.3.3.6.6.4.1 Antigen retrieval

Slides were placed in a plastic microwavable container filled with citrate buffer (sodium salt of citric acid; 10 mM and pH 6.0). For heating induced epitope retrieval, the microwavable container was wrapped with pierced cling film and heated at 600W (medium-high power (NN-E201W, Panasonic) for 20 min with topping up of citrate buffer when necessary. Slides were then left to cool down for 30 min and washed twice in TBS solution (pH 7.55) for 5 minutes.

2.3.3.6.6.4.2 Endogenous peroxidase and nonspecific staining block

The quenching of endogenous peroxidase activates was performed by incubation of slides for 15 minutes in freshly prepared 3% hydrogen peroxide (H_2O_2) in distilled water. Following this, nonspecific blocking was done with 1.5% normal serum (horse or goat) for 30 minutes at room temperature, then excess serum was removed by pipette and covered with αIIb or β3 primary antibodies at dilution given in Table 3 and incubated overnight at 4ºC in a humidity chamber. Negative controls were incubated with 1.5% normal serum (horse or goat) without primary antibody for the same period of time. The following day, slides were washed 3 times with TBS buffer for 3 minutes. The slides were then covered with 1:200 biotinylated secondary antibody (anti-rabbit or anti-mouse IgG (H+L) incubation for 30 minutes at RT. Meanwhile, ABC reagent (Avidin-Biotin Complex) working solution of peroxidase–labelled streptavidin was prepared by mixing 10µl solution A with10µl solution B in 1 ml of TBS buffer. Excess secondary antibody was removed by washing three times with Tris buffered Saline (TBS) solution for 3 minutes.

The sections were then incubated with ABC reagent for 30 minutes, then washed twice with TBS solution for 5 minutes. The colour was developed by using DAB detection kit (Vector Laboratories). DAB solution was prepared by mixing1 drop of buffer stock solution, 2 drops of DAB and 1 drop of H_2O_2 in 2.5 ml of distilled water. Sections were then counterstained with Harris' hematoxylin for 10 minutes followed by washing with tap water and stained in Scott's tap water for 2 minutes. Sections were dehydrated and cleared by immersing

sequentially in 70% ethanol, 90% ethanol, absolute 100% ethanol, 50% xylene-ethanol, 100% xylene and 100% fresh xylene (5 minutes each). Slides were mounted with coverslips by using DPX slide mount medium.

2.4 Results

2.4.1 Characterisation of growth curves of cancer cell lines

Growth curves were measured to identify the lag phase, log phase and saturation phase, in order to analyse the cellular growth and determine the best time for using the cells in subsequent assays. Figure 9 shows growth curves of K562 and prostate cell lines. K562 cell lines began exponential growth from day 1 which continued until day 7 for most concentrations except $1X10^5$ cells/ml. Prostate cells lines also began exponential growth from day 1. LNCaP cells ($2X10^5$cells/ml) showed diminution in cells number from day 5 whereas PC-3 numbers began to decline from day 4 at 5 $X10^4$cells/ml and $1X10^5$ cells /ml.

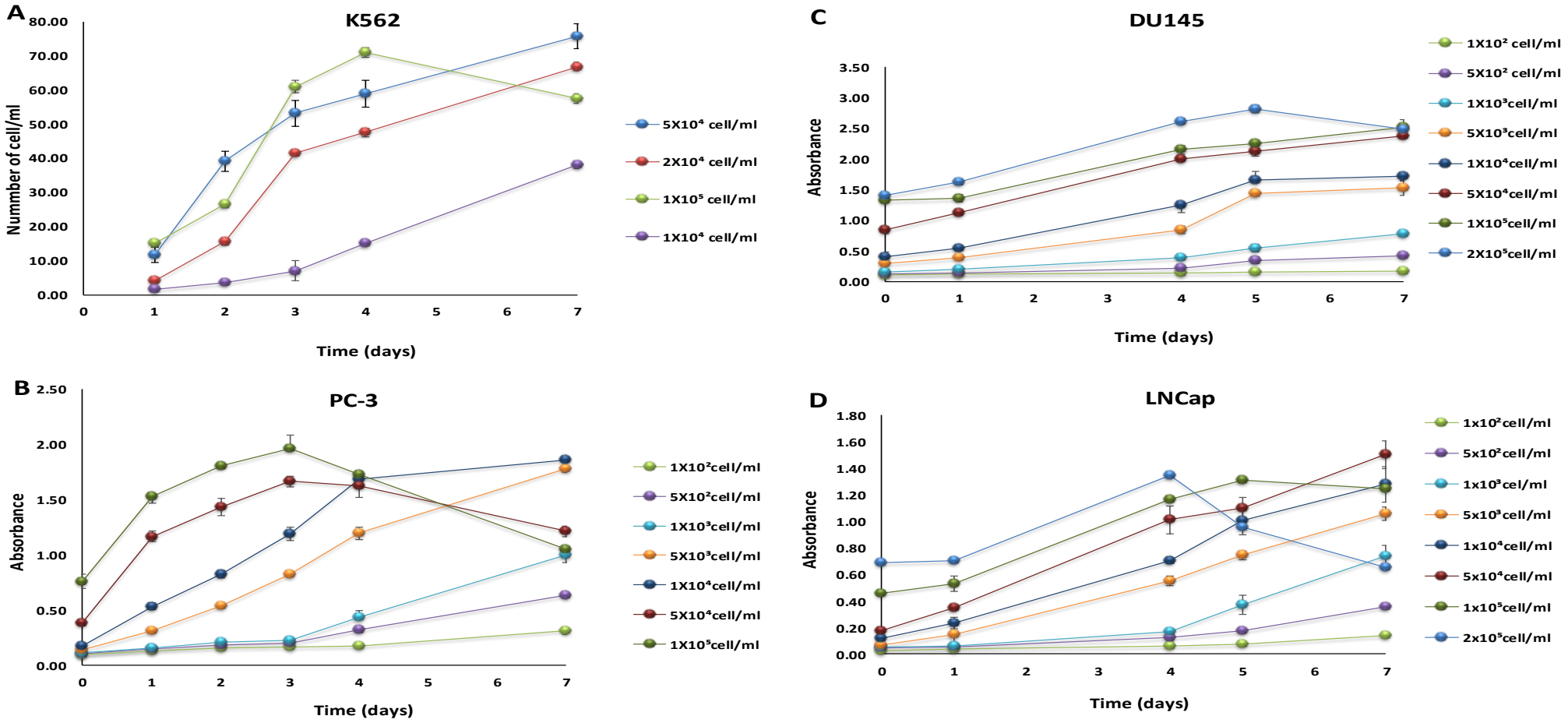

Figure 9 : Cellular growth curves. (A) K562 were assessed using a haemocytometer method and growth curves of prostate cell lines, (B) PC-3, (C) DU-145 and (D) LNCap, were assessed by the MTT assay (see sections 2.3.3.3 and 2.3.3.3 for details). Data are shown as mean ± SE of 3 independent experiments.

2.4.2 Investigation of the expression of integrin subunits using immunofluorescence

2.4.2.1 Screening of αv, α5, αIIb, β3 and β5 in K562, LNCap, DU-145, PC-3 and MCF-7

The human erythromyeloblastoid leukaemia cell line K562, and prostate cancer cell lines DU-145, LNCap and PC-3, were investigated for the expression of αv, α5, αIIb, β3 and β5 integrin subunits using protocols previously optimised in our research group (Table 3) (Ahmedah, 2015). The expression of these integrin subunits is shown in Figures 10 -14. In K562 cells, high cytoplasmic expression of αv and α5, moderate cytoplasmic expression of β3 and moderate cytoplasmic expression of β5 were detected, but no expression of αIIb was detected. In LNCap cells, high cytoplasmic expression of αv and α5 was detected, moderate cytoplasmic expression of β5 was detected, low expression of β3 was detected, but no expression of αIIb was detected. In DU-145 cells, high membrane expression of αv and αIIb and high cytoplasmic expression of β5 were detected, and moderate membrane expression of α5 and moderate cytoplasmic expression of β3 were detected. In PC-3 cells, high cellular membrane expression of αv and αIIb was detected, moderate cytoplasmic expression of α5 and β3 was detected, and moderate cellular membrane expression of β5 was detected. In MCF-7 cells, high cellular membrane expression of αv, αIIb and β3 was detected, moderate cellular membrane and cytoplasm expression of β5 was detected, and no expression of α5 was detected.

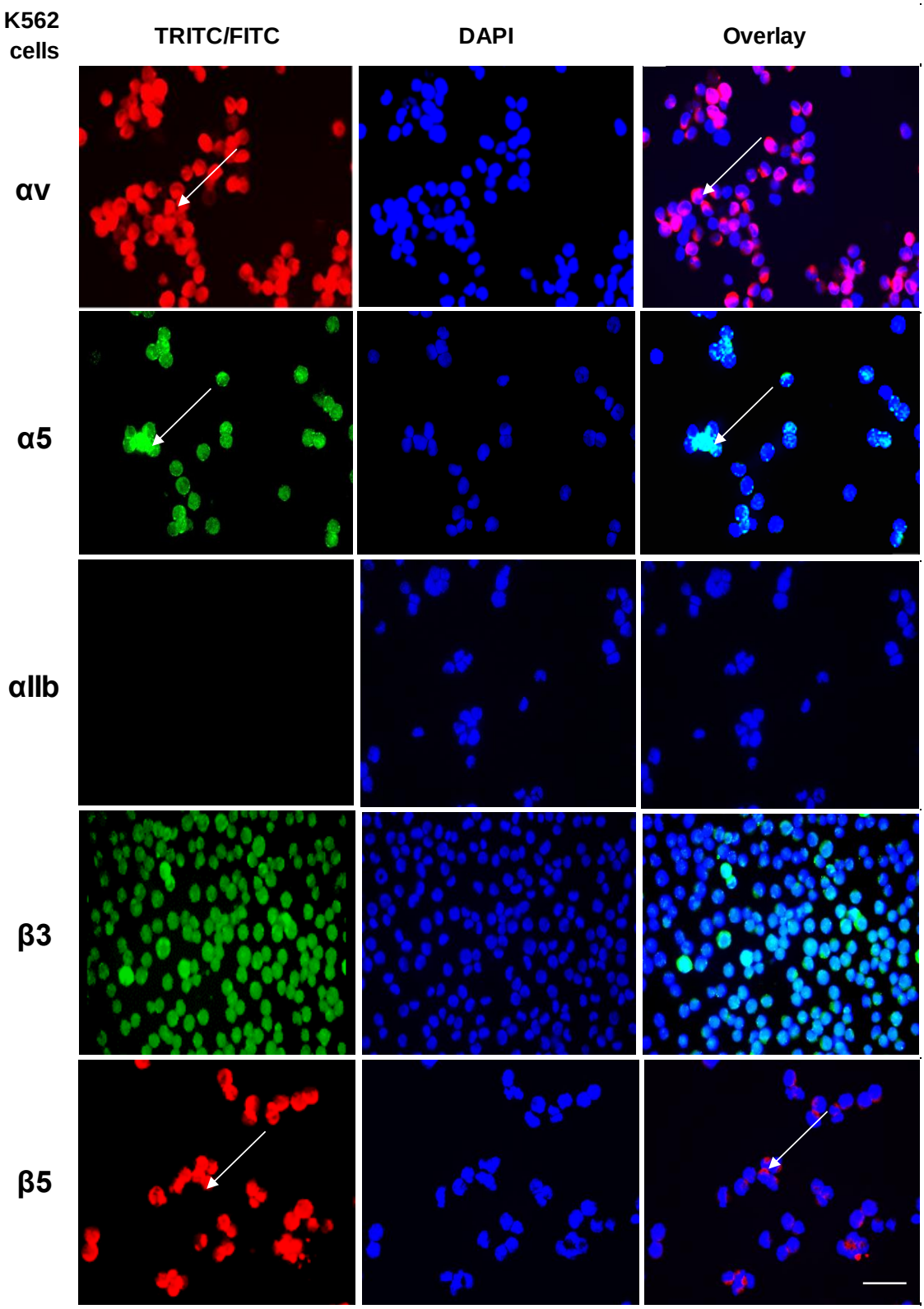

Figure 10: Expression of αv, α5, αIIb, β3 and β5 integrin subunits in K562 cells. Integrins were detected using immunofluorescence with Q20 anti-αv, C9 anti-α5, EPR4330 anti-αIIb, B7 anti-β3, and ab15459 anti-β5 integrin antibodies. Bar Length = 50 μm. Blue-fluorescent DAPI is nuclear staining and colours (green and red) represent integrin expression detected by a fluorophor. White arrows point to positive labelling of αv, α5, αIIb, β3 and β5 integrin subunits in K562 cells.

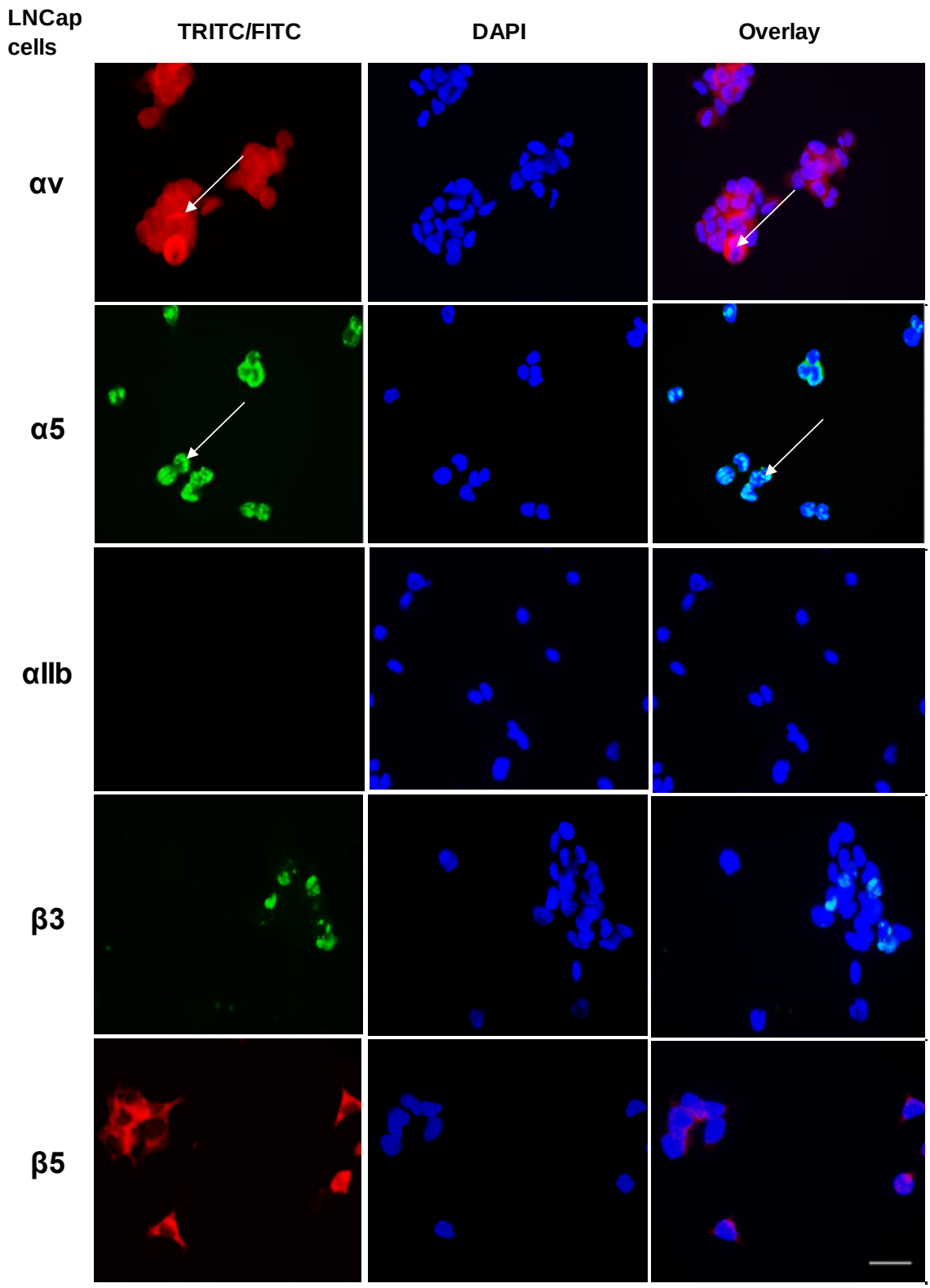

Figure 11: Expression of αv, α5, αIIb, β3 and β5 integrin subunits in LNCap cells. Integrins were detected using immunofluorescence with Q20 anti-αv, C9 anti-α5, EPR4330 anti-αIIb, B7 anti-β3, and ab15459 anti-β5 integrin antibodies. Bar Length = 50 μm. Blue-fluorescent DAPI is nuclear staining and colours (green and red) represent integrin expression detected by a fluorophore. White arrows point to the positive labelling of αv, α5, αIIb, β3 and β5 integrin subunits in LNCap cells.

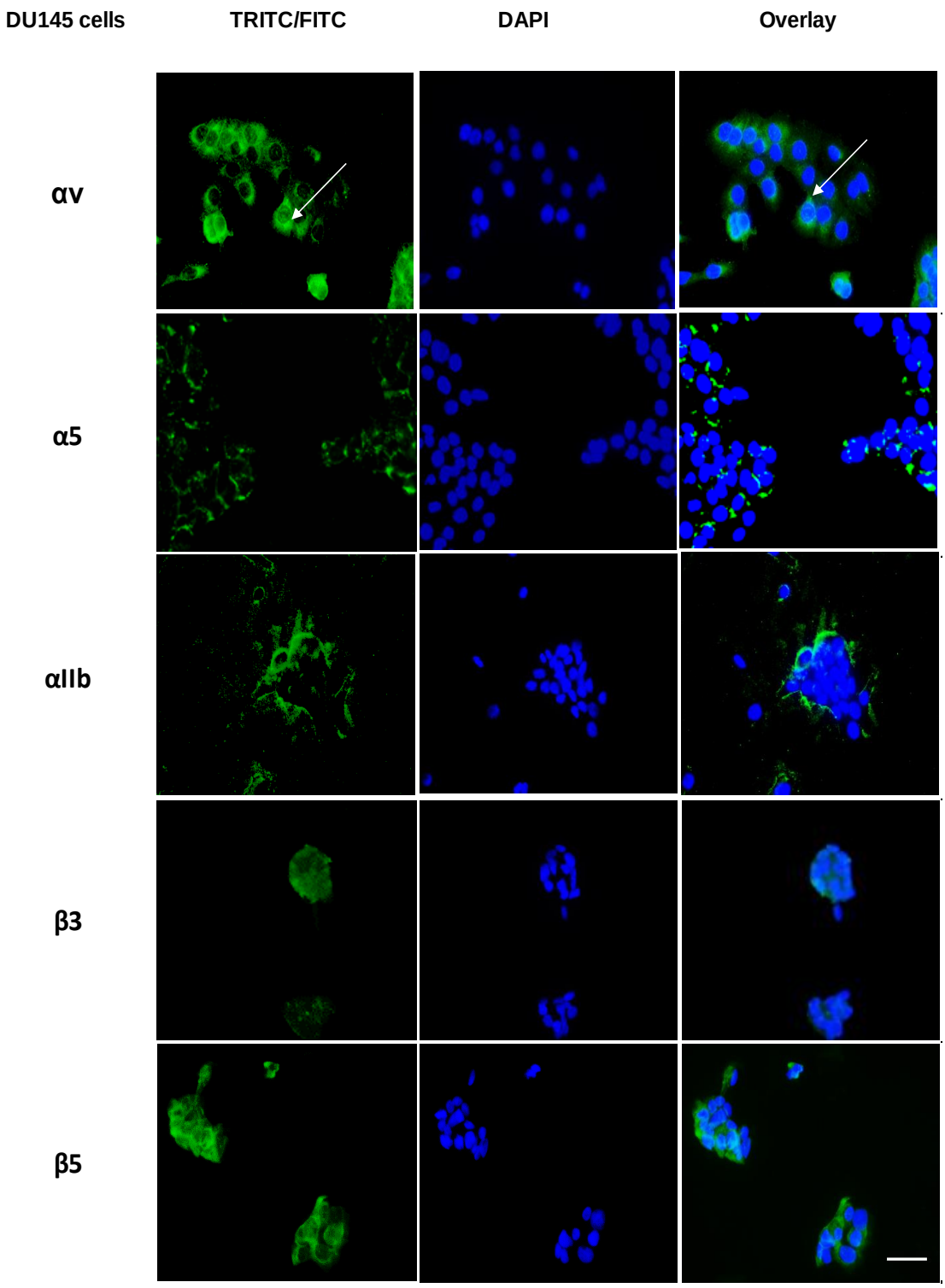

Figure 12: Expression of αv, α5, αIIb, β3 and β5 integrin subunits in DU-145 cells. Integrins were detected using immunofluorescence with Q20 anti-αv, C9 anti-α5, EPR4330 anti-αIIb, B7 anti-β3, and ab15459 anti-β5 integrin antibodies. Bar Length = 50 μm. Blue-fluorescent DAPI is nuclear staining, and green colour represents integrin expression detected by a fluorophore. White arrows point to the positive labelling of αv, α5, αIIb, β3 and β5 integrin subunits in DU-145 cells.

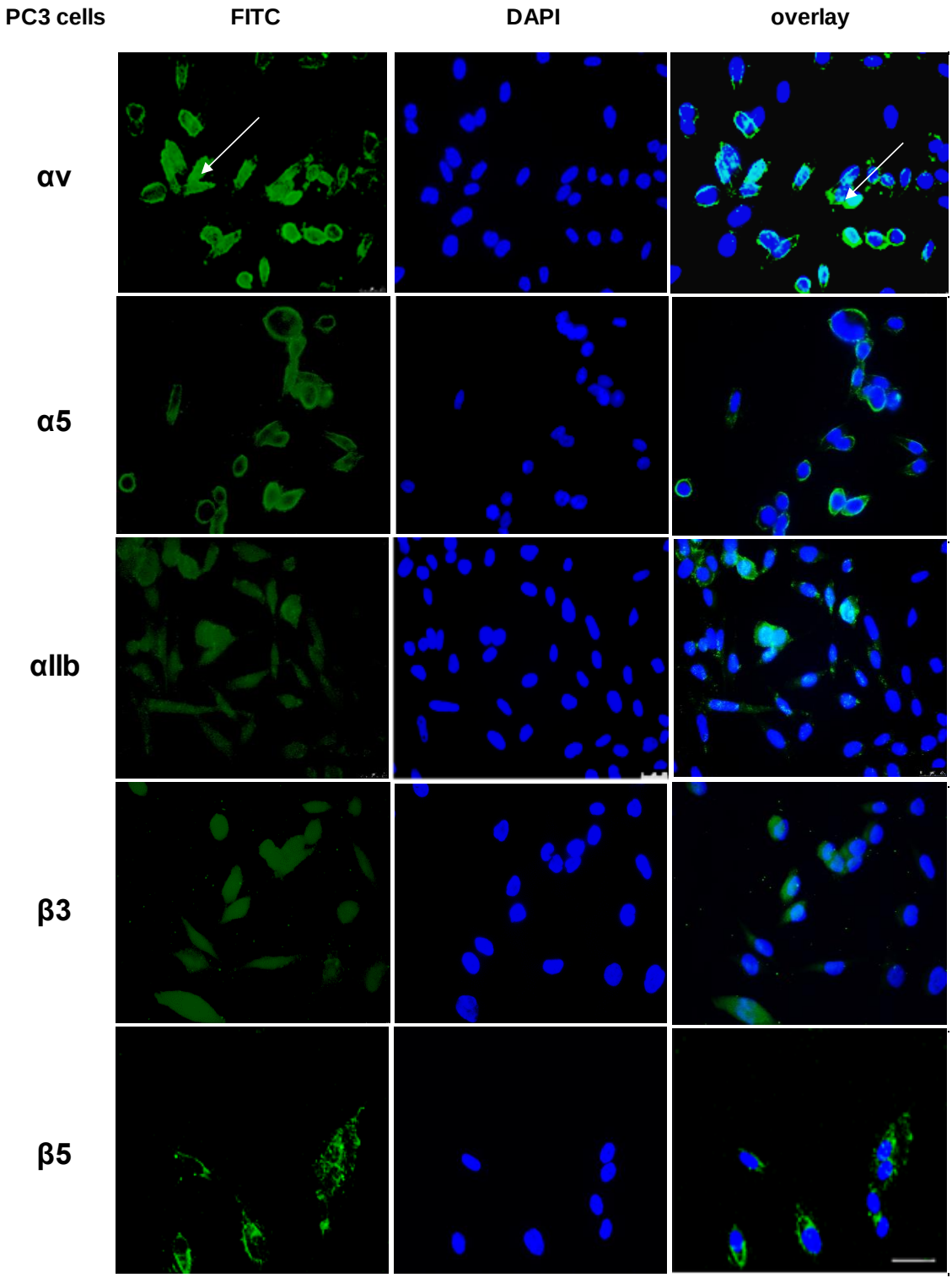

Figure 13 : Expression of αv, α5, αIIb, β3 and β5 integrin subunits in PC-3 cells. Integrins were detected using immunofluorescence with Q20 anti-αv, C9 anti-α5, EPR4330 anti-αIIb, B7 anti-β3, and ab15459 anti-β5 integrin antibodies. Bar Length = 50 μm. Blue-fluorescent DAPI is nuclear staining, and green colour represents integrin expression detected by a fluorophore.

White arrows point to the positive labelling of αv, α5, αIIb, β3 and β5 integrin subunits in PC-3 cells.

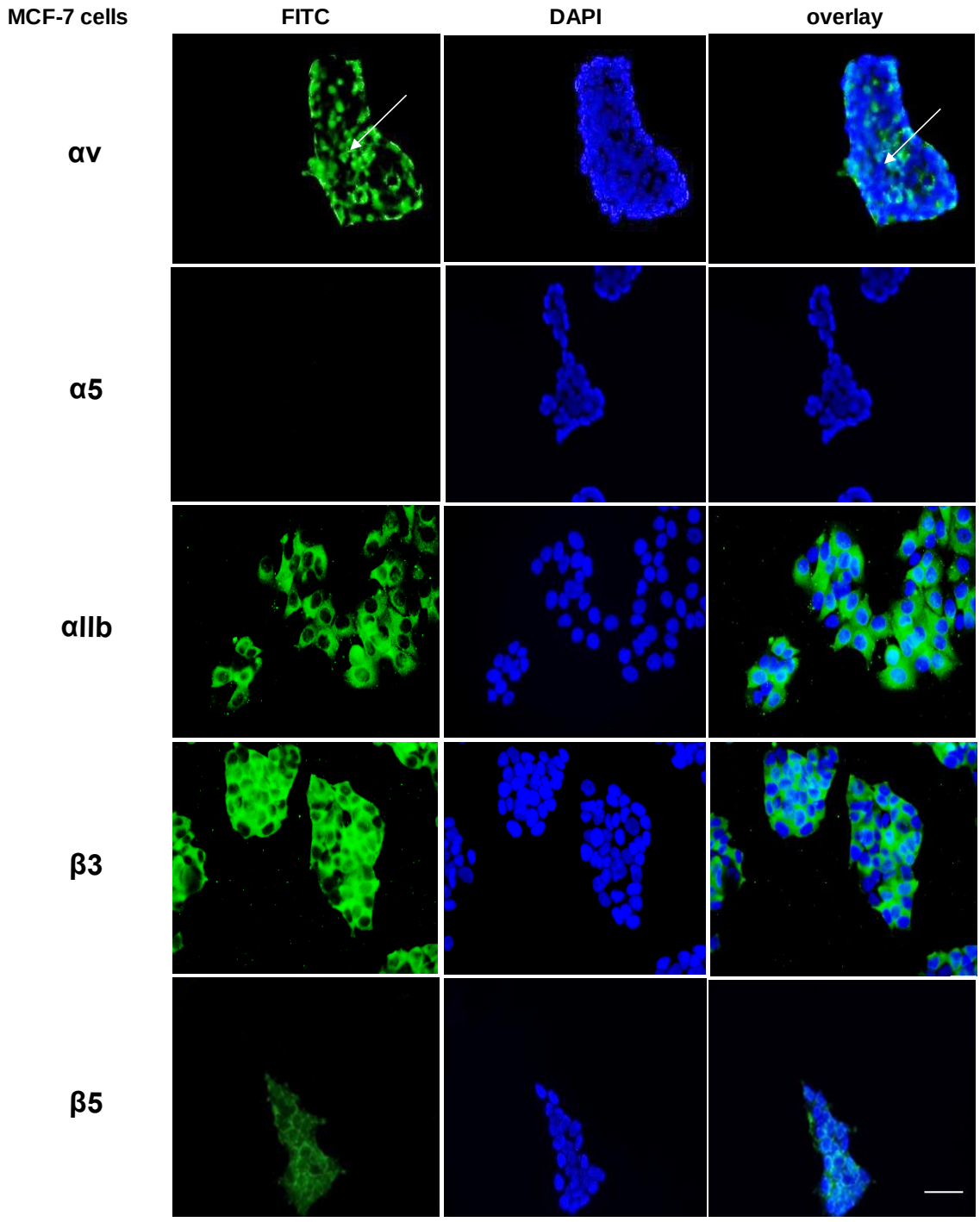

Figure 14: Expression of αv, α5, αIIb, β3 and β5 integrin subunits in MCF-7 cells. Integrins were detected using immunofluorescence with Q20 anti-αv, C9 anti-α5, EPR4330 anti-αIIb, B7 anti-β3, and ab15459 anti-β5 integrin antibodies. Bar Length = 50 μm. Blue-fluorescent DAPI is nuclear staining, and green colour represents integrins expression detected by a fluorophore.

White arrows point to the positive labelling of αv, α5, αIIb, β3 and β5 integrin subunits in MCF-7 cells.

2.4.2.2 Use of Adhirons to detect αvβ5 integrin in MCF-7

Adhirons A8 and C3 are novel reagents, artificical binding proteins (ABPs) developed to bind to αvβ5 by Dr. Darren Tomlinson. Their performance was compared to the commercially available antibodies used to detect αvβ5 expression on MCF-7 cells using the protocol detailed in Table 3. High membrane and cytoplasm expression of αvβ5 were observed with Adhiron A8 and Adhiron C3, whereas high membrane expression of αv and moderate membrane and cytoplasm expression of β5 were observed uisng antibodies. These data showed similar performance between adhirons and antibodies (Figure 15) suggesting the adhirons have similar sensitivity and specificity.

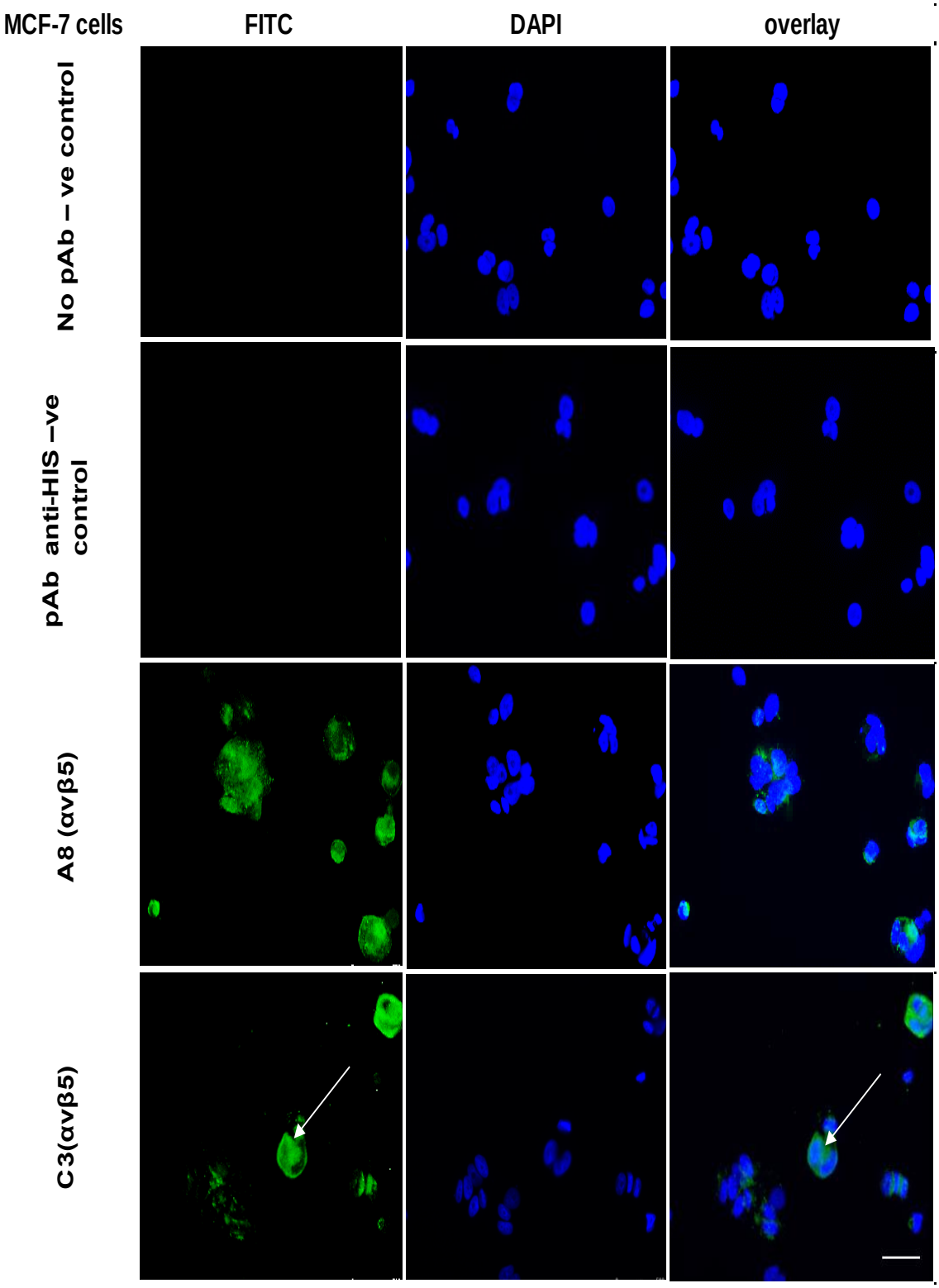

Figure 15 : Expression of αvβ5 integrin in MCF-7 cells.

αvβ5 was detected using immunofluorescence with adhiron A8 and C3 (anti αvβ5). Bar Length = 50 µm. Blue-fluorescent DAPI is nuclear staining, and green colour represents integrin expression detected by a fluorophore. White arrows point to the positive labelling of αvβ5 integrin in MCF-7 cells.

2.4.2.3 Expression of αIIb and β3 in HT-29, M14, MeWo and UACC-62

The melanoma cell lines, MEWO, M14 and UACC-62 were selected as known models of melanoma expressing β3 (Hieken et al., 1996), and HT-29 as a non-β3 expressing line. They were investigated for the expression of αIIb and β3 integrin subunits according to the optimised protocols (Table 3).

The αIIb integrin subunit screening results showed that the majority of these cell lines did not express the αIIb integrin subunit on cell membranes or cytoplasmically. The exception was UACC-62 cells, where moderate membrane expression of αIIb was detected. Whereas high expression of β3 integrin subunit was detected in the membrane of UACC-62 cells and the cytoplasm of M14 cells but no expression was detected in HT-29 and MEWO cells as shown in Figures 16 and 17.

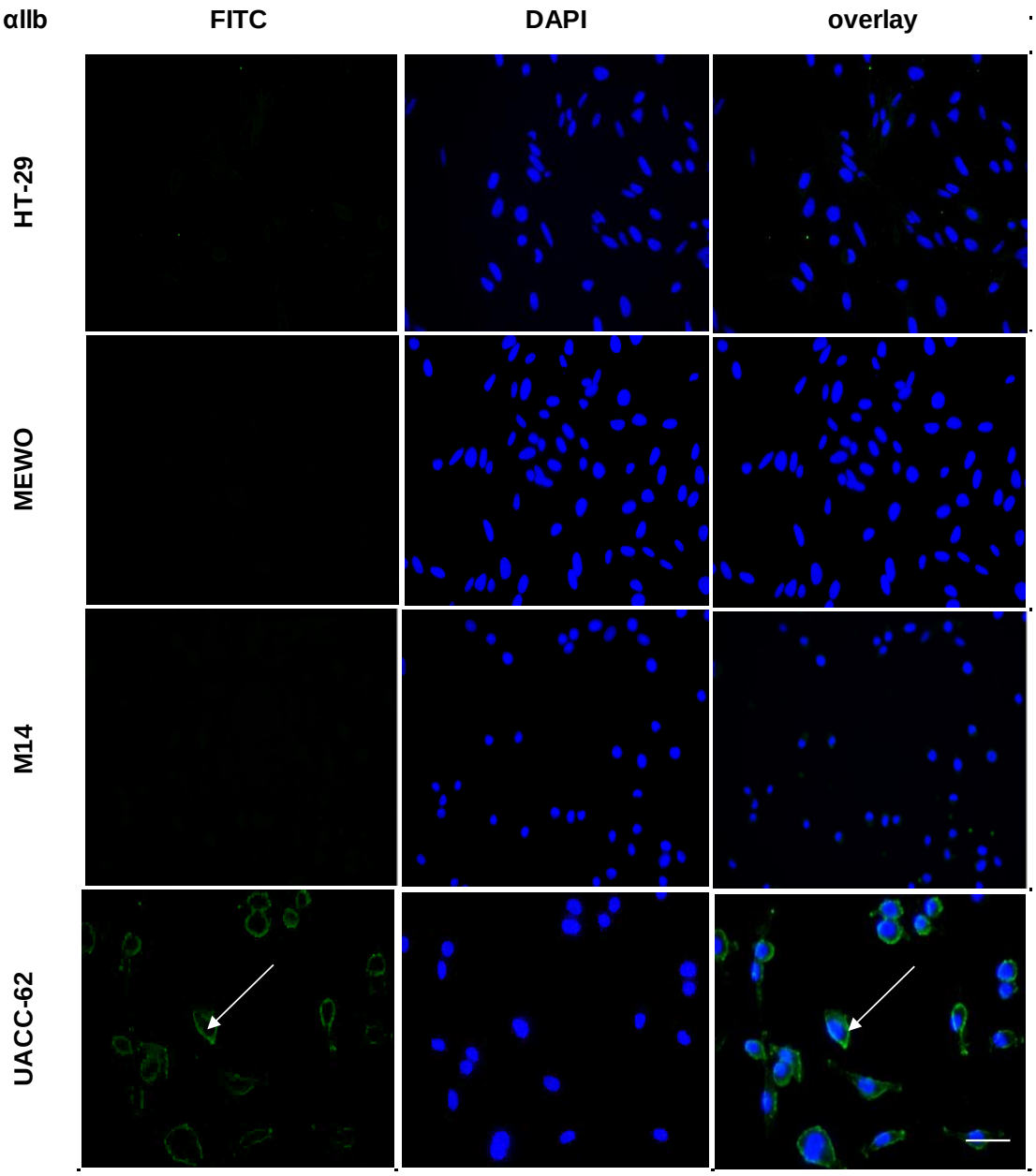

Figure 16: Expression of the αIIb integrin subunit in HT-29, MEWO, M14 and UACC-62 cells. αIIb was detected using immunofluorescence with EPR4330 anti-αIIb integrin antibody. Bar Length = 50μm. Blue-fluorescent DAPI is nuclear staining, and green colour represents integrin expression detected by a fluorophore. White arrows point to the positive labelling of αIIb integrin subunits in the selected cell lines.

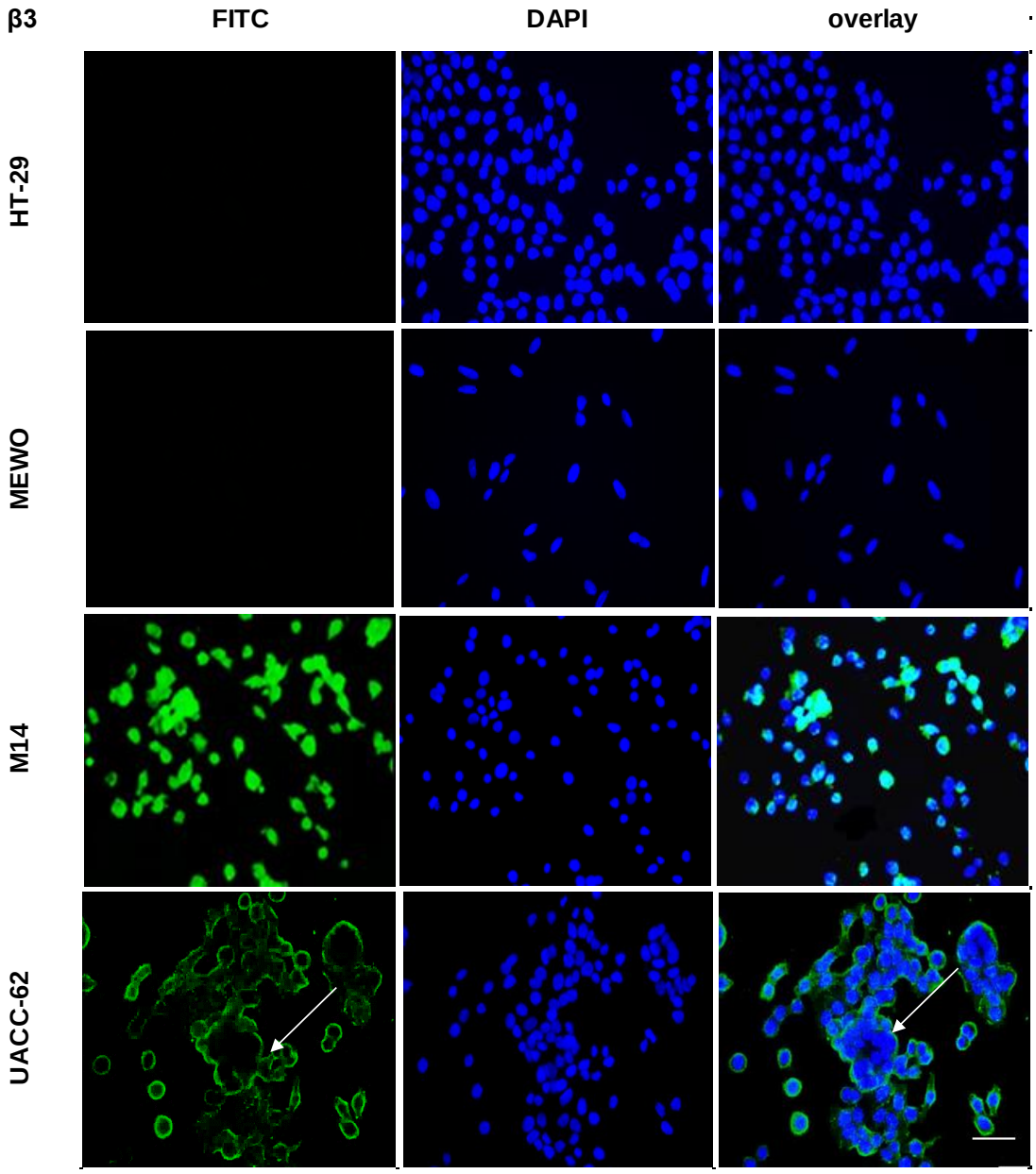

Figure 17: Expression of the β3 integrin subunit in HT-29, MEWO, M14 and UACC-62 cells. β3 was detected using immunofluorescence with B7 anti-β3 integrin antibody. Bar Length = 50μm. Blue-fluorescent DAPI is nuclear staining, and green colour represents integrin expression detected by a fluorophore. White arrows point to the positive labelling of integrin subunits in the selected cell cells.

2.4.3 Quantification of the expression of αv, α5, αIIb, β3 and β5 integrin subunits

2.4.3.1 Quantification of αv, α5, αIIb, β3 and β5 in K562, DU145, PC-3, LNCap and MCF-7 cells using FACS

The cell lines were harvested and incubated with anti αv, αIIb, α5, β3 and β5 antibodies and their expression determined by FACS analysis of mean fluorescence intensity (Figure 18). For histograms, see Appendix III. Very high levels of αv expression were observed in all cells lines, whereas moderate αIIb expression was observed on MCF-7 cells; low levels on PC-3 cells, weak staining on K562 cells and DU145 cells and no expression on LNCap cells. High levels of α5 expression were seen in K562 cells, moderate on LNCap cells and low levels on DU145 cells and PC-3 cells, and no expression on MCF-7 cells. High levels of β3 were observed in K562 and MCF-7 cells, moderate levels on DU145 and low levels were observed in LNCap and PC3 cells. The expression of β5 was cells moderate in all cell lines except PC3, which expressed a low level.

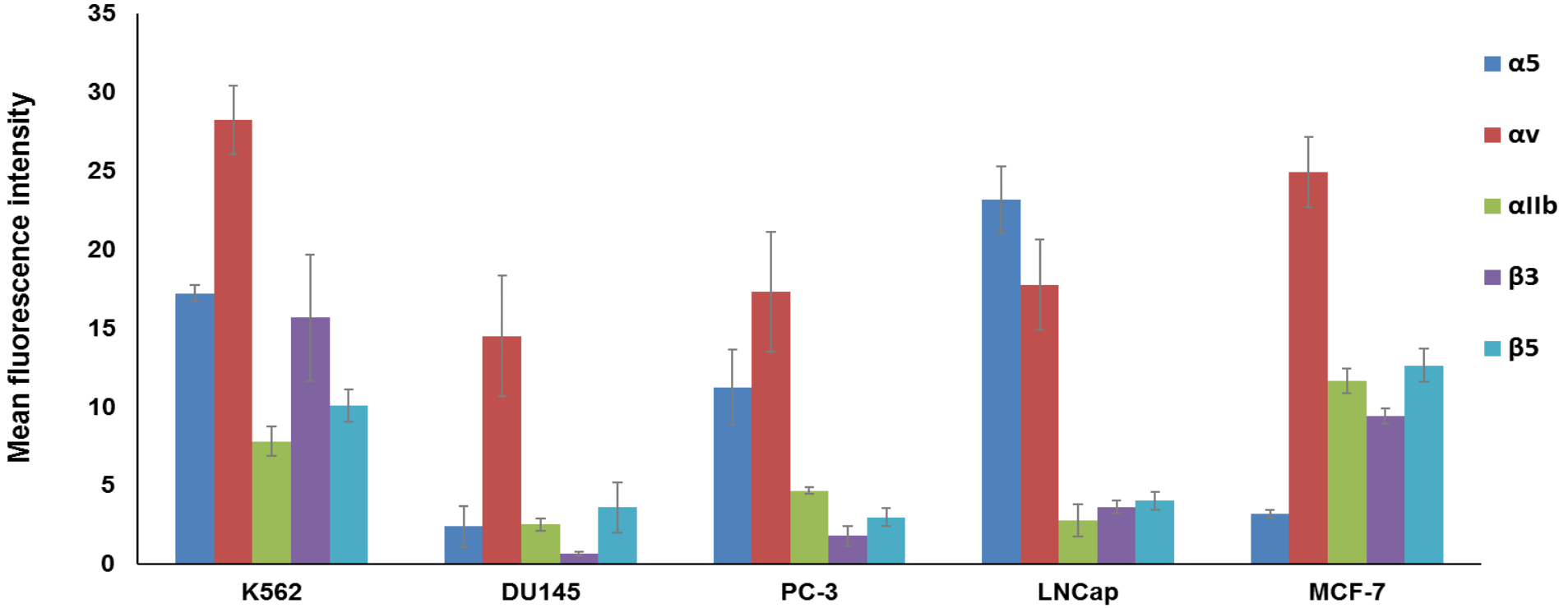

Figure 18: Expression of αv, α5, αIIb, β3 and β5 integrin subunits in K562, DU145, PC-3, LNcap and MCF-7 cells. The mean fluorescence intensity of αv, α5, αIIb, β3 and β5 subunits. Values are the average of 3 independent experiments and error bars are SE.

2.4.3.2 Quantification of αIIb and β3 integrin subunits in M14, MeWo, UACC-62 and HT-29 cells using FACS

The cell lines were harvested and incubated with anti αIIb and β3 antibodies and their expression determined by FACS analysis of mean fluorescence intensity (Figure 19). For histograms, see Appendix IV. No expression of αIIb and β3 was detected in any of these cell lines except M14 had low expression of β3.

The comparison of αIIb and β3 integrin expression in all cell lines tested using the two detection techniques is shown in Table 4.

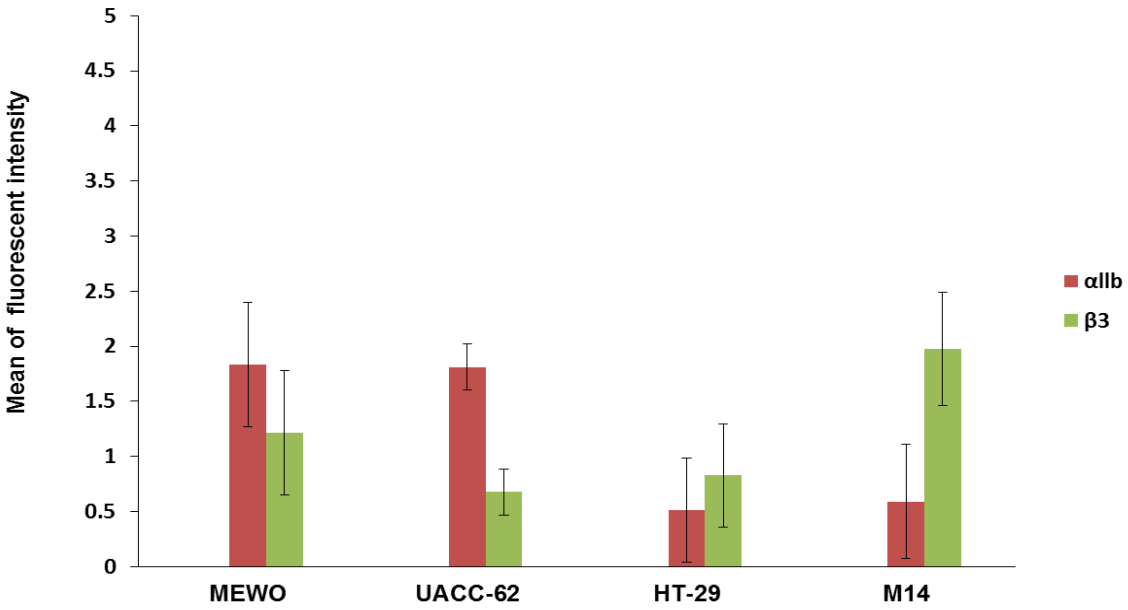

Figure 19: Expression of αIIb and β3 integrin subunits in M14, MeWo, UACC-62 and HT-29 cells using FACS analysis. The mean fluorescence intensity of αIIb and β3 integrin subunits. Values are the average of 3 independent experiments and error bars are SE.

Table 4: Comparison of integrin expression in different tumour cell lines with specific antibodies for αIIb and β3 integrin subunits using IF and FACS. Keys for IF and FACS -: no expression. ±: Weak expression, +: Low expression, ++: Moderate expression, +++: High expression.

Types of cells	Human cancer cell lines	αIIb		β3	
		IF	FACS	IF	FACS
Leukaemia	K562	-	±	+++	+++
Prostate cancer	DU145	+++	+	++	++
	PC3	+++	+	++	+
	LNCap	-	-	+	+
Colon cancer	HT-29	-	-	-	-
Melanoma	MEWO	-	-	+	-
	M14	-	-	++	+
	UACC-62	+	-	++	-
Breast cancer	MCF-7	+++	++	+++	+++

2.4.4 Expression of αIIb and β3 integrin subunits in spheroids

2.4.4.1 Spheroid generation.

Since integrin expression was seen for MCF-7 and K562 cells by IF and FACS, both was selected as 3D models for use in *vitro* under conditions more similar to those *in vivo*. 10^4 cells/100 µl of MCF-7 and K562 cells was used to optimise spheroid formation to obtain regular and large (>500 µm) diameter of spheroids (Figure 20 B). Spheroid growth was monitored every day and the optimal parameters were determined to control their morphology. MCF-7 cells formed a compact spherical shape which grew over time, but K562 cells were not a

successful model for spheroids due to increasing in their size without coherent compacting together (Figure 20 A).

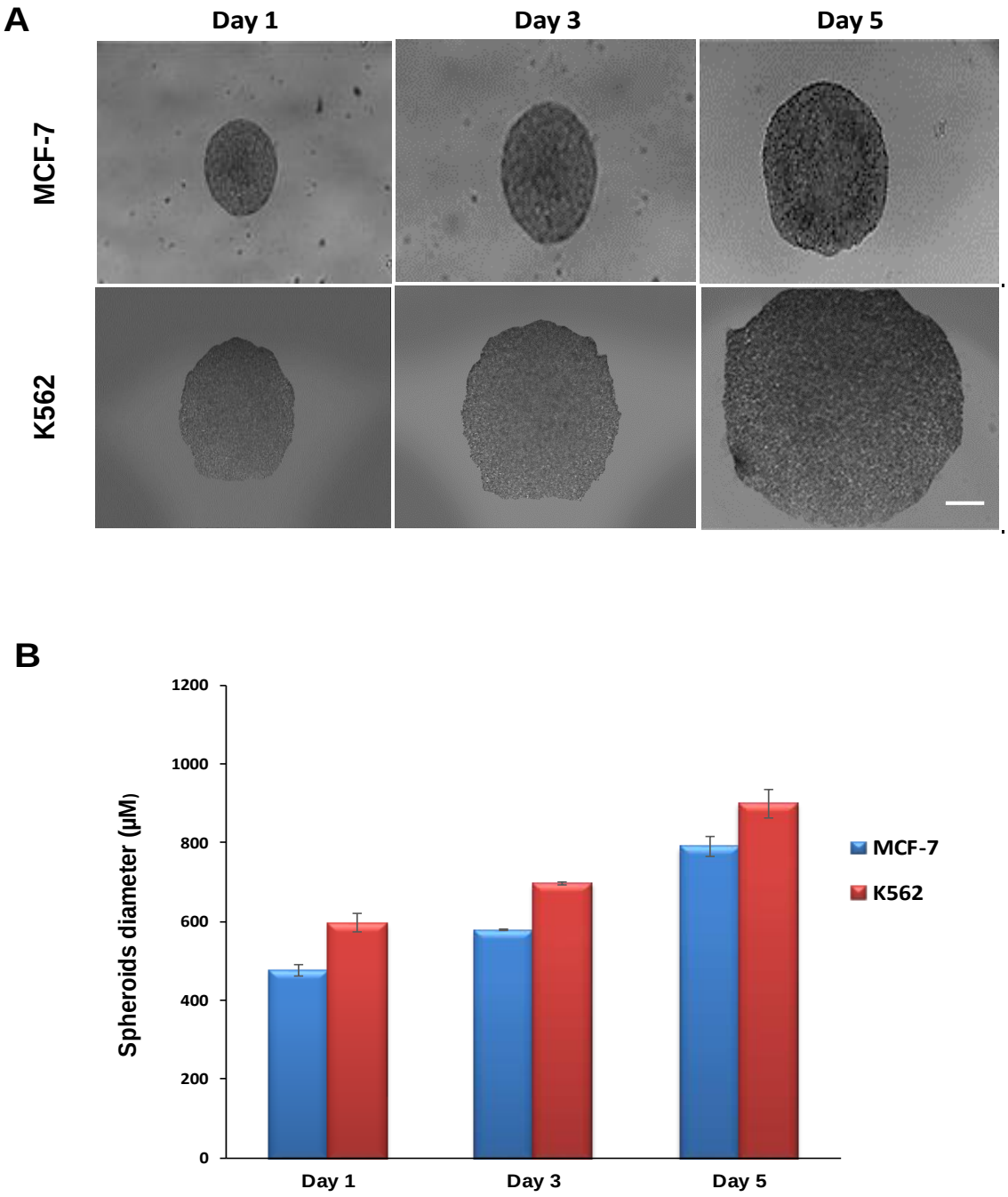

Figure 20: Formation of spheroids in 96 well plates. (A) Transmission microscope images of MCF-7 and K562 spheroids. Scale bar = 100 µm at 20X objective lens. (B) Effect of time of incubation on spheroid diameter. Values are the average of 3 independent experiments and error bars are SE.

2.4.4.2 Spheroid histology

Haematoxylin and Eosin (H&E) staining was carried out on MCF-7 spheroid sections at day 3. Microscopic examination revealed the spheroid to be clearly differentiated with the presence of mitotic nuclear and cytoplasmic regions and absence of necrotic or hypoxic regions (Figure 21).

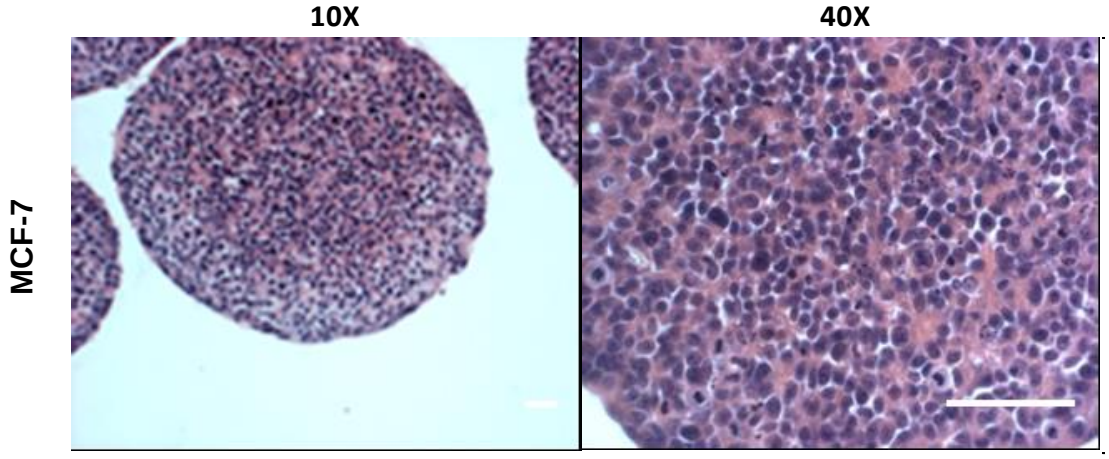

Figure 21: Histology of MCF-7 cell spheroids. Spheroids were processed and stained with H&E staining at day 3. Scale bar = 25 µm and 100 µm at 10X and 40X objective lens respectively.

2.4.4.3 Immuno-detection of αIIb and β3 integrin subunits in spheroids.

Expression of αIIb and β3 integrin subunits in MCF-7 spheroids was assessed using IHC staining as previously described in Materials and Methods, section 2.3.3.7.3.4.

Moderate expression of αIIb and high expression of β3 were observed in MCF-7 spheroids (Figure 22), the level of β3 was consistent with that observed for monolayer (2D) cultures (Figure 14 and 18). But the level of αIIb expression was changed from high to moderate level in 3 dimensional.

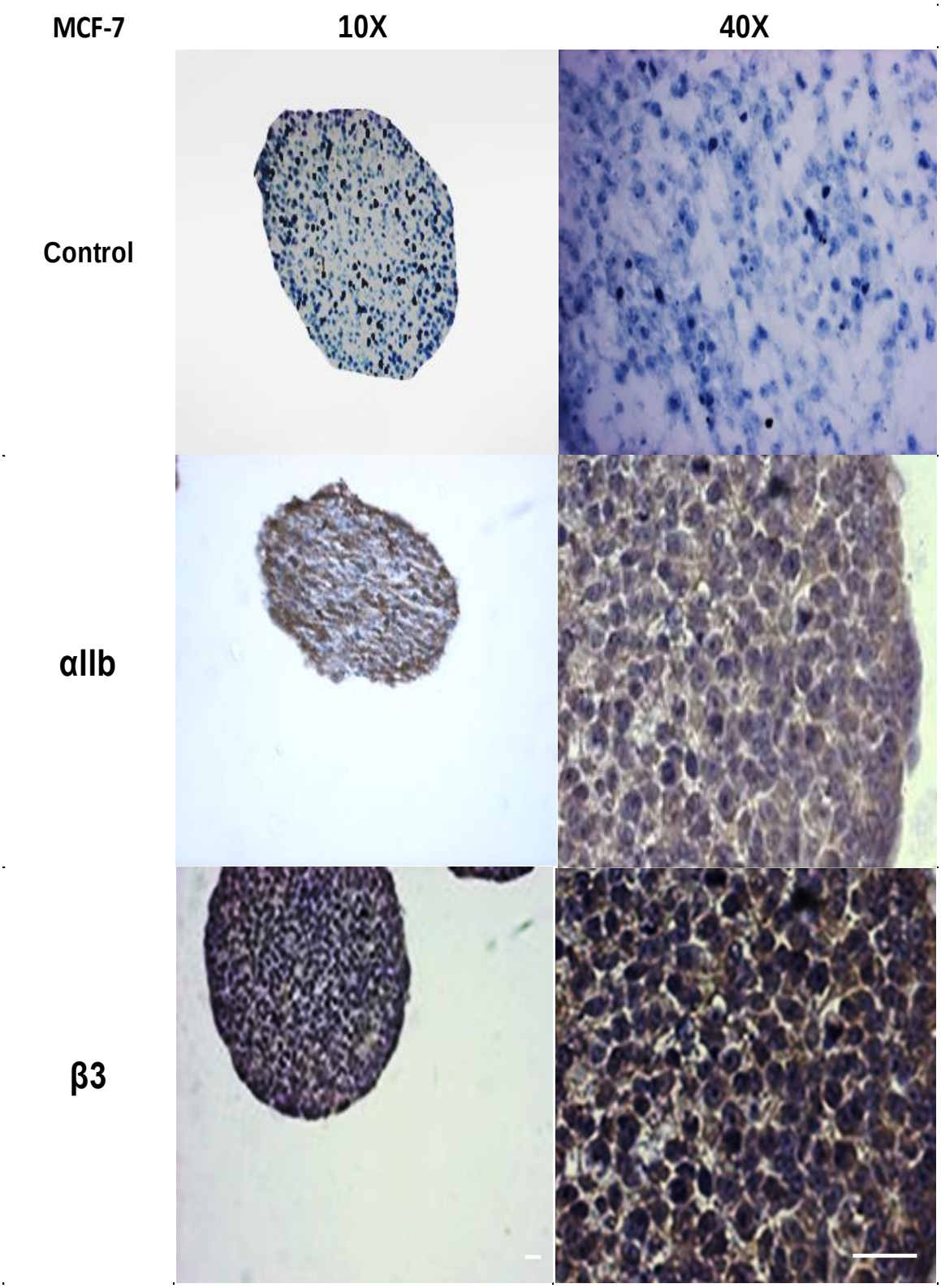

Figure 22: Expression of αIIb and β3 integrin subunits in MCF-7 spheroids. Subunits were detected using IHC with EPR4330 anti-αIIb and B7 anti-β3. Brown colour indicates positive staining (αIIb and β3 expression). Scale bar = 25 µm and 100 µm at 10X and 40X objective lens respectively.

2.5 Discussion

Integrins as heterodimeric receptors are vital molecules which function in cell adhesion, growth and migration because of serving as cell-cell adhesion receptors which bind to other cells and respond to the ECM. As described previously in chapter 1, the expression and function of integrins are involved in cancer progression, angiogenesis and metastasis. Consequently, there are many extensive research studies about integrin expression in *in vitro* and *in vivo* (Goodman and Picard, 2012; Stachurska et al., 2012).

The aim of this chapter was to characterise the expression of integrins in a panel of human cancer cell lines, in order to determine which could be utilised as models for screening novel integrin antagonists. Growth curves of cancer several cell types were measured to determine the log phase (exponential growth), where cells are dividing rapidly.

Immunofluorescence and flow cytometry showed the expression of αv, αIIb, α5, β3 and β5 integrin subunits in the panel of cancer cell lines, was either in the cytoplasm or on the cell membrane. The selectivity and specificity of the primary antibodies for integrin subunit detection had previously been determined in-house using Western blotting (Ahmedah, 2015).

Zheng et al. have demonstrated the absence of the expression of αvβ3 and αIIbβ3 integrin in normal prostate cells. For instance, human prostate adenocarcinoma tissue expressed the β3 subunit, whereas normal human prostate tissue did not (Zheng et al., 1999).

Previous studies have also revealed the expression of αv and β3 integrin subunits as well as αvβ3 integrin in the MCF-7 breast tumour cell line (Beauvais et al., 2004).

The expression of αv and β3 integrin subunits on DU145 and PC-3 cells has been detected, although it was not confirmed on LNCap cells (Cooper et al., 2002; Witkowski et al., 1993). Although the expression of these subunits has been detected in LNCap cells (Cooper et al., 2002), Zheng et al. found that αv and β3 integrin subunits were not expressed in LNCap (Zheng et al., 2000). Another study has also demonstrated low αvβ3 expression in PC-3 compared to LNCaP (Chatterjee et al., 2001).

In the present study, the results of immunofluorescence show that the prostate cancer cells DU145, PC-3 and LNCap express a relatively high level of αv integrin subunit but only moderate expression of β3 was detected on DU145 and PC-3 cells, and low expression was detected on LNCap cells. These results were generally consistent with previous studies which found moderate expression of αv in PC3 cells by flow cytometry (Goodman and Picard, 2012; Zheng et al., 2000).

LNCap cells expressed a moderate level of α5 and β5; no expression of αIIb was detected. In DU145 cells, high expression of αIIb and β5 were detected and moderate expression of α5 was detected. In PC-3 cells, high expression of αIIb was detected and moderate expression of α5 and β5 was detected. In previous studies, the intracellular expression of αIIbβ3 has been detected in PC-3 cells whereas it is localised to the cell membrane in DU-145 as measured by immunofluorescence (Trikha et al., 1998). The expression of β5 in DU145 and PC3 cells found by Trikha et al., 1998 is contrary to that of Bauer et al. who

found very low expression of β5 in DU145 and PC3 (Bauer et al., 2007). These conflicting data might be a result of the types of antibodies utilised in each of the research studies and cell lines being derived from various laboratories.

In MCF-7 cells, high membrane expression of αv, αIIb and β3 was detected, moderate expression of β5 was detected, and no expression of α5 was detected. These data match those observed in earlier studies (Meyer et al., 1998; Taherian et al., 2011).

A high level of αIIb was detected in MCF-7 cells by the EPR4330 antibody, in contrast with other in-house results using the C20 antibody (Alshammari, 2013). The EPR4330 antibody is a rabbit monoclonal CD41 antibody, but the C20 is goat polyclonal IgG antibody, the homogeneity of monoclonal antibodies is very high relative to polyclonal.

Adhirons are new artificial binding protein scaffolds depend on a designed consensus phytocystatin protein. Adhirons are well expressed and highly stable permitting highly specific binding reagents to be developed for molecular recognition applications (Tiede et al., 2014). Adhirons are proposed as an alternative to antibodies, and are one of a number of non-antibody binding reagents which have been developed, usually through adaptation of a naturally occurring protein or protein domain (Bedford et al., 2017).

Adhirons A8 and C3 were compared in performance to anti-αvβ5 antibodies in MCF-7 cells. High expression of αvβ5 was shown with both A8 and C3 adhirons; Q20 anti-αv antibody showed high expression, and ab15459 anti-β5 antibody gave moderate expression. Similar staining patterns were obtained with both the anti-αv and β5 antibody and adhiron A8 and C3. This indicates that these adhirons are effective for detecting αvβ5, providing a good

fluorescent signal. The selectivity appears comparable at this stage, but further studies will be required in αvβ5-negative cells to confirm the adhirons do not recognise any unexpected targets.

M14, MeWo, UACC-62 and HT-29 cells were further screened using immunofluorescence anti αIIb EPR4330, anti β3 B7 antibodies. There was no detectable expression of αIIb on these cells except the low level of expression, in UACC-62 cells whereas high expression of β3 was observed in M14 and UACC-62 but no expression in other cell types. These data agree with Li et al.(2001) who found that high level of β3 integrin subunits was expressed in melanoma human tumour cell lines (M14 and UACC-62), and confirms previous results in the group, as well as the observation in clinical tissues that overexpression of β3 is a hallmark of melanoma.

Using immunofluorescence, the expression gives only the localisation of antibodies as there is a component of intensity. Therefore, the flow cytometry was used to evaluate the sensitivity of the antibodies as well as quantify the level of integrin expression. FACS analysis may be more sensitive than immunofluorescence for detecting very low levels of protein (Jenson et al., 1998).

Flow cytometry data generally confirmed the results of immunofluorescence in the panel of cancer cells, except for the expression of αIIb and β3 in UACC-62 cells, which was positive by IF but negative by FACS. The expression of αv, αIIb and β3 subunits was fluorescence shifted more than control in MCF-7, in contrast with other in-house results for expressing of αIIb and β3 subunits, where weak expression of β3 and no expression of αIIb were observed

(Alshammari, 2013). This suggests that integrin expression is dependent on the batch of cells used as well as the identity of the cell line.

Stachurska et al.(2012) suggested that there are many reasons for differing in integrin expression found in different studies researchers, including different specificity of the antibody, methods of integrin detection, heterogeneity of cell subpopulations and different cell culture conditions. In this current work, different specificity of the antibody and FACS were used whereas western blot was used in other in-house work.

A high level of αv was expressed in all tested cell lines, which was to be expected; as mentioned in the literature review; αv can associate with not only β3 but also β1, β5, β6, and β8. This result is consistent with data obtained in earlier studies (Goodman et al., 2012; Trikha et al., 2002a).

MCF-7 was identified as a suitable αv, αIIb and β3 integrin-expressing cell line by flow cytometry and immunofluorescence. This result is in agreement with the finding of other studies which showed that MCF-7 cells express αvβ3 and αIIbβ3 integrins using both flow cytometry and immunofluorescence (Kononczuk et al., 2015; Oleksowicz et al., 1995).

The expression of αIIb and β3 integrin subunits was determined in MCF-7 3D model. Spheroids are used as they are a surrogate for the tumour environment, allowing cells to interact in 3 dimensions (Li et al., 2008). According to previous studies, spheroids also show zones reminiscent of tumours and proliferation gradients. Thus, expression of proteins in multicellular tumour spheroids is more similar to expression profiles *in vivo* than those in 2D cell culture (Friedrich et al., 2009; Katt et al., 2016), which confers a high degree of biological and clinical relevance on them (Fennema et al., 2013). Hauptmann et al. also found

that the expression of integrins in tumour cells depends on the system of culture and its expression in spheroids is much closer to the situation in nude mouse tumours (Hauptmann et al., 1995). The contrast of protein expression levels between cell lines, comprising breast cancer, and their tissue origins showed that almost 30% of proteins are differently expressed in *in vitro* cell lines. 3D cultures differ in cellular responses due to both the 3D organisation of the cell surface receptors involved in interactions with surrounding cells, but it also encouraged physical constraints to cells (Edmondson et al., 2014). K562 cells were not suitable for use in model of spheroids because of the inability of cells to compact together. Usually, in 2D, K562 cells grow fast and tend to aggregate when reaching a high density without compacting. A high level of β3 membrane expression was observed in 2D and 3D MCF-7 models but αIIb was moderately expressed in 3D compared to 2D. This may suggest αIIb is less important in cancer cell-cancer cell interactions than it is with soluble proteins found in cell culture medium. It is also noteworthy that these spheroids did not contain necrotic or hypoxic regions because spheroid formation at day three was chosen to confirm the integrin expression in MCF-7, not to investigate changes in integrin expression as part of tumour progress in 3D.

In this part of the study, MCF-7 cells were chosen as a useful native dual β3-expressing model to investigate novel dual αvβ3 and αIIbβ3 antagonists in the functional assays. In the next chapter, the effect of PMA treatment on integrin expression in K562 will be described to develop an inducible model as a known αIIb-expressing model.

Chapter 3: Investigation of K562 cells as a potential dual αIIbβ3/αvβ3-expressing functional model

3.1 Introduction

In normal human tissues, the expression of αIIbβ3 is mainly on platelets but it is also expressed in some types of tumours including melanoma and prostate. αIIbβ3 is considered an essential part of the metastatic process (Hynes, 2002a; Jin et al., 2011; Trikha et al., 1998). For example, some prostate cancer cells express αIIbβ3 integrin, which is involved in the invasion of tumours (Gay and Felding-Habermann, 2011; Hynes, 2002). αIIbβ3 integrin makes an interaction between platelets and cancer cells, leading to metastasis and making it a promising cancer target (Bakewell et al., 2003).

Additionally, αvβ3 is involved in the migration of endothelial cells which results in angiogenesis. αvβ3 also contributes to the tumorigenesis of several cancer types (Borsig et al., 2002; Liu et al., 2009). For example, no expression of β3 integrin was found in normal breast tissue compared to breast carcinoma tissue (Havaki et al., 2007).

Phorbol 12-myristate 13-acetate (PMA) is a Protein Kinase C activator that participates in the regulation of megakaryocyte differentiation and activates the downstream mitogen-activated protein kinase (MEK/MAPK) pathway. PMA treatment of K562 cells upregulates proto-oncogene transcription factors notably jun/Fos. The change in cell adhesion ability is correlated to integrin expression and cytoskeleton changes (Huang et al., 2014). PMA has been extensively utilised in studying megakaryocyte biology. PMA is a potent activator of immediate early response genes and enhances megakaryocytic phenotype in leukemic cell lines including K562. PMA promotes early growth response protein 1 (EGR-1) expression in K562 and HEL cells, and this is

related to upregulation of megakaryocyte specific αIIb (Cheng et al., 1994; Jalagadugula et al., 2008). Phorbol esters are known to enhance transcription of the C-sis gene which results in expression of αIIb in K562 cells (Zanyk et al., 1988). Phorbol esters induce expression of integrins in K562 cells including αv and β3, but αIIb was not detected (Jarvinen et al., 1993). Other studies showed that PMA induced several integrins in leukaemia cell lines and also enhanced the secretion of thrombospondin, which may be utilised as a binding ligand for αvβ3 integrin (Ylanne et al., 1990).

3.2 Aims and objectives

The main aim of the work described in this chapter was to evaluate αIIb integrin subunit expression in K562 cells treated with PMA (Phorbol 12-myristate 13-acetate), a putative inducer of integrin expression. The obtained results were valuable in order to develop a functional assay model for testing the effect of dual β3 antagonism in cancer, and screening novel dual integrin antagonists.

The aim was addressed by the following experiments

- Investigate by immunofluorescence and flow cytometry, the effect of PMA on the expression of the αIIb and αv integrin subunits in K562 and DU145 cells.
- Determine, using flow cytometry, the optimal concentration of PMA for increasing the expression of αIIb subunit in K562 cells.
- Evaluate the effect of the selected concentration of PMA on the expression of αIIb integrin subunit in K562 cells by Western blot.
- Investigate, using the MTT assay, the effect of PMA on K562 cell survival.

3.3 Materials and methods

3.3.1 Materials

Human tumour cell lines K562 and DU145 were maintained as described in section 2.2.2.1. All reagents if not specified, were obtained from Sigma-Aldrich (Poole, UK). Primary antibodies and secondary antibodies used in immunofluorescence and flow cytometry are as listed in Chapter 2, Table 2. Primary antibodies and secondary antibodies used in Western blotting are summarised in Table 5

Table 5: Primary antibodies and related secondary antibodies used in Western blot experiments

Primary antibody	Company	Secondary antibodies	
Anti-β3 (B-7), monoclonal mouse antibody	Santa Cruz Biotechnology	Polyclonal rabbit anti mouse immunoglobulins horseradish peroxidase (P0260, Dako Cytomation Glostrup, Denmark)	Western dot 625 fluorescence based anti-mouse secondary antibody (Life technologies)
Anti-αv (Q-20), polyclonal rabbit antibody	Santa Cruz Biotechnology	Polyclonal goat anti-rabbit immunoglobulins horseradish peroxidase (P0260, Dako Cytomation, Glostrup, Denmark)	Western dot 625 fluorescence based anti-rabbit secondary antibody (Life technologies)
Anti-αIIb (Anti-CD41 antibody [EPR4330]), monoclonal rabbit antibod	Abcam (Cambridge, UK)	Polyclonal goat anti-rabbit immunoglobulins horseradish peroxidase	Western dot 625 fluorescence based anti-rabbit secondary antibody (Life technologies)
Anti–β actin (A1978), Monoclonal mouse antibody	Sigma-Aldrich, Poole UK	Polyclonal rabbit anti -mouse, immunoglobulins horseradish peroxidase	Western dot 625 fluorescence based anti-mouse secondary antibody (Life technologies)

3.3.2 Methods

3.3.2.1 Induction of αIIb integrin subunit in K562 cells by PMA using Immunocytochemistry

K562 cells were treated with 0.04, 0.08 or 0.1 μM of PMA for 24, 48, or 72 hours. After incubation, the expression of αIIb integrin subunit was detected as described in Section 2.3.3.5.

3.3.2.2 Induction of integrin subunits in K562 and DU145 cells by PMA.

K562 cells were treated with 0.1 μM of PMA and DU-145 cells with 0.5 μM of PMA for 24 hours. After incubation, the expression of α5, αv, β3, and β5 integrin subunits was detected using primary antibodies as previously described in sections 2.3.3.5.1 and Table 2 (Chapter 2).

3.3.2.3 Flow cytometry

3.3.2.3.1 Optimization of induction of αv and αIIb integrin subunits expression in K562 and DU145 cells by PMA.

After determining the concentration of cells, $5X10^5$ cells/ml of cell suspension was added to each well of 6-well plates at various concentrations of PMA (0.5 μM, 1 μM, or 2 μM) for incubation of durations 24, 48 or 72 h respectively. After incubation, the methods as described in section 2.4.4.1.1 were used to detect αv and αIIb integrin subunits, and following incubation, cellular expression of α5, β3, and β5 integrin subunits was measured. Unlabelled (without primary antibody) treated and untreated cells were used as controls. See section 2.3.3.6.1 for experimental details.

3.3.2.4 The effect of PMA on cell viability

The cells were stimulated with different concentrations of PMA (0.1 μM, 0.5 μM, 1 μM or 2 μM), for 2, 24, and 96 h at 37 ºC. After incubation, cells were washed with PBS and centrifuged at 1000 rpm for 5 minutes. After each incubation times, cells were washed with PBS and fresh media added and then incubated for 96 hours. Cell survival was measured by the MTT assay (section 2.3.3.4 in chapter 2).

3.3.2.5 Western Blotting

Western Blotting of the αIIb integrin subunit was performed on whole cell lysates of ±PMA treated K562 cell line as described below.

3.3.2.5.1 Cell Lysis

Cells were collected from incubation flasks after stimulation with PMA (0.04 uM) for 40 hours then washed with PBS by centrifugation (1000 x g). Complete RIPA lysis buffer (300 μl); [100 mM Tris pH 8.8, 5 mM EDTA, 300 mM NaCl, 2% Triton X-100] and protease inhibitor mix (PI, Complete mini EDTA-free, Roche, Mannheim, Germany) and water (50 μl/ml of PI added in RIPA) were added for 30 min on ice, after which sonication (Philip Harries Scientific Sonicator, Scientific Laboratory) was applied for 5 cycles of four seconds and speedial on 10% with cooling on ice between each sample to avoid overheating. Sonicated cells were centrifuged at 13,000 rpm for 15 min at 4 ºC. The supernatant of the lysed cells was collected into new Eppendorf tubes and stored at -20 °C until analysed.

3.3.2.5.2 Bradford assay

Protein concentrations in cell lysates were measured using the Bradford Assay (Coomassie Brilliant Blue). Bovine serum albumin (BSA) was used to calibrate the assay by preparing six serial dilutions of protein (2 mg/ml of BSA dissolved in HPLC water) from 0.0625 - 1.0 mg/ml. 50 µl from each BSA dilution was added to 1.5 ml of Bradford reagent. All tubes were vortexed and left to stand at room temperature for 15 minutes to allow the Coomassie Brilliant Blue dye to react with the protein. Dilutions of cell lysates were prepared in HPLC grade water (2.5 µl of lysate added to 47.5 µl of water) and mixed with 1.5 ml of Bradford reagent. 1 ml from each BSA dilution and lysate were vortexed and transferred to plastic cuvettes. Absorbance readings were measured at 595 nm using a spectrophotometer (Thermo Scientific Multiskan Spectrum, 1500, Thermo Fisher Scientific, Finland) and a standard curve was plotted (Figure 23).

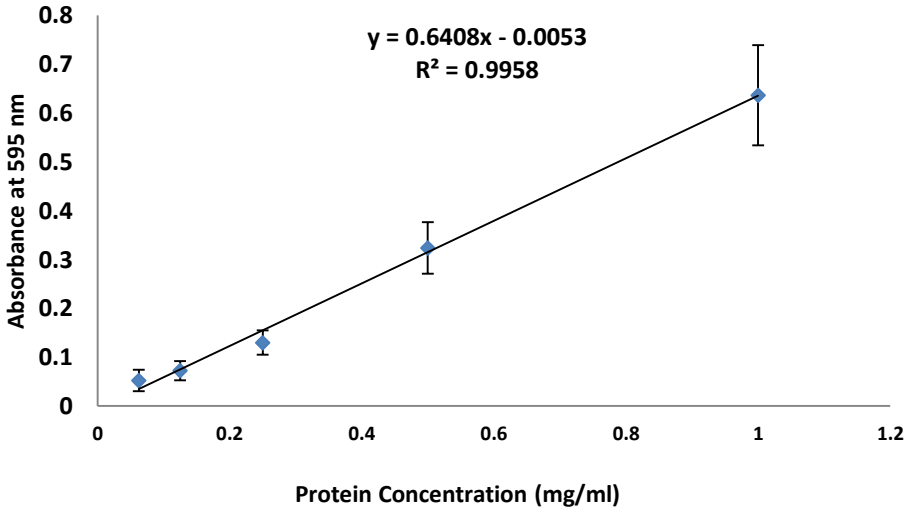

Figure 23: Representative calibration graph for protein concentration using the Bradford assay. Data points represent the mean ± SE of three determinations.

3.3.2.5.3 Polyacrylamide gel electrophoresis

Proteins were separated using pre-cast 12% polyacrylamide SDS gels (Bio-Rad, Hertfordshire, UK). The gel was immersed in running buffer (10X Tris-glycine electrophoresis buffer: 25 mM Tris, 250 mM glycine pH 8.3, 0.1% SDS). 50 µg of protein was diluted in 10 µl SDS loading buffer (Laemmli sample buffer, Sigma Aldrich, UK) and 10 µl distilled water, then heated at 80 °C for ten minutes followed by rapid cooling on ice to denature proteins. Sample (20 µl) was loaded into each well. PageRuler™ Plus Prestained Protein Ladder marker with a size range from 10 to 250 kDa (26619, Thermo Fisher Scientific Inc. Rockford, USA) was loaded into the first lane. The electrophoresis of proteins was carried out at 120 V for 1 hour.

3.3.2.5.4 Western Blot processing

Proteins were transferred from the SDS-polyacrylamide gel to nitrocellulose membrane (GE Healthcare Life Sciences) using transfer buffer (2.9 g glycine, 5.8 g Tris base, 0.37 g SDS, 200 ml methanol, 800 ml water pH 8.3). Protein transfer was run at 100 volts for 1 to 2 hours. After transfer, membranes were immersed in Ponceau S solution (1 g Ponceau S plus 50 ml acetic acid, made up to 1 L with distilled water) for 3 minutes to confirm protein transfer then washed with distilled water in order to de-stain the membrane.

3.3.2.5.5 Immunoblotting of nitrocellulose membrane

The nitrocellulose membranes were blocked with either 3% non-fat dried milk in TBST or 5% BSA in PBS for one hour at room temperature, followed by application of primary antibody. The membrane was then washed with TBST or PBS (3 washes for 10 minutes each) followed by application of secondary antibodies (HRP secondary antibody or Western blot 625 fluorescence based secondary antibody) as specified in Table 5.

Membranes were developed using either the enhanced chemiluminescent system (Roche) method or the transilluminator system depending on the secondary antibody type. For the chemiluminescent system, the ECL plus Western blotting detection system (NEL104, Perkin Elmer LAS) reagents A and B were mixed in a 1:1 ratio and applied to the membrane for one minute, then the detection reagent was discarded, and the membrane placed in an X-ray film cassette (Amersham hyperfilm^{TM} ECL, GE Healthcare) before being developed in an Ilford Developer for 2 minutes and Ilford fixer solution for another 2 minutes in the dark.

The same membrane was washed with PBST (3 X 5 minutes) and re-probed with primary and secondary antibodies that detect β-actin protein. For the transilluminator system, the membrane was placed in the transilluminator in which the proteins side of the membrane faces the UV light for image development. The results were analysed by ImageJ Software (National Institutes of Health, U.S.A) which was utilised to quantify each blot by dividing the protein signal intensity by the signal of β actin control.

3.4 Results

3.4.1 Effect of PMA on the expression of αIIb in K562 cells.

K562 cells treated with different concentrations of PMA (0.04 μM, 0.08 μM or 0.1 μM) were investigated at different incubation times (24, 40 and 72 hours) for αIIb subunit expression using the αIIb antibody EPR4330. At all concentrations of PMA used the expression of αIIb increased with time (Figure 24).

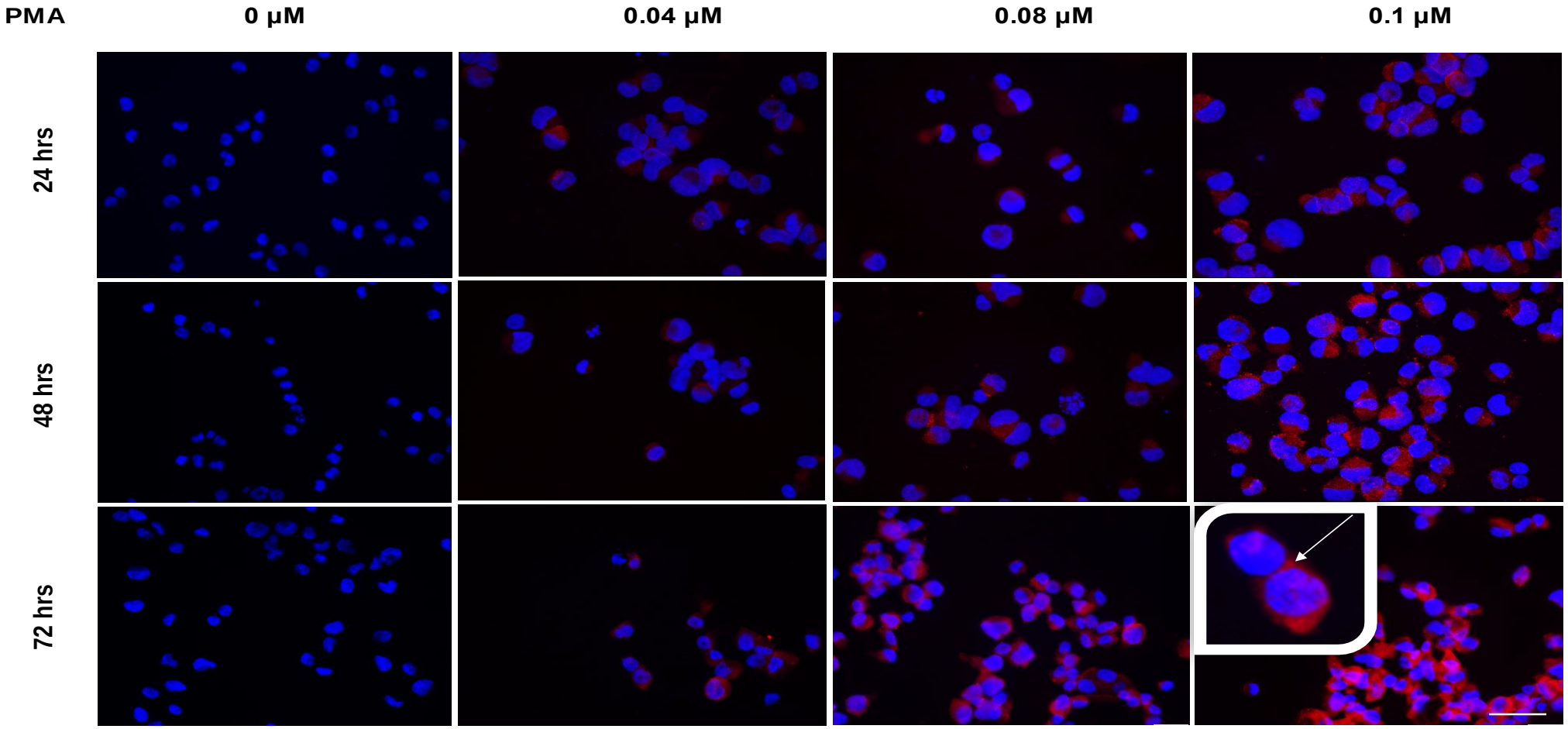

Figure 24: Effect of time of incubation and PMA concentration on expression of αIIb subunit in K562 cells. Blue-fluorescent DAPI is nuclear staining and the red colour represents αIIb expression detected by a fluorophore TRITC. White arrows point to membrane expression of αIIb in higher magnification image of cells. Bar length = 50 µm at 40X objective lens.

3.4.2 Effect of PMA on the expression of αv, α5, β3 and β5 integrin subunits in K562 and DU145 cells.

The expression of αv, α5, and β3 and β5 integrin subunits in K562 cells treated with PMA after 24 hours incubation was higher than in untreated cells (Figure 25).

DU-145 cells treated with PMA were also investigated for the expression of αv, αIIb, α5, β3 and β5 integrin subunits. No difference was detected in the level of αv, α5, αIIb, and β3 and β5 integrin subunit expression in DU145 cells which had been treated with PMA compared to untreated cells (Figure 26).

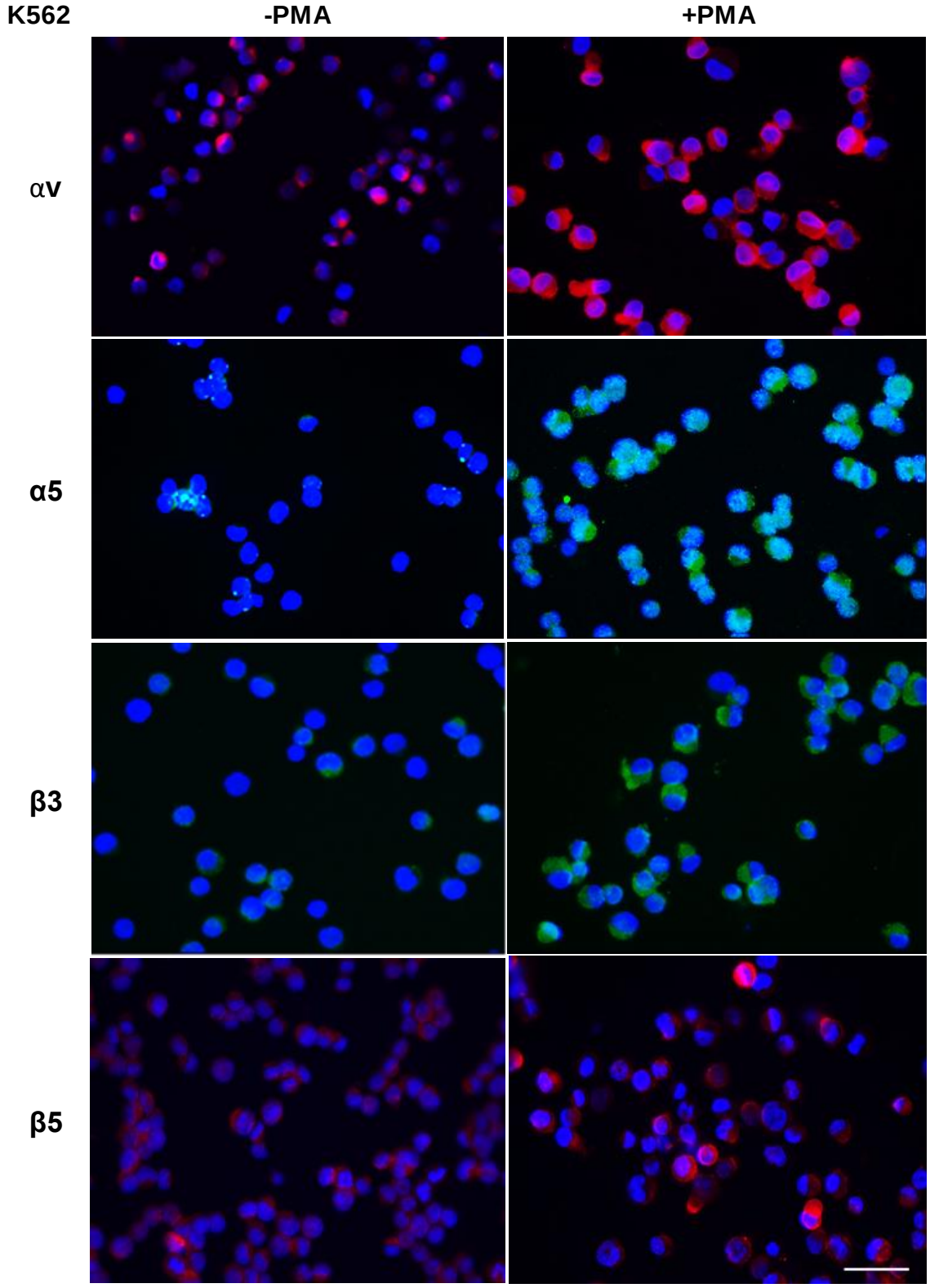

Figure 25: Effect of PMA treatment on αv, α5, and β3 and β5 expression in K562 cells. K562 cells were treated with PMA (0.1 μM) and incubated for 24 hrs. The expression of αv, α5, β3 and β5 integrin subunits was detected by immunofluorescence with Q20 anti-αv, C9 anti-α5, B7 anti-β3, and ab15459 anti-β5 integrin antibodies. Bar Length = 50 μm. Blue-fluorescent DAPI is nuclear staining and colours (green and red) represent integrin expression detected by a fluorophore (TRITC or FITC).

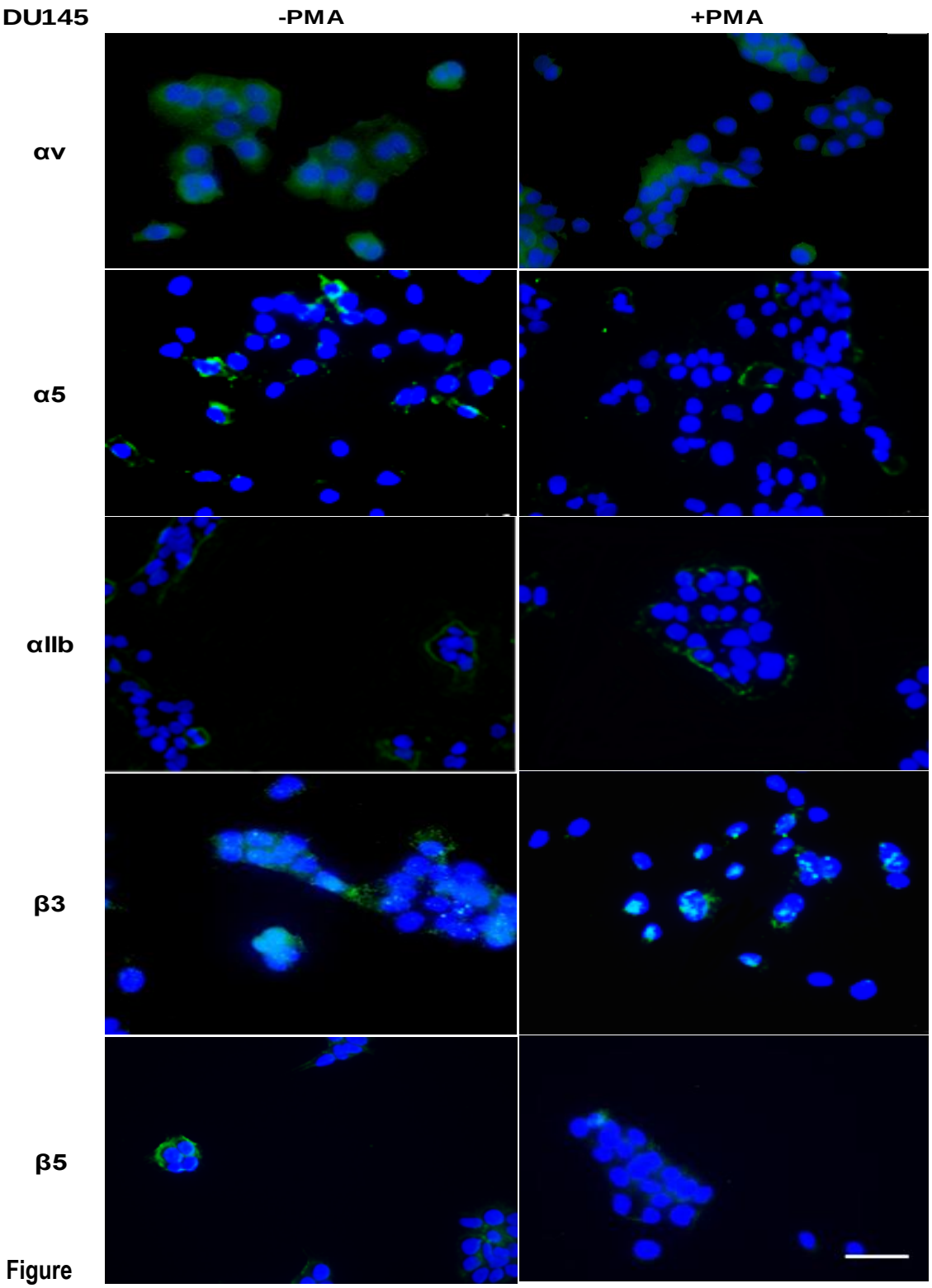

Figure 26: Effect of PMA treatment on αv, α5, β3 and β5 expression in DU145 cells. DU145 cells were treated with PMA (0.5 μM) and incubated for 24 hrs. The expression of αv, α5, β3 and β5 integrin subunits was detected by immunofluorescence with Q20 anti-αv, C9 anti-α5, B7 anti-β3, and ab15459 anti-β5 integrin antibodies. Bar Length = 50 μm. Blue-fluorescent DAPI is nuclear staining and green colour represents integrin expression detected by a fluorophore FITC.

3.4.3 Quantification of the effect of PMA concentrations and incubation times on αv and αIIb integrin subunit expression by flow cytometry.

The expression of αv and αIIb integrin subunit in K562 cell lines stimulated with 1 nM, 2 nM and 5 nM of PMA for 2 and 24 hours was quantified using FACS. The expression of αv and αIIb in PMA treated cells were not changed compared to untreated cells after 2 hours. The mean fluorescence intensities for αv in treated cells showed no observed difference compared to untreated cells but αIIb was not clear (Figure 27). However, the expression of αv in PMA treated cells for 24 hours increased with increasing PMA concentration (Appendix V). The expression of αIIb in cells treated with PMA for 24 hours was slightly shifted, see figure 28 (showing a double peak in the histogram, see Appendix VI).

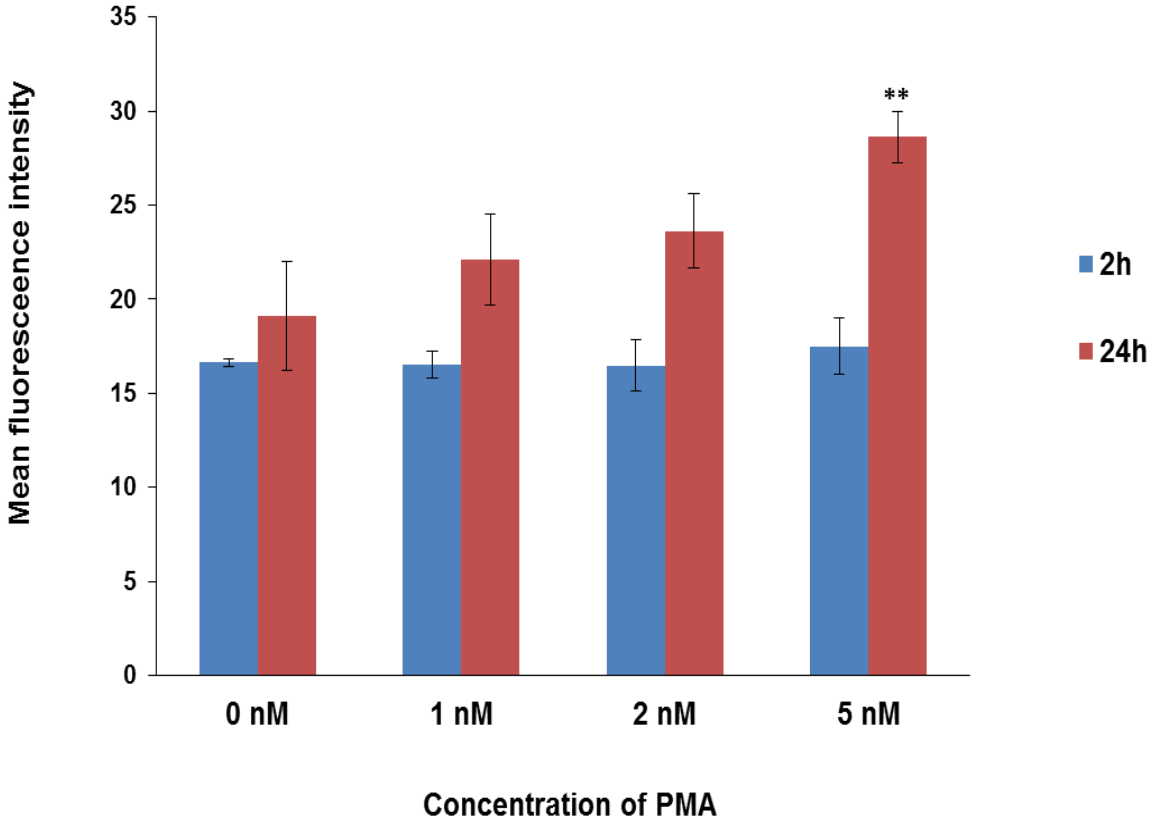

Figure 27: Effect of PMA concentration on expression of αv in K562 cells.

Cells were pre-treated with PMA for 2 or 24 hours prior to analysis (see section 3.2.2.2.1 for experimental detail). Mean fluorescence intensity of anti αv (using primary antibody B-7).

** p>0.01.

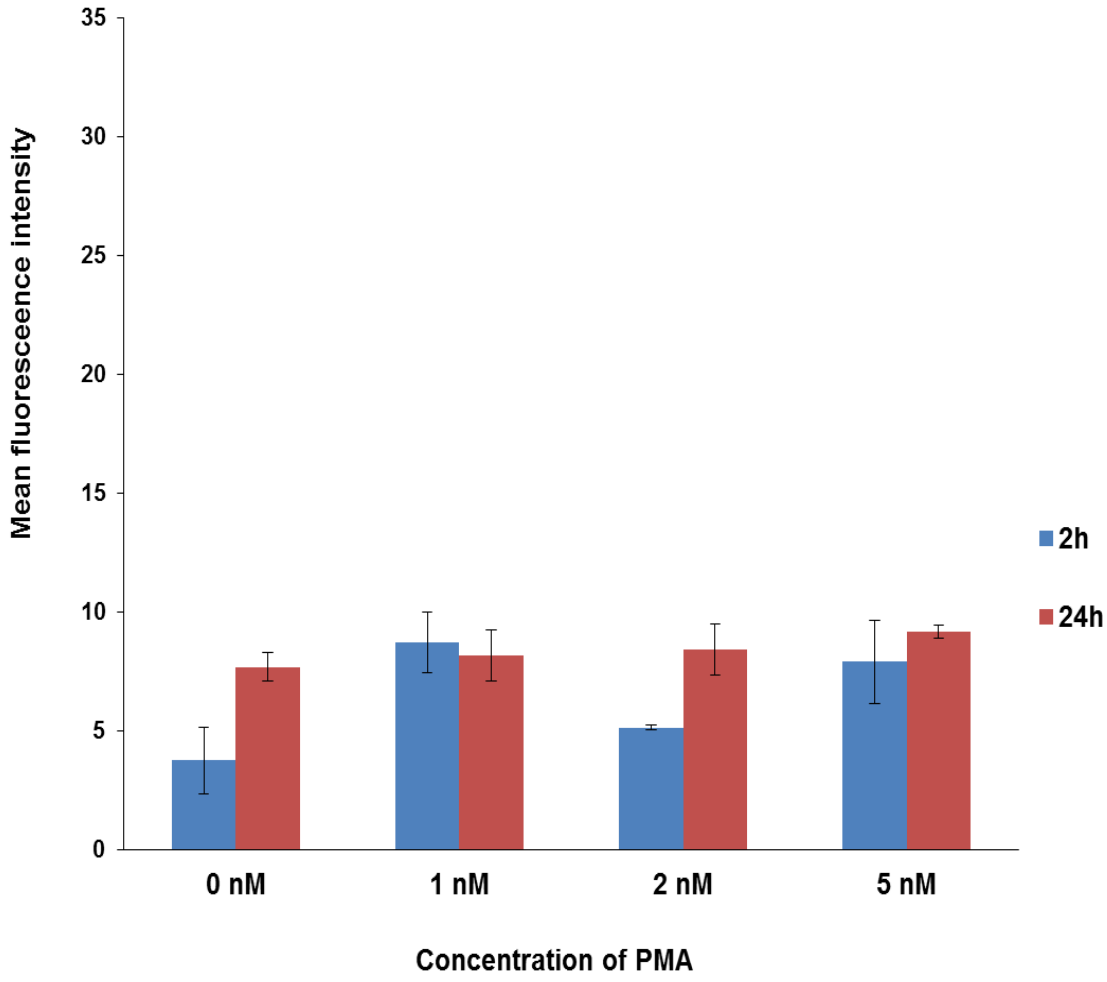

Figure 28: Effect of PMA concentration on expression of αIIb in K562 cells.

Cells were pre-treated with PMA for 2 or 24 hours prior to analysis (see section 3.2.2.2.1 for experimental detail). Mean fluorescence intensity of anti αIIb (using EPR4330 primary antibody).

The effect of PMA on integrin expression was further evaluated using 1000-fold increased concentrations of PMA. To this effect K562 and DU-145 cells were treated with 0.5 μM, 1 μM or 2 μM of PMA for 24 hours, 48 hours h or 72 hours respectively. The cells were then harvested and labelled with anti-αv and anti-αIIb antibodies and presence of both integrin subunits assessed by FACS analysis.

In K562 cells, all concentrations of PMA used produced an increase in αIIb integrin expression although there was no clear dose response relationship with PMA concentration or time of PMA exposure. 2 μM of PMA for 24 hours produced the largest increase in the expression of αv integrin (Figure 29). The largest shift for αIIb was obtained with 0.5 μM of PMA for 48 hours (Figure 30). For FACS data of K562 cells, see Appendix VII.

In DU-145 cells, treatment with 0.5 μM of PMA for 24 hours gave the highest shift from control and the highest mean fluorescence intensity for the expression of αv (Figure 31), whereas treatment for 24 hours caused no clear shift in the expression of αIIb but the mean fluorescence intensity with 2 μM of PMA was higher than control. There was no significant difference in the shift and mean fluorescence intensity between all three concentrations at 48 and 72 hours (Figure 32). For FACS data of DU-145 cells, see Appendix VIII.

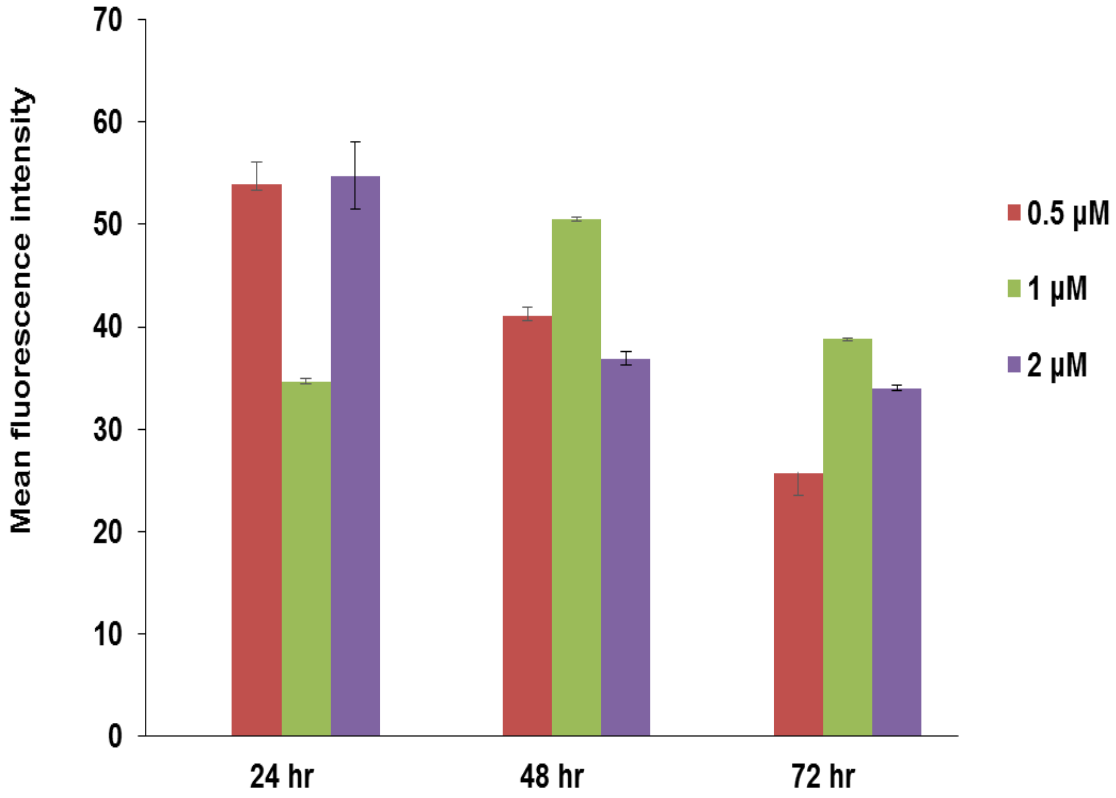

Figure 29: Effect of PMA concentration and treatment time on αv integrin expression in K562 cells. Comparison of αv expression in K562 induced by three concentrations (0.5 µM 1 µM, 2 µM of PMA) for 24h, 48 h, and 72h. B-7 primary antibody was utilised to detect expression of the αv using flow cytometry.

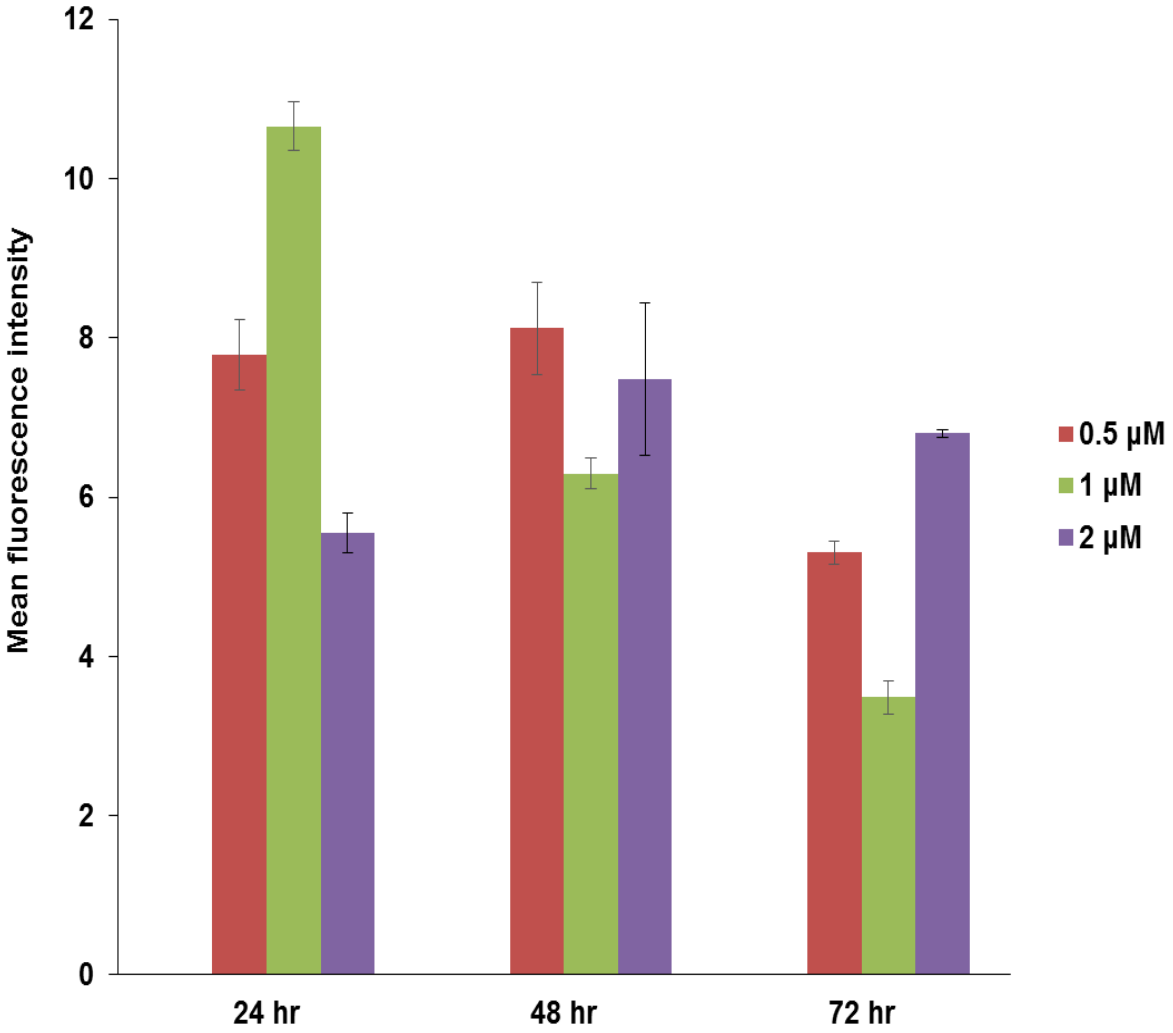

Figure 30: Effect of PMA concentration and treatment time on αIIb integrin expression in K562 cells. Comparison of αIIb expression in K562 treated by three concentrations (0.5 µM 1 µM, 2 µM of PMA) for 24h 48 h and 72h. EPR4330 primary antibody was utilised to detect expression of the αIIb using flow cytometry.

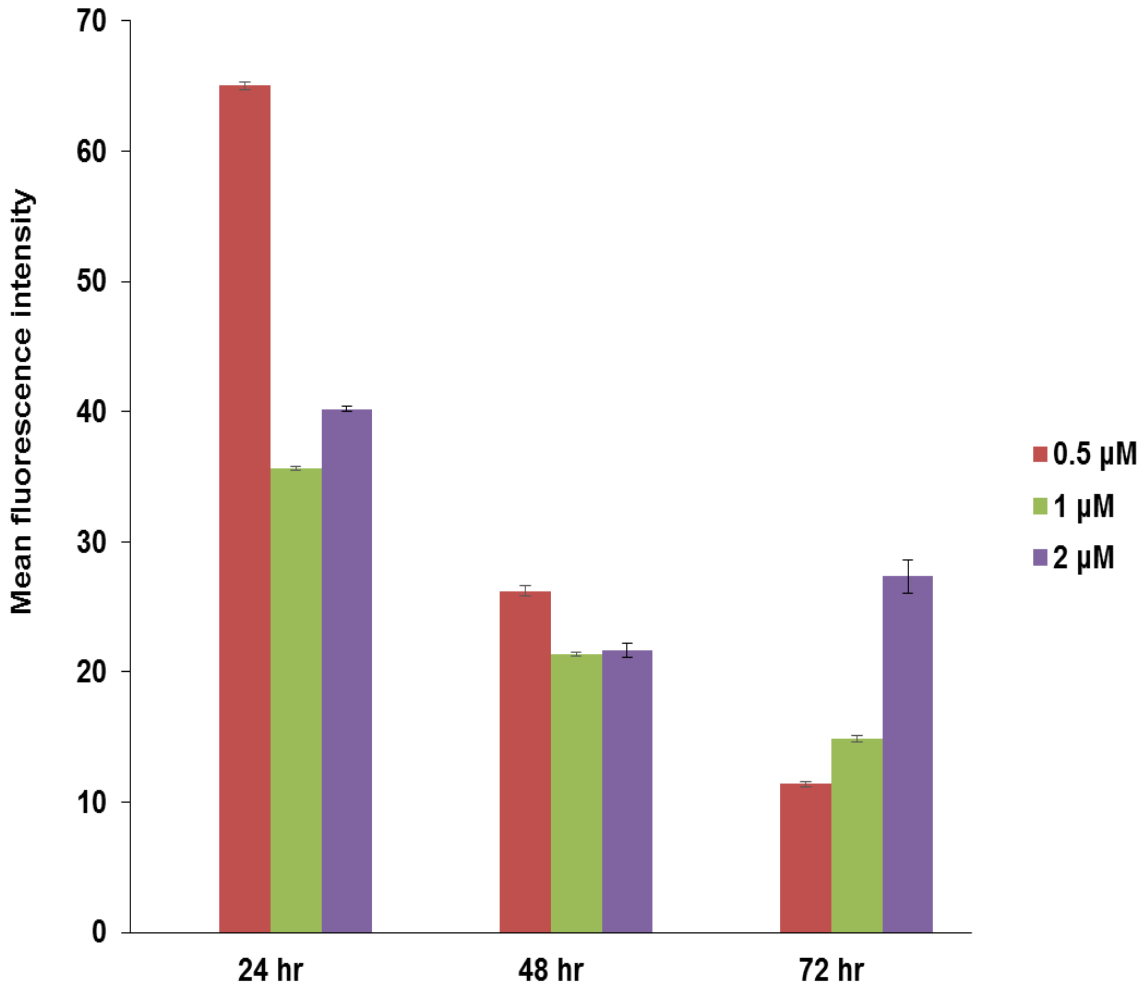

Figure 31: Effect of PMA concentration and treatment time on αv integrin expression in DU145 cells. Comparison of αv expression in DU145 treated by three concentrations (0.5 µM 1 µM, 2 µM of PMA) for 24h, 48 h and 72h. B-7 primary antibody was utilised to detect expression of the αv using flow cytometry.

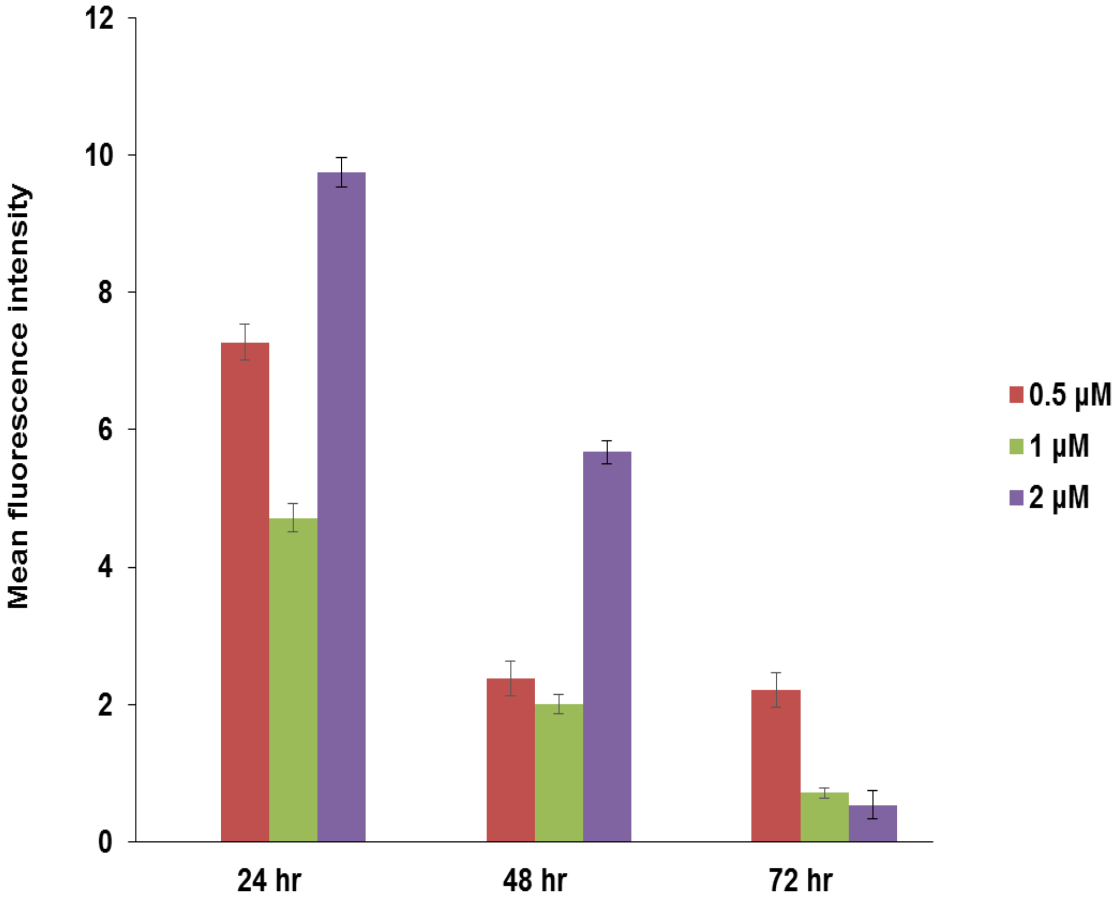

Figure 32: Effect of PMA concentration and treatment time on αIIb integrin expression in DU145 cells. Comparison of αIIb expression in DU145 treated by three concentrations (0.5 µM 1 µM, 2 µM of PMA) for 24h, 48 h and 72h. EPR4330 primary antibody was utilised to detect expression of the αv using flow cytometry.

3.4.4 Effect of PMA on expression of α5, β3 and β5 integrin subunits: comparison with αIIb and αv in K562 and DU145 cells.

The expression of αv, α5, αIIb, β3 and β5 integrin subunits in K562 cells stimulated with PMA (0.1 μM, 24 hours) compared to unstimulated cells was quantified. The expression of integrin subunits αv α5, αIIb, β3 and β5 was increased compared to untreated cells (Figure 33). For FACS data, see Appendix IX.

Increasing the K562 cell exposure to a 20-fold PMA concentration (i.e. 2 μM) exposure also stimulated the expression of αv α5, αIIb, β3 and β5 subunits, compared to PMA-untreated cells. The baseline expression level of the αv subunit was increased by approximately 4-fold compared to untreated cells. (Figure 34). The expression level of αIIb was also measured in K562 cells treated with PMA (0.04μM) at incubation times (0, 24 and 40 hours) (Figure 36). The expression level of αIIb was highest (more than 2-fold increase) compared to untreated cells after 40 hours. For FACS data, see Appendix X and Appendix XII.

DU-145 cells treated with PMA (0.5 μM, 24 h) did not show a significant increase in the expression of αv α5, αIIb, β3 and β5 subunits. Instead all subunits other than α5 showed a decrease in fluorescence intensity following PMA treatment (Figure 35). For FACS data of DU-145 cells, see Appendix XI.

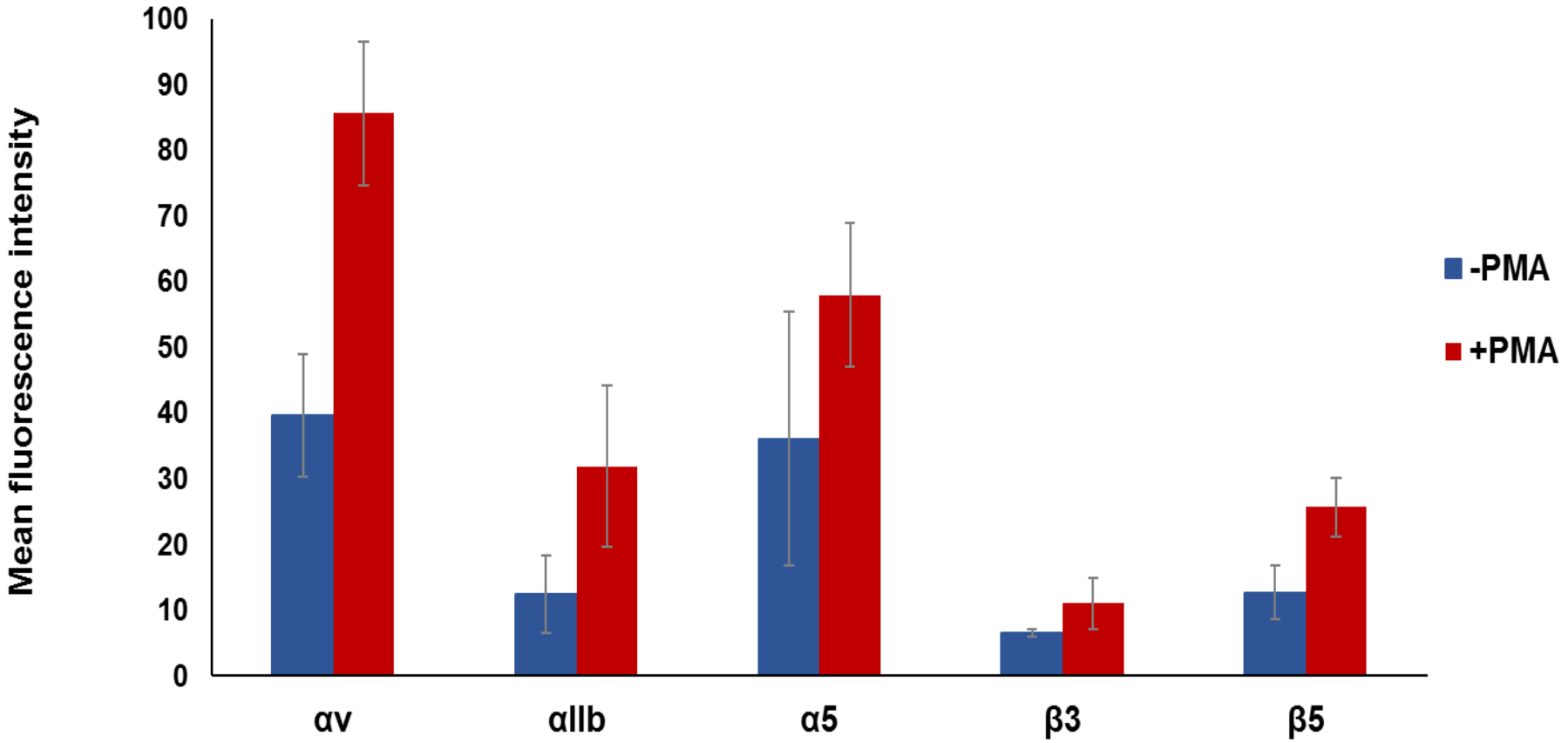

Figure 33: Expression of αv, αIIb, α5, β3 and β5 subunits in PMA stimulated K562 cells.

The anti-αv (Q20), anti-αIIb, anti-α5, anti-β3 (B-7), and anti-β5 (C-9) antibodies were utilized to detect expression of αv, αIIb, α5, β3 and β5 subunits in K562 cells in the presence of PMA (0.1 μM) using flow cytometry. Data are shown as mean ± standard error of 3 independent repeats.

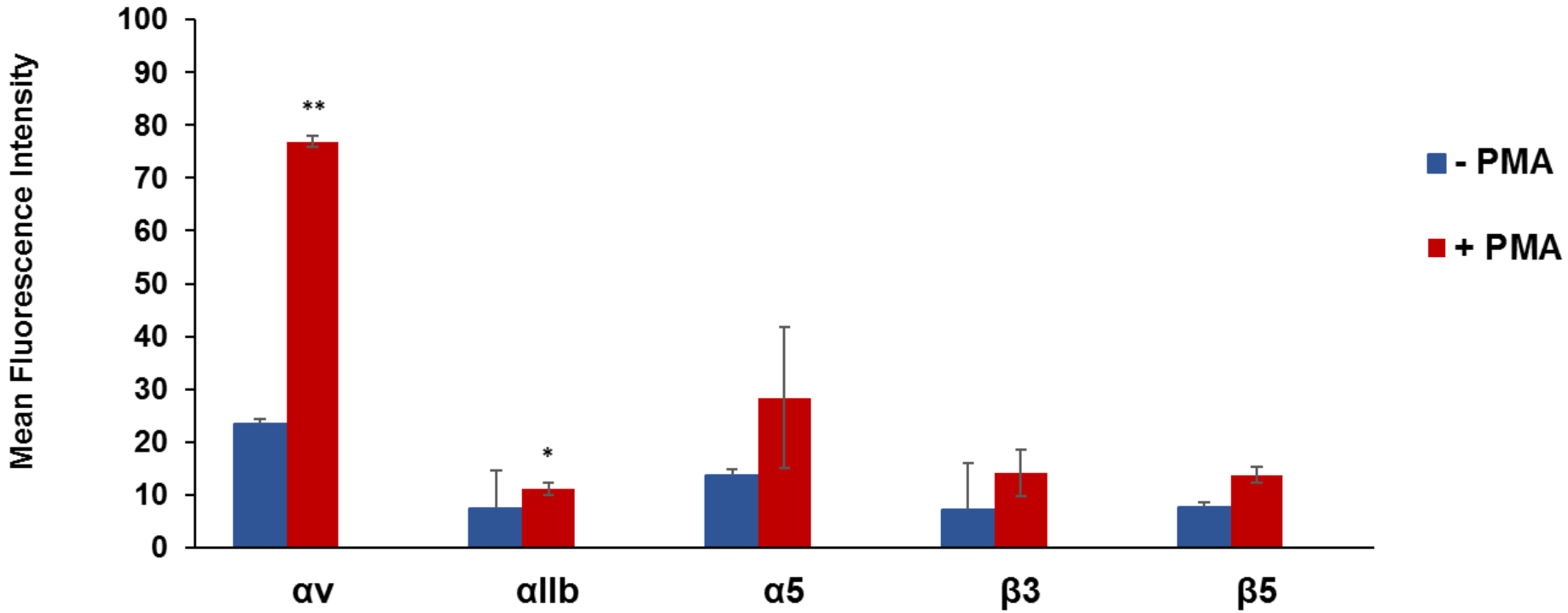

Figure 34: Expression of αv, αIIb, α5, β3 and β5 subunits in PMA stimulated K562 cells.

The anti-αv (Q20), anti-αIIb, anti-α5, anti-β3 (B-7), and anti-β5 (C-9) antibodies were utilised to detect expression of αv, αIIb, α5, β3 and β5 subunits in K562 cells in the presence of 2 μM PMA and in its absence using flow cytometry. Data are shown as mean ± standard error of 3 independent repeats. * indicated p <0.05, ** indicated p < 0.01

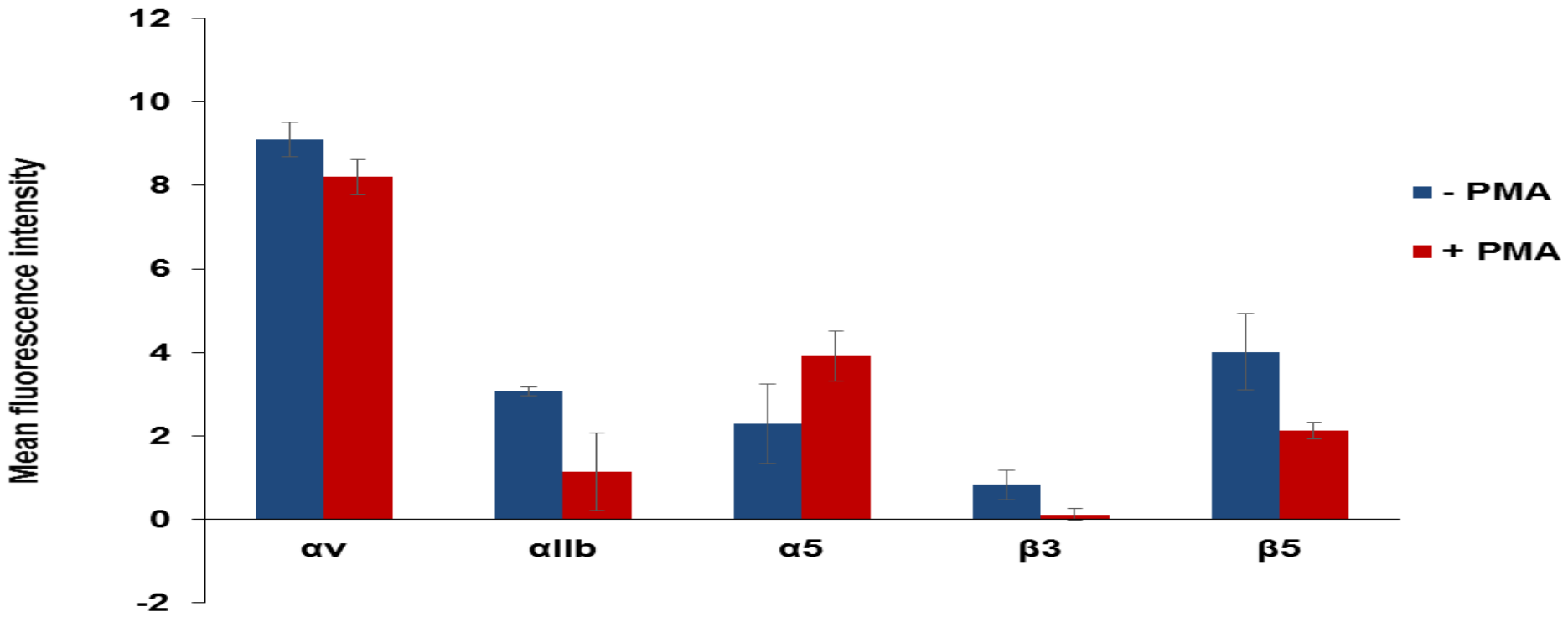

Figure 35: Expression of αv, αIIb, α5, β3 and β5 subunits in PMA stimulated DU145 cells.

The anti-αv (Q20), anti-αIIb, anti-α5, anti-β3 (B-7), and anti-β5 (C-9) antibodies were utilised to detect expression of αv, αIIb, α5, β3 and β5 subunits in DU145 cells in the presence of 0.5 μM PMA and in its absence using flow cytometry. Data are shown as mean ± standard error of 3 independent results.

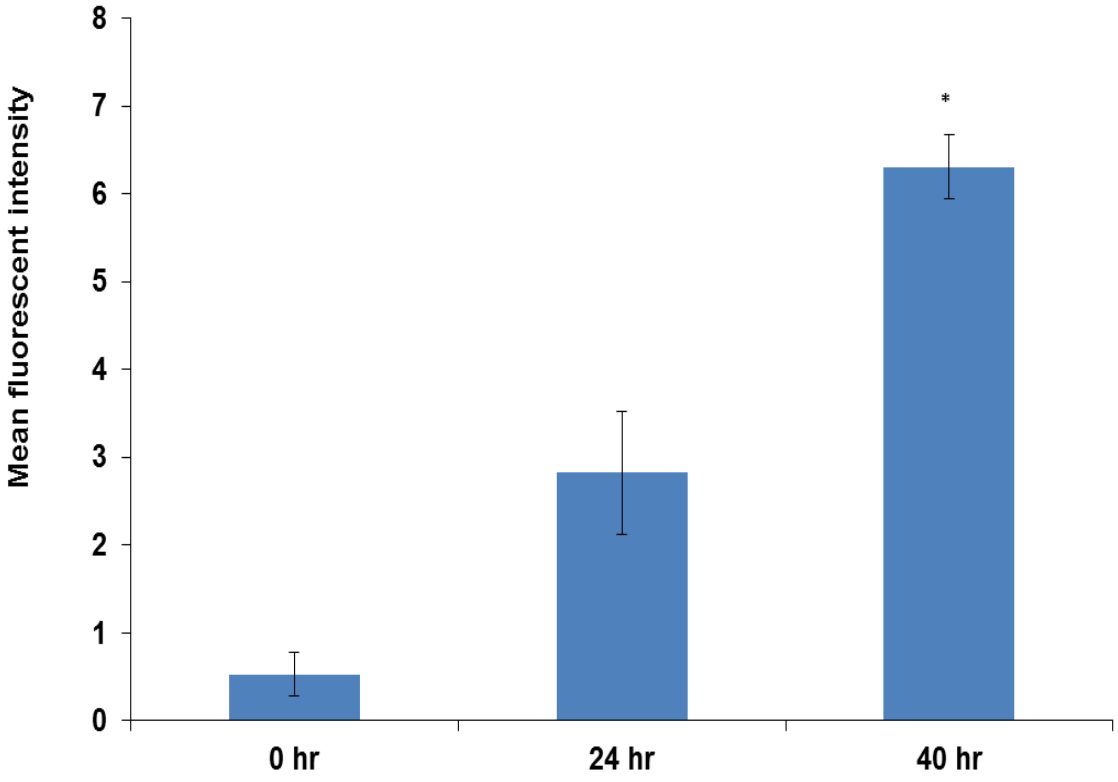

Figure 36: Effect of time on PMA (40 nM) induced expression of αIIb in K562 cells. Analysis of FACS data using mean fluorescence intensity. Data are shown as mean ± standard error of 3 independent results. * $p < 0.05$.

3.4.5 Expression of αIIb, αv and β3 using Western blot

The expression of αIIb, αv and β3 were also investigated in K562 cells treated with 0.04 μM PMA for 40 hours using the semi quantitative Western blot technique to confirm the results of the flow cytometry and to show if there is any difference between the membrane expressions of integrin subunits and the whole cell expression. The results of Western blot (Figure 37) confirmed the FACS analysis; Q-20 anti-αv antibody gave a band at 132 kDa in K562

(±PMA). The expression of αv was higher in PMA treated K562 than untreated. The anti-β3 antibody (B-7) gave a band at 120 kDa in K562 (± PMA) and showed moderate expression. There was no apparent difference between two bands in stimulated and unstimulated cells. The expression of αIIb was present in stimulated cells only and αIIb antibody (EPR4330) gave a band at 113 kDa.

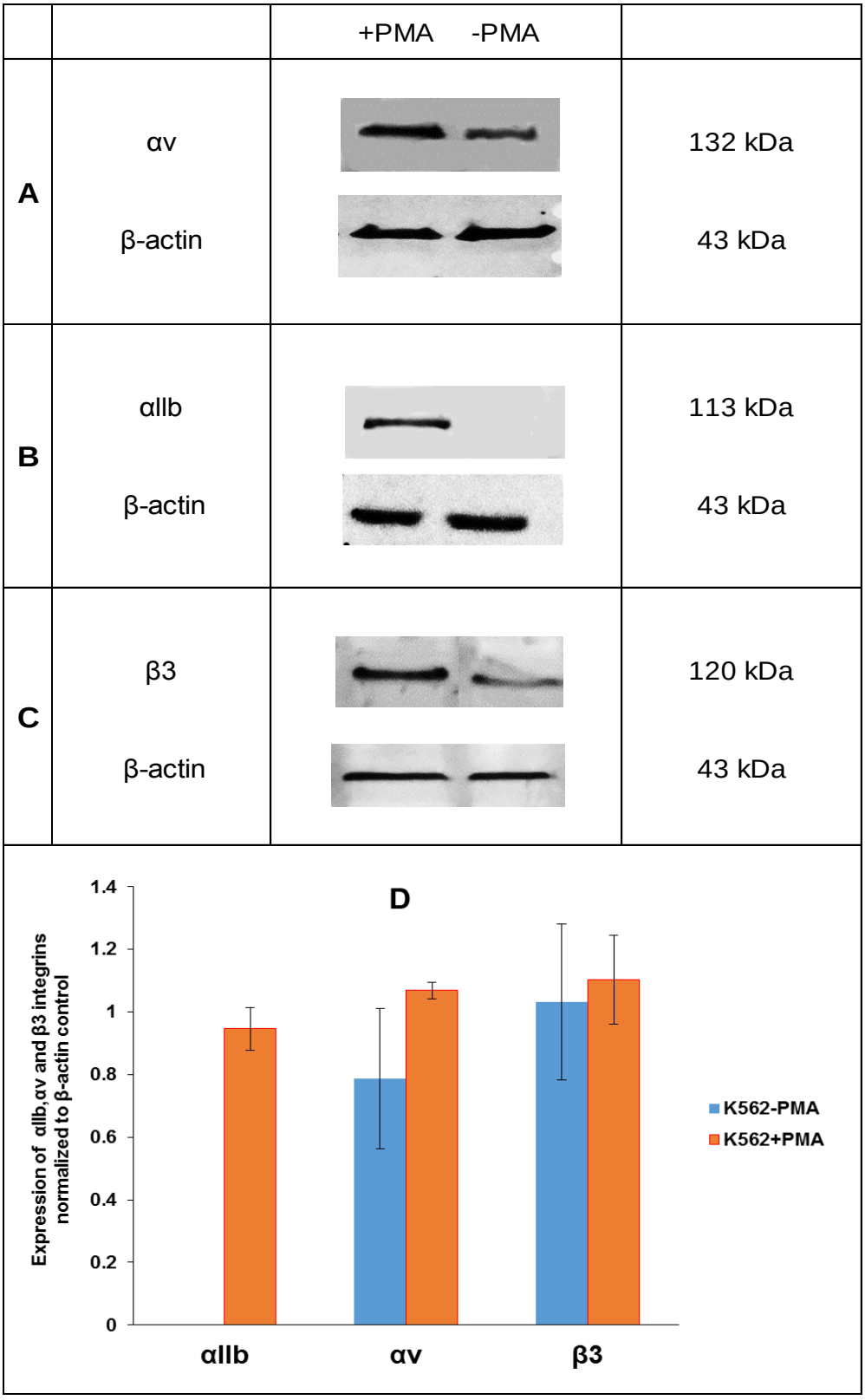

Figure 37: Expression of αv, αIIb and β3 integrin subunits in PMA-treated K562 cells compared to untreated cells. Membranes were blotted with anti αv (Q20), anti αIIb (EPR4330) and anti-β3 (B7) integrin antibodies and β-actin antibody as a loading control. Data are average of 2 experiments.

3.4.6 The effect of PMA on K562 cell survival and cell morphology

The effect of PMA on cell viability was determined to assist selection of a concentration of PMA and incubation time that would be stimulatory in term of integrin expression with minimal effect on cell viability. PMA concentrations in the range (0.04 - 2 μM) and incubation time used for subsequent stimulation of integrin expression were investigated (see figures 26 - 37). The data obtained show that PMA affected cell viability in a dose dependent manner. At an incubation time of 2 hours, in which no cell division would be anticipated, PMA (up to 0.5 μM) had no effect on cell viability but did decrease cell numbers at higher concentrations of PMA (1 or 2 μM). Increasing the PMA incubation time to 24 hours had a moderate effect on cell viability whereas, exposure to PMA at all concentrations for 96 hours produced a cytotoxic effect (Figure 38). Treatment of cells with approximately ten-fold lower concentration (0.04 μM PMA) for 24 and 40 hours (Figure 39) upregulated expression of αIIb whilst producing a minimal effect on cell survival.

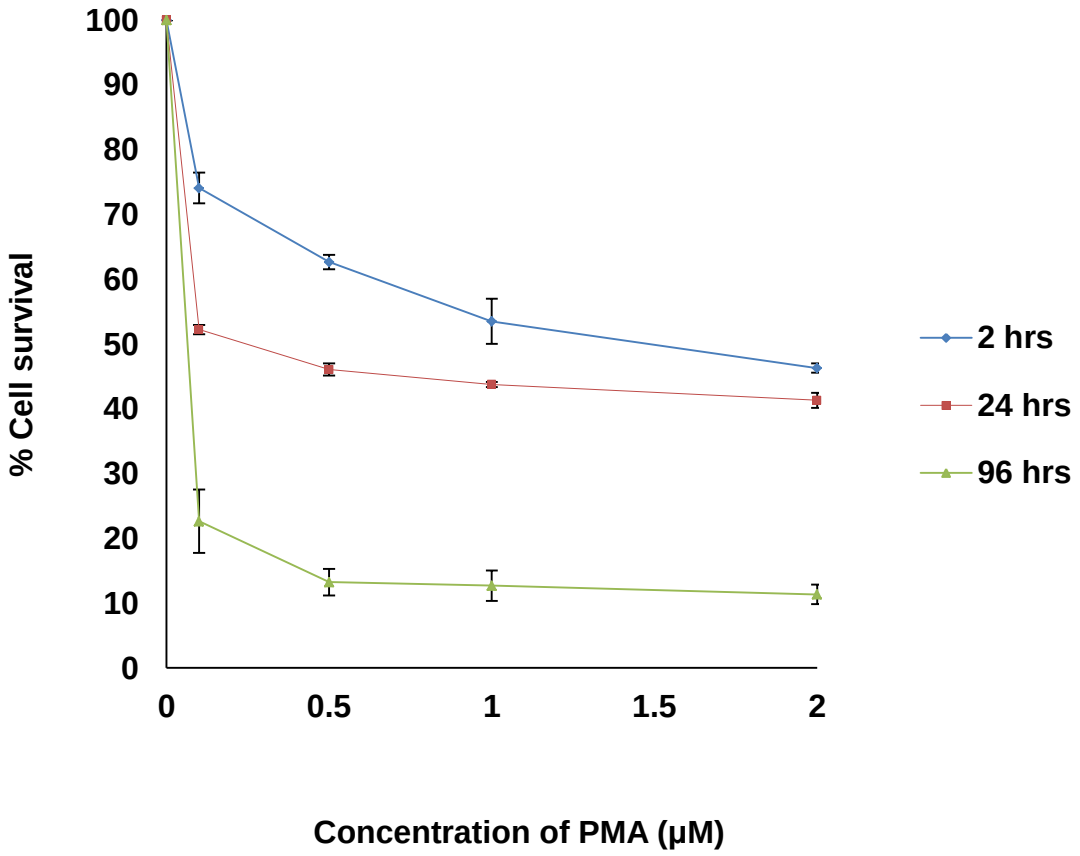

Figure 38: Effect of PMA on K562 cell viability. Cell viability versus PMA concentration at incubation times of 2, 24 and 96 hours. Cell viability was determined using the MTT assay as described in section 2.3.3.4. Data are shown is the mean ± standard error of 3 independent results.

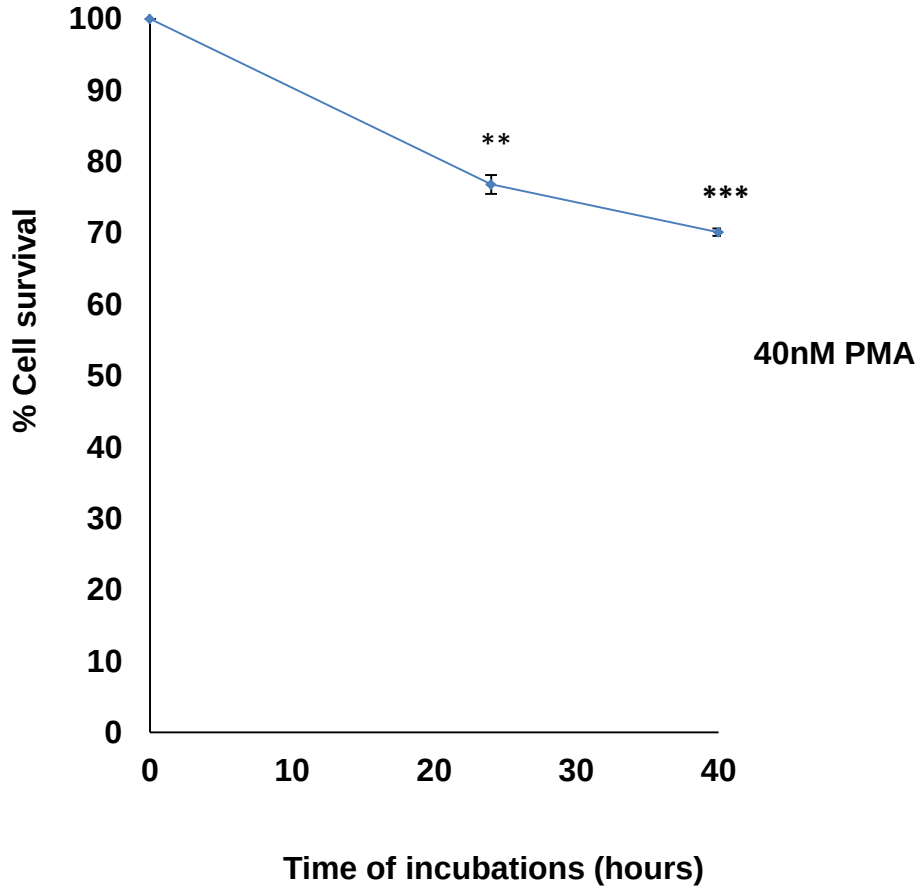

Figure 39: Effect of PMA (40nM) on K562 cell viability. Cells were treated with 40 nM PMA for 24 and 40 hours. Cell viability was determined using the MTT assay as described in section 2.3.3.4. Data are shown as mean ± standard error of 3 independent results. ** indicated $p < 0.01$, *** indicated $p < 0.001$.

A significant difference in morphology and integrin expression levels was observed using FITC immunofluorescence (Figure 40). PMA treatment induced changes of cell shape; irregular cell surfaces and cell size became slightly larger. Expression of both subunits αv and αIIb was increased.

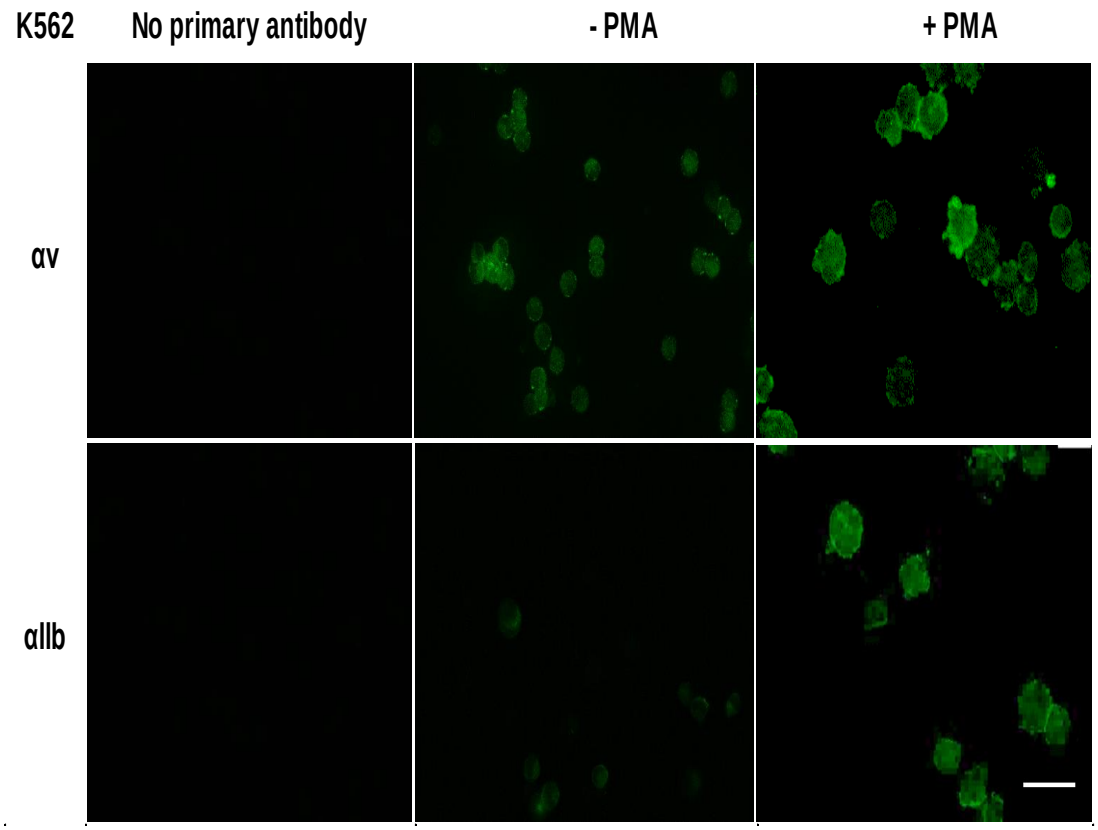

Figure 40: Effect of PMA treatment on αv and αIIb integrin subunit expression in K562 cells. Cells were treated with PMA (2 μM) for 24h. Cells were labelled with anti-αv (Q20) and anti-αIIb (EPR4330) integrin antibodies for FITC immunofluorescence. Bar length = 50 μm.

3.5 Discussion

The importance of targeting integrins as a therapeutic strategy arises from their overexpression in various diseases (Engebraaten et al., 2009; Sheldrake and Patterson, 2014). Blocking integrins has an essential function in inhibiting angiogenesis and cancer metastasis (Liu et al., 2009). Inhibition of both cancer cells and endothelial αvβ3, and platelets αIIbβ3, can promote blockade of tumour growth *in vivo* (Engebraaten et al., 2009; Trikha et al., 2002b). Therefore, we hypothesise of that a dual αIIbβ3/αvβ3 antagonist would have a direct anti-proliferative effect on dual β3 expressing models and inhibit angiogenesis and metastasis through targeting cancer cell interaction with platelet αIIbβ3 and endothelial cell αvβ3.

The major purpose of this chapter was to investigate potential dual αIIbβ3 and αvβ3 expressing functional models. The leukaemia cell line (K562) was chosen for investigation in order to develop functional assay models for testing dual β3 antagonism. PMA treatment of K562 cells is known to upregulate αIIbβ3 integrin expression (Galletti et al., 2014; Stupp et al., 2014). In order to investigate the utility of K562 cells as an inducible model of αIIbβ3 expression PMA treatment was used to stimulate protein expression on the cell surface.

To determine the best conditions for αIIbβ3 induction, K562 cells were treated with three different low concentrations (0.04 μM, 0.08 μM, and 0.1 μM) of PMA and different PMA incubation times to increase αIIb subunit expression which we then measured using immunofluorescence. An increase in the expression of the αIIb integrin subunit was observed; expression increased with increasing

time of incubation with PMA and with increasing dose. These data agree with previous research, which links PMA to the induced surface expression of integrins. That research described this to be through its activation of protein kinase C (PKC) that requires mitogen-activated protein kinases (MAPK) pathway activity for regulating the cell cycle (see Figure 8). This has an effect on cell surface expression of integrins (Conran and Hemming, 1998). For example, PMA-induced differentiation of human erythroleukaemia cells caused an increase in the expression of functionally active αvβ3, αIIbβ3 and α5β1 which simultaneously considerably altered their morphology and allowed them to spread on ECM fibronectin and vitronectin (Ylanne et al., 1990). Very low concentrations (1 nM, 2 nM and 5 nM) of PMA did not induce a significant increase in αIIb and αv expression.

As the upregulated expression of αIIb was achieved with PMA treatment, the effect of PMA (0.1 μM) on αv, α5, β3, and β5 integrin subunits expression in K562 was investigated by using immunofluorescence and flow cytometry to check the localisation and quantity of integrin expression. Expression of all subunits detected by both techniques was increased compared to untreated cells particularly αv. Since a dual expressing model is desired, increased αv, and β3 levels is not an issue, but increased levels of α5, and β5 will need to be taken into account in functional assays.

The effects of 1000-fold increase concentrations of PMA on the expression of αv and αIIb integrin subunits in K562 and DU145 were investigated to explore whether the effects of PMA are cell line dependent. PMA (2 μM) led to a rapid increase in αv expression and upregulation in αIIb expression in K562 cells. The expression of all other subunits (α5, β3, and β5) was also increased on PMA treatment. However, no significant change in integrin subunit expression on

treatment with PMA was detected by flow cytometry or immunofluorescence in DU-145 cells. This was not unexpected, since there are no literature reports of DU145 cells undergoing differentiation or changing integrin expression in response to phorbol esters. This result may suggest that K562 has upregulated levels of PKC isozyme, while DU145 has deregulated expression. K562 cells undergo differentiation in response to PMA which involves changes in integrin expression. Phorbol esters also affect cell signalling in DU145 cells (Stewart and O'Brian, 2005).

Comparing morphological changes in PMA-stimulated K562 cells with unstimulated K562 cells revealed that the PMA caused phenotypic alterations, such as irregular cell shape and increased size. The morphological changes agree with the findings of other studies (Burger et al., 1992). PMA-induced megakaryocytic differentiation of K562 cells has been shown to be accompanied by alterations in cell morphology, specific markers expressing on the cell surface of megakaryocytes, the acquisition of adhesion properties, cell growth arrest, and other changes. The change in cell adhesion is associated with cytoskeleton alterations and integrin expression (Butler et al., 1990; Huang et al., 2014; Whalen et al., 1997).

To allow the use of an adhesion assay with stimulated cell lines at the optimum concentration (0.04μM), evaluating the effect of PMA on cell survival was required. Therefore, the same concentrations that gave increased integrin expression above were used to screen the effect of PMA on cell survival for different incubation times (2, 24 & 96 hours). The absorbance values for PMA-treated cells were lower than untreated cells. This means treatment with PMA inhibited the cellular growth as well as enhancing the differentiation and increasing adhesion.

However, the MTT absorbance decrease is not necessarily a reflection of PMA mediated cytotoxicity because PMA is a differentiating agent then one of the effects of cell differentiation is cells no longer divide and undergo growth arrest. In this regard, PMA induces the inhibition of cell growth because of an arrest of the phase of G1 cell cycle and leads to a marked decrease in cdk2 activity (cyclin-dependent kinase 2), which is related to complete cdk2 dephosphorylation (Asiedu et al., 1997). Furthermore, the growth inhibition for PMA-treated cells may be because of other proteins being activated after PKC activation, such as caspase-3, serine protease(s), and pro-apoptotic proteins, which induces apoptosis (Park et al., 2001). This may interfere with the use of stimulated cells in functional assays as it is difficult to measure changes in low absorption values. For this reason, the effect of PMA on the cell survival and αIIb integrin subunit expression was investigated with 0.04 µM PMA which was used previously by Galletti et al (Galletti et al., 2014) for 0, 24 and 40 hours. I found that the cell density was very suitable at 0.04 µM PMA for 40 hours and, αIIb was significantly upregulated.

In conclusion, I have identified that treating K562 cells with 0.04 µM PMA for 40 hours is appropriate to create a dual αv/αIIbβ3 expressing cell line which will be a useful model to screen novel dual αvβ3 and αIIbβ3 antagonists in the functional assays reported in the next chapter.

Chapter 4: Investigation of the effect of novel β3 integrin antagonists in functional cell assays

4.1 Introduction

In the previous chapter, αIIb integrin subunit expression in PMA treated K562 cells was assessed by qualitative and quantitative analysis. The demonstration that αIIb expression was induced suggests PMA-treated cells may be useful in assays to measure the effect of integrin inhibitors on cell adhesion and detachment.

Cell adhesion and detachment have severe effects on the function and behaviour of cells. For instance, cell adhesion and detachment are involved in promulgating a diverse range of biological phenomena including embryonic development, wound healing, cancer development, progression, and dissemination. Therefore abnormality in cell adhesion and detachment can lead to consequences associated with pathophysiologies (Yoon and Mofrad, 2011) such as osteoporosis (Cho et al., 2006; Perinpanayagam et al., 2001), arthritis (Lasky et al., 1992; Szekanecz and Koch, 2000), cancer (Hirohashi and Kanai, 2003; Huang and Ingber, 1999; Okegawa et al., 2004) and atherosclerosis (Serhan and Savill, 2005; Simon and Green, 2005). When cells adhere to components of ECM, integrins are activated; the activated integrins connect target ligands; the linked integrins cluster together by altering their affinity (Yoon and Mofrad, 2011).

In general, there are two key events in cancer cell adhesion: cell attachment and cell detachment. Attachment events of cell adhesion focus on the mechanism of cell attachment to the ligand, whereas the detachment events of cell adhesion include load application to detach the adhered cells from the ligand (Khalili and Ahmad, 2015).

In the development and validation of cell functional assays to explore the effect of integrin antagonist, cRGDfV, a cyclic RGD peptide which is a known αvβ3/β5 integrin antagonist, and GR144053, a small molecule αIIbβ3 antagonist, were used as positive controls.

This chapter describes the validation and use of adhesion and detachment assays to evaluate potential novel β3 integrin subunit antagonists synthesised at the Institute of Cancer Therapeutics, University of Bradford. K562 cells were used as an inducible model of αIIb expression for investigating the inhibition of cellular adhesion to fibrinogen and breaking cell-ECM interactions in order to detach from fibrinogen. MCF-7 cells also were used in these functional assays as a dual β3-expressing modal.

4.2 Aims and objectives

The aims of this chapter were to evaluate a panel of novel small molecules designed to antagonise the β3 integrin subunits, for their cytotoxicity and effects on integrin-mediated tumour cell adhesion, detachment and migration. These aims achieved through the following experiments:

- Evaluation of the cytotoxicity of known integrin inhibitors (cRGDfV and GR144053) as control compounds and comparing this activity with the novel compounds using the MTT assay.
- Validation of the K562 and MCF-7 cell-based integrin functional assays using control β3 antagonists.
- Evaluation of the effects of novel compounds on K562 and MCF-7 cell adhesion and detachment.
- Evaluation of the effects of novel compounds on K562 and MCF-7 cell migration using the transwell migration assay.

4.3 Materials and methods

4.3.1 Materials

Fibrinogen from human plasma (Fg) and Hoechst stain solution were obtained from Sigma-Aldrich. The Hoechst stain solution was prepared by diluting 5 µl of 1 µg/ml of Hoechst staining into 495 µl of PBS. GR144053 was sourced from Tocris Bioscience and cRGDfV from Peptinova.

A group of small molecule β3 antagonists synthesised in-house by Dr. Helen Sheldrake were investigated in this chapter (Table 6). The compounds were initially dissolved in DMSO at a concentration of 10mM or 100mM. The stock solutions were kept at -20ºC and working solutions were prepared in complete RPMI medium immediately prior to use.

4.3.1.1 Cancer cell lines

K562 and MCF-7 cancer cell lines were maintained as described in chapter 2

Table 6 : Molecular weights of novel antagonists. See insert card for structures (confidential due to intellectual property embargo). These compounds were synthesised by Dr. Helen Sheldrake.

ICT compounds	Molecular weight (g/mol)
ICT9001	305
ICT9025	517
ICT9026	475
ICT9055	542
ICT9066	345
ICT9072	474
ICT9073	516
ICT9085	500
ICT9094	557
ICT9099	542
ICT9101	514
ICT9103A	600

4.3.2 Methods

4.3.2.1 Cytotoxicity assay using MTT assay

The cytotoxicity assay was performed in triplicate wells per drug concentration. 180 µl cell suspension per well (2 x 10^4 cell/ml of K562 and 1x10^4 cell/ml of MCF-7) were plated into the required number of 96 well plates. 20 µl of the control compounds (GR144053 and cRGDfV): 1, 2, 5, 10, 20, 50, 100, and 200 µM and ICT compounds: serial dilutions of each compound 0.01 to 100 µM were prepared using cell culture medium as a diluent. The compounds were added to all wells except the blank control (200 µl of RPMI medium) and untreated control. Control cells were treated with 0.1% DMSO with the same concentrations that used with drugs as seen in Appendix I. The 96 well plates were incubated for 4 hours at 37 °C and then centrifuged for 5 minutes at 1000 rpm and then thus the supernatant was removed. 200 µl PBS was added to wash the cells and centrifuged again to remove PBS. 200 µl of fresh RPMI medium was added and incubated for 92 hours at 37 °C. Following incubation for 96 hours, cell survival was quantified using the MTT assay.

96-hours drug exposure: after 4 hrs treatment, the plate was incubated directly for a further 92 hours at 37 °C. Following 96 hours incubation, cell survival was quantified using the MTT assay. The IC_{50} is defined as the compound concentration that is required to causes a decrease in the percentage of surviving cells to 50 %. The following equation was used to calculate cell survival as following:

$$\%\ \text{Cell survival} = \frac{\text{Average of the absorbance of treated wells} - \text{blank}}{\text{Average of the absorbance of untreated wells (control)} - \text{blank}} \times 100$$

4.3.2.2 Adhesion assay

4.3.2.2.1 Fibrinogen preparation

2 mg/ml of fibrinogen from human plasma powder was dissolved in 1 ml of saline (0.9% NaCl). The fibrinogen saline solution was incubated at 37°C (warm water bath) without mixing for 3 – 4 hours and then filtered through a 0.2 µm filter using a syringe. After filtration, the fibrinogen stock solution was used immediately or stored for up to one week at 4°C.

4.3.2.2.2 Fibrinogen adhesion assay

96 well plates (treated microplate, Costar, Corning, NY) were coated with 100 µl/well of fibrinogen (2 µg/ml or 5 µg/ml) and incubated overnight at 4°C. The wells were blocked with 3% BSA in PBS (100 µl/well) for 1 - 2 hrs at 37 °C. K562 cells were stimulated with PMA (0.04 µM) and incubated for 40 hrs at 37 °C, then prepared in FCS-free medium ($5X10^5$ cells/ml) and MCF-7 cells were also prepared in FCS-free medium ($4X10^5$ cells/ml) and then treated with different concentrations of drugs for 4 hours on a rotator at room temperature. Control cells were treated identically apart from the absence of drugs. After the 4 hours incubation, cells were added to the fibrinogen-coated plates and incubated at 37 °C for one hour. The supernatant was removed, and the wells washed twice with PBS to remove non-adherent cells. 180 µl of complete medium was added to each well and incubated overnight at 37°C. Finally, 20 µl of MTT was added and incubated for 4 hours at 37°C, and then measured spectrophotometrically by the plate reader at 540 nm. This experiment was repeated three times. The following equation was used to calculate cell adhesion as following:

$$\% \text{ Adhesion } = \frac{\text{Average of the optical density of treated cells } - \text{blank}}{\text{Average of the optical density of untreated cells} - \text{blank}} \times 100$$

4.3.2.2.3 Non-adherent cell viability assay

K562 cells were treated with different concentrations of ICT9055 for 0, 4 and 24 hours. After the exposure times, cells were plated on the fibrinogen-coated plates and incubated at 37°C for one hour. Non-adherent cells were removed by washing gently twice with PBS then centrifuged at 1000 RPM for 5 minutes. The viability of cells was evaluated using the trypan blue assay, where 100 µL of cell suspension was added to100 µL of trypan blue stain and mixed gently. 10 µL of trypan blue-treated cell suspension was applied to the haemocytometer to calculate live and dead cells by the followed equations:

$$\% \text{ Viability } = \frac{\text{Average number of live cells}}{\text{Average number of total cells}} \times 100$$

$$\% \text{ Nonviability } = \frac{\text{Average number of dead cells}}{\text{Average number of total cells}} \times 100$$

The sample of untreated and treated non-adherent cells were stained with Hoechst 33342 (5 µg/ml) for 5 -10 minutes at room tempreturere to indicate the morphology of cells, and if they had any signs of apoptosis or necrosis. The slides were then examined using a LEICA fluorescence microscope at 40X objective lens magnification and photographed.

4.3.2.3 Fibrinogen detachment assay

96 well plates (non-treated microplate, Corning) were coated with 100 µl/well of fibrinogen (2 µg/ml or 5 µg/ml) or coated with100 µl/well of 5% BSA in PBS as a blocking agent (control for non-specific adhesion). The coated plates were incubated overnight at 4°C. K562 cells were stimulated with PMA (0.04 µM) and incubated for 40 hrs at 37°C, then seeded in complete medium (5 X10^5 cells/ml) and incubated overnight at 37°C. The next day, the cells were treated with or without different concentrations of drugs for a range of time points: 2, 4 & 6 hours at 37°C for detachment. After each incubation period, the supernatants were collected in labelled Eppendorf tubes, and the wells washed gently with PBS to remove non-adherent cells which were added to the suspension and then centrifuged at 1000 RPM for 5 minutes. The supernatant was removed and washed with PBS at 1000 RPM for 5 minutes. 10 µL of cells were taken and applied to the haemocytometer for counting. The equation below was used to calculate cell detachment. The remaining attached cells were measured using the MTT assay as described above. Half maximal effective concentrations (EC_{50}) were calculated to measure a response of drug to detach 50 % of cells from fibrinogen.

$$\%\ \text{Detachment} = \frac{\text{Average number of treated detached cells}}{\text{Average number of untreated detached cells (control)}} \times 100$$

4.3.2.1.1 Analysis of integrin subunit expression in fibrinogen detachment assay

The fibrinogen detachment assay was set up in 12 well plates. The detached cells were collected as described above (Section 4.2.4.3). Attached cells were removed using a scraper and washed with PBS at 1000 RPM for 5 minutes. Following this the supernatant was removed and 100 µl of 4% PFA was added. The suspension was kept for 5 – 10 minutes at room temperature. The supernatant was removed, and fixed cells were obtained. Dilution of primary antibodies was made in 1% BSA/PBS. 100 µl of diluted primary antibodies were added to each tube according to their optimal concentrations in Table 3 and incubated for 45 – 60 minutes at 4°C in the dark. The cells were centrifuged with cold PBS three times at 1000 rpm for 5 minutes. The secondary antibody was diluted (1:500) in 1% BSA/PBS. 100 µl of diluted secondary antibodies were added to each tube and incubated for at least 20 – 30 minutes at 4°C in the dark. The cells were centrifuged again with cold PBS three times at 1000 rpm for 5 minutes. 1% BSA/PBS (300µl) was added to the cells and then 50µl of the suspension mixed with one drop of DAPI stain and applied to the slide and photographed by LEICA fluorescence microscope at 40X objective lens magnification.

4.3.2.2 Transwell migration assay (Boyden chamber assay)

The Transwell migration assay is a common alternative approach to scratch assays. A diagram of the assay is shown in Figure 41. The transwell insert has a polycarbonate membrane with pore size 8 µm (Corning® Costar® Transwell® cell culture inserts). When placed in the well, it divides the chamber into two compartments. 150 µl of cell suspension treated with different concentrations of compounds were seeded in serum-free medium in the top compartment so they can migrate directly through the pores towards a chemoattractant (10% FBS) in the bottom reservoir. After 24 hours of incubation at 37 °C, the cell suspension was removed from the insert of the top compartment and the rest of cells were washed with PBS and wiped off with a cotton swab. Cells on the lower side of the membrane were fixed with 70% ethanol for 2 minutes and left to air dry. The membrane was cut off using a scalpel and placed on a microscopic slide upside down with DAPI staining. Images were taken using LEICA fluorescence microscope at 20X objective lens magnification, and the cells were counted using Image J software as shown in Figure 42. Cell migration was calculated as following:

$$\%\ \text{Migration} = \frac{\text{Average number of treated cells migrating through membrane}}{\text{Average number of untreated cells migrating through membrane}} \times 100$$

Figure 41: Diagram of Transwell migration assay. Cells are added to the upper chamber and then migrate through the porous membrane and adhere to the bottom surface of the membrane in response to the chemoattractant added to the lower chamber. This diagram was modified from (Strazielle et al., 2016).

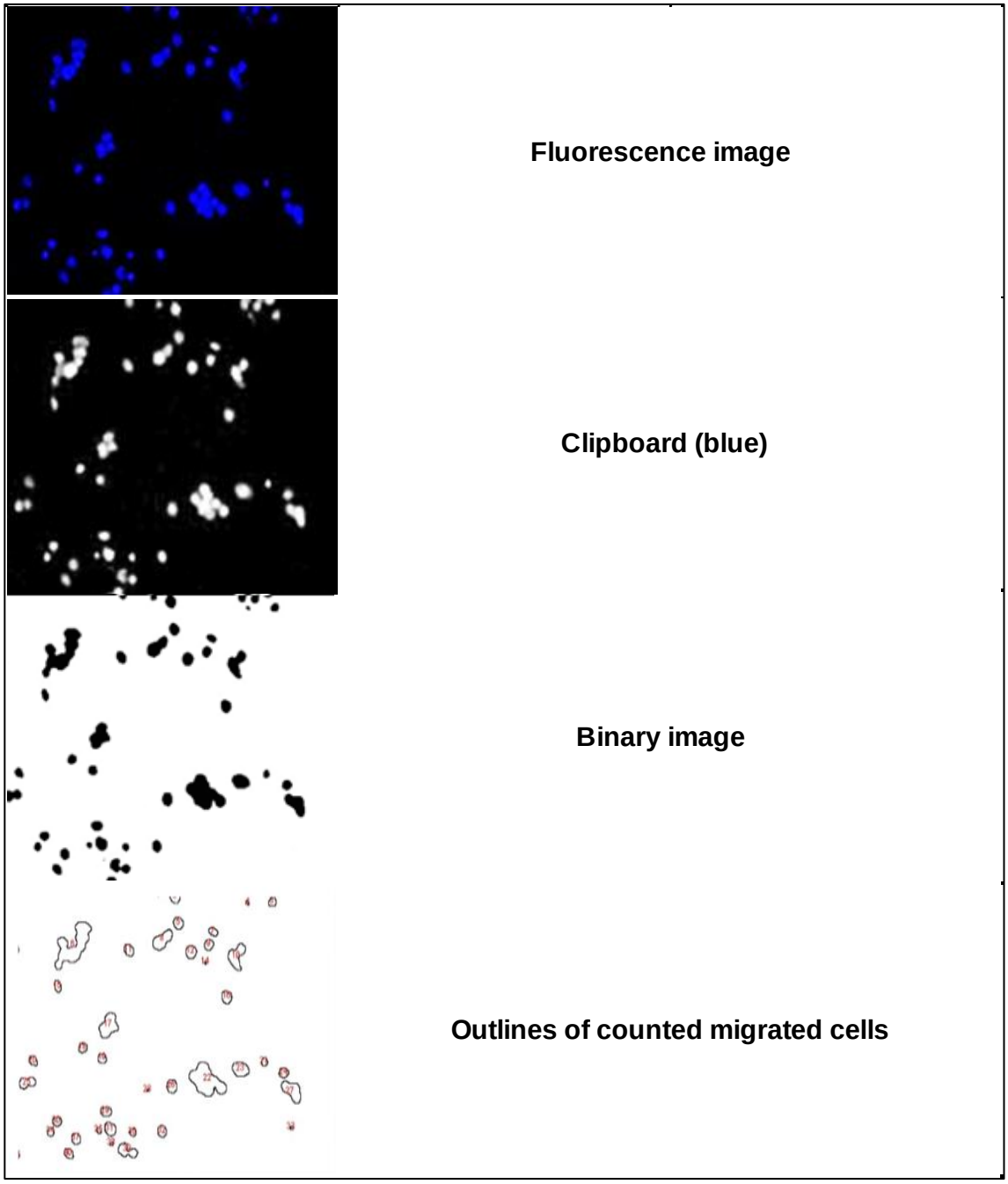

Figure 42: Analysis of Transwell migration assay using ImageJ. The fluorescence images were analysed through Image J and images converted to binary for Image J recognition then cells were counted using Image J.

4.3.2.3 Statistical analysis

Student's t-test (two tailed) was utilised for statistical analysis of functional assay using Excel software. The results considered statistically significant for $p < 0.05$ and highly significant for $p < 0.01$. CompuSyn version 1.0 (Combosyn Inc) was sed to calculate the combination index (CI) in drug combinations. CI<1, CI=1 and CI>1 indicate synergistic, additive, and antagonistic effects, respectively.

4.4 Results

4.4.1 Cytotoxicity of GR144053 and cRGDfV against K562 cells

The MTT assay was utilised to measure the cytotoxicity of GR144053 and cRGDfV against K562 with or without PMA and MCF-7 cells at concentrations of 0, 1, 2, 5, 10, 50, 100, and 200 μM for two different drug exposure times; 4 hours of drug exposure and 96 hours of drug exposure (Figure 43 and Figure 44). Both drugs were non-toxic to K562 and MCF-7 cells except at the highest concentrations (50, 100 and 200 μM to K562 cells and 100 and 200 μM to MCF-7 cells for 96 hours) which killed 40-50% of cells. Therefore, the antagonists could be utilised in the functional assays at lower concentrations.

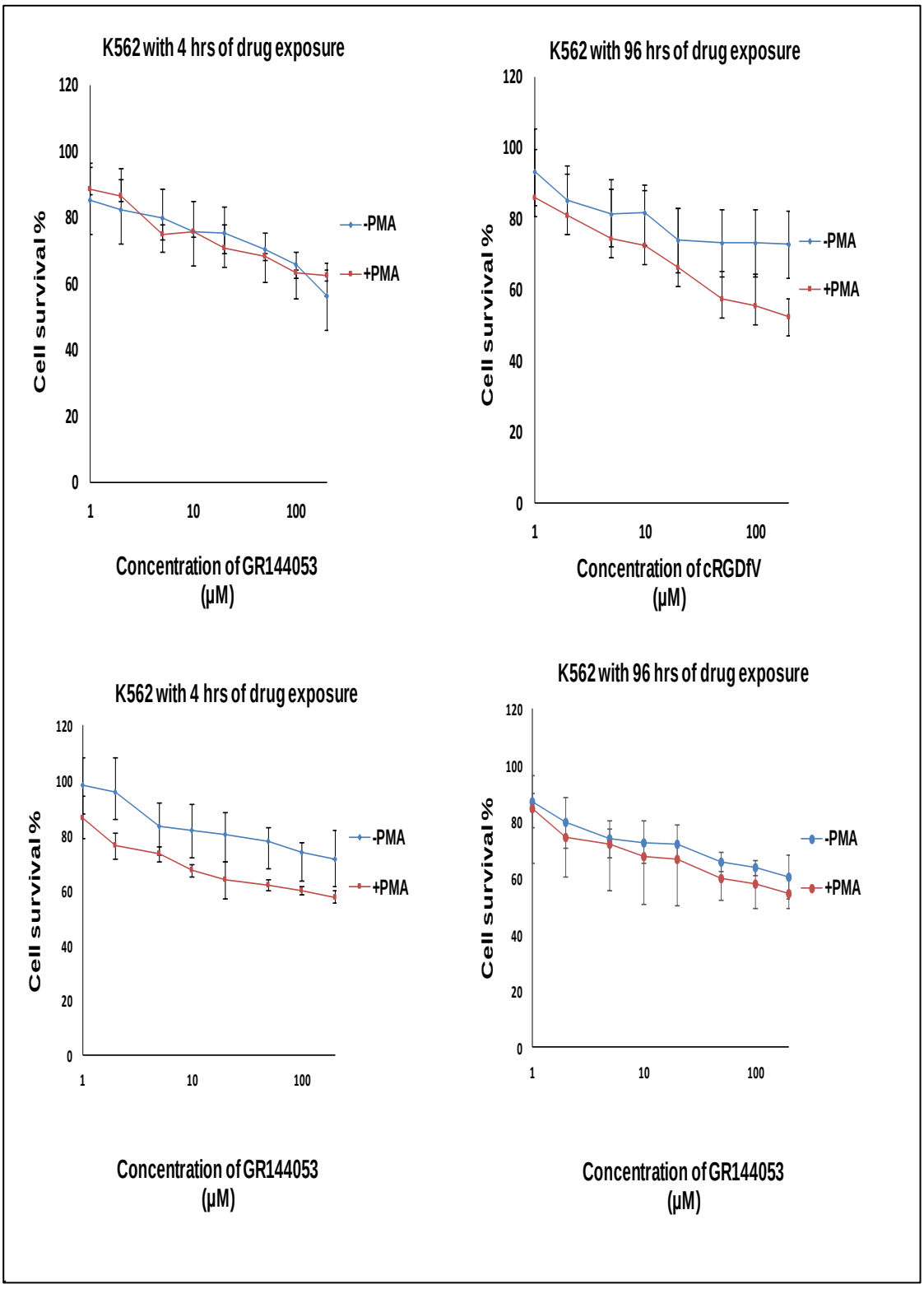

Figure 43: Evaluation of the cytotoxicity of GR144053 and cRGDfV on K562 cells using the MTT assay. Cells (± 0.04 µM PMA) were exposed to the drugs for 4 hrs and 96 hrs.

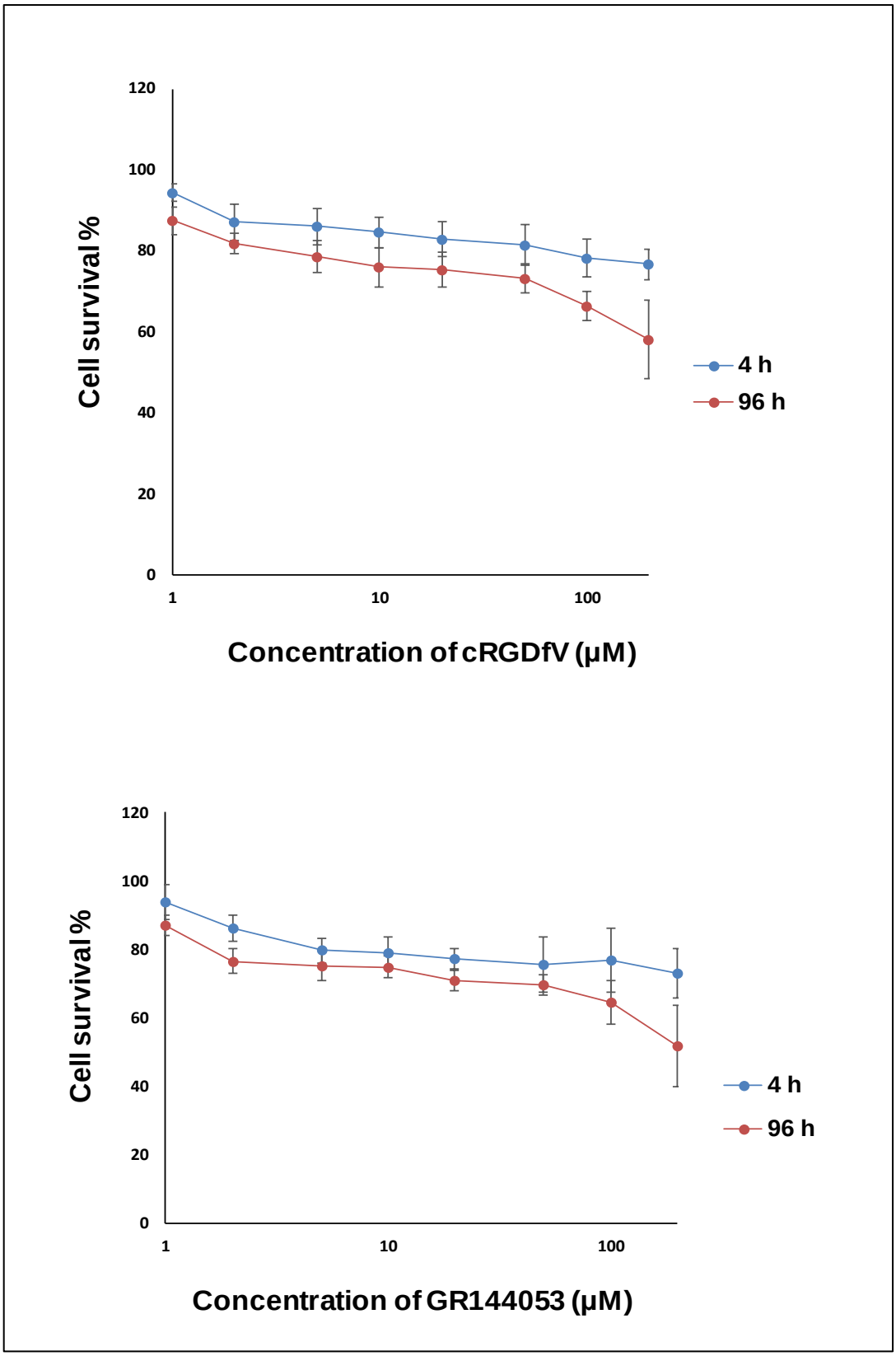

Figure 44: Measurement of the cytotoxicity of GR144053 and cRGDfV on MCF-7 cells using the MTT assay. Cells were exposed to the drugs for 4 hrs and 96 hrs.

4.4.2 Evaluation of the cytotoxicity of potential novel β3 integrin antagonists

The MTT assay was used to assess the cytotoxicity of potential novel β3 integrin antagonists against K562 and MCF-7 cells over a range of different concentrations (0.01, 0.1, 1, 10 & 100 μM) for 4 and 96 hours of drug exposure. As shown in Figure 45A and B, Figure 46 A and B and Figure 47 A and B most of tested ICT compounds were non-toxic to K562 and MCF-7 within the range of concentrations tested for 4 hours of drug exposure; at 96 hours: ICT9094 and ICT9099 proved toxic in all cell lines. ICT9025 was toxic and ICT9101 had a moderate effect in K562 + PMA. ICT9066, ICT9072 and ICT9073 at higher concentrations had a toxic effect on MCF-7 cells only. IC_{50} values are shown in Table 7.

Table 7: IC_{50} values for new small molecule integrin antagonists in the MTT cytotoxicity assay for 96 hours.

ICT compounds	K562 IC_{50} ± SD (μM)	K562 (+PMA) IC_{50} ± SD (μM)	MCF-7 IC_{50} ± SD (μM)
ICT9001	> 100	> 100	> 100
ICT9025	> 100	68.1 ± 8.6	> 100
ICT9026	> 100	> 100	> 100
ICT9055	> 100	> 100	> 100
ICT9066	> 100	> 100	81 ± 26.5
ICT9085	> 100	> 100	> 100
ICT9072	> 100	> 100	74.1 ± 21.7
ICT9073	> 100	> 100	65.9 ± 8.3
ICT9094	21.9 ± 8.4	6.5 ± 3.1	23.2 ± 7.1
ICT9099	51.4 ± 9.3	42.7 ± 0.2	55.9 ±12.7
ICT9101	> 100	75.7 ± 3.4	> 100
ICT9103A	> 100	> 100	> 100

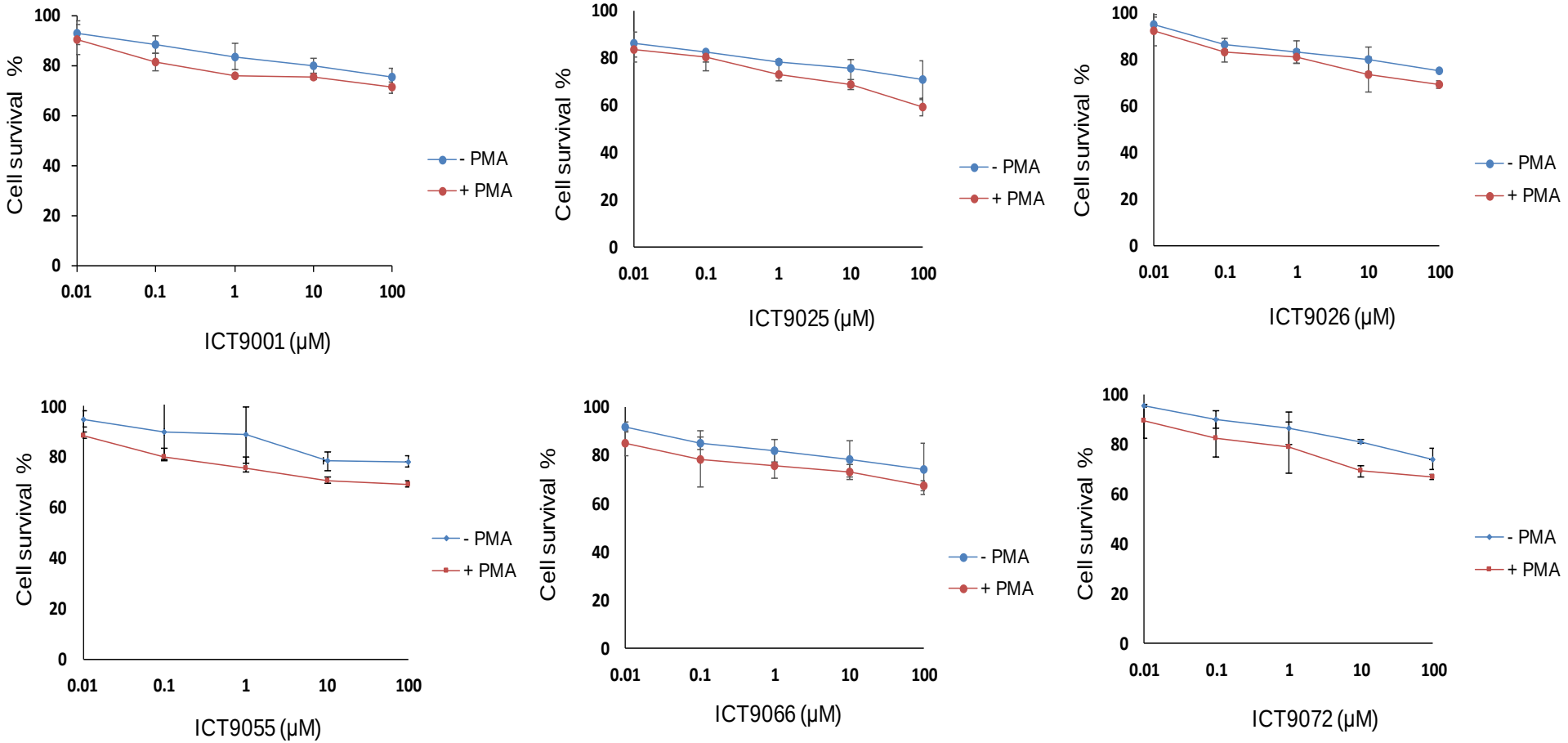

Figure 45 A: Measurement of the cytotoxicity of the first part of new small molecule integrin antagonist's panel for 4 h of drug exposure in K562 cells. Cells were pre-treated with 0.04 μM PMA for 40 h (red line) or not treated with PMA (blue line). Data are shown as mean ± standard deviation of 3 independent results.

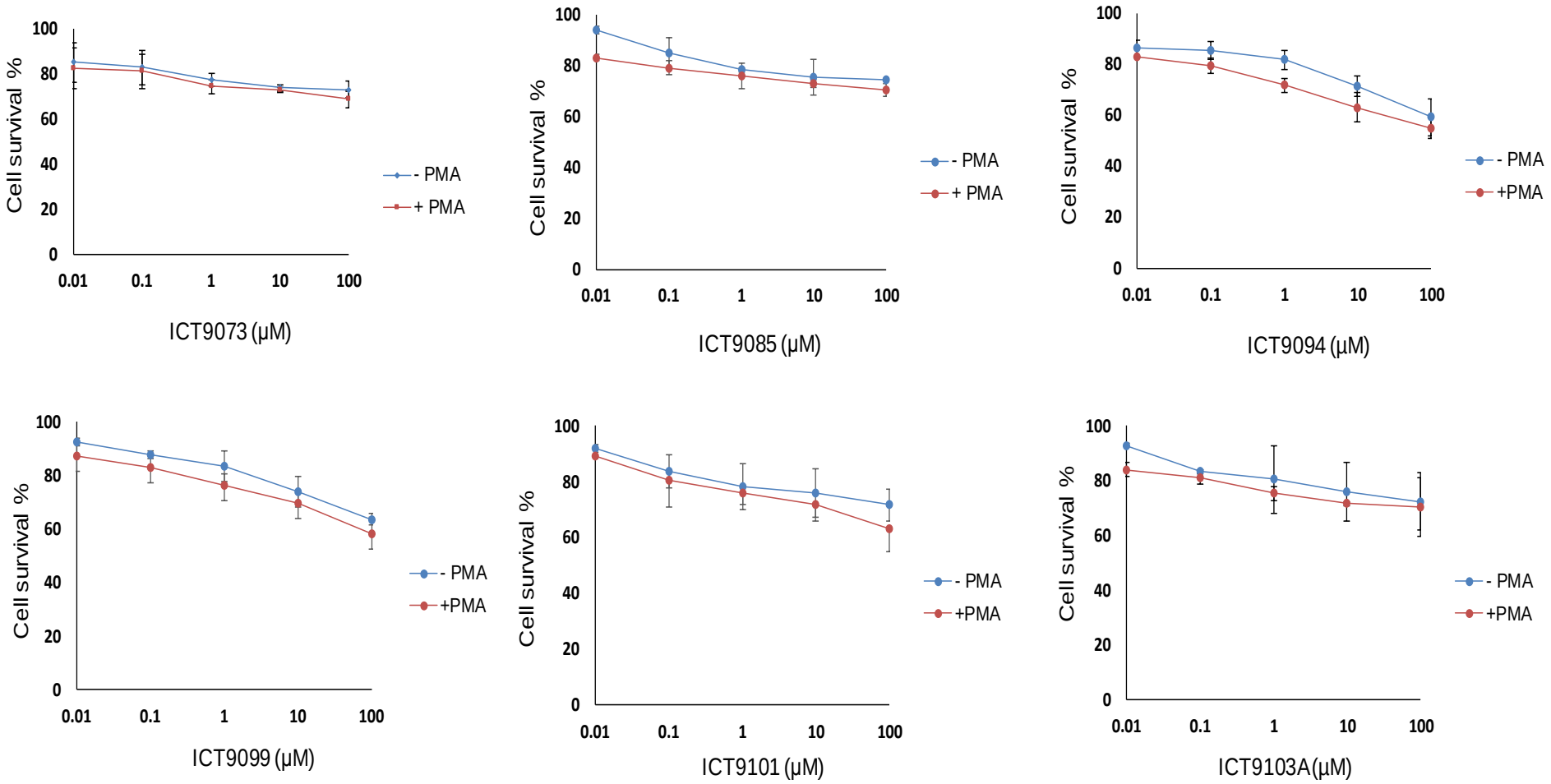

Figure 45 B: Measurement of the cytotoxicity of the second part of new small molecule integrin antagonist's panel for 4 h of drug exposure in K562 cells. Cells were pre-treated with 0.04 µM PMA for 40 h (red line) or not treated with PMA (blue line). Data are shown as mean ± standard deviation of 3 independent results.

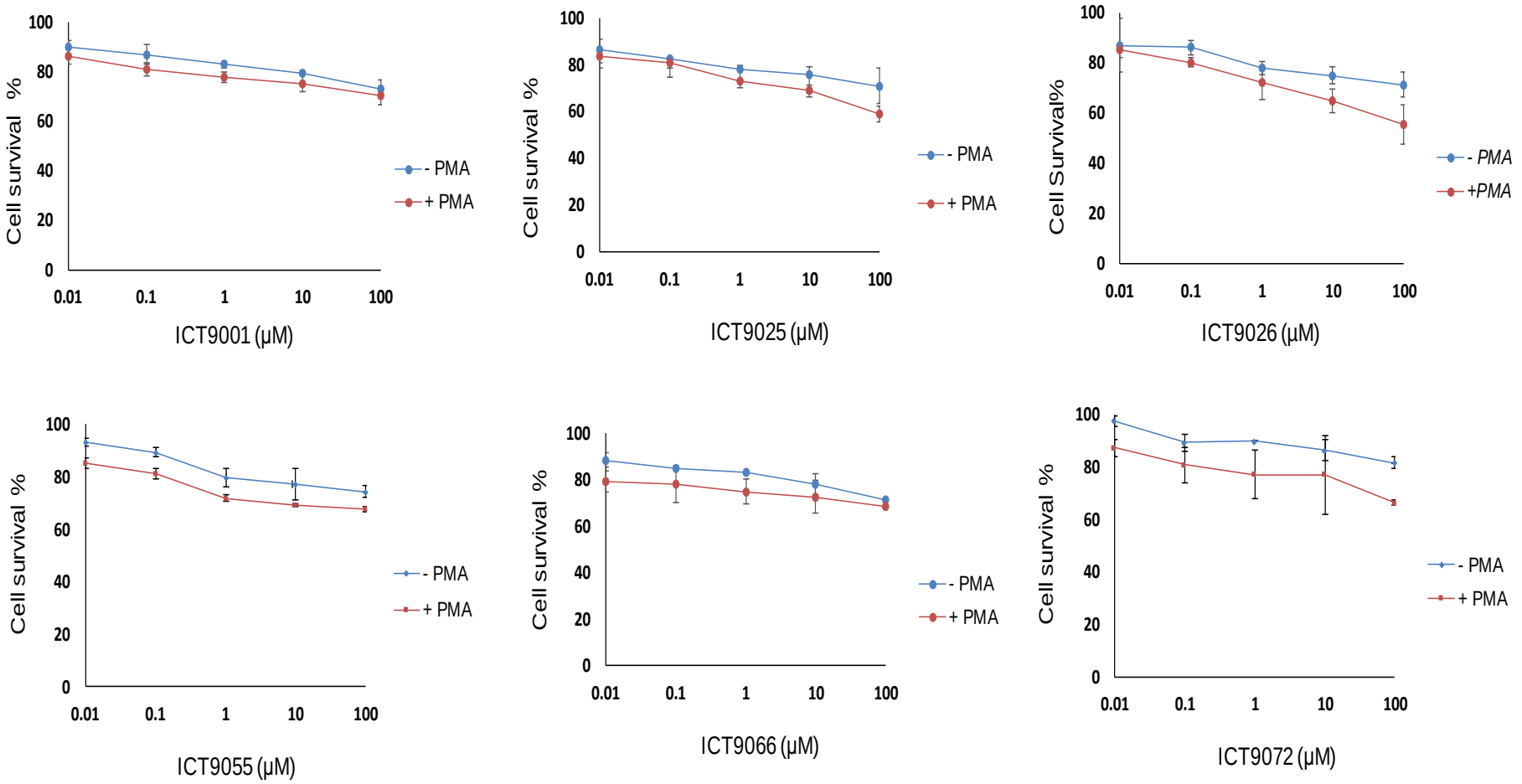

Figure 46 A: Measurement of the cytotoxicity of the first part of new small molecule integrin antagonist's panel for 96 h of drug exposure in K562 cells. Cells were pre-treated with 0.04µM PMA for 40 h (red line) or not treated with PMA (blue line). Data are shown as mean ± standard deviation of 3 independent results.

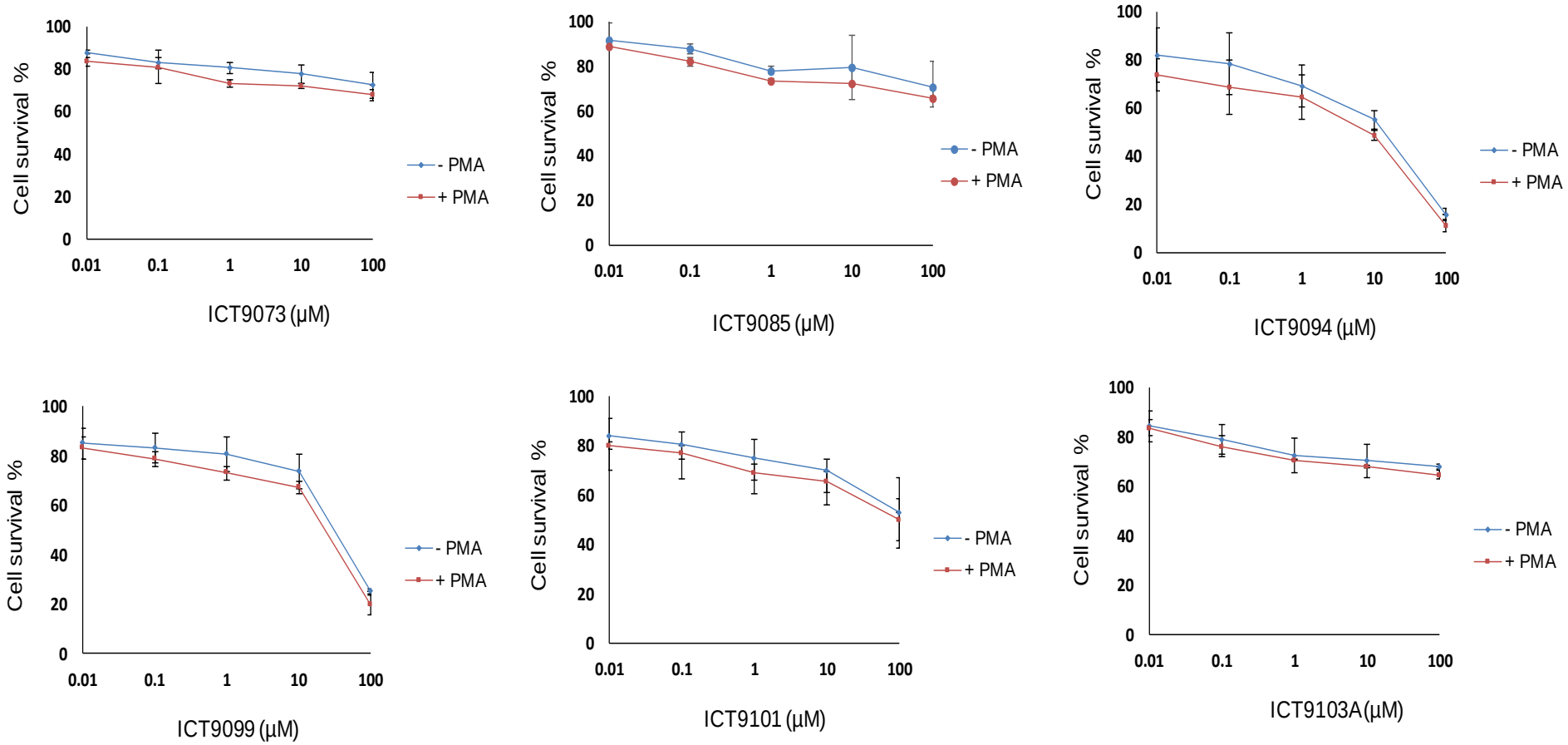

Figure 46 B: Measurement of the cytotoxicity of the second part of new small molecule integrin antagonist's panel for 96 h of drug exposure in K562 cells. Cells were pre-treated with 0.04µM PMA for 40 h (red line) or not treated with PMA (blue line). Data are shown as mean ± standard deviation of 3 independent results.

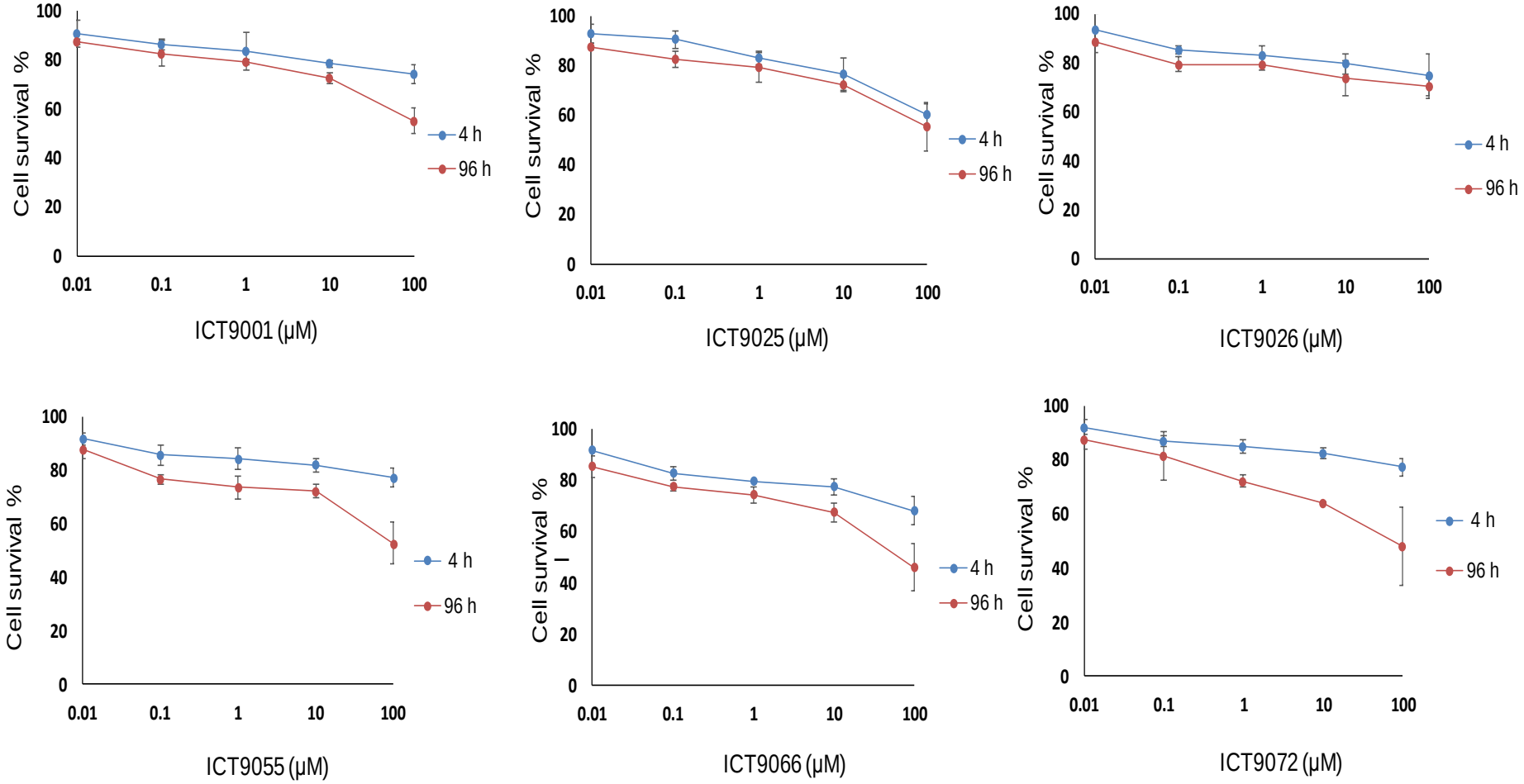

Figure 47 A: Measurement of the cytotoxicity of the first part of potential novel β3 integrin antagonist's panel in MCF-7 cells. Cells were treated with drug for 4 (blue lines) and 96 (red lines) hrs. Data are shown as mean ± standard deviation of 3 independent results.

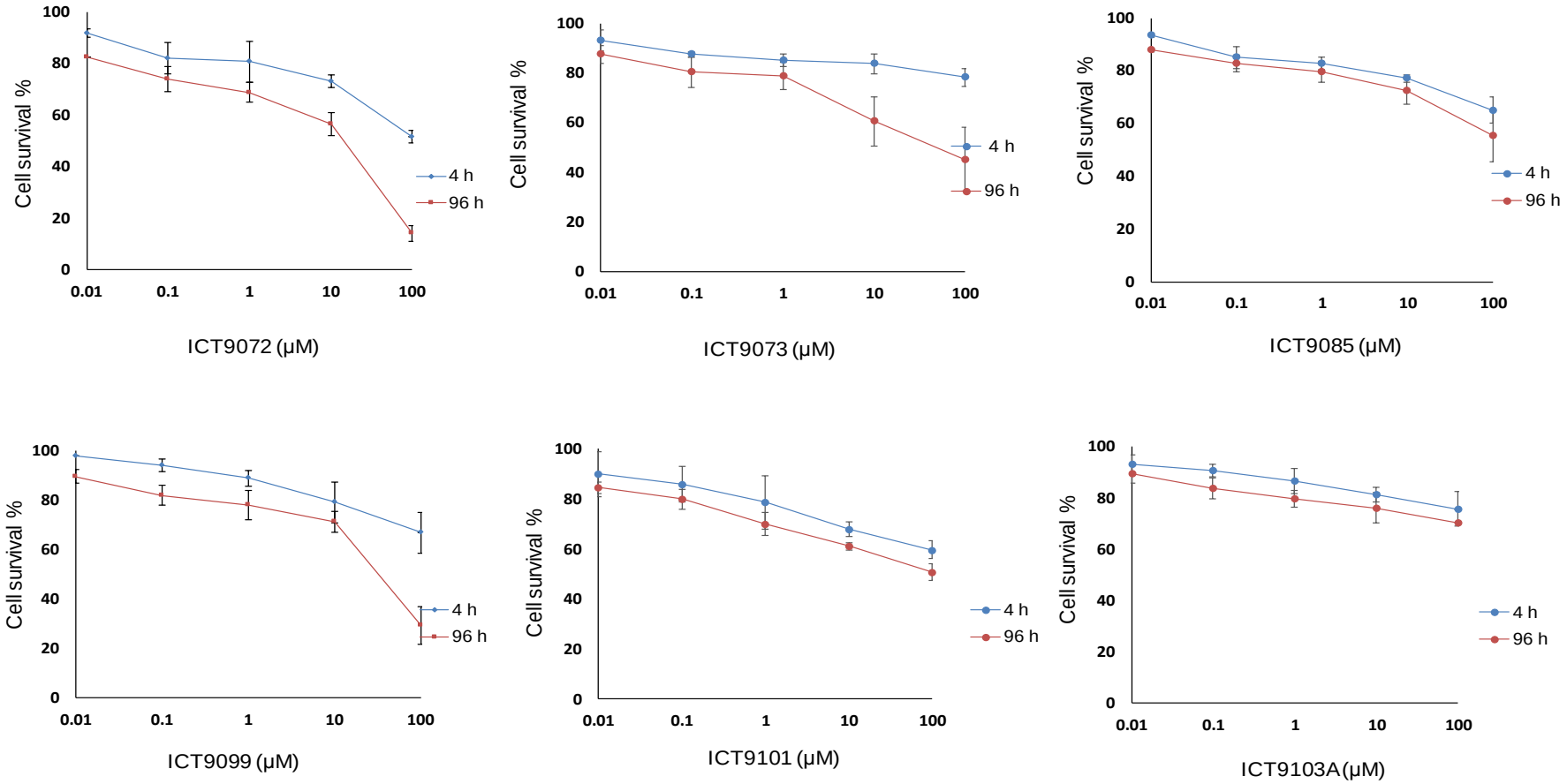

Figure 47 B: Measurement of the cytotoxicity of the second part of potential novel β3 integrin antagonist's panel in MCF-7 cells. Cells were treated with drug for 4 (blue lines) and 96 (red lines) hrs. Data are shown as mean ± standard deviation of 3 independent results.

4.4.3 Fibrinogen adhesion assay

The ability of K562 cells to adhere to fibrinogen in the presence and absence of PMA was investigated to determine whether PMA induced functionally active integrins and therefore whether the cell line could be used for an adhesion assay. The ability of MCF-7 cells to adhere to fibrinogen was determined.

4.4.3.1 Initial investigation of K562 cell binding to fibrinogen

Adhesion assay methods depend on the ability of integrin receptors on the cell surface to interact with extracellular matrix proteins on a coated plate. The adhesion of three different concentrations, $1X10^4$, 5X104 and $1X10^5$ K562 cells/ml, to two different concentrations of fibrinogen (2 and 5 µg/ml) was determined in the presence of PMA and absence (2 µM). Three different adhesion conditions were used: at 37°C for 4 hours, room temperature for 4 hours and no incubation. K562 cells treated with PMA showed greater adhesion than untreated cells. The optimum conditions for K562 cells (±PMA) to adhere to 2 µg/ml of fibrinogen in a 96-well plate were 37 °C for 4 hrs (Figure 48). However, the absorbance values of K562 cells in the presence of PMA (2 µM) were lower than desired.

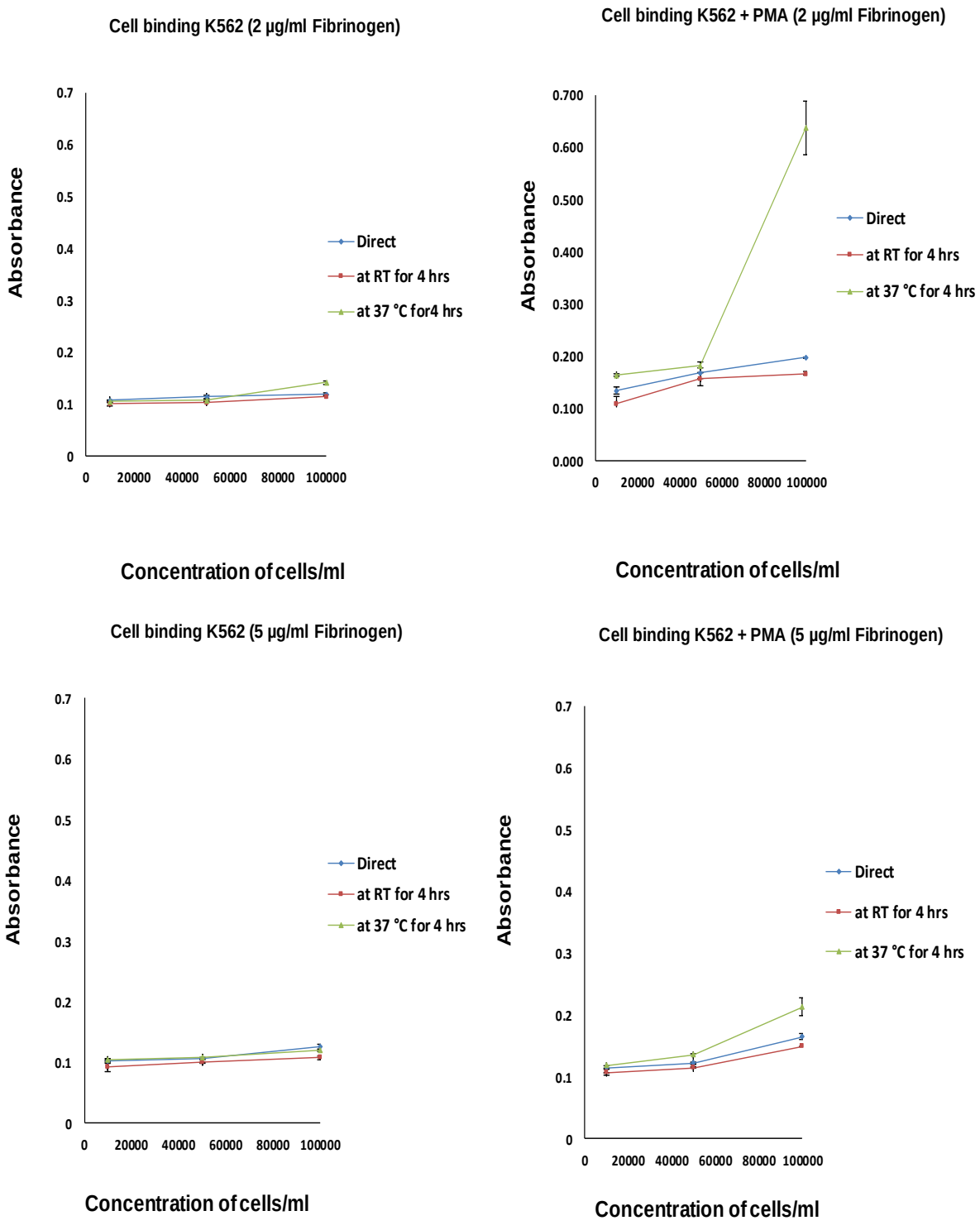

Figure 48: Optimization of K562 cell binding to fibrinogen. K562 (± 2 µM PMA) cells were applied to plates coated with 2 and 5 µg/ml of fibrinogen and adhered cells quantified either immediately (blue lines), after 4 hours at room temperature (red lines) or after 4 hours at 37 °C (green lines). Results shown are the mean ± SE of 3 independent experiments.

4.4.3.2 Optimisation of K562 cell binding to fibrinogen

The best cell binding was observed with cells incubated at 37 °C for 4 hours with 2 µg/ml of fibrinogen but the number of bound cells was low. To optimise the cell number, six different concentrations of cells (5 $X10^4$ - 5 $X10^5$ cell/ml) treated with 0.04 µM PMA (ideal dose was described in Chapter3) or untreated in the FCS-free medium were used. The results, as shown in Figure 49, indicate treatment with PMA increased cell binding to fibrinogen 500,000 cells/ml gave the greatest absorption value, therefore this was chosen as the best cell density for further experiments.

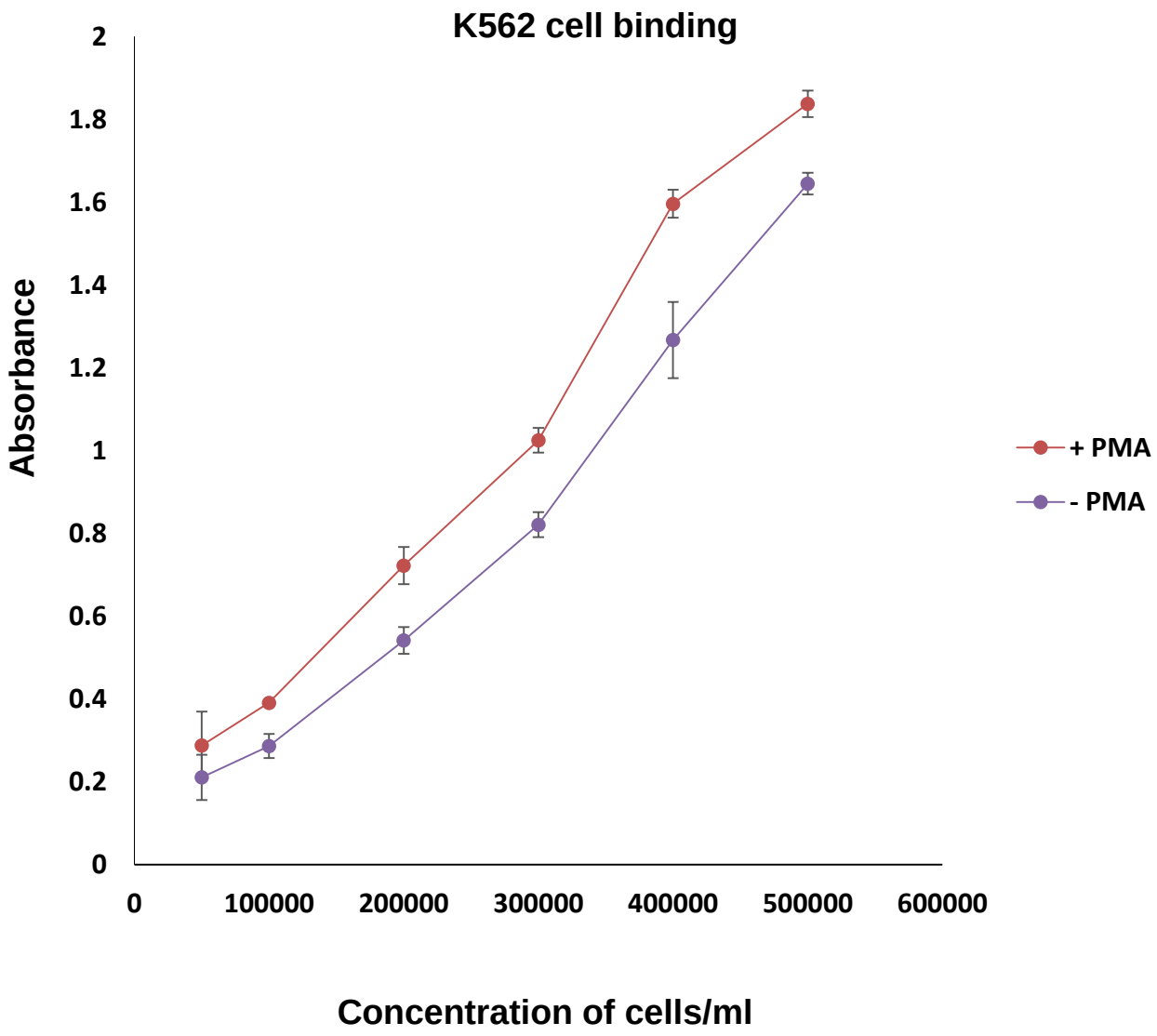

Figure 49: K562 cell binding to fibrinogen. K562 cells (± 0.04μM PMA) were allowed to adhere to a plate coated with 2 μg/ml of fibrinogen at 37 °C for 4 hours. Results shown are the mean ± standard error of 3 independent experiments.

4.4.3.3 Evaluation of MCF-7 cell binding to fibrinogen

The ability of MCF-7 cells to adhere to two different concentrations of fibrinogen (2 and 5 µg/ml) was investigated. To optimise the cell number, six different concentrations of cells (5 $X10^4$ – 5 $X10^5$ cell/ml) in FCS-free medium were used. Cell adhesion was higher on 5 µg/mL fibrinogen than 2 µg/mL fibrinogen. The highest absorbance was seen with 400,000 cells/ml (Figure 50).

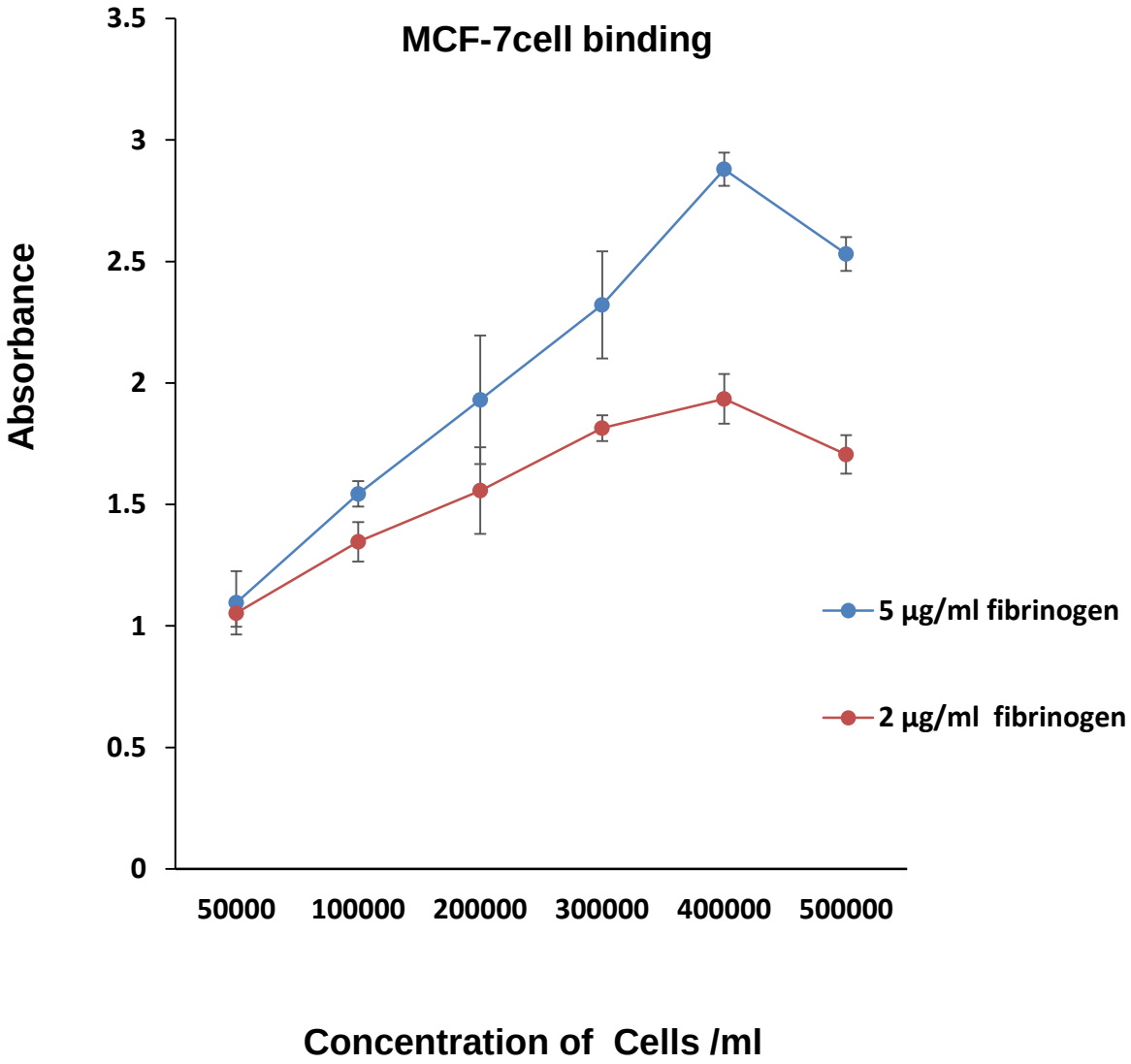

Figure 50: Optimisation of MCF-7 cell binding to fibrinogen. MCF-7 cells were allowed to adhere to a plate coated with 5 µg/ml of fibrinogen at 37 °C for 4 hours. Data are shown as mean ± standard error of 3 independent results.

4.4.3.4 Validation of the fibrinogen adhesion assay using cRGDfV and GR144053

In order to validate the fibrinogen adhesion assay for using with novel compounds which are expected to inhibit adhesion, the response of the cells to the positive controls cRGDfV and GR144053 was evaluated. Controls were used singly and in combination at different concentrations. There was an apparent inhibitory effect of combined drugs on the ability of K562 (±PMA) and MCF-7 cells to adhere to fibrinogen in a dose dependent manner whereas cRGDfV alone had a moderate effect and GR144053 had lower effect (Figure 51 and Figure 52). Adhesion was partially reliant on the β3 integrins in untreated K562 cells, and more dependent in PMA-treated cells, where 20 μM of combined antagonists almost completely blocked cell adhesion. In addition, adhesion was inhibited more than 50% in MCF-7 cells treated with 50 μM combined antagonists. The specific interaction between cRGDfV and GR144053 on these cell lines was evaluated by the combination index (CI) analysis where CI<1 indicates a synergistic effect. The results of all concentrations from each compound used (5, 10 and 20 μM with K562 and 5, 10, 20 and 50 μM with MCF-7) gave the synergistic effect. CI values for actual experimental points can be seen in Table 8, and IC_{50} values in Table 9.

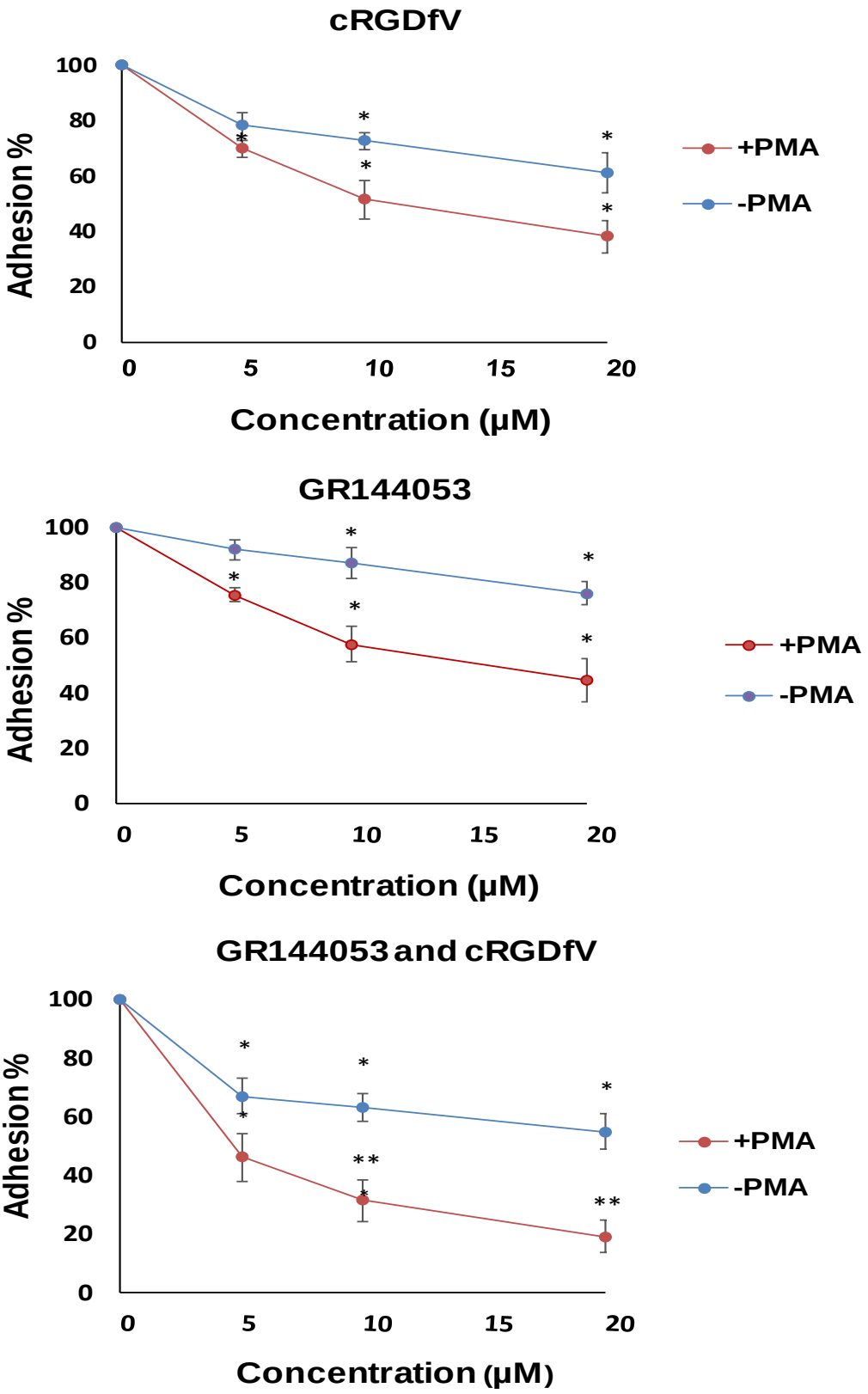

Figure 51: Effects of GR144053 and cRGDfV on K562 adhesion to fibrinogen. K562 cells (±0.04μM PMA) were treated with the compounds for 4 h. Values are the average of 3 independent experiments and error bars are SE. P values: * $p<0.05$ and ** $p<0.01$.

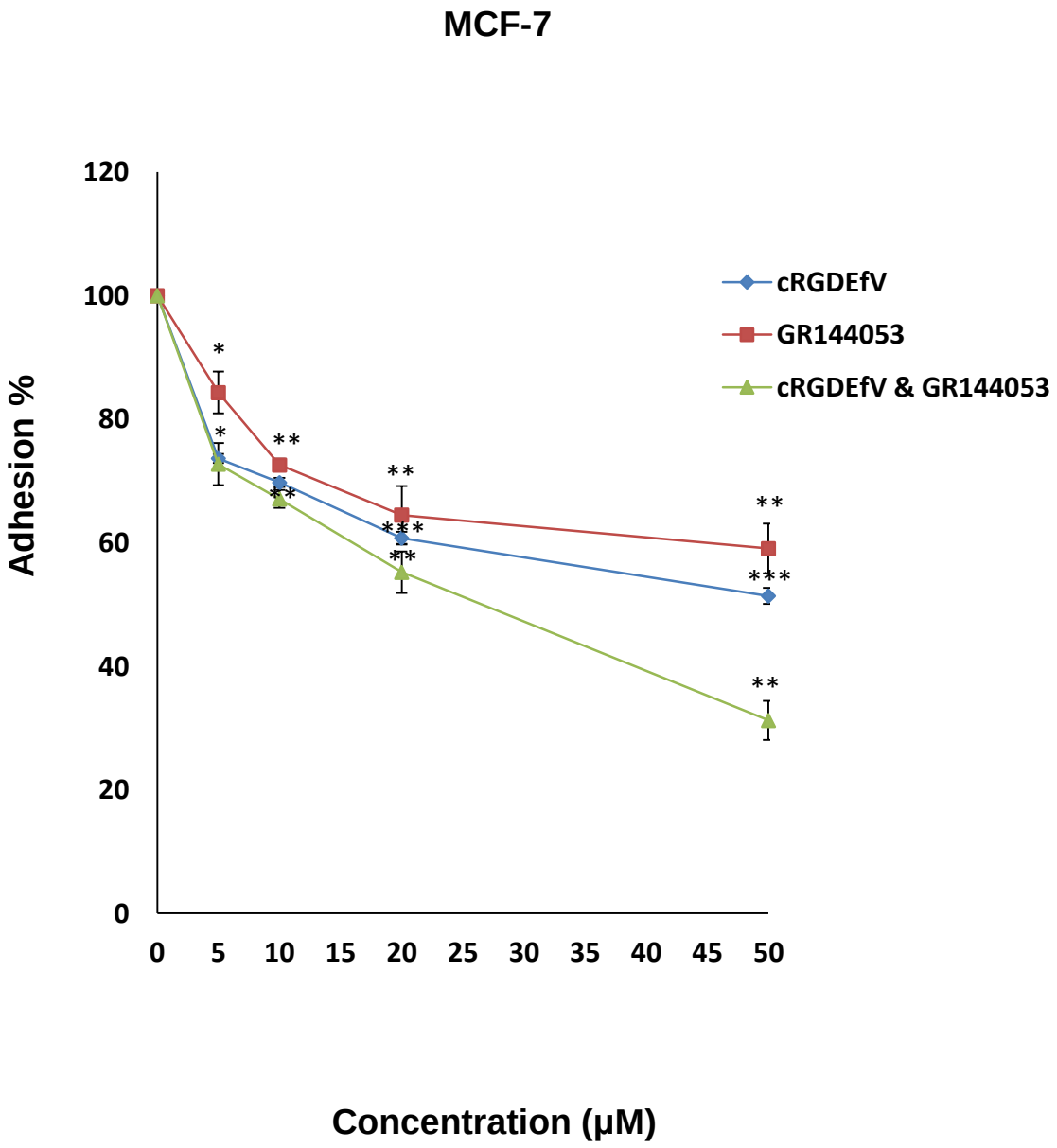

Figure 52: Effects of GR144053 and cRGDfV on MCF-7 adhesion to fibrinogen. MCF-7 cells were treated with the compounds for 4 h. Values are the average of 3 independent experiments and error bars are SE. P values: * P<0.05, **P.0.01 and ***P>0.001.

Table 8: Combination index (CI) values for the effect of GR144053 and cRGDfV on adhesion to fibrinogen. CI < 0.1 very strong synergism, 0.1 - 0.3 strong synergism, 0.3 - 0.7 synergism, 0.7 - 0.85 moderate synergism, 0.85 - 0.90 slight synergism, and 0.90 -1.10 additive.

Type of Cell	Total Dose	CI Value	Interpretation
K562 with PMA	5.0	0.33	Synergism
	10.0	0.34	Synergism
	20.0	0.34	Synergism
K562 without PMA	5.0	0.25	Strong synergism
	10.0	0.42	Synergism
	20.0	0.51	Synergism
MCF-7	5.0	0.46	Synergism
	10.0	0.62	Synergism
	20.0	0.42	Synergism
	50.0	0.16	Strong synergism

4.4.3.5 Effects of potential β3 integrin antagonists on K562 (±PMA) cell adhesion.

The compounds were tested at a range (0.1, 1.0, 10 and 100 μM) of nontoxic concentrations in the fibrinogen adhesion assay. The compounds developed in house have been tested using in K562 cells with and without PMA. Initial screening concentrations were selected based on their cytotoxicity results for 96 hours. In the adhesion assay, the K562 cells were treated for 4 hours only. Consequently, as the exposure time was shorter than it was expected that these concentrations would not have a cytotoxic effect. The compounds tested inhibited cell adhesion to fibrinogen at different concentrations (0.1, 1.0, 10 and 100 μM). ICT9055 showed the highest effect of inhibiting PMA treated K562 cell adhesion at the lowest concentration while ICT9072 and ICT9073 had lower effects at the same concentration compared to untreated cells. IC_{50} values were calculated for ICT9055, ICT9072 and ICT9073 and are given in Table 9. Compared to cRGDfV (anti-αvβ3) and GR144053 (anti-αIIbβ3) controls, in the presence of PMA (66 ± 3%, $P<0.001$), the ICT9055 (77 ± 4.2%) had a higher effect than the combined control, while ICT9072 (63 ± 3.9%) and ICT9073 (59 ± 1.92%) had a slightly lower effect than combined control. In the absence of PMA, all three compounds had a highest showed greater anti-adhesive activity than the positive control (40 ± 5%, $P<0.01$) (Figure 53). ICT9026 (40 ±12%), ICT9094 (42 ± 7%), ICT9099 (51 ± 4%), ICT9101 (42 ±11%), and ICT9103A (49.5 ± 5%) were moderately effective at inhibiting PMA treated K562 cell adhesion at 10 μM, but these compounds showed lower anti-adhesive activity than the combined controls (Figures 54 A and B). A summary of the effect of all the β3 integrin antagonists on the adhesion of

K562±PMA at 10 μM is shown in Figure 55. ICT9055 (77± 4.2%) had a higher effect than the combined control, while ICT9072 (63 ± 3.9%) and ICT9073 (59 ± 1.9%) had a lower effect than combined control. In the absence of PMA, all three compounds had a higher effect than the positive control (40 ± 5%, $P<0.01$).

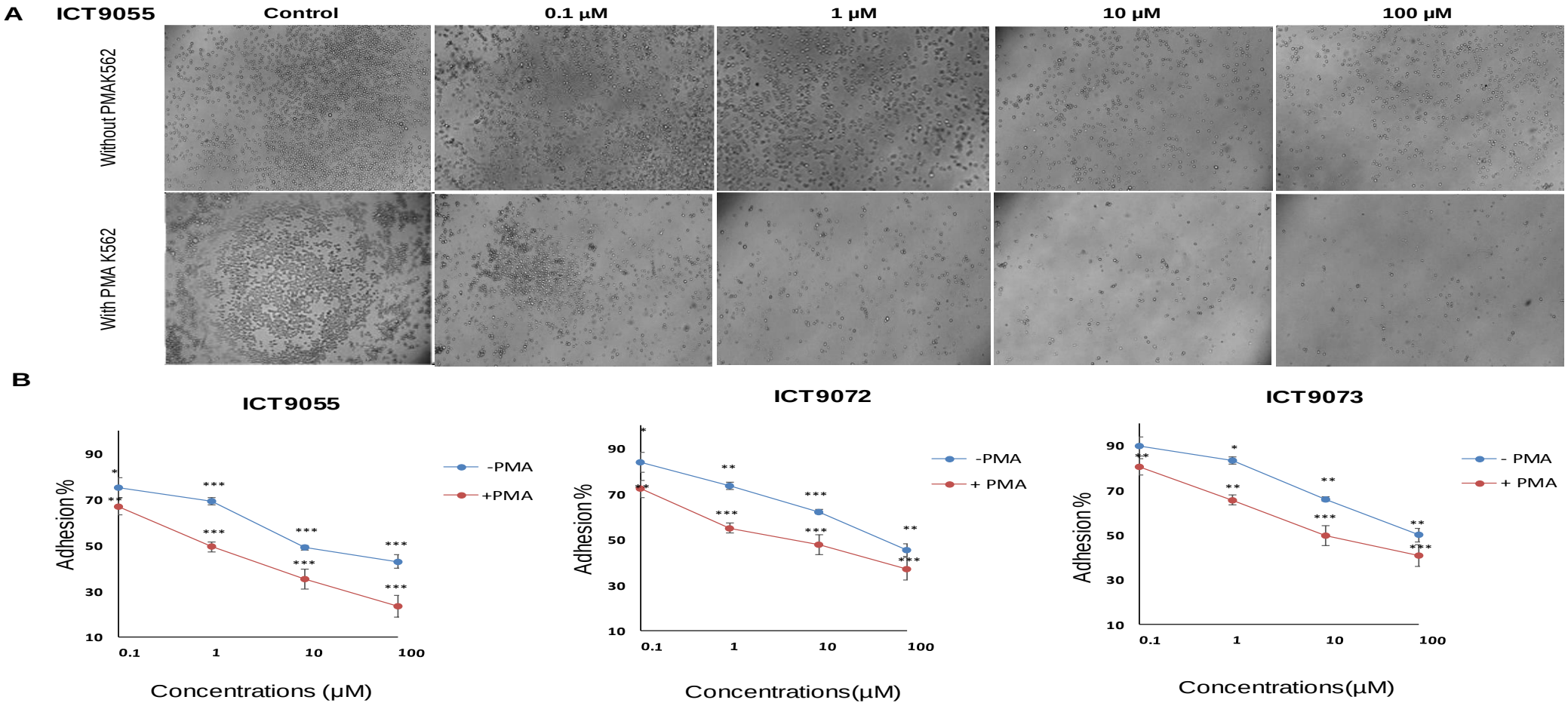

Figure 53: Effect of small molecule integrin antagonists on K562 cell adhesion to fibrinogen. **(**A) Representative images the fibrinogen adhesion assay with K562 cells treated with the indicated concentrations of ICT9055 for 4 hours compared to untreated cells. (B) Quantification of anti-adhesive effects of ICT9055, ICT9072 and ICT9073 on K562 cells with (red lines) and without (blue lines) 0.04µM PMA * p <0.05, ** p < 0.01, *** p < 0.001.

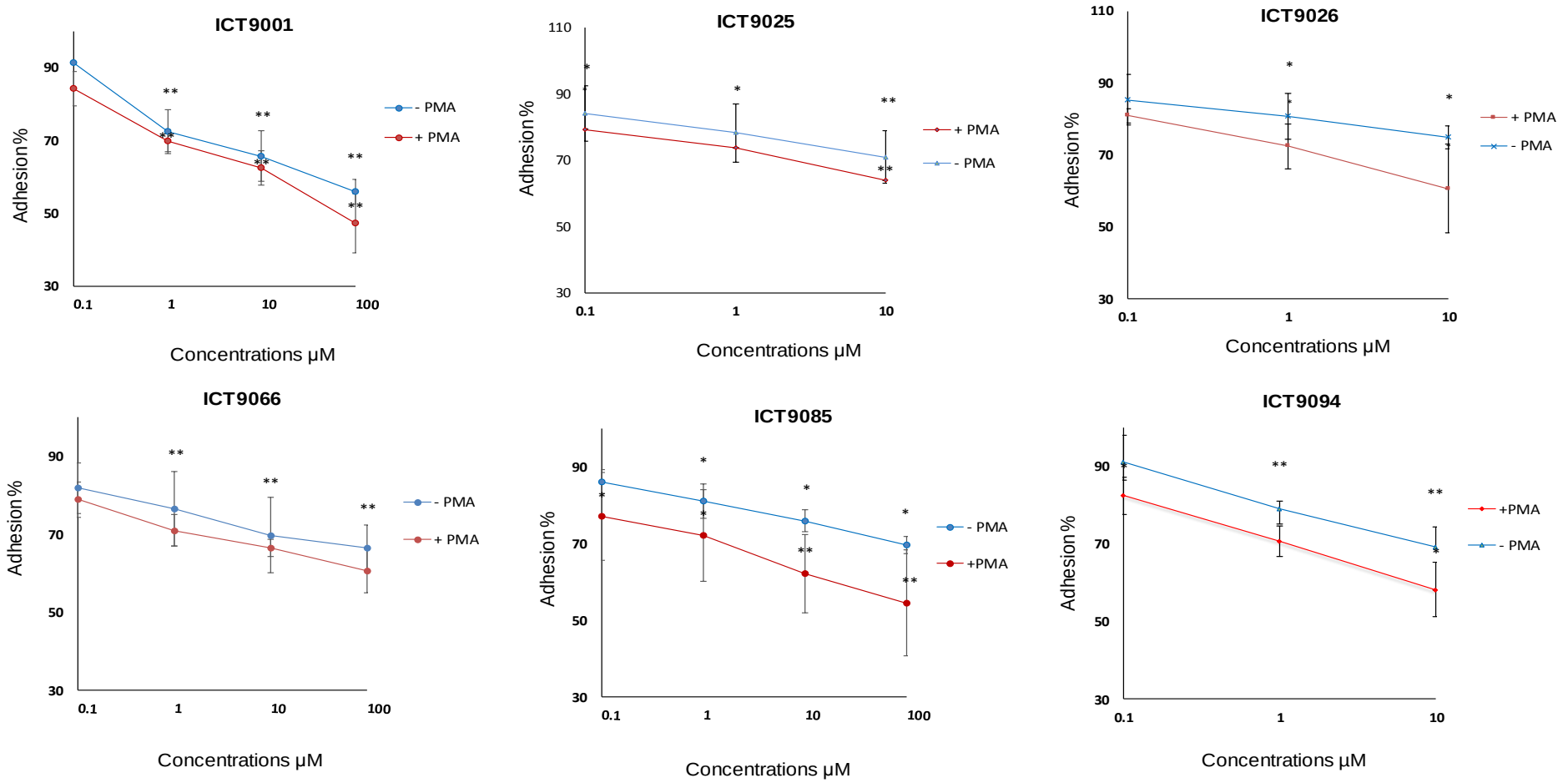

Figure 54 A: Effect of small molecule integrin antagonists on K562 cell adhesion to fibrinogen. Quantification of anti-adhesive effects of ICT9001, ICT9025, ICT9026, ICT9066, ICT9085 and ICT9094 on K562 cells with (red lines) and without (blue lines) 0.04µM PMA. * $p < 0.05$, ** $p < 0.01$.

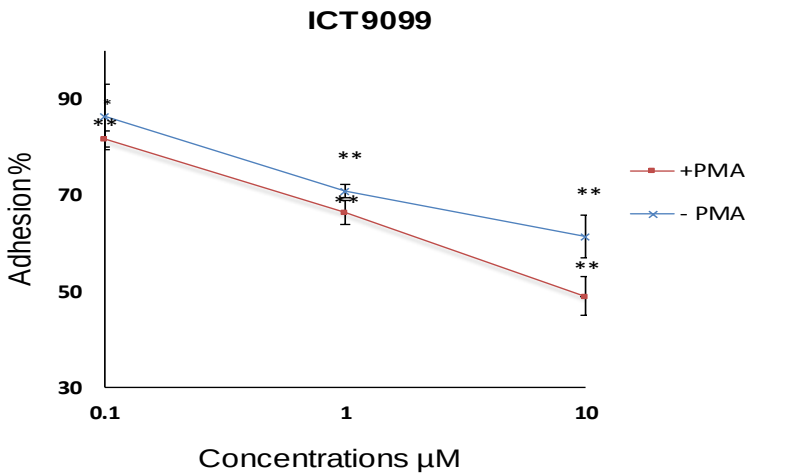

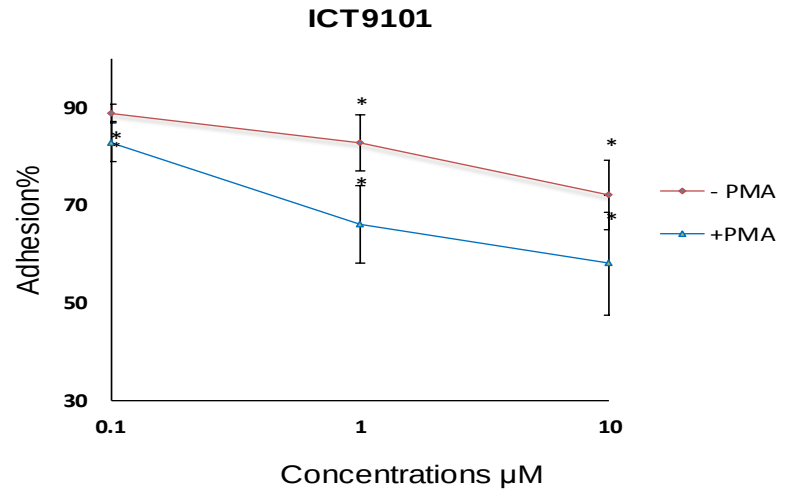

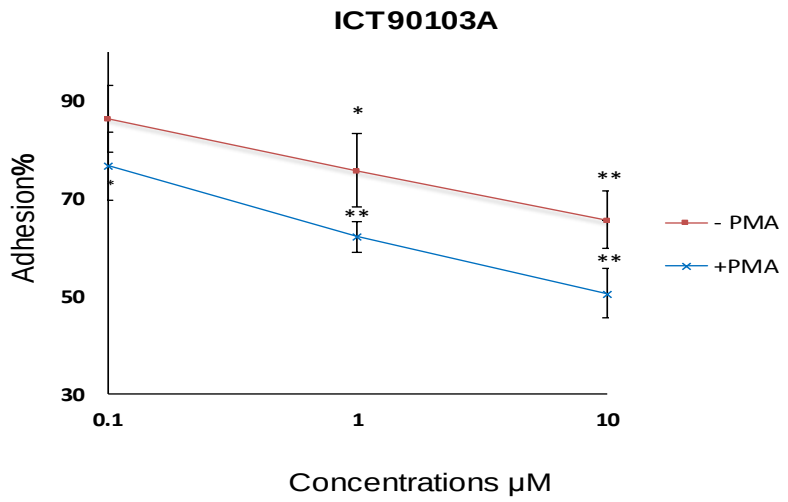

Figure 54 B: Effect of small molecule integrin antagonists on K562 cell adhesion to fibrinogen. Quantification of anti-adhesive effects of ICT9099, ICT9101 and ICT9103A on K562 cells with (red lines) and without (blue lines) 0.04µM PMA. * p <0.05, ** p < 0.01.

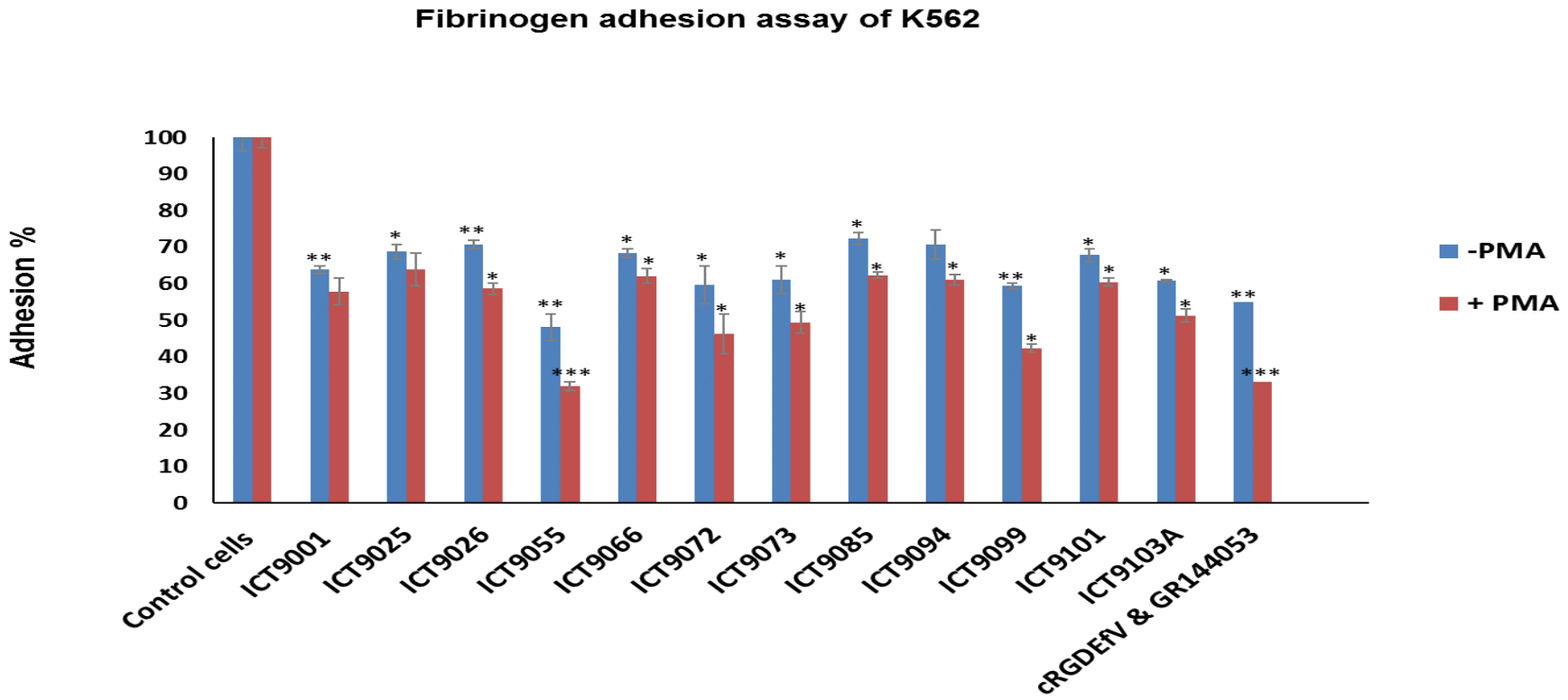

Figure 55: Inhibition of K562 cell adhesion to fibrinogen by ICT compounds. Cells pre-treated with 0.04 μM PMA (red bars) or not treated with PMA (blue bars) were treated with 10 μM compound for 4 hours. % adhesion is normalised compared to cells not treated by ICT compounds. * p <0.05, ** p <0.01 and *** p <0.0001.

4.4.3.6 Effects of novel integrin antagonists on MCF-7 cell adhesion.

The compounds were also tested in MCF-7 cells according to the same procedure. IC_{50} values are given in Table 9. ICT9055, ICT9072 and ICT9073 significantly reduced the adhesion of the MCF-7 cells to fibrinogen at the lowest concentration, while other ICT compounds had smaller effects at the same concentration (Figure 56 and Figures 57 A and B). Compared to the positive control (61 ± 2.2%), ICT9055 (68 ± 6.3%) at 10 μM was more potent, whereas ICT9072 (55.7 ± 4%), ICT9073 (50 ± 4.5%) at 1 μM and ICT9099 (57.5 ± 5.8%) at 10 μM were less potent. The rest of the ICT compounds at 10 μM were less potent (< 40%) than control (59 ± 7.9%).

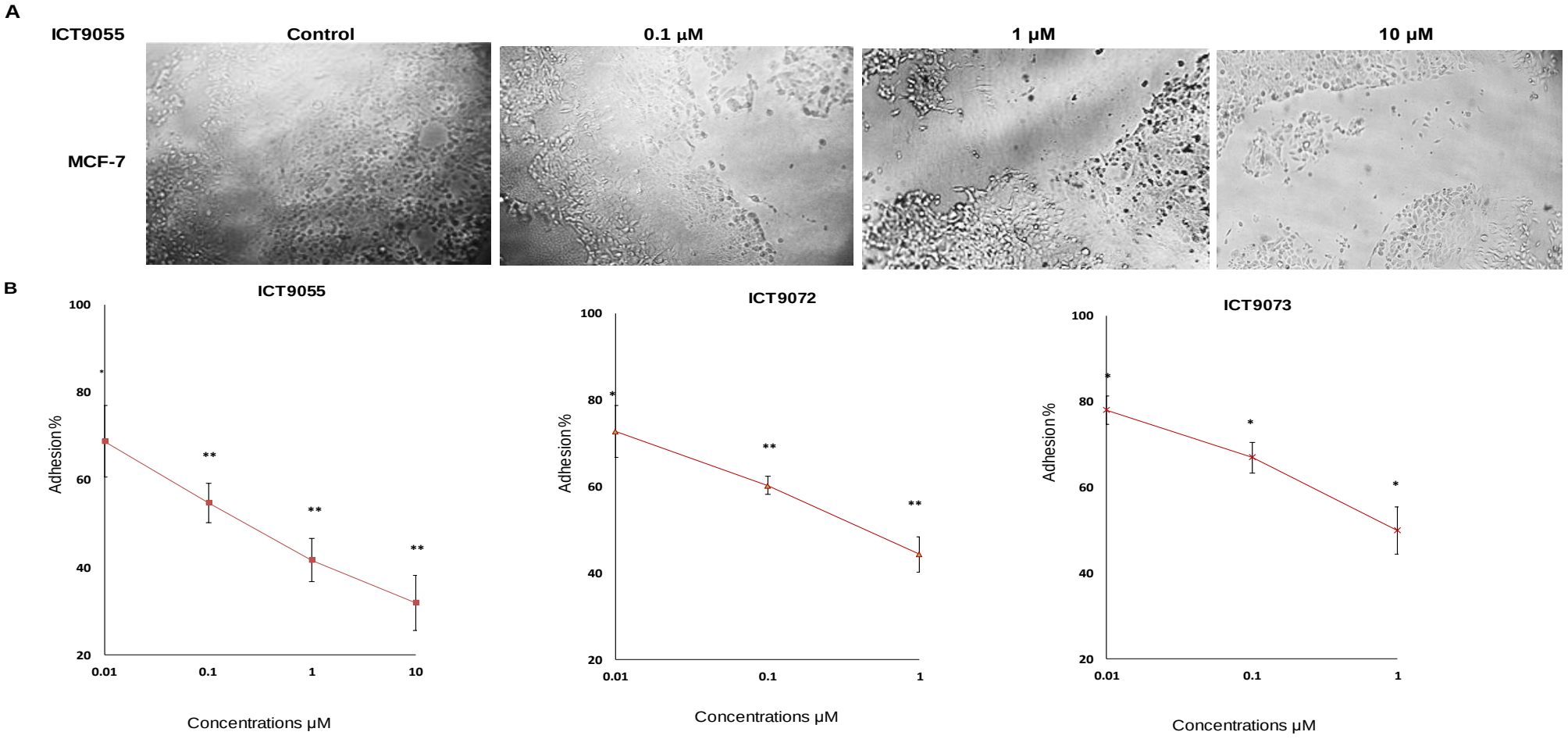

Figure 56: Effect of small molecule integrin antagonists on MCF-7 cell adhesion to fibrinogen. (A) Representative images the fibrinogen adhesion assay with MCF-7 cells treated with the indicated concentrations of ICT9055 for 4 hours. (B) Quantification of anti-adhesive effects of ICT9055, ICT9072 and ICT9073 on MCF-7 cells. * p <0.05, ** p <0.01.

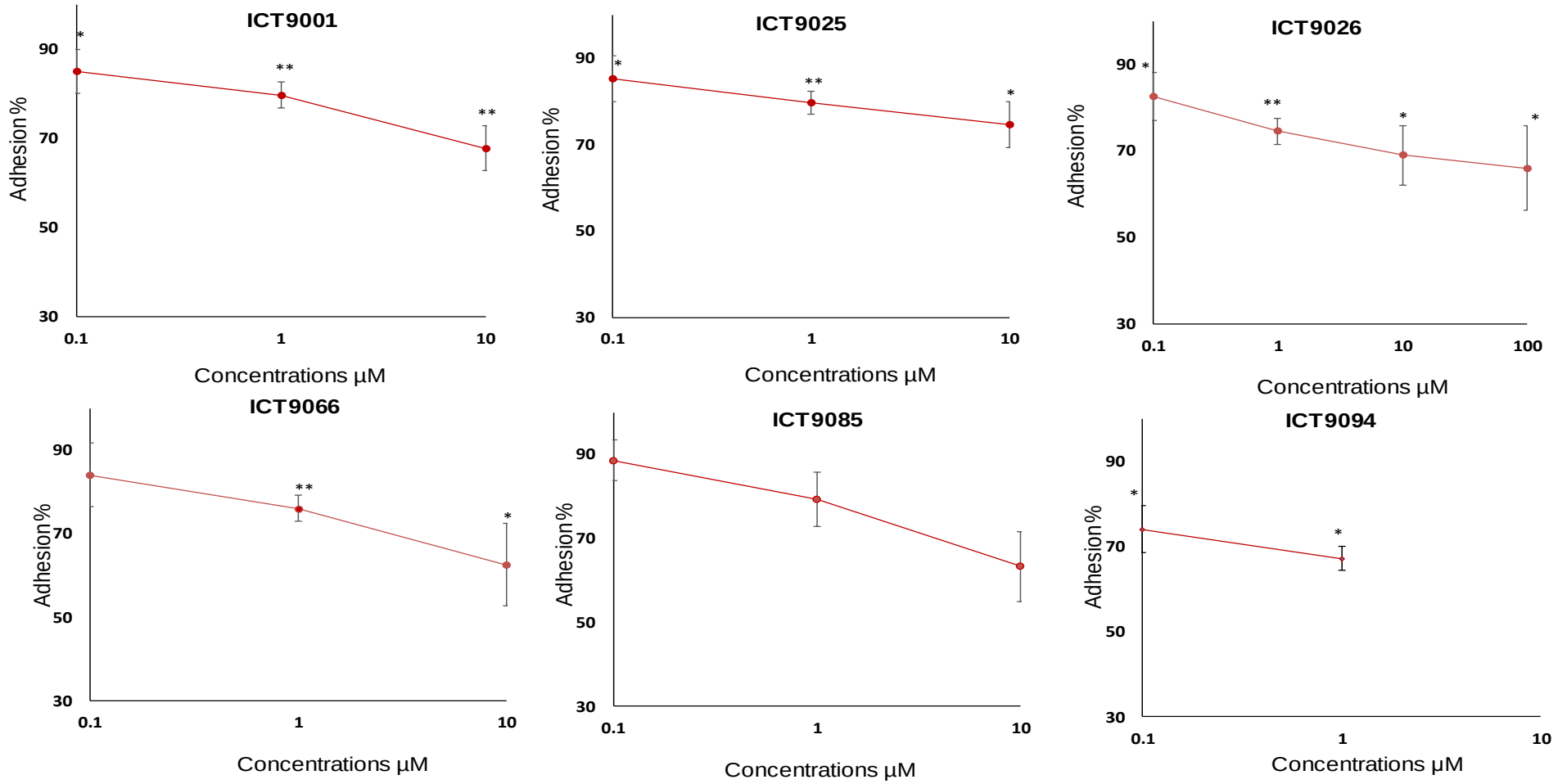

Figure 57 A: Effect of small molecule integrin antagonists MCF-7 cell adhesion to fibrinogen. Quantification of anti-adhesive effects of ICT9001, ICT9025, ICT9076, ICT9066, ICT9085 and ICT9094 on MCF-7 cells compared to untreated cells. * $p < 0.05$, ** $p < 0.01$.

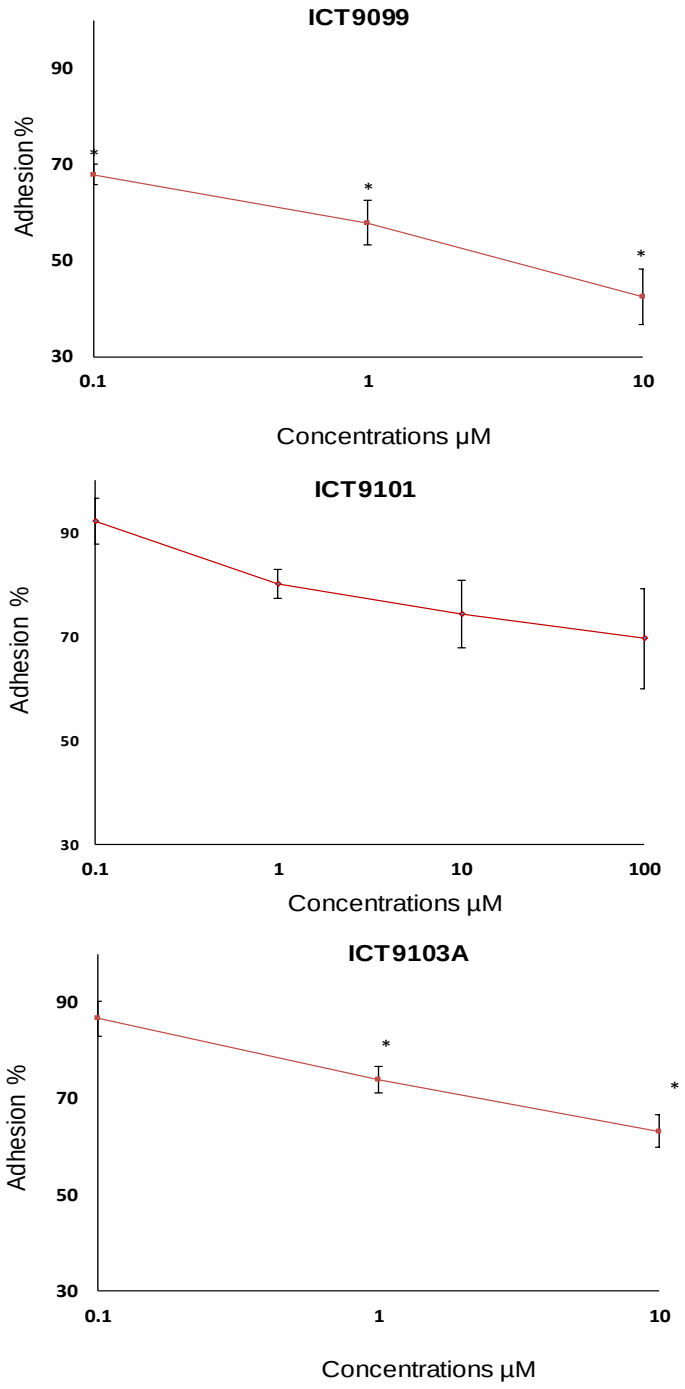

Figure 57 B: Effect of small molecule integrin antagonists MCF-7 cell adhesion to fibrinogen. Quantification of anti-adhesive effects of ICT9099, ICT9101 and ICT9103A on MCF-7 cells compared to untreated cells. * $p < 0.05$.

Table 9: IC_{50} values for inhibition of cell adhesion by β3 integrin antagonists.

ICT compounds	K562-PMA IC_{50} ± SD (μM)	K562 +PMA IC_{50} ± SD (μM)	MCF7 IC_{50} ± SD (μM)
ICT9001	>100	84.66 ± 24	>100
ICT9025	> 100	> 100	> 100
ICT9026	> 100	> 100	> 100
ICT9055	9.3 ± 0.75	0.96 ± 0.1	0. 43 ± 0.34
ICT9066	> 100	> 100	> 100
ICT9085	> 100	> 100	> 100
ICT9072	79.7 ±17.7	6.6 ± 4	0.71 ± 0.2
ICT9073	98 ± 3.6	13.7 ± 7.97	0.86 ± 0.2
ICT9094	> 100	> 100	> 100
ICT9099	> 100	8.58 ± 1.3	2.6 ± 2.3
ICT9101	> 100	> 100	> 100
ICT9103A	> 100	8.64 ± 1.9	> 100
cRGDfV	20	12.6 ± 6.4	50
GR144053	> 20	14.1 ± 5.2	> 50
GR144053 and cRGDfV	17.7 ± 3.2	5.9 ±1	24.4 ± 4.8

4.4.3.6.1 Effect of ICT9055 on the viability of non-adherent cells.

To further investigate the mechanism of action of ICT compounds on cancer cell lines, the most active compound, ICT9055, was selected for use in a viability assay. The viability of non-adherent cells collected during adhesion assays was determined using the trypan blue exclusion test. The results showed no apparent effect on the K562 cells (±PMA) after 4 hours of treatment. However, at 24 hours, cell viability was reduced by both ICT9055 and control compounds. The viability of MCF-7 cells was decreased after both 4 and 24 hours. Hoechst staining was used to determine whether the cell death in this assay was associated with apoptotic changes by IF. Cells with signs of apoptosis (fragmented nuclei) were observed (Figure 58 A and B and Figure 59 A and B).

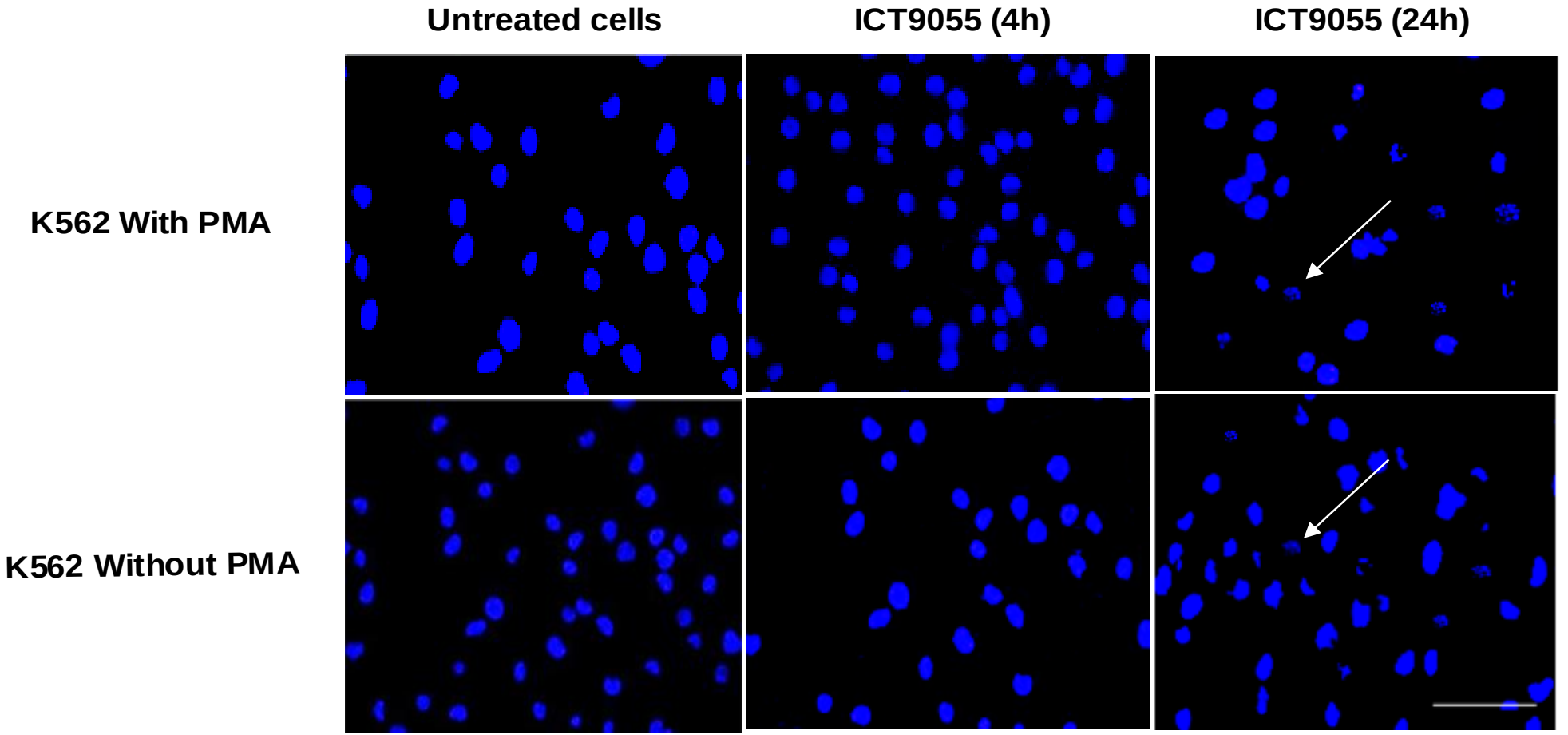

Figure 58 A: Viability of K562 non-adherent cells upon ICT9055 treatment. Nuclei staining with Hoechst in K562 (±PMA) non-adherent cells treated with ICT9055 showing signs of apoptotic morphology (white arrows). Scale bar = 50µm.

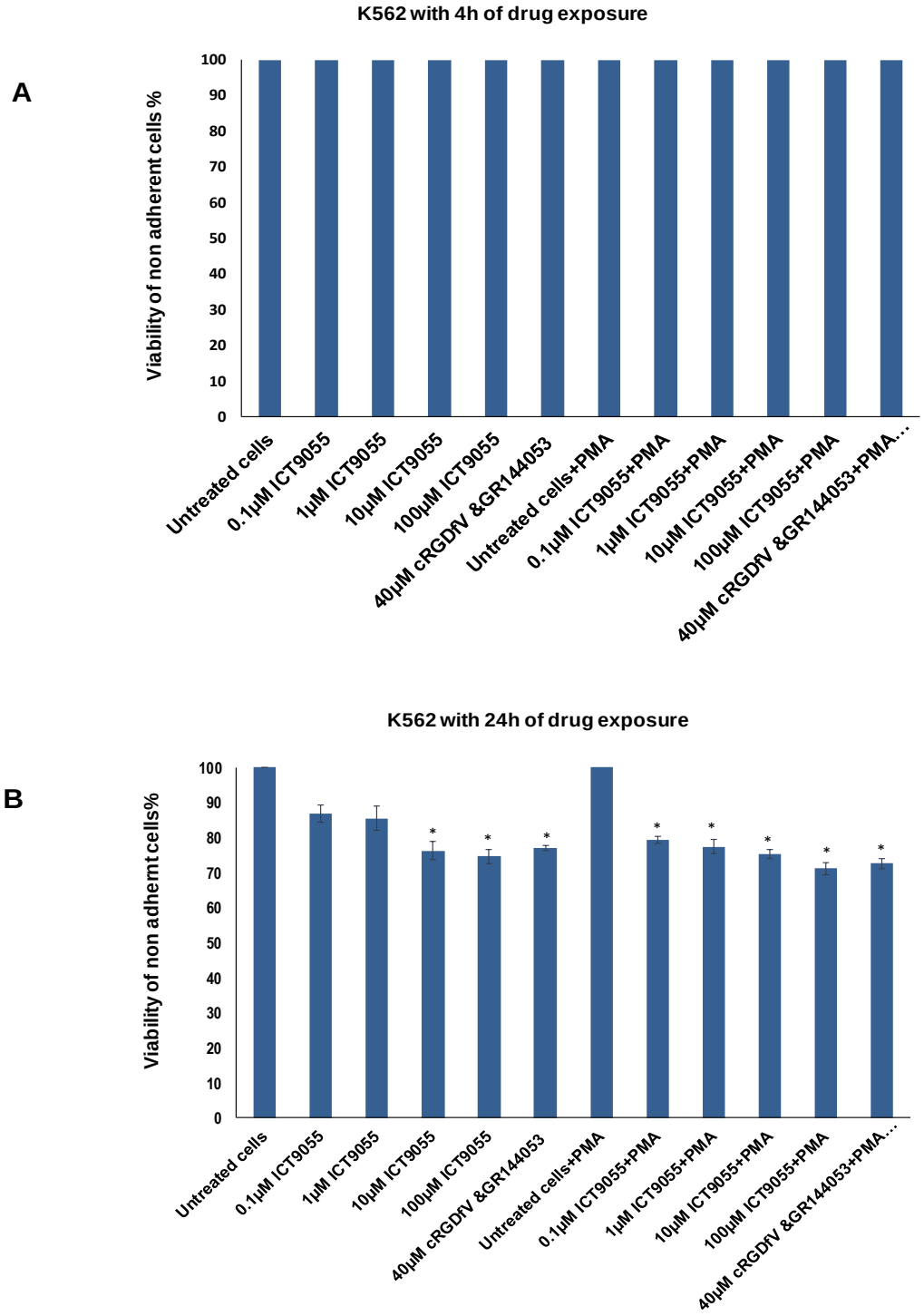

Figure 58 B: Viability of K562 non-adherent cells upon ICT9055 treatment. (A) Viability of K562 (±PMA) cells treated with ICT9055 for 4 hrs determined using the trypan blue assay. (B) Viability of K562 (±PMA) cells treated with ICT9055 for 24 hrs determined using the trypan blue assay. * P<0.05.

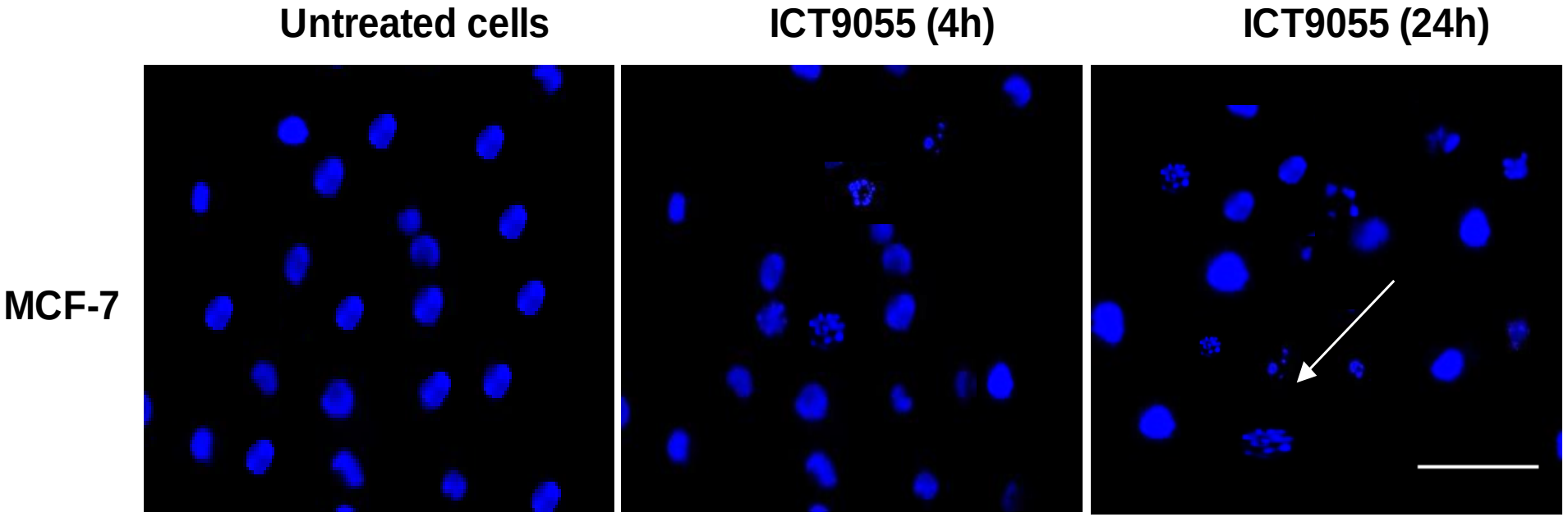

Figure 59 A: Viability of MCF-7 non-adherent cells upon ICT9055 treatment using the trypan blue assay. Nuclei staining with Hoechst in MCF-7 non-adherent cells treated with ICT9055 showing signs of apoptotic morphology (white arrows). Scale bar = 50µm.

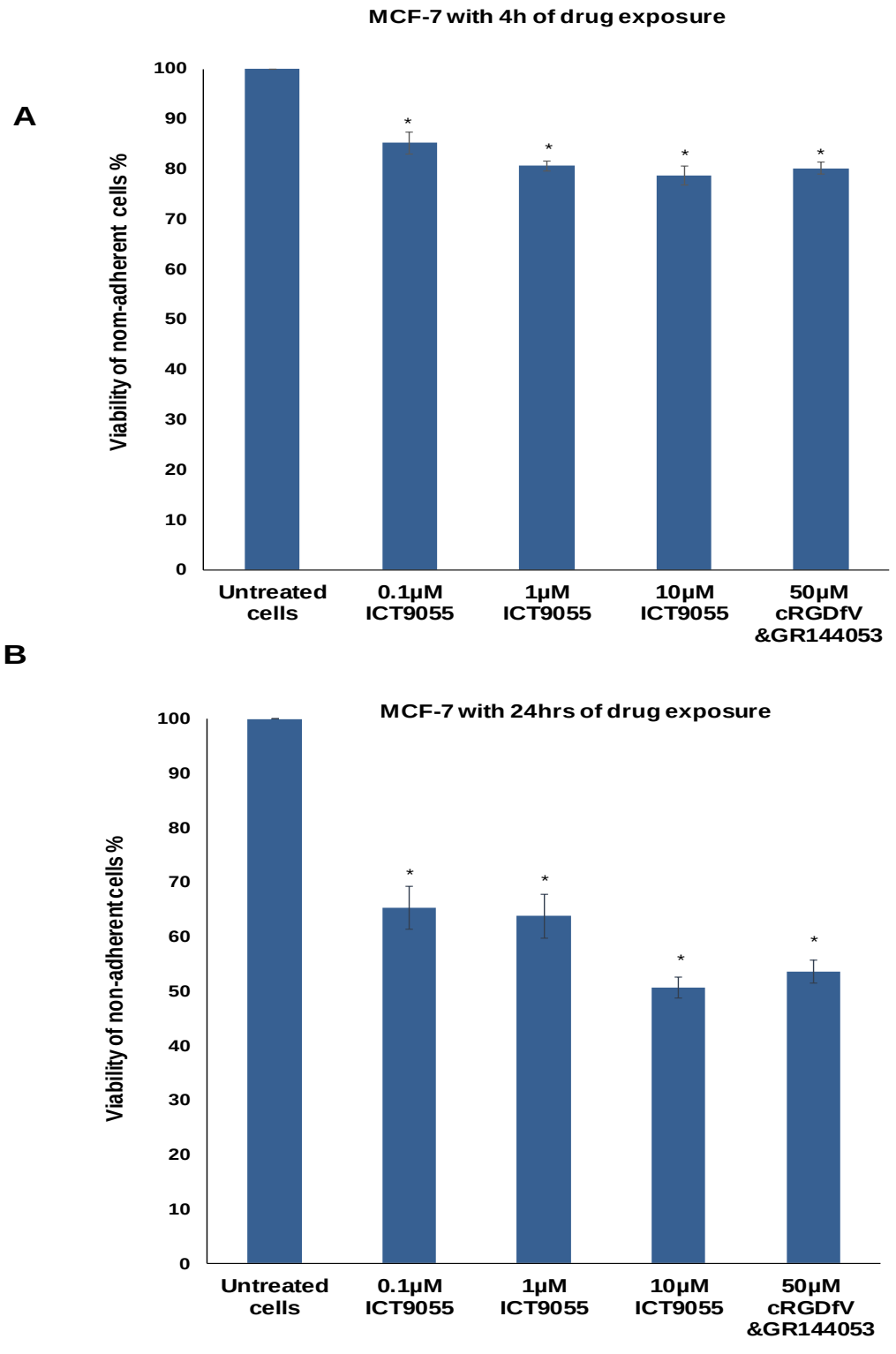

Figure 59 B: Viability of MCF-7 non-adherent cells upon ICT9055 treatment using the trypan blue assay. (A) MCF-7 cells treated with ICT9055 for 4 hrs determined using the trypan blue assay. (B) Viability of MCF-7 cells treated with ICT9055 for 24 hrs determined using the trypan blue assay**.** * $p<0.05$.

4.4.4 Validation of the fibrinogen detachment assay using cRGDfV and GR144053

The detachment of K562 and MCF-7 cells from fibrinogen induced by integrin antagonists was first investigated using cRGDfV and GR144053 singly and in combination. Combination of the control compounds caused a larger amount of cell detachment than single compounds. Inhibition of β3 function caused partial detachment of untreated K562 cells and greater detachment of PMA-treated cells, where 40 μM combined antagonists had more effect than single compounds (Figure 60). Inhibition of β3 function also caused partial detachment of MCF-7 cells, with 50 μM combined antagonists having a greater effect than single compounds (Figure 61). Combination index analysis showed the two compounds had a strongly synergistic effect at all concentrations tested (Table 10).

Table 10: Combination index values for cRGDfV/GR144053-induced detachment from fibrinogen. CI < 0.1 very strong synergism, 0.1 - 0.3 strong synergism 0.3 - 0.7 synergism, 0.7 - 0.85 moderate synergism, 0.85 - 0.90 slight synergism, and 0.90 -1.10 additive

Type of Cells	Total Dose (μM)	CI Value	Interpretation
K562 with PMA	5.0	0.20	Strong synergism
	10.0	0.12	Strong synergism
	20.0	0.17	Strong synergism
	40.0	0.16	Strong synergism
K562 without PMA	5.0	0.18	Strong synergism
	10.0	0.13	Strong synergism
	20.0	0.17	Strong synergism
	40.0	0.19	Strong synergism
MCF-7	5.0	0.34	Synergism
	10.0	0.26	Strong synergism
	20.0	0.30	Strong synergism
	50.0	0.44	Synergism

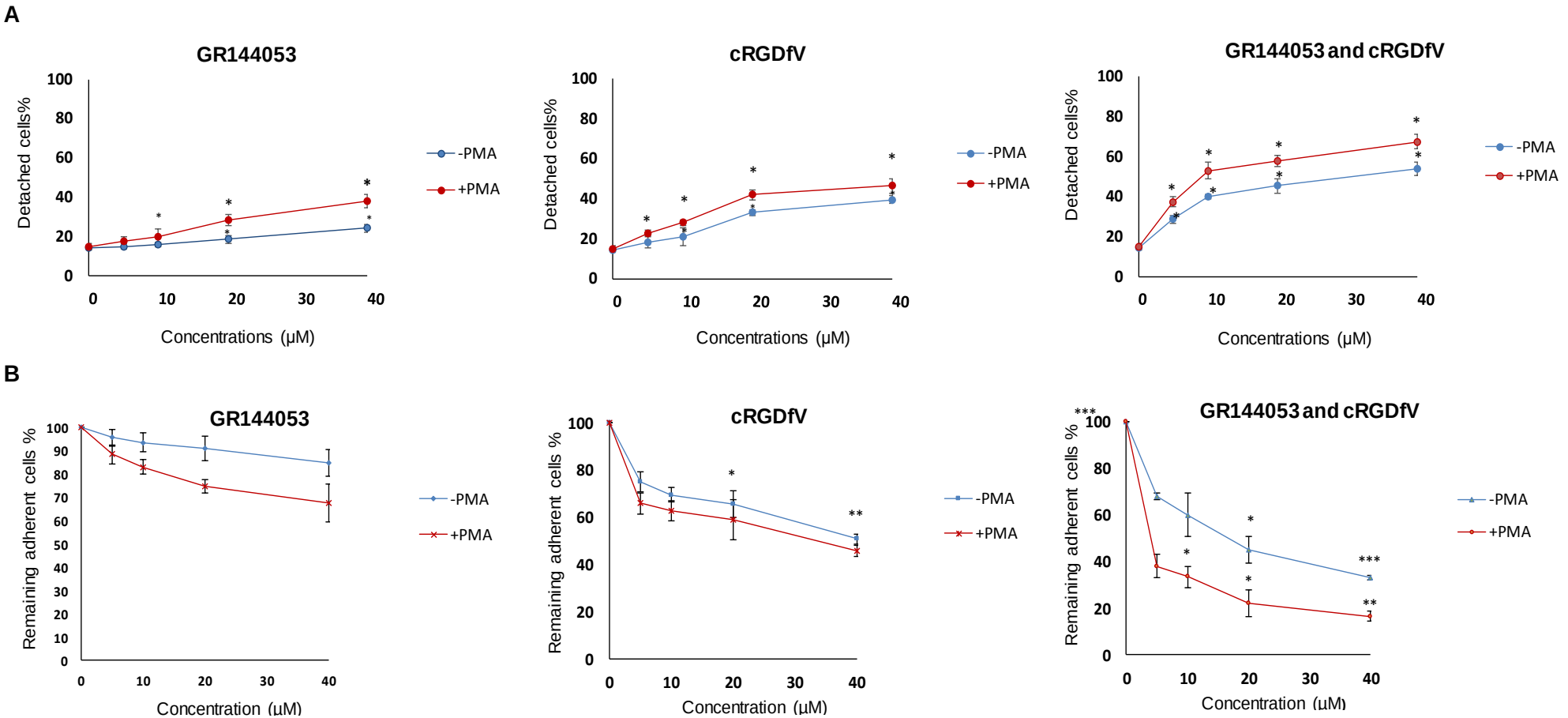

Figure 60: Effects of cRGDfV and GR144053 on K562 cells detachment. Cells (± 0.04μM PMA) were treated with the stated concentration of compounds for 6 h, then number of detached cells quantified by counting with haemocytometer. (A) Number of detached cells (B) Number of remaining attached cells. Values are the average of 3 independent experiments and error bars are SE. * $p<0.05$

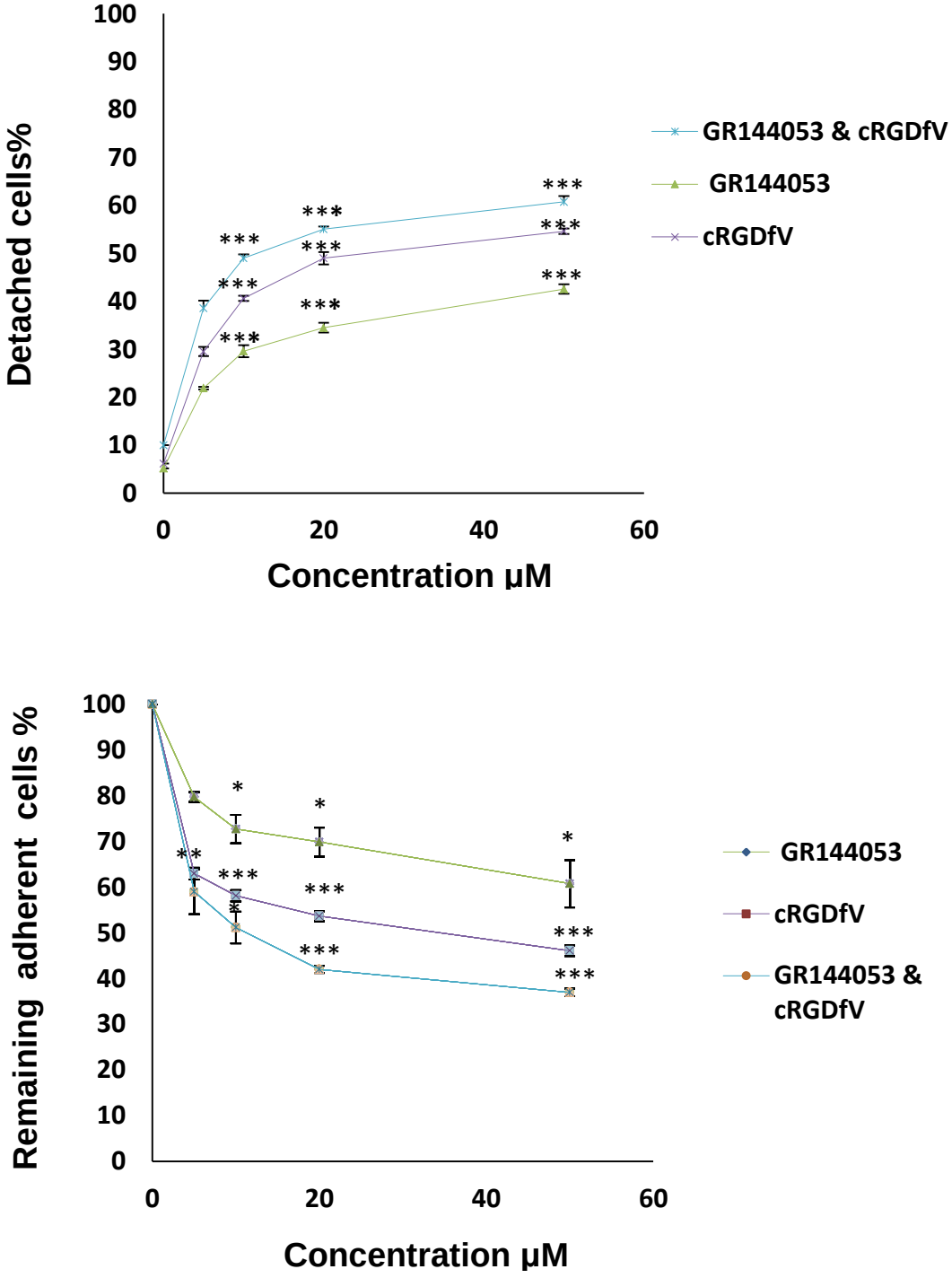

Figure 61: Effects of cRGDfV and GR144053 on MCF-7 cells detachment. Cells were treated with the stated concentration of compounds for 6 hours, then number of detached cells quantified by counting with haemocytometer. (A) Number of detached cells (B) Number of remaining attached cells. Values are the average of 3 independent experiments and error bars are SE. *p <0.05, ** p<0.01 and *** p<0.001.

Subsequently, a time course of cell detachment was performed (Figure 62 and Figure 63). Detachment determinations were performed after 2, 4 and 6 hour's incubation with cRGDfV and GR144053 singly and in combination at 50 μM. As anticipated, a time-dependent increase in the percentage of detached cells was shown which was accompanied by a corresponding decrease in the percentage of remaining attached cells in both cell lines. Combined antagonists had a greater effect than single compounds. Doses of 40 μM and 50 μM of the combined controls for 6 hours were selected for use in K562 and MCF-7 respectively as comparators with ICT compounds.

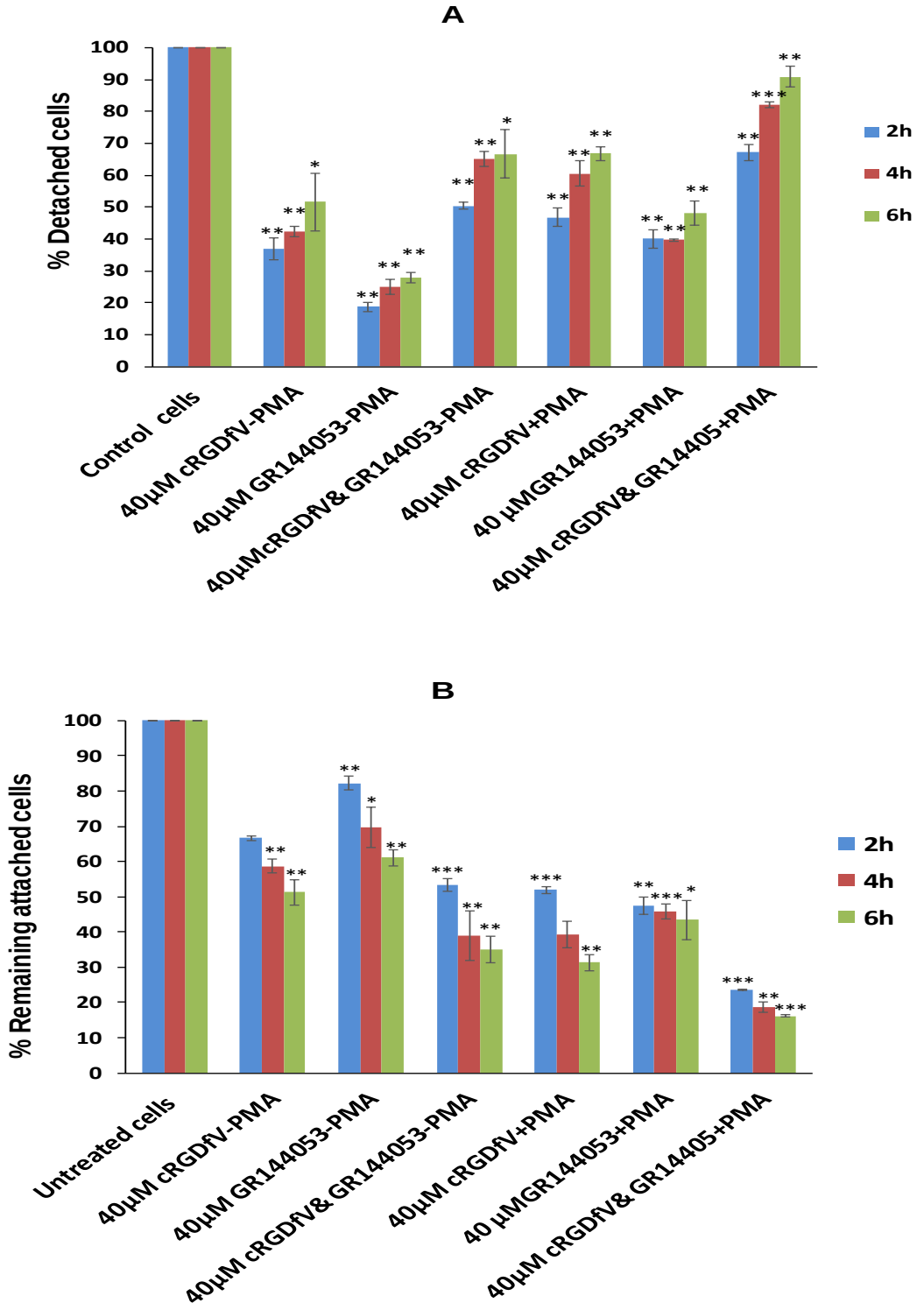

Figure 62: Effects of cRGDfV and GR144053 on K562 cell adhesion. Cells (± 0.04µM PMA) were treated with the stated concentration of compounds for 2, 4 and 6 hours, then number of detached cells quantified by counting with haemocytometer. (A) Number of detached cells (B) Number of remaining attached cells. Values are the average of 3 independent experiments and error bars are SE. * $p < 0.05$. ** $p < 0.01$ and *** $p < 0.001$.

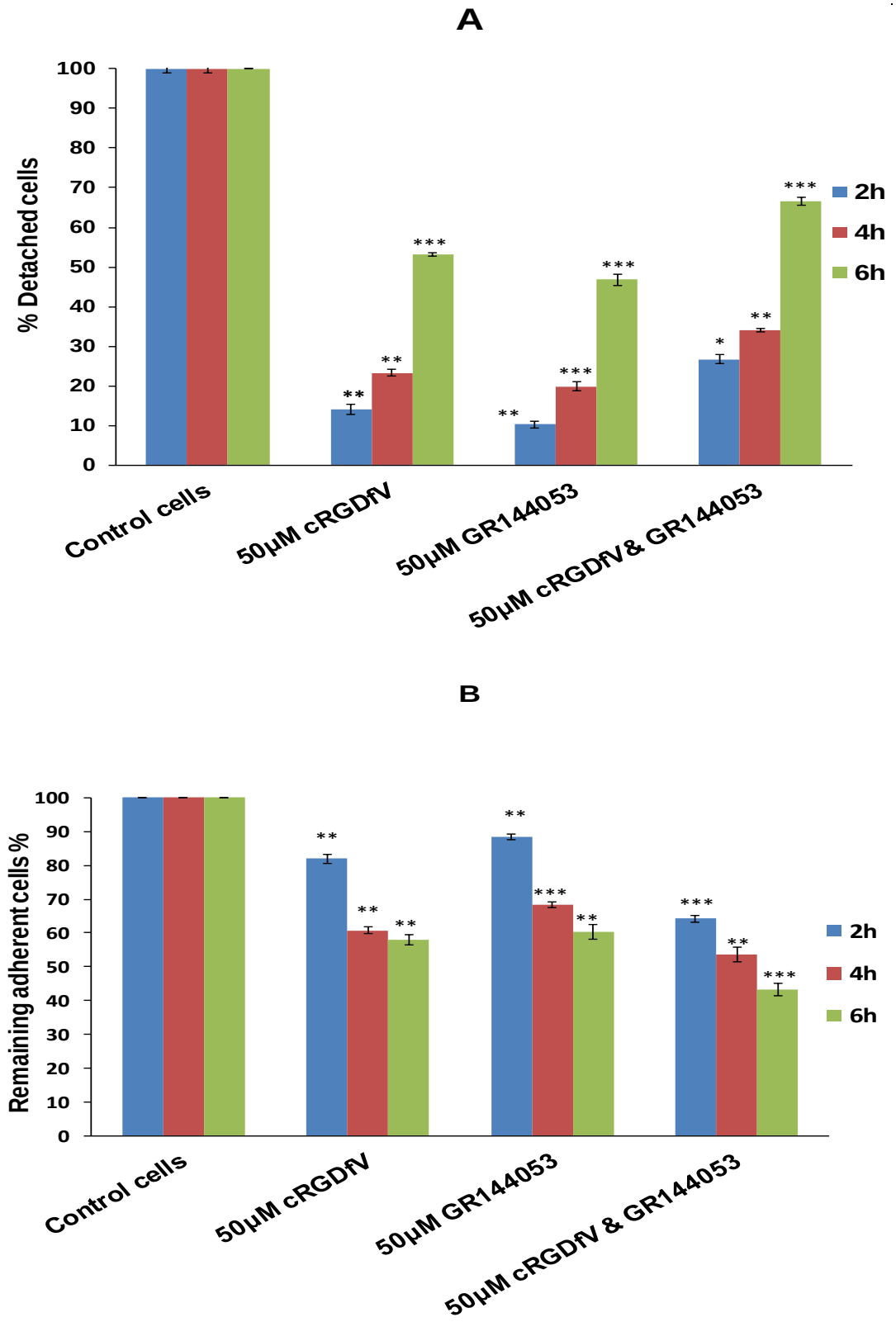

Figure 63: Effects of cRGDfV and GR144053 on MCF-7 cell adhesion. Cells (± 0.04µM PMA) were treated with the stated concentration of compounds for 2, 4 and 6 hours, then number of detached cells quantified by counting with haemocytometer. (A) Number of detached cells (B) Number of remaining attached cells. Values are the average of 3 independent experiments and error bars are SE. * $p < 0.05$ ** $p < 0.01$ and *** $p < 0.001$.

4.4.4.1 Effects of novel β3 integrin antagonists on cell detachment

Detachment determinations were performed after 2, 4 and 6 hour's incubations with different concentrations (0.1, 1, and 10 μM) of ICT9055 evaluated by counting with haemocytometer (Figure 64 and Figure 65). ICT9055 showed the highest effect of detaching PMA treated K562 cells from fibrinogen compared to untreated cells in a time and dose dependent manner.

ICT9055, ICT9072, ICT9073 and ICT9099 were selected for further investigation in the detachment assay as they had been demonstrated (sections 4.4.3.5 and 4.4.3.6) to give significant inhibition of the adhesion of K562 cells ±PMA and MCF-7 cells to fibrinogen. The selected cells were plated on fibrinogen coated wells and treated with different concentrations (0.1, 1 and 10 μM) of the compounds for 6 hours. The detached cells from the fibrinogen-coated plates were counted. The number of cells remaining on the plates decreased with increasing compound concentration, whereas the number of the detached cells increased with increasing compound concentration (Figure 66). The most successful compound at causing K562 cell detachment at 10 μM was ICT9055 then ICT9072, ICT9099 and ICT9073 respectively. Positive control (49 ± 0.5%, $P<0.01$ without PMA and 66 $\pm$ 3.6%, $P<0.05$ with PMA) was less effective at causing cell detachment than all tested compound except ICT9073 (±PMA) and ICT9099 (+PMA), which were a slightly less effective. EC_{50} are given in Table 11.

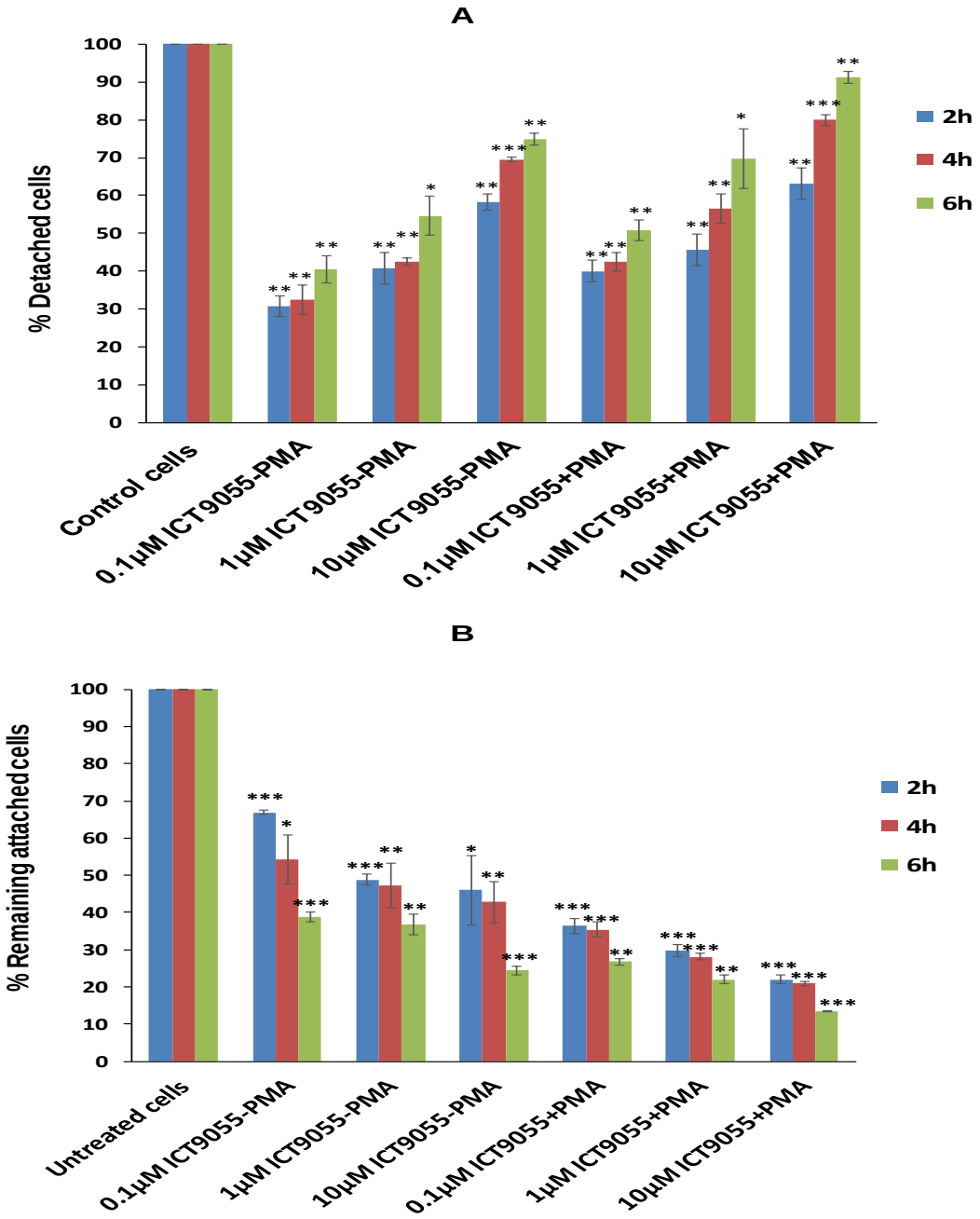

Figure 64: Effects of ICT9055 on K562 cell adhesion. Cells (± 0.04 μM PMA) were treated with the stated concentration of compound for 2, 4 and 6 hours, then number of detached cells quantified by counting with haemocytometer. (A) Number of detached cells (B) Number of remaining attached cells. Values are the average of 3 independent experiments and error bars are SE. * $p < 0.05$. ** $p < 0.01$, *** $p < 0.001$.

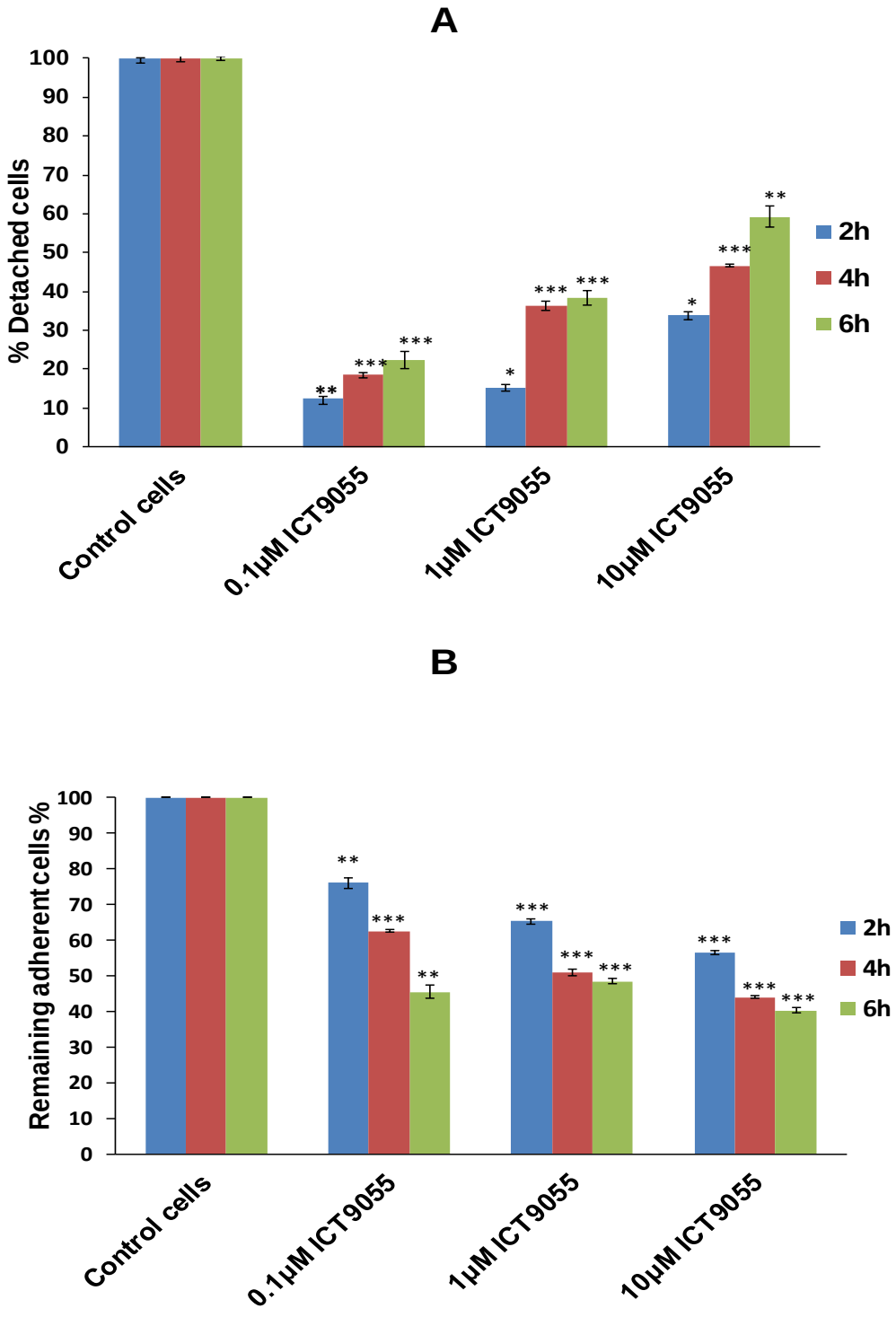

Figure 65: Effects of ICT9055 on MCF-7 cell adhesion. Cells were treated with the stated concentration of compound for 2, 4 and 6 hours, then number of detached cells quantified by counting with haemocytometer. (A) Number of detached cells (B) Number of remaining attached cells. Values are the average of 3 independent experiments and error bars are SE. * $p < 0.05$ ** $p < 0.01$ and *** $p < 0.001$.

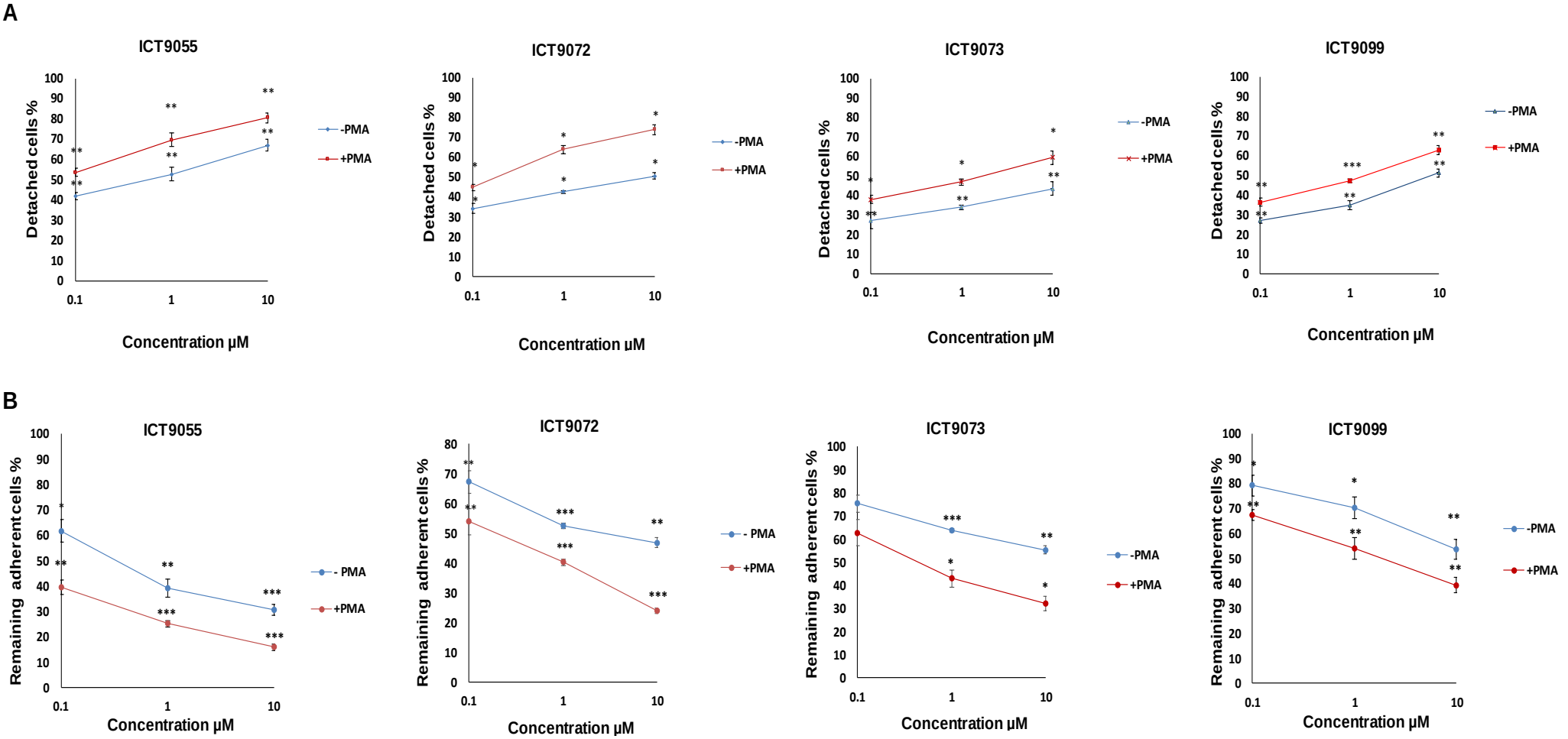

Figure 66: Induction of K562 detachment from fibrinogen by ICT compounds. Cells (± 0.4 µM PMA) were treated with the stated concentration of compound for 6 h, then number of detached cells quantified by counting with haemocytometer. (A) Number of detached cells (B) Number of remaining attached cells. Values are the average of 3 independent experiments and error bars are SE. * $p < 0.05$. ** $p < 0.01$ and *** $p < 0.001$.

Table 11: EC_{50} values for cell detachment caused by ICT compounds, GR144053 and cRGDfV.

Compounds	K562 (- PMA) EC_{50} ± SD (μM)	K562(+PMA) EC_{50} ± SD (μM)	MCF-7 EC_{50} ± SD (μM)
ICT9055	0.8 ± 0.1	0.1	1. 8 1 ± 1.1
ICT9072	9.1 ± 0.7	0.47 ± 0.08	3.4 ± 3.8
ICT9073	> 10	4.4 ± 1.9	> 10
ICT9099	8.5 ± 2	2.3 ± 0.4	> 10
CRGDfV	> 40	> 40	25.42 ± 5.5
GR144053	> 40	> 40	> 50
GR144053 and cRGDfV	30.4 ± 2.2	9.1 ± 1.3	11.88 ± 2

4.4.4.1.1 Characterisation of αv, αIIb and β3 integrin subunit expression in detached and attached PMA-treated K562 cells.

Analysis of αv, αIIb and β3 integrin subunit expression after 6 hours of exposure to ICT9055 showed no alterations in expression in detached K562 cells compared to untreated cells. In contrast, attached cells showed lower expression of αv, αIIb and β3 integrin subunits than untreated cells and detached cells (Figure 67). ICT9055 caused significant detachment of PMA-treated K562 cells from fibrinogen coated plates, which suggests it is able to disrupt binding to αIIbβ3 and αvβ3. However, reduced expression levels of αv, αIIb and β3 integrin subunits were observed in cells which remained attached to fibrinogen-coated plates in the presence of ICT9055. These findings may be explained by the existence of subpopulations of PMA induced K562 cells which attach to fibrinogen via other integrins such as α5β1; a clear expression of α5 was previously shown in K562 cells (Figure 25, Figure 33 and Figure 34).

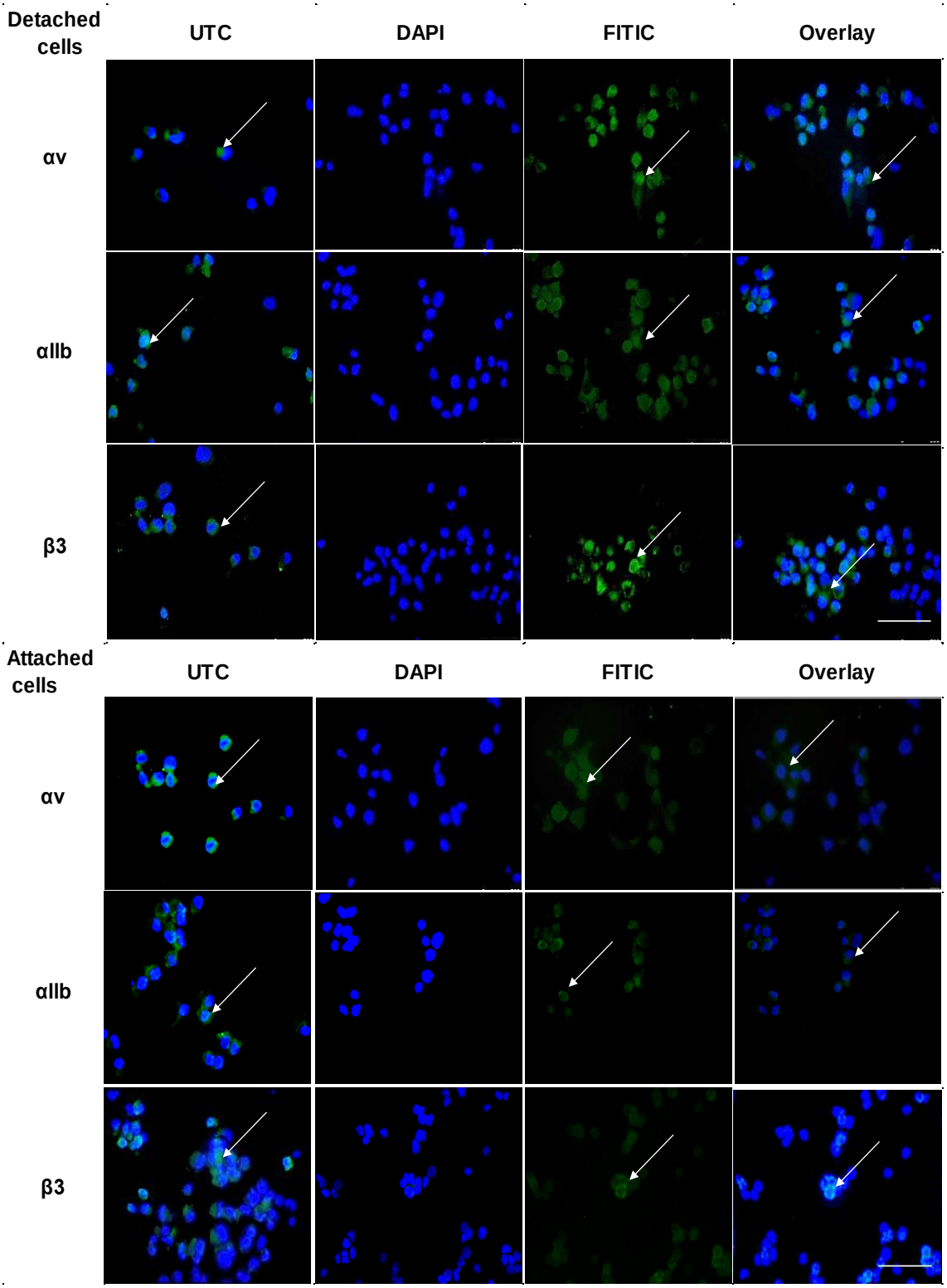

Figure 67: Expression of αv, αIIb and β3 integrin subunits in K562 cells treated with ICT9055. (A) The expression of integrin subunits in detached cells and (B) the expression of integrin subunits in attached cells compared to untreated cells (UTC) using immunofluorescence with Q20 anti-αv, EPR4330 anti-αIIb, and B7 anti-β3. Scale bar = 50 μm. Blue-fluorescent DAPI is nuclear staining and green colour represents integrins expression detected by a green fluorophor. White arrows point to positive labelling of αv, αIIb, β3 integrin subunits in the detached and attached cells.

4.4.4.2 Effects of novel β3 integrin antagonists on MCF-7 cell detachment

ICT9055, ICT9072, ICT9073 and ICT9099 were also investigated on detachment and remaining attachment of MCF-7 cells. The cells were plated on fibrinogen coated wells and treated with different concentrations (0.1, 1 and 10 μM) of the compounds for 6 hours. The detached cells from the fibrinogen-coated plates were counted. As with K562 cells, a dose dependent increase in cell detachment was observed, and ICT9055 was the most effective compound identified (Figure 68). EC_{50} are given in Table 11.

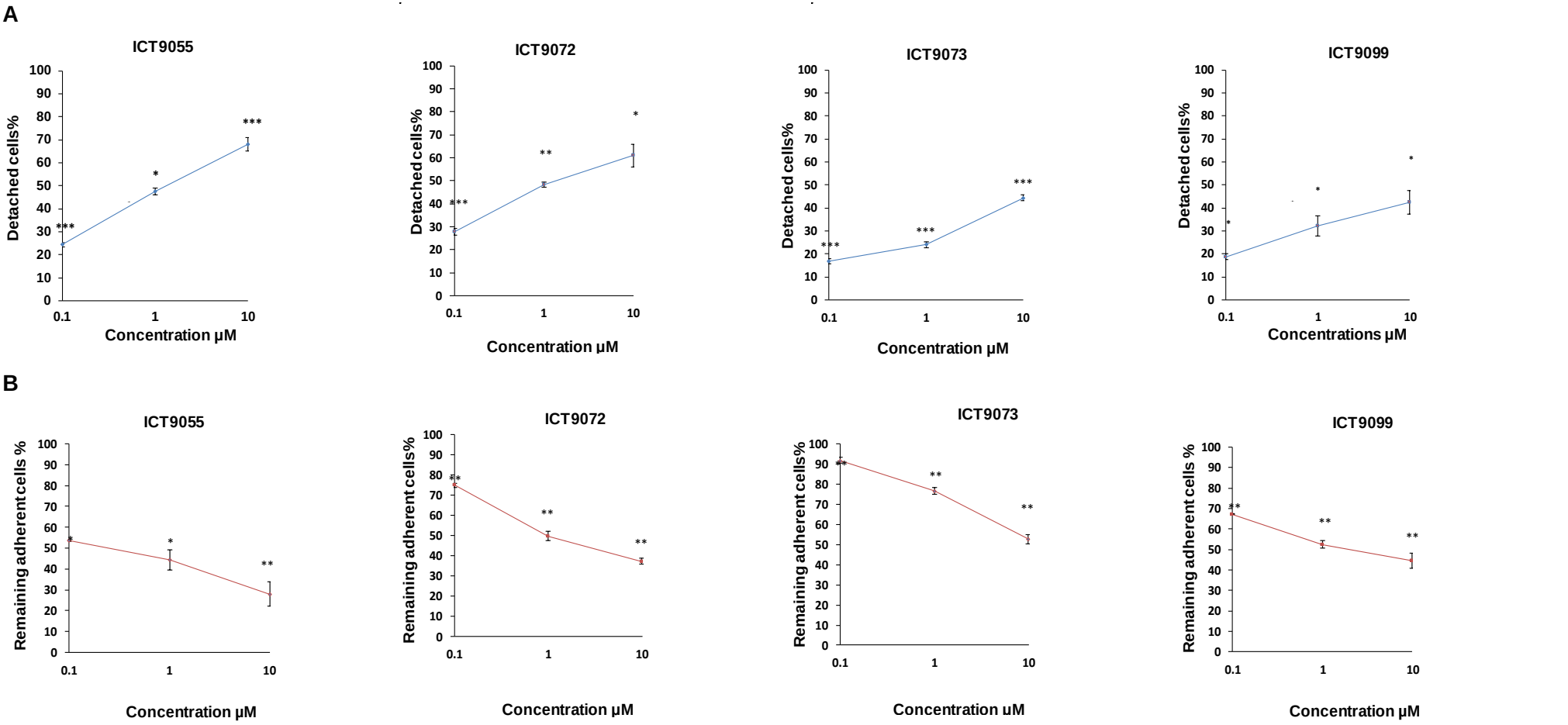

Figure 68: Induction of MCF-7 cells from fibrinogen by ICT compounds. Cells were treated with the stated concentration of compound for 6 h, then number of detached cells quantified by counting with haemocytometer. (A) Number of detached cells (B) Number of remaining attached cells. Values are the average of 3 independent experiments and error bars are SE. * p <0.05 ** p < 0.01, *** p < 0.001.

4.4.5 Transwell migration assays

The ability of K562 and MCF-7 cells to migrate through a porous membrane was investigated in order to determine whether models are fit for measuring inhibition of migration.

4.4.5.1 Cell migration

Cell migration depends on the ability of cells to move from one area to another in response to a chemoattractant. The transwell migration assay was optimised using different concentrations of FCS as a chemoattractant. The best results were obtained with unstimulated K562 and MCF-7 cells. K562 cells treated with PMA were unable to migrate through the pores successfully (Figure 69 and Figure 70)

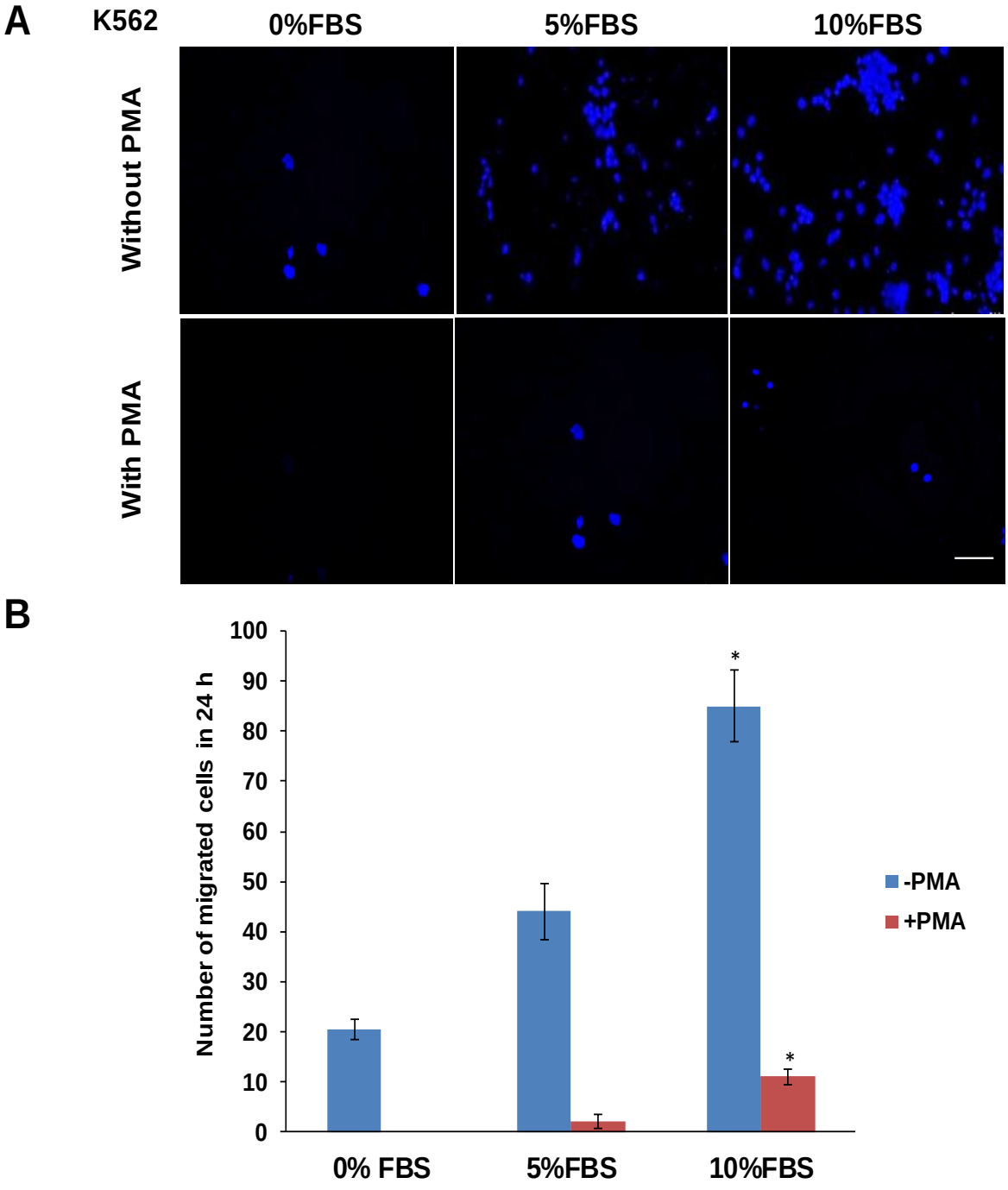

Figure 69: Optimisation of chemoattractant concentration for K562 cell migration through a transwell membrane. 5 X 10^5 cells were seeded in the upper chamber of a transwell insert and allowed to migrate towards FBS for 24 hours. (A) Representative images of the migrated cells visualised with. Scale bar = 100 µm (B) Quantification of cell migration in response to different concentrations of FBS. * $p < 0.05$.

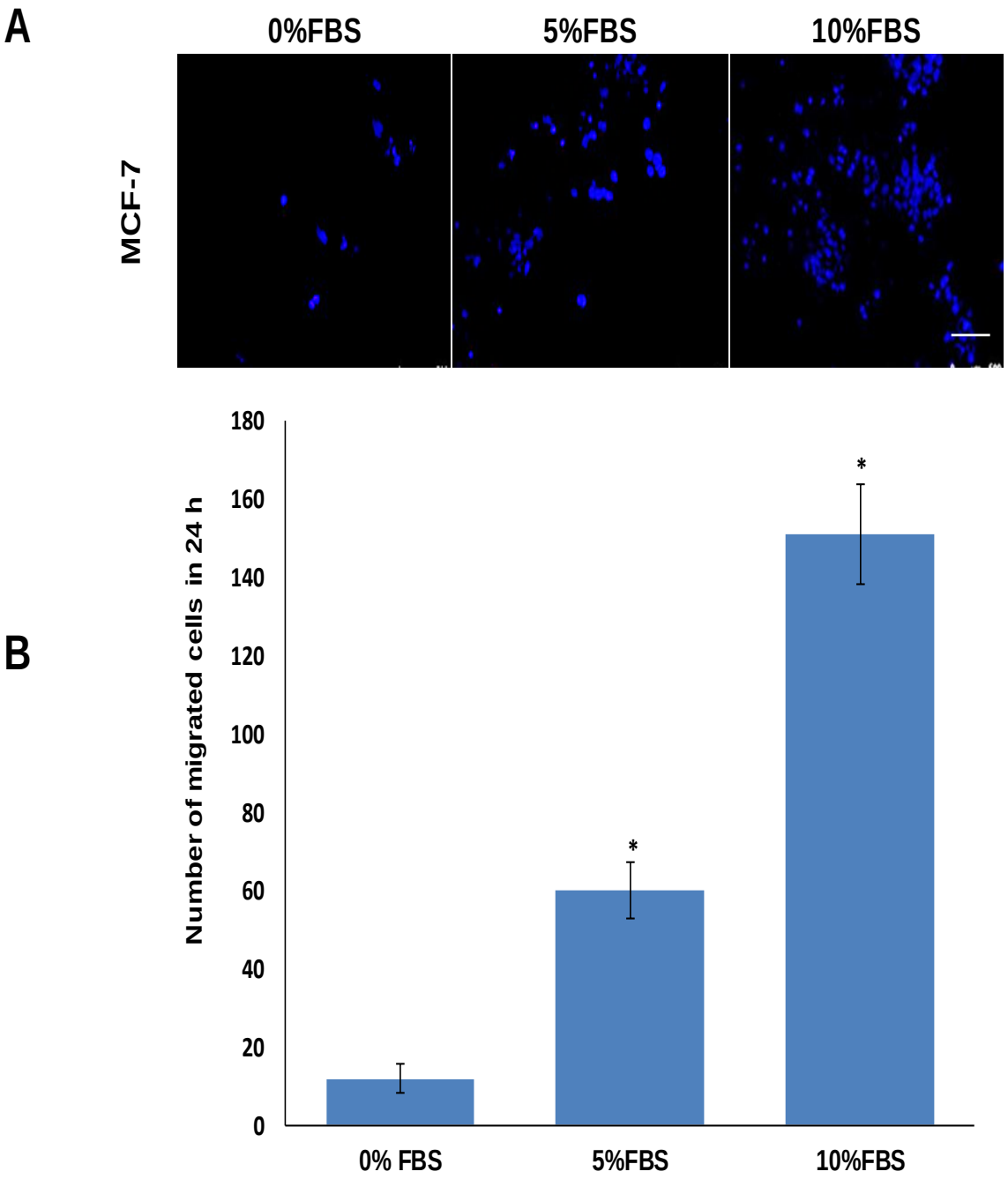

Figure 70: Optimisation of chemoattractant concentration for MCF-7 cell migration through a transwell membrane. 4 X 10^5 cells were seeded in the upper chamber of a traswell insert and allowed to migrate towards FBS for 24 hours. (A) Representative images of the migrated cells visualised with. Scale bar = 100 µm (B) Quantification of cell migration in response to different concentrations of FBS. * $p < 0.05$.

4.4.5.2 Validation of the transwell migration assay using cRGDfV and GR144053

Different concentrations of cRGDfV and GR44053 were used singly and in combination for 24 hours in the transwell migration assay to confirm migration was β3 integrin dependent and provide a baseline to compare new antagonists (Figure 71 A and B and Figure 72 A and B). The ability of combined compounds to inhibit migration of K562 and MCF-7 cells through the membrane of the chamber was higher than single compounds and combination index analysis indicated the interaction was synergistic at all doses tested (Table 12). GR144053 alone had little effect, indicating migration is not αIIbβ3 dependent.

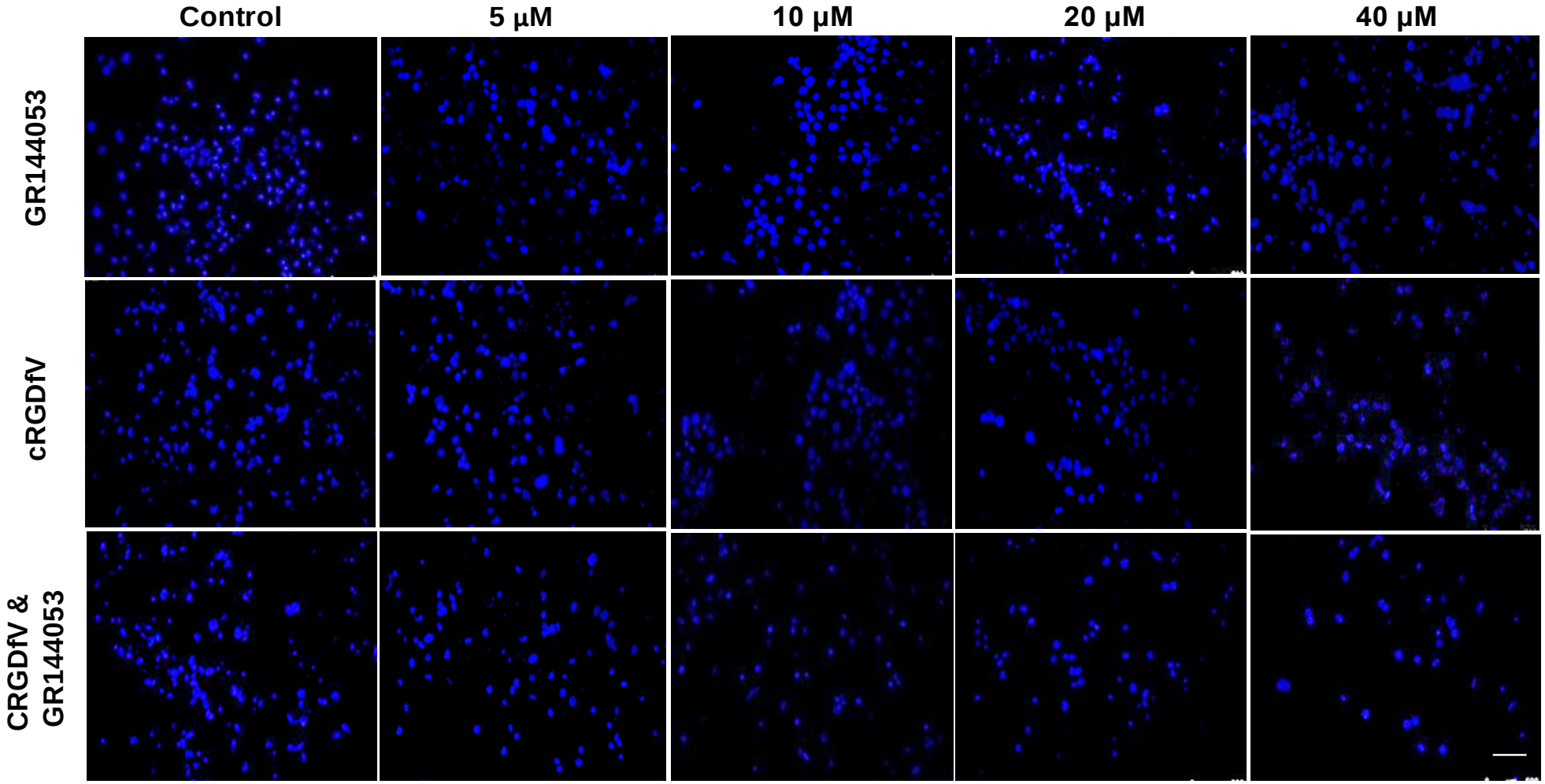

Figure 71 A: The effect of cRGDfV and GR144053 on K562 cell migration. Representative images of the bottom surface of a transwell plate are shownfor each compound. Scale bar = 100 µm at 20X objective lens.

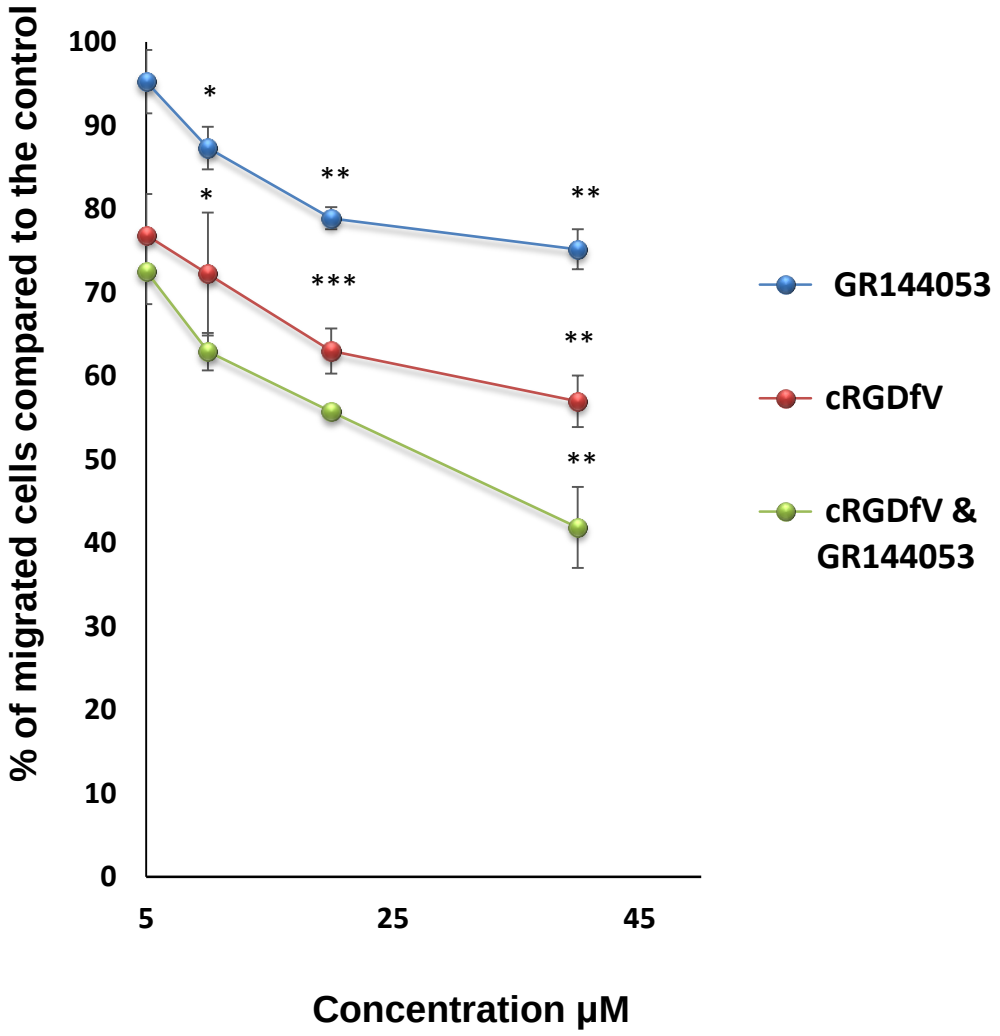

Figure 71 B: The effect of cRGDfV and GR144053 on K562 cell migration. Quantification of reduction in migration; results presented are an average of 3 random microscopic fields (20X) from 3 independent experiments error bars are SE. * p <0.05, ** p <0.01 and *** p <0.001.

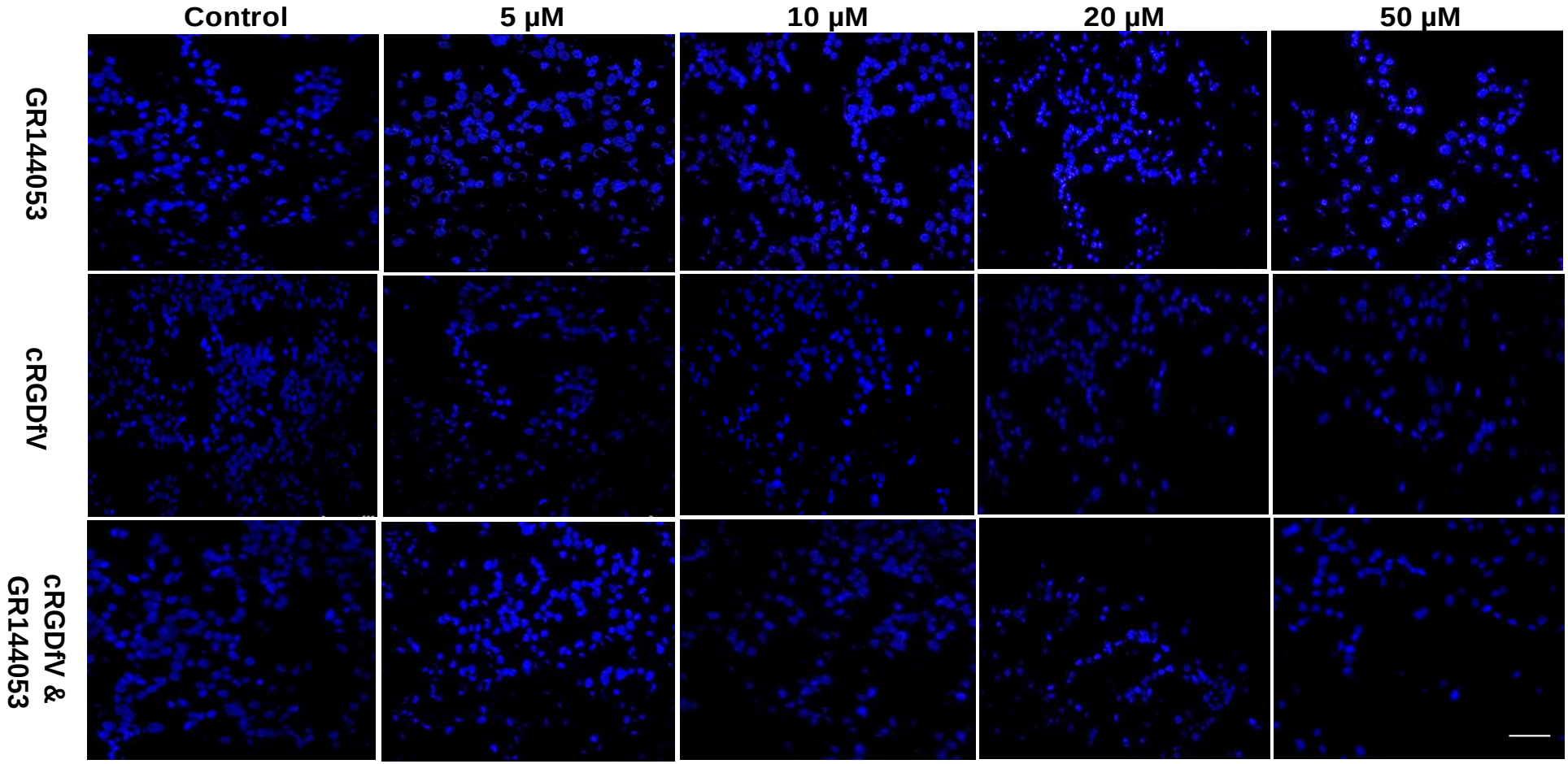

Figure 72 A: The effect of cRGDfV and GR144053 on MCF-7 cell migration. (A) Representative images of the bottom surface of a transwell plate are shown for each compound. Scale bar = 100 µm at 20X objective lens.

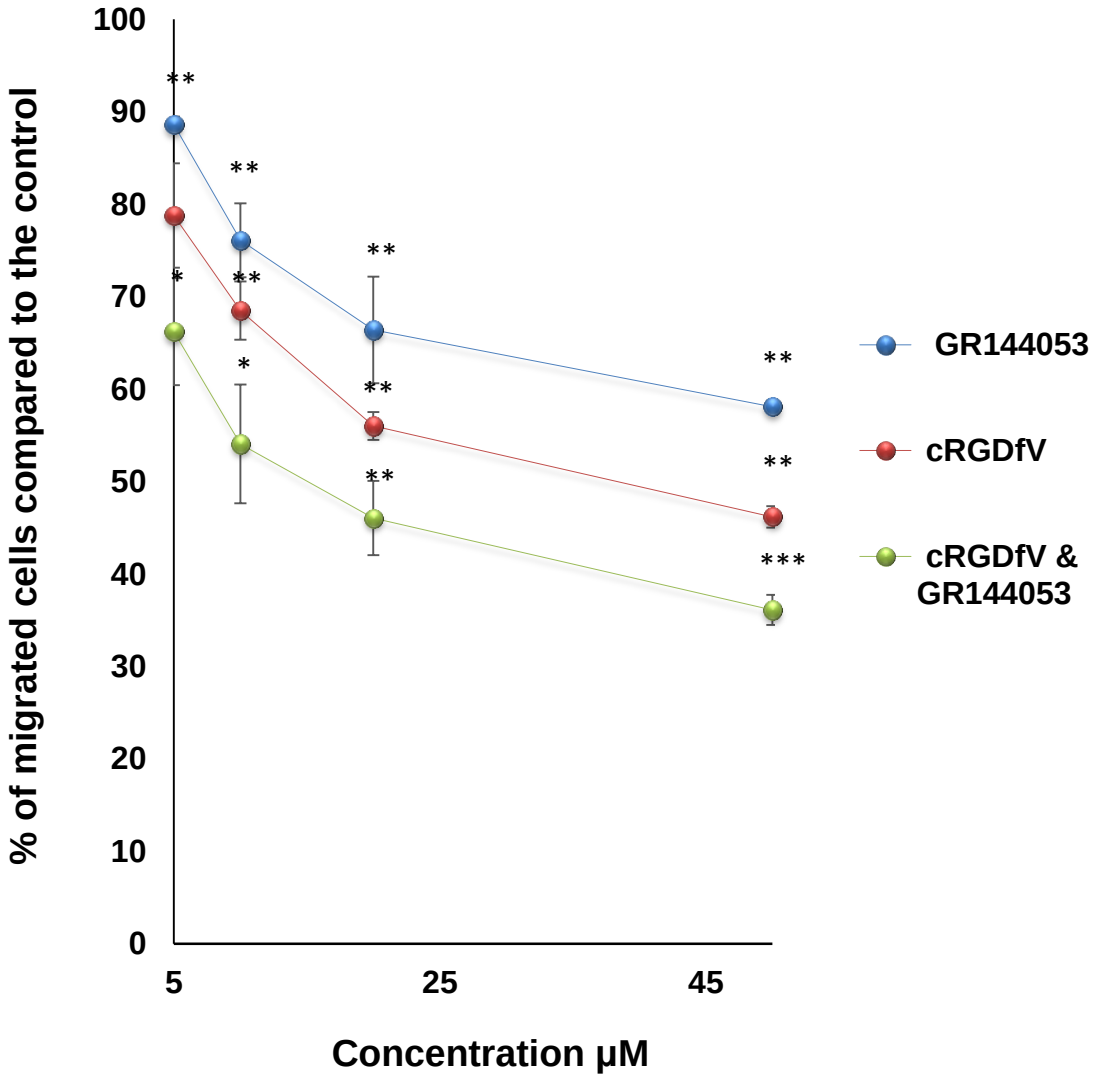

Figure 72 B: The effect of cRGDfV and GR144053 on MCF-7 cell migration. Quantification of reduction in migration; results presented are an average of 3 random microscopic fields (20X) from 3 independent experiments and error bars are SE. * p <0.05, ** p <0.01 and *** p <0.001.

Table 12: Combination index values of GR144053 and cRGDfV on transwell migration. CI < 0.1 very strong synergism, 0.1 - 0.3 strong synergism 0.3 - 0.7 synergism, 0.7- 0.85 moderate synergism, 0.85 - 0.90 slight synergism, and 0.90 -1.10 additive.

Type of Cells	Total Dose (μM)	CI Value	Interpretation
K562	5.0	0.35	Synergism
	10.0	0.29	Strong synergism
	20.0	0.32	Synergism
	40.0	0.23	Strong synergism
MCF-7	5.0	0.28	Strong synergism
	10.0	0.24	Strong synergism
	20.0	0.27	Strong synergism
	50.0	0.34	Synergism

4.4.5.3 Characterisation of the anti-migratory effect of novel β3 integrin antagonists

To investigate whether ICT9055, ICT9072 and ICT9073 are able to block the migration of K562 and MCF-7 cells, I performed *in vitro* migration assays using transwell chambers *in vitro.* ICT9055 produced a greater effect than ICT9072 and ICT9073 at all concentrations tested. ICT9055 and ICT9072 had a higher effect than the combination of anti-αvβ3 and anti-αIIbβ3 controls (55.5% + 4.7 in MCF-7 cells and 45.5% + 3.3 in K562 cells, $P<0.01$) while ICT9073 was less effective (Figure 73 A and B and Figure 74 A and B). IC_{50} values are given in Table 13.

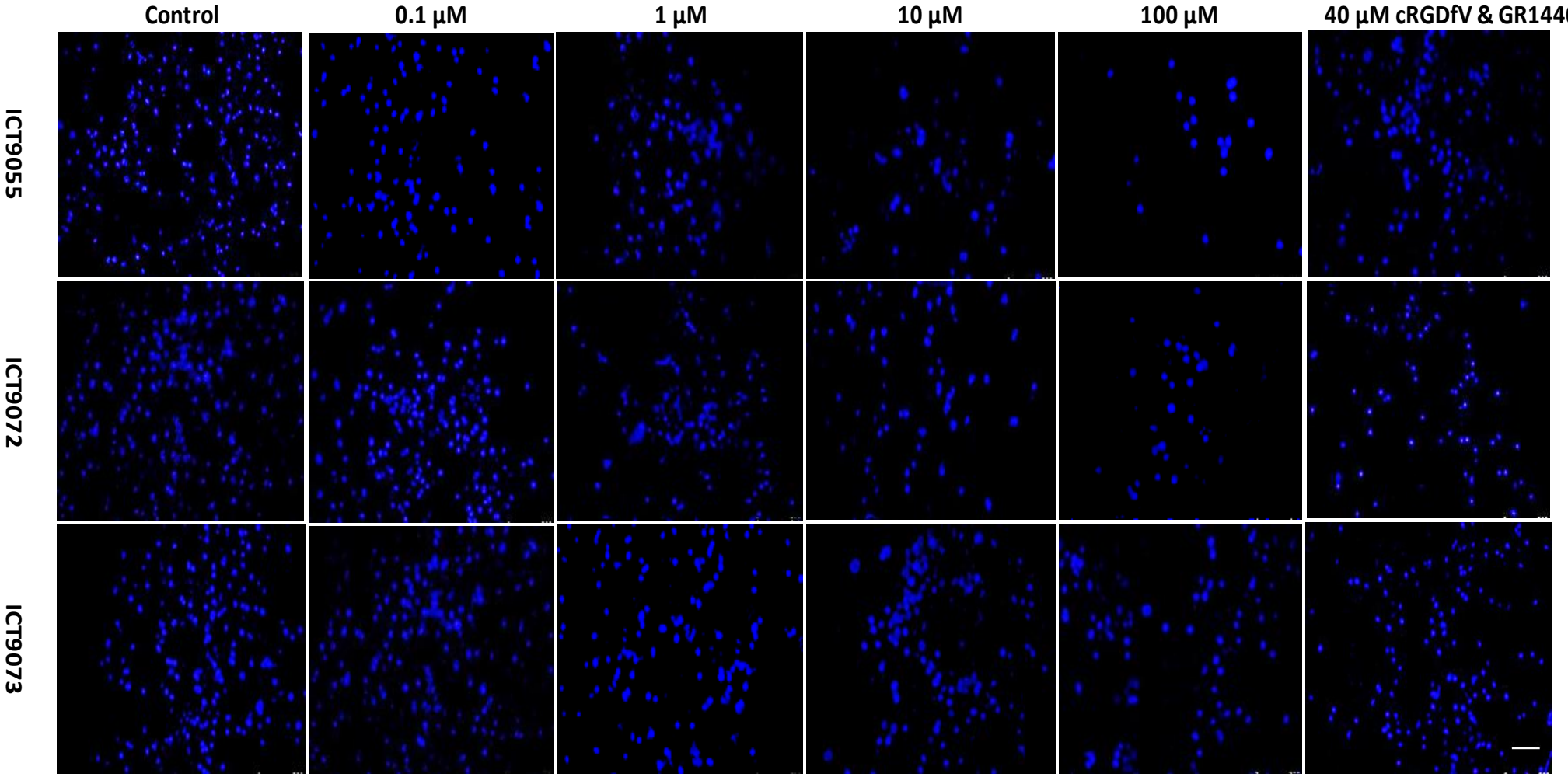

Figure 73 A: The effect of ICT compounds on K562 cell migration. Representative images of the bottom surface of a transwell plate are shown for each ICT compound. Scale bar= 100 µm at 20X objective lens.

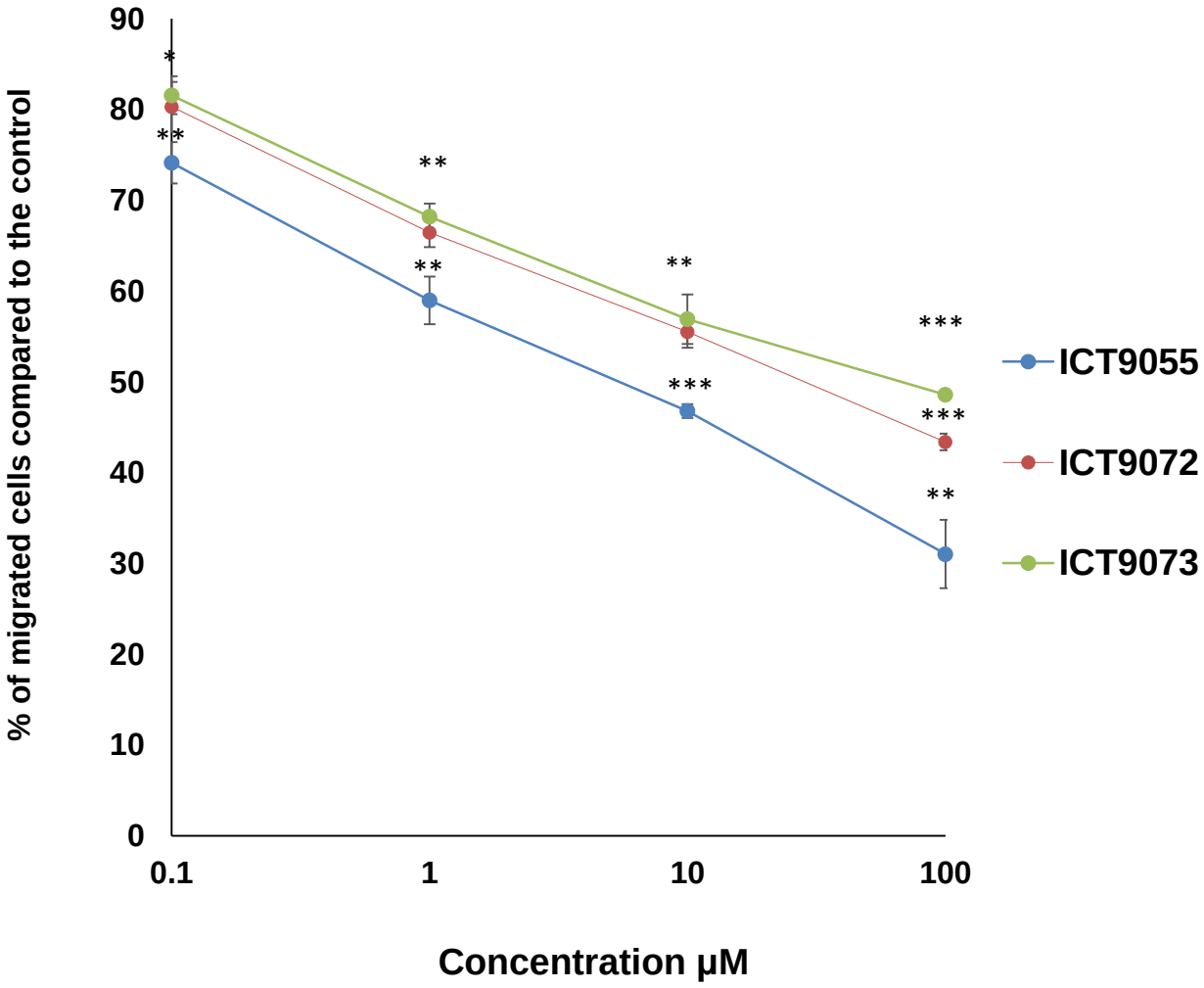

Figure 73 B: The effect of ICT compounds on K562 cell migration. Quantification of reduction in migration; results presented are an average of 3 random microscopic fields (20X) from 3 independent experiments and error bars are SE. * p <0.05, ** p <0.01, *** p <0.001.

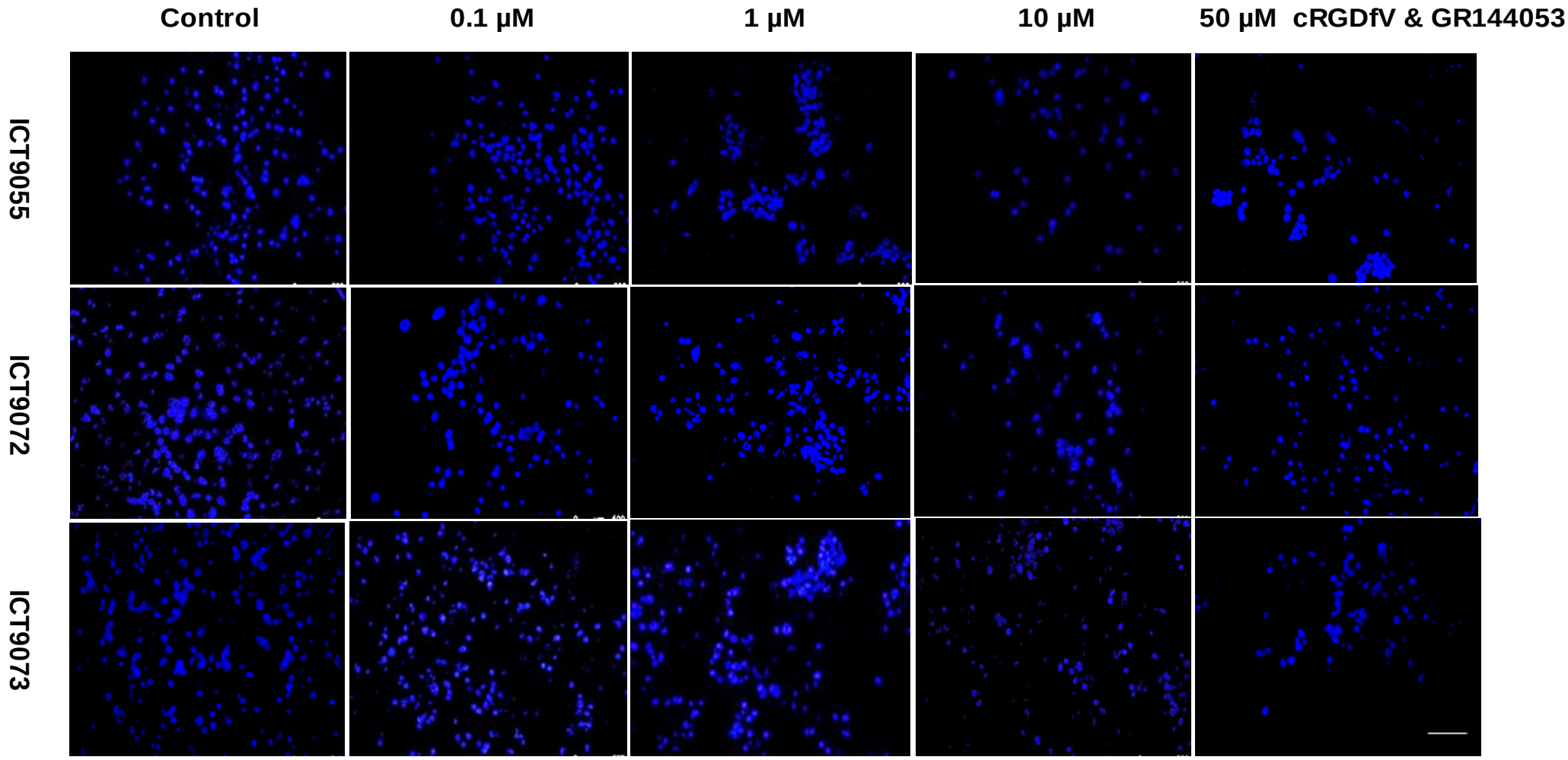

Figure 74 A: Effect of ICT compounds on MCF-7 cell migration. Representative images of the bottom surface of a transwell plate are shown for each ICT compound. Scale bar = 100 µm at 20X objective lens.

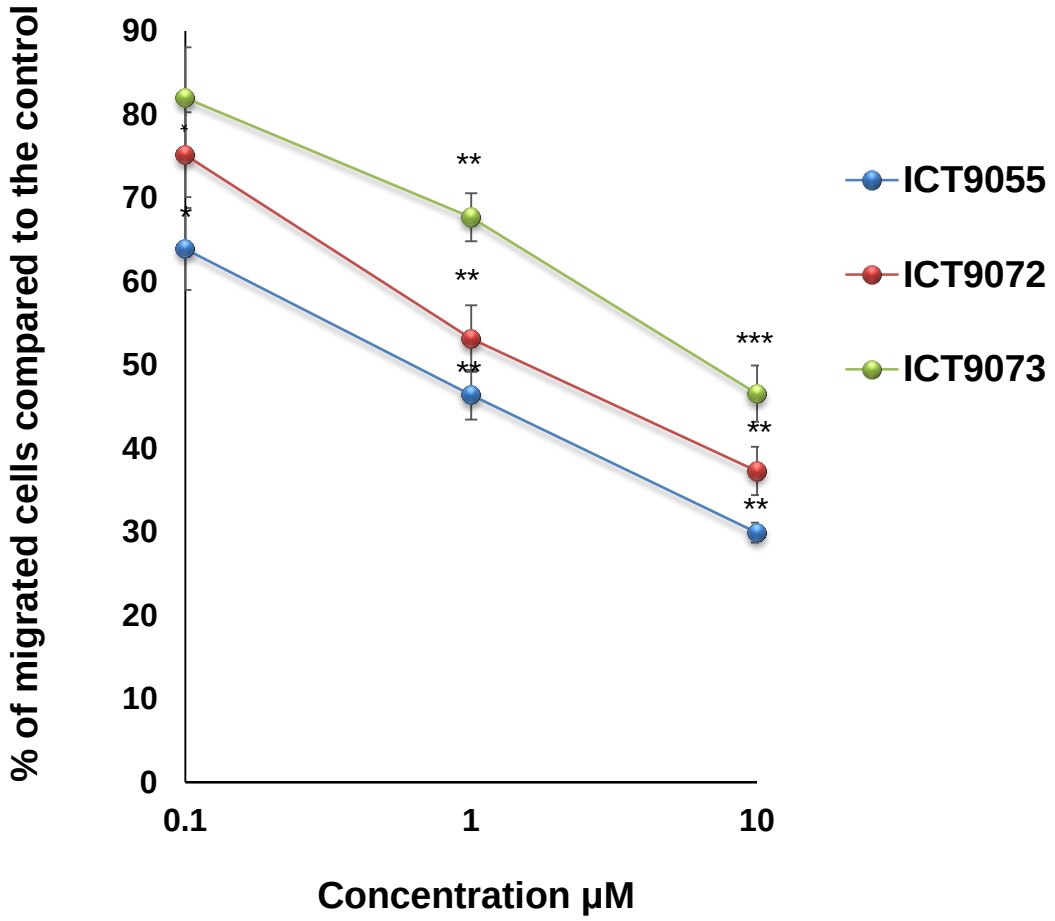

Figure 74 B: Effect of ICT compounds on MCF-7 cell migration. Quantification of reduction in migration; results presented are an average of 3 random microscopic fields (20X) from 3 independent experiments and error bars are SE. * p <0.05, ** p <0.01, *** p <0.001.

Table 13: IC_{50} values for β3 integrin antagonists in inhibition of cell migration.

Compound	K562 IC_{50} ± SD (μM)	MCF-7 IC_{50} ± SD (μM)
ICT9055	7.3 ± 1.7	1.08 ± 0.96
ICT9072	48.9 ± 8	3.4 ± 2.3
ICT9073	78.6 ± 10.1	8.4 ±1.2
CRGDfV	> 50	39.7 ± 10.1
GR144053	> 50	> 50
GR144053 and cRGDfV	30.5 ± 5.6	14.8 ± 9.5

4.5 Discussion

The metastatic cascade of tumour cells includes sequential multi-steps: detaching from the primary tumour, migrating to distant sites and attaching to the tumoural niche (Hanahan and Weinberg, 2011). During the steps of metastasis formation, the capability of cells to interact with ECM proteins through integrins provides the traction necessary for regulating both adhesion and migration processes. Consequently, blocking tumour cells binding to the ECM is an important strategy to prevent their spreading (Desgrosellier and Cheresh, 2010).

In the previous chapters the β3 integrin expressing cancer cell lines, K562 and MCF-7 were characterised and selected to use in the functional assays. In this chapter, these selected models were validated using known β3 antagonists cRGDfV and GR144053 as positive controls. The purpose of these validations was to demonstrate that the models are suitable for assessing inhibition of cell adhesion; induction of cell detachment and anti-migration properties in that the models were responsive to β3. The validated models were then used to investigate the effect of novel small molecule β3 integrin antagonists.

Subsequently, the novel small molecule β3 integrin antagonists were evaluated for their relative cytotoxicity before they were used in the functional assays, in order to determine the safe dose of the antagonists that would show effects through blocking β3 integrin function in mediating cell adhesion and migration rather than inducing cytotoxicity. Firstly, the cytotoxicity of αIIbβ3 antagonist (GR144053) and αvβ3/β5 antagonist (cRGDfV) against K562 cells (in the presence of PMA and its absence), and MCF-7 cells was investigated utilising the MTT assay, to determine concentrations that could be used in the functional

assays without causing cell killing. cRGDfV and GR144053 had no toxic effects on the K562 cell lines (±PMA) and MCF-7 compared to their control except at higher doses.

As seen in Table 7, different anti β3 integrin antagonists had different cytotoxic effects. ICT9001, ICT9026, ICT9055 and ICT9103A were not toxic to K562 and MCF-7 cells. ICT9066, ICT9072 and ICT9073 had a cytotoxic effect on MCF-7 only, and ICT9025 and ICT9101 were cytotoxic to K562 in the presence of PMA. ICT9094 and ICT9099 showed the cytotoxic effect with all tested cell lines. Previous studies have also found cytotoxic effects of αvβ3 antagonists are highly variable within a library (Dayam et al., 2006).

The cell adhesion assay is an important method in cell biology because cellular adhesion is a contributing factor in many diseases, including inflammatory diseases, tumour progression, and metastasis. These cellular responses are based on the attachment of adhesion receptors to existing extracellular matrix proteins or another cell's surface, and also cellular adhesion is essential for the growth and survival of the cell (Soloviev et al., 2007). Therefore, a cell adhesion assay is often utilised to evaluate the metastatic ability of cancer cells and also provides a low-cost method for screening integrin antagonists.

In order to identify models of cellular adhesion, the concentration of K562 cells binding to fibrinogen was optimised with and without PMA. PMA stimulation of K562 cells increased adhesion on fibrinogen compared to unstimulated cells, indicating that the integrin receptors induced by PMA treatment were functionally competent.

Likewise, cell detachment is fundamental to several phenomena of cellular dynamic such as cell migration (Geiger et al., 2001a, b; Ridley et al., 2003).

Cheng et al.(2016) found that blocking the activity of αvβ3 and αvβ5 integrin induced the detachment of all three papillary thyroid cancer cell lines. In endothelial cells, inhibiting integrin activity usually results in cell detachment and leads to a form of programmed cell death called anoikis.

Further, cellular adhesion and detachment were validated with controls singly and in combination. K562 cells (with and without PMA) were treated with different concentrations of GR144053 and cRGDfV to measure the antagonists' ability to inhibit the adherence of cells to fibrinogen and to break the established binding interactions between the targeted integrin receptors and fibrinogen.

The inhibitory and detaching effects were greater in PMA-stimulated cells than in unstimulated. These data showed that the known β3 antagonists, GR144053 and cRGDfV, decrease cellular adhesion to fibrinogen in the adhesion assay and increase cellular detachment from fibrinogen in the detachment assay. Adhesion and detachment were partially dependent on the β3 integrins in untreated cells and more dependent in PMA-treated cells, where 20 μM and 40 μM combined antagonists respectively in adhesion and detachment assays almost completely blocked cell adhesion and induced cell detachment with the synergistic effects in the analysis of combination index (CI<1). The importance of synergistic effects arises through pharmacokinetic and/or pharmacodynamics interactions that occur between two or more agents which result in an effect greater than the sum of individual effects. The pharmacodynamic synergy refers to two or more compounds that work on the same biological targets or receptors that lead to induced therapeutic results through their positive interactions (Zhou et al., 2016a). Synergistic effects also arise from working on the targets that have different modes of action. For instance, the combination of cilengitide and temozolomide gave synergistic antiproliferative effects against endothelial and

malignant melanoma cells *in vitro* and enhanced a statistically significant decrease in melanoma growth *in vivo*, thereby providing novel insights for the utilisation of integrin inhibitors not only in an adjuvant therapy to inhibit tumour spreading but also to improve the efficiency of chemotherapy (Tentori et al., 2008). In MCF-7 cells, 50 μM combined antagonists reduced cell adhesion to fibrinogen and induced cell detachment with a synergistic effect. These data indicate that blocking of integrin by either GR144053 or cRGDfV particularly with PMA treated K562 incompletely inhibits integrin function, through acting on either αIIbβ3 or αvβ3, whereas the combination improves β3 integrin receptors' occupation by covering both targets, which can inhibit adhesion completely or completely induce detachment. The present data suggest that targeting αIIβ3 alone is insufficient to inhibit cell adhesion, whereas targeting αvβ3 and αIIbβ3 integrins has a greater effect on cancer cell interactions with a biologically relevant extracellular matrix derived ligand, such as fibrinogen in these particular dual expression models. This result corresponds with the finding of Gomes et al.(2004) which identified cooperation between αIIbβ3 and αvβ3 in breast adenocarcinoma cells' adhesion to ECM under flow conditions. The αIIbβ3 antagonist lamifiban (Ro 44-9883) reduced adhesion of cancer cells to ECM while the αvβ3 antagonist (SB-273005) did not affect cancer cell adhesion to the ECM. However, the combination of both antagonists (SB-273005 and Ro 44-9883) had a synergistic effect on adhesion compared to the effects of single antagonists.

The effect of the novel β3 integrin antagonists was investigated using the fibrinogen adhesion assay. GR144053 and cRGDfV were included as combined control integrin antagonists. The data obtained showed that different

antagonists had different effects on inhibition of K562 (±PMA) and MCF-7. ICT9055 which contains the tetrahydronaphthyridine (THN) αv-binding functional group was an effective inhibitor of PMA treated K562 cell adhesion and showed a 10-fold difference in the effect between untreated and PMA treated K562. ICT9055 was, therefore, the most effective functional antagonist with no toxic effect on PMA treated K562 cells, which had upregulated integrin expression. ICT9055 also was significantly more potent at inhibiting MCF-7 attachment to fibrinogen compared to the combined control.

ICT9094 also contains the THN group, and a longer β3 binding group. It has cytotoxic effect on all tested cells and had minor effect on adhesion. ICT9101 has a very similar structure and similar efficacy.

Many of the tested compounds are methyl esters which are expected to be rapidly hydrolysed by cell esterases, releasing active carboxylic acids. ICT9099 contains a tert-butyl ester group which is a non-physiologial group and sterically hindered so might not be hydrolysed by cells. ICT9099 effectively inhibited K562 and MCF-7 cells' adhesion *in vitro*, which suggests the tert-butyl ester is being hydrolysed releasing ICT9103A.

The positive effect on K562 (±PMA) and MCF-7 was seen with the compounds ICT9072 and ICT9073. The carboxylic acids ICT9001 and ICT9103A were effective inhibitors of K562 cell adhesion in the presence of PMA only, which it suggests they act on the upregulated integrins. The effect of ICT9001 is surprising as it does not contain an exosite binding group so would be expected to have lower affinity for β3 integrins than other compounds. The other compounds including ICT9025, ICT9026, ICT9066, ICT9085, and ICT9101 showed a minor effect compared to ICT9055 on all tested cells. ICT9066 has

the THN αv binding group, which is generally more active than the αv binding group found in ICT9001, and like ICT9001 has no exosite binding group. These results indicate that the observed activity of compounds is not dependent on one particular functional group and it is difficult to identify SAR or predict activity in this chemical library.

Further analysis during the fibrinogen adhesion assay found ICT9055 demonstrated time-dependent effects on cellular viability of non-adherent K562 cells. The viability of non-adherent cells declined with increasing time (Figure 59) indicating that the effects of ICT9055 might be associated with an initial loss of cellular attachment followed by cell death. However, the viability of non-adherent MCF-7 cells was reduced with short and long exposure times. The analysis of non-adherent cells with Hoechst staining revealed a time-dependent increase in the number of cells displaying apoptotic morphology. Results presented herein demonstrate that the compounds' effects on cellular viability depend on the cell lines as MCF-7 was more affected than K562. This in agreement with Frisch and Ruoslahti., (1997) who confirm that the loss of integrin-mediated cell–matrix interaction can enhance programmed cell death of some cell types such as mammary epithelial cells. Other cell lines might be more resistant to a drug than others; insensitivity to loss of normal cell-matrix interactions is a feature of cancer progression, promoting migration and invasion (He et al., 2010).

Additionally, the data obtained from the cell detachment assay showed that β3 integrin antagonists induced a statistically significant concentration and time dependent increase in the detachment of cells. Similar data have been obtained with other αvβ3 small molecule antagonists (Christenheit et al., 2016). However, in cell-free systems, integrin antagonists have been found to be unable to

reverse pre-existing integrin-matrix interactions. For example, RGD-based inhibitor such as cilengitide was unable to induce cell detachment. A non-reversible complex formed very rapidly that did not depend on the integrin leg regions or the time-dependent formation of a high-affinity state of the integrin, Compared to RGD-based inhibitor, Ca^{2+} (but not Mg^{2+}) caused on increased detachment rate of integrin-fibronectin complexes (Mould et al., 2014). Humphries et al.(2015) have suggested this may be a reason for the failure of RGD-based competitive antagonists in the clinic. These results suggest there are significant differences between the effect of RGD-mimetic antagonists in cell-free and cell-based systems so the inability to reverse binding interactions may not be a problem in vivo.

Using the detachment assay, analysis of αv, αIIb and β3 integrin subunit expression in attached and detached cells showed no changes in integrin expression in detached cells compared to control cells. In contrast, attached cells showed lower expression of αv, αIIb and β3 integrin subunit than in untreated control or treated detached cells. Most probably these observations may be explained by a fraction of PMA treated K562 cells with low expression of the integrins targeted by ICT9055 binding to fibrinogen via integrin α5β1 as a clear expression of α5 was observed in the presence of PMA.

In addition to investigating the effects of novel β3 antagonists on the adhesion and detachment of the cells *in vitro*, it was important to study their effect on other features that characterise cancer spreading such as cell migration. The determination of the migratory and invasive potential and activity of cancer cells is essential for offering novel clinical strategies in cancer prognosis, diagnosis and drug development, since the acquisition of a migratory phenotype is needed for metastatic spreading. A wide range of assays are available to

evaluate the migratory or invasive potential of cells *in vitro*. These assays range from cheap and simple ones to expensive ones (Justus et al., 2014) such as the scratch assay, the cell-exclusion zone assay and the transwell migration assay.

The advantages of the transwell migration assay are the availability of different cell culture inserts and sizes, a short path length medium/chemokine gradient between the upper and lower culture medium reservoir and the relative ease of the experimental setup. Therefore, this assay is commonly used to evaluate cell migration (Justus et al., 2014). The transwell migration assay was used in this work since the selected cell lines were not suitable for the scratch assay; K562 cells are suspension cells while MCF-7 cells did not completely close a scratch after 72 hours (Appendix ll).

The transwell migration assay was optimised for use with K562 and MCF-7 cells. MCF-7 and K562 cells with and without PMA were investigated using different concentrations of FBS as chemoattractant to evaluate the ability of the cells to migrate through pores of the membrane. PMA stimulation of K562 cells reduced migration through the pores compared to unstimulated cells (K562 and MCF-7). Zhou et al., (2016) demonstrated that K562 cells treated with PMA showed increased strength of binding to other cells, which was attributed to increased E-cadherin expression, and decreased migration in a transwell assay due to increased traction forces.

Anti-migratory effects were shown with all β3 antagonists investigated. cRGDfV had a greater effect than GR144053 when used singly, indicating migration of K562 and MCF-7 cells is more dependent on αvβ3 than αIIbβ3. cRGDfV and GR144053 shows synergistic effects in the analysis of combination index when used together at all

concentrations tested. ICT9055, ICT9072 and ICT9073 suppressed migration of K562 and MCF-7 cells in a dose-dependent manner. ICT9055 and ICT9072 were more potent, but ICT9073 was less potent. No SAR is apparent here.

To sum up, these findings (Table 14, Appendix III) demonstrate the ability of novel small molecule β3 integrin antagonists to inhibit cell adhesion and migratory potential effectively, both of which are critical factors for infiltration of remote tissues and cancer spreading in vivo.

Chapter 5: General discussion, conclusion and future work

4.6 General discussion

Metastasis depends on the regulation of some specific cellular properties, amongst them cell survival/programmed cell death, cell migration/invasion and cell proliferation. These processes are partially regulated by cell attachment and detachment, which require the involvement of integrin receptors. Integrins are also recognised as being important for mediating cell migration in tumours (Felding-Habermann et al., 2001; Huttenlocher and Horwitz, 2011), in addition to interactions of tumour cell and tumour cell-platelet binding (Weber et al., 2016), functions which are essential for immune evasion and metastasis (Yacobovich et al., 2016).

The expression of selected integrins is upregulated, often dramatically, during human cancers and inflammatory diseases (Raab-Westphal et al., 2017). Therefore, due to their involvement in these process have become popular targets in the battle against metastasis (Ganguly et al., 2013).

Small molecule drugs are popular as antagonists as they have better stability and are less costly to manufacture than antibodies (Millard et al., 2011). For example, pharmacokinetics of small molecules are often better than antibodies *in vivo*; half-life, typically less than 5 hours and attractive plasma protein binding and daily dosing. Antibodies may have half-lives of many weeks and require monthly dosing and no renal filtration. They are also subject to target mediated clearance (Carter, 2006; Hatley et al., 2017; Vugmeyster et al., 2012).

Integrin targeted therapies are employed in two strategies: blockade of integrin function; and the utilisation of integrin expression patterns to facilitate drug delivery (Currier et al., 2016). Blockade of integrin function has so far been the main therapeutic strategy that has reached the clinic (Raab-Westphal et al.,

2017), although it has not been successfully used to treat cancers. Notably, selective integrin ligands have been widely utilised to target tumours with high integrin expression as inhibitors of cancer angiogenesis (Desgrosellier and Cheresh, 2010; Kapp et al., 2017).

Inhibition of β3 integrins (platelet αIIbβ3 and endothelial and cancer cell-αvβ3) has an important role preventing tumour angiogenesis and cancer metastasis (Gay and Felding-Habermann, 2011). Accordingly, we hypothesise that dual β3 antagonists will have superior efficacy in a dual β3 integrin expressing model by reducing proliferation, as well as preventing angiogenesis and metastasis through targeting dual expressing cancer cell interaction with platelet αIIbβ3 and endothelial cells αvβ3.

In this thesis, the overall aim was to evaluate the effect of ICT compounds on the inhibition of human tumour cell adhesion and migration; and induction of cell detachment utilising functional assays. The main objectives of the work were to develop models that can be used for evaluation of novel β3 integrin antagonists by detecting expression of integrin subunits particularly αIIb, αv and β3 in human cancer cell lines.

Initially, the expression of αv, αIIb, α5, β3 and β5 integrin subunits was investigated in the panel of human cancer cell lines (K562, DU145, PC-3, LNCap, MCF-7, M14, MeWo, UACC-62 and HT-29) using IF and FACS (Chapter 2). Since FACS analysis is quantitative and sensitive measurements, it can be used to investigate even weak expression (Goodman and Picard, 2012; Nolan and Sklar, 1998). However, FACS does not evaluate the location of protein expression, so it must still be run in comparison with IF.

αv, αIIb and β3 integrin subunits were found to be highly expressed in MCF-7 cells. This is in agreement with IF and FACS analysis that showed expression of αIIbβ3 and αvβ3 in MCF-7 (Oleksowicz et al., 1995). Therefore, MCF-7 was chosen as a suitable dual β3-expressing model in its native state to investigate novel dual αvβ3 and αIIbβ antagonists in the functional assays.

Integrin expression in the leukaemia cell line K562, which has been shown to express αIIbβ3 when treated with PMA (Galletti et al., 2014; Stupp et al., 2010), was also investigated in order to develop a functional assay model for testing dual β3 antagonism.

The different times of induction at different concentrations of PMA were investigated to explore its effect on integrin expression as discussed in Chapter 3; 0.04 μM PMA for 40 hours was chosen as a safe concentration and time to induce αIIb in K562 cells. PMA stimulation of K562 cells increased adhesion on fibrinogen compared to unstimulated controls. This suggests that the functional response of stimulated cells depends on integrin-mediated binding. Zhou found increased E-cadherin was responsible for increased adhesion in PMA-treated leukaemia cell lines (Zhou et al., 2016b). Therefore, known β3 antagonists, GR144053 and cRGDfV were used singly and in combination to validate cell adhesion and detachment assays, confirming the binding was β3 integrin mediated. Their inhibitory and detaching effects were dose dependent and greater in PMA-stimulated K562 cells than in unstimulated cells. Combination of the control compounds inhibited cellular adhesion and induced cellular detachment more than single compounds with a combination index CI<1, indicating there was a synergistic interaction between the two agents. The same effects were seen in MCF-7 cells. The synergy of two or more agents is a highly

pursued goal for developing combined drugs which lead to greater efficacy than monotherapy because their interaction is accompanied by a greater response in the tumour microenvironment. In this case, the efficacy of the combination indicates the two β3 integrins both contribute to cell functions and are partially redundant if one is inhibited, and support our hypothesis that dual antagonism is required for effective control of dual integrin expressing tumours.

After establishing the fibrinogen adhesion assay response to controls, novel β3 integrin antagonists were screened. From investigating a panel of 12 small molecules, ICT9055 was not toxic and had the greatest effect in inhibition of K562 (±PMA) and MCF-7 cell adhesion compared to the combined controls. Other compounds had different cytotoxicity such as ICT9072 and ICT9073 which were toxic to MCF-7 cells but not toxic to K562 cells. The difference in the cytotoxic effect of some integrin antagonists on some tumour cells is a common observation. For example, the effects of cilengitide were investigated against the three papillary thyroid cancer cell lines (BCPAP, TPC1, and K1). These data showed a moderate effect on cell viability of BCPAP and K1 cells but cilengitide was toxic in TPC1 cells which had the highest expression of the target integrins (Cheng et al., 2016).

Cheng et al., (2016) suggested that integrin antagonists may be most useful in subgroups of patients with high integrin expressing tumours. The toxicity results in this study are more likely to result from idiosyncratic or off target effects of particular compounds, and may suggest that these compounds are also pro-apoptotic.

ICT9072, ICT9073 and ICT9099 reduced the adhesion of K562 cells treated with PMA more than untreated controls. ICT9001 and ICT9103A reduced

adhesion only in the presence of PMA suggesting they are acting specifically on the upregulated integrins rather than those expressed on untreated cells.

In addition, the viability of non-adherent K562 cells (±PMA) and MCF-7 treated with ICT9055 during the adhesion assay was investigated and showed that ICT9055 affected cell survival in a time-dependent manner. When K562 cells were treated with ICT9055, no difference in the number of viable cells was detected within 4 hours, but the number of viable K562 cells had decreased by 24 hours. The number of viable MCF-7 cells declined with both short and long times of exposure. The effects of ICT9055 may be related to the initial loss of cell adhesion leading later to cell death, with different cell lines being more sensitive to loss of adhesion. The proteins of the pro-apoptotic BH3 family are essential players within the intrinsic pathway of the anoikis programme (Bouillet and Strasser, 2002). Bid and Bim are members of the BH3-only protein family which are activated following cells detachment from ECM and stimulate the assembly of Bax–Bak oligomers within the outer mitochondrial membrane (Taylor et al., 2008). Bim is isolated in the dynein cytoskeletal complexes until loss of cell adhesion promotes a release of Bim from these complexes and leads to its translocation to the mitochondria (Cheng et al., 2001; Paoli et al., 2013). Loss of cell adhesion also results in accumulating of Bim, during the prevention of its proteasomal degradation caused by an ERK and PI3K/Akt-mediated phosphorylation of Bim, elicited upon engagement of integrin (Le Gall et al., 2000; Paoli et al., 2013; Qi et al., 2006).

Hoechst staining of K562 and MCF-7 indicated apoptosis was taking place. As noted by Hook and Schagat., (2012) the same compound may induce programmed cell death in one cell type but not in other cells, and the time of

drug exposure required to induce a response which also may change with cell type.

The effect of compounds on cellular detachment was investigated, as Mould et al., (2014) had postulated that RGD-mimetic antagonists were ineffective due to their inability to detach integrins from their ligands, demonstrated with Cilengitide and cycloGRGDSP. Amino acid residues involved in integrin-fibronectin binding become masked in the ligand-occupied state which prevents binding competitive antagonists. As a result of location of the epitopes of some function-blocking anti-integrin mAbs close to the ligand-binding pocket, it follows that the epitopes of these mAbs may become protected in the ligand-occupied state. mAbs could fail to cause dissociation of integrin-fibronectin interactions (Mould et al., 2016).

ICT9055, ICT9072, ICT9073, and ICT9099 were chosen to investigate their effect on cellular detachment as they significantly inhibited the adhesion of K562 ±PMA and MCF-7 to fibrinogen. ICT9055 had a greater effect in inducing cell detachment than other tested compounds.

The findings of this current study are consistent with those of Oliveira-Ferrer et al., (2008) who demonstrated that cilengitide causes cellular detachment, disassembly of the cytoskeleton and induction of a cell death programme in glioma and endothelial cells thereby clarifying the activity of integrin inhibitors in gliomas. Earlier data suggested that cilengitide also enhances cellular detachment from the ECM proteins vitronectin and tenascin present in the brain (Taga et al., 2002).

The expression of αv, αIIb and β3 integrin subunits was analysed in detached and attached PMA treated K562 cells resulting from treatment with ICT9055 for

6 hours to investigate a possible mechanism of action. The observation showed no changes in integrin expression in detached cells compared to control untreated cells. In contrast, attached cells showed reduced expression of αv, αIIb and β3 integrin subunit compared to the untreated control and or treated detached cells. These data may be explained by the attached cell binding to fibrinogen using another integrin which is not targeted by ICT9055, such as α5β1.

After investigating the library of ICT compounds in adhesion and detachment assays, it was important to study their impact on other biological functions such as cell migration. Cell migration is a fundamental cellular behaviour that not only contributes to developing homeostasis but also to cancer metastasis. Because of its relevance to numerous aspects of human health, many approaches have been developed to measure cell migration (Glenn et al., 2016). Integrins regulate complex molecular processes including the interaction between the ECM and cell receptors, and the signal integration that modulates cell phenotype and migration rate (Friedl and Wolf, 2003; Madrazo et al., 2017). The expression of integrin αvβ3 has been revealed to have a significant effect on the invasive and migratory potential of various cell types (Christenheit et al., 2016; Hynes, 2003).

The anti-migratory effects of the novel integrin antagonists comprising ICT9055, ICT9072 and ICT9073 in comparison with combined controls were evaluated in K562 and MCF-7 cells using a transwell migration assay. ICT9055, ICT9072 and ICT9073 inhibit migration of K562 and MCF-7 cells in a dose-dependent manner. ICT9055 and ICT9072 had greatest efficacy but ICT9073 had a lesser impact than combined cRGDfV/GR144053.

Small molecule RGD-mimetic antagonists have been shown to inhibit migration and adhesion of U251 and U373 human glioblastoma cell lines via modulation of a FAK-dependent pathway (Russo et al., 2013). FAK is the connection between downstream signalling transduction pathways and integrins and activates the PI3K/AKT and ERK pathways implicated in cell migration and proliferation (Schaller, 2010). Treatment of endothelial and glioma cells with cilengitide for a short period causes inhibition of the FAK/Src/AKT-dependent pathway but did not impact on ERK activation in human umbilical vein endothelial cells (Oliveira-Ferrer et al., 2008). Cells treated with a small molecule integrin antagonist 1a-RGD showed a significant decrease of FAK phosphorylation but no obvious effect on phosphorylation of AKT and ERK was observed, suggesting other receptor systems (possibly including other integrins) can activate the AKT and ERK dependent pathways after αvβ3 inhibition (Russo et al., 2013).

4.7 Conclusion

In conclusion, this thesis validates the use of αvβ3 and αIIbβ3 integrin expressing models using both naturally and induced expression for functional assays which have been utilised to evaluate a group of novel small molecule β3 integrin antagonists. The findings presented here show the importance of the RGD binding integrin expression in cancer cell adhesion, detachment and migration. Of note, ICT9055 resulted in significant inhibition of cell adhesion and migration and significant induction of cell detachment.

4.8 Future work

The future experiments could be achieved in the short, medium and long term are described below.

4.8.1 Short-term work

Apoptosis assessment by a quantitative *in vitro* assay (Annexin V apoptosis detection assay) should be utilised to confirm our qualitative analysis, and a wider range of cell lines used to rule out line specific effects when selecting compounds for progression. It may also be worthwhile to investigate whether pro-apoptotic BH3 family proteins are involved in cell detachment and apoptosis caused by ICT compounds. For example, ICT9049 had cytotoxic effects on selected cells in this work, therefore, we need to determine whether ICT9094 is more effective in pro-apoptotic cells expressing β3 integrins, or whether this antagonist has cytotoxic effects, using tumour and healthy cells.

Further research is necessary to determine whether the adherent cells are a subpopulation with naturally low expression of the β3 integrins, or whether treatment with the antagonist decreases expression of its target. This should be followed by investigating the effect of ICT9055 on the subpopulation by characterising their integrin expression.

In further work, it may be worthwhile to look the impacts of integrin antagonists on cell signalling pathways, such as the FAK and ERK pathways, to explore the mechanism that facilitates cell migration, as well as exploring combinations of integrin antagonists with other pathway inhibitors. For example, Inhibition of αv integrins and Src has been shown to be more effective than integrin antagonism alone (Jia et al., 2013).

In this work the effect of novel compounds was investigated by a 2D migration assay (a transwell migration assay). Although it has advantages, as described earlier in Chapter 4, investigating the effect of ICT compounds using a 3D migration assay would give further understanding in a situation more closely mimicking the tumour *in vivo*.

Another aspect that should be considered is evaluating the effect of ICT compounds on angiogenesis, utilising an *in vitro* matrigel-based angiogenic assay.

4.8.2 Medium term work

Investigating the effect of selected antagonists on xenograft models in mice would be a next step. Developing a model for *in vivo* analysis of anti-metastatic

effects would be the next stage for the evaluation of integrin antagonists. This would additionally allow assessment of possible side effects of treatment, and also synergistic effects when in combination with other treatments. Further steps would include assessment of pharmacokinetics, off-target effects, safety and toxicology.

4.8.3 Long term work

Ultimately, the final goal would be assessment of a candidate inhibitor in a phase I clinical trial in cancer patients. There are many factors would need to be taken into consideration that could be the effect on the sensitivity of integrin antagonist. For example, Glut3-addicted glioblastoma tumours are extremely sensitive to drugs targeting αvβ3 (Cosset et al., 2017).

Chapter 6: References

4.9 References

Aguayo, A., Estey, E., Kantarjian, H., Mansouri, T., Gidel, C., Keating, M., Giles, F., Estrov, Z., Barlogie, B., and Albitar, M. (1999). Cellular vascular endothelial growth factor is a predictor of outcome in patients with acute myeloid leukemia. Blood *94*, 3717-3721.

Aguayo, A., Kantarjian, H., Manshouri, T., Gidel, C., Estey, E., Thomas, D., Koller, C., Estrov, Z., O'Brien, S., and Keating, M. (2000). Angiogenesis in acute and chronic leukemias and myelodysplastic syndromes. Blood *96*, 2240-2245.

Ahmedah, H. (2015). Correlation between the expression of integrin and their role in cancer progression. PhD thesis. (University of Bradford).

Al-Asadi, M.G., Brindle, G., Castellanos, M., May, S.T., Mills, K.I., Russell, N.H., Seedhouse, C.H., and Pallis, M. (2017). A molecular signature of dormancy in CD34(+)CD38(-) acute myeloid leukaemia cells. Oncotarget *8*, 111405-111418.

Al-Husein, B., Abdalla, M., Trepte, M., Deremer, D.L., and Somanath, P.R. (2012). Antiangiogenic therapy for cancer: an update. Pharmacotherapy *32*, 1095-1111.

Al-Mehdi, A.B., Tozawa, K., Fisher, A.B., Shientag, L., Lee, A., and Muschel, R.J. (2000). Intravascular origin of metastasis from the proliferation of endothelium-attached tumor cells: a new model for metastasis. Nat Med *6*, 100-102.

Albelda, S.M. (1990). Integrin distribution in malignant melanoma: association of the [beta]3 subunit with tumor progression. Cancer Res *50*, 6757-6764.

Albelda, S.M., Mette, S.A., Elder, D.E., Stewart, R., Damjanovich, L., Herlyn, M., and Buck, C.A. (1990). Integrin distribution in malignant melanoma: association of the beta 3 subunit with tumor progression. Cancer Res *50*, 6757-6764.

Alghisi, G.C., Ponsonnet, L., and Ruegg, C. (2009). The integrin antagonist cilengitide activates alphaVbeta3, disrupts VE-cadherin localization at cell junctions and enhances permeability in endothelial cells. PLoS One *4*, e4449.

Alshammari, F.O.F.O. (2013). An immunohistopathological and functional investigation of β3 integrin antagonism as a therapeutic strategy in cancer. In ICT (Bradford: PhD Thesis. University of Bradford).

Arias-Salgado, E.G. (2003). Src kinase activation by direct interaction with the integrin [beta]cytoplasmic domain. Proc Natl Acad Sci USA *100*, 13298-13302.

Arnaout, M.A., Mahalingam, B., and Xiong, J.P. (2005). Integrin structure, allostery, and bidirectional signaling. Annu Rev Cell Dev Biol *21*, 381-410.

Asiedu, C., Biggs, J., and Kraft, A.S. (1997). Complex regulation of CDK2 during phorbol ester-induced hematopoietic differentiation. Blood *90*, 3430-3437.

Atkinson, S.J., Ellison, T.S., Steri, V., Gould, E., and Robinson, S.D. (2014). Redefining the role(s) of endothelial alphavbeta3-integrin in angiogenesis. Biochem Soc Trans *42*, 1590-1595.

Avraamides, C.J., Garmy-Susini, B., and Varner, J.A. (2008). Integrins in angiogenesis and lymphangiogenesis. Nat Rev Cancer *8*, 604-617.

Ayala, F., Dewar, R., Kieran, M., and Kalluri, R. (2009). Contribution of bone microenvironment to leukemogenesis and leukemia progression. Leukemia *23*, 2233-2241.

Bachsais, M., Naddaf, N., Yacoub, D., Salti, S., Alaaeddine, N., Aoudjit, F., Hassan, G.S., and Mourad, W. (2016). The Interaction of CD154 with the alpha5beta1 Integrin Inhibits Fas-Induced T Cell Death. PLoS One *11*, 158987.

Bakewell, S.J., Nestor, P., Prasad, S., Tomasson, M.H., Dowland, N., Mehrotra, M., Scarborough, R., Kanter, J., Abe, K., Phillips, D.*, et al.* (2003). Platelet and osteoclast beta3 integrins are critical for bone metastasis. Proc Natl Acad Sci U S A *100*, 14205-14210.

Ball, E.D., and Kagan, A. (2007).100 questions and answers about leukemia (Jones & Bartlett Learning),pp.134.

Bauer, K., Mierke, C., and Behrens, J. (2007). Expression profiling reveals genes associated with transendothelial migration of tumor cells: a functional role for alphavbeta3 integrin. Int J Cancer *121*, 1910-1918.

Beauvais, D.M., Burbach, B.J., and Rapraeger, A.C. (2004). The syndecan-1 ectodomain regulates alphavbeta3 integrin activity in human mammary carcinoma cells. J Cell Biol *167*, 171-181.

Becker, A., von Richter, O., Kovar, A., Scheible, H., van Lier, J.J., and Johne, A. (2015). Metabolism and disposition of the αv-integrin ß3/ß5 receptor antagonist cilengitide, a cyclic polypeptide, in humans. J Clin Pharmacol 55,815-24.

Guinn, K.M., Matthews, C.M., Ho, S.N., Barve, M., Gilbert, L., Penson, R.T., Lengyel, E., Palapareptide, in humans. J Clin Pharmacol *55*, 815-824.

Becker, P.S., and Appelbaum, F.R. (2015). VLA-4 Function and Prognosis in Acute Myeloid Leukemia. In Targeted Therapy of Acute Myeloid Leukemia, M. Andreeff, ed. (New York, NY: Springer New York), pp. 627-635.

Bedford, R., Tiede, C., Hughes, R., Curd, A., McPherson, M.J., Peckham, M., and Tomlinson, D.C. (2017). Alternative reagents to antibodies in imaging applications. Biophys Rev *9*, 299-308.

Bell-Mcthy, R., Gilder, K., Vassos, A.*, et al.* (2011). A phase II, single-arm study of the anti-alpha5beta1 integrin antibody volociximab as monotherapy in

patients with platinum-resistant advanced epithelial ovarian or primary peritoneal cancer. Gynecol Oncol *121*, 273-279.

Bendall, L.J., Daniel, A., Kortlepel, K., and Gottlieb, D.J. (1994). Bone marrow adherent layers inhibit apoptosis of acute myeloid leukemia cells. Exp Hematol *22*, 1252-1260.

Bendas, G., and Borsig, L. (2012). Cancer cell adhesion and metastasis: selectins, integrins, and the inhibitory potential of heparins. Int J Cell Biol *2012*, 676731.

Berger, M.D., Heini, A.D., Seipel, K., Mueller, B., Angelillo-Scherrer, A., and Pabst, T. (2017). Increased fibrinogen levels at diagnosis are associated with adverse outcome in patients with acute myeloid leukemia. Hematol Oncol *35*, 789-796.

Bergers, G., and Benjamin, L.E. (2003). Tumorigenesis and the angiogenic switch. Nat Rev Cancer *3*, 401-410.

Besse, B., Tsao, L.C., Chao, D.T., Fang, Y., Soria, J.C., Almokadem, S., and Belani, C.P. (2013). Phase Ib safety and pharmacokinetic study of volociximab, an anti-alpha5beta1 integrin antibody, in combination with carboplatin and paclitaxel in advanced non-small-cell lung cancer. Ann Oncol *24*, 90-96.

Bhaskar, V., Fox, M., Breinberg, D., Wong, M.H., Wales, P.E., Rhodes, S., DuBridge, R.B., and Ramakrishnan, V. (2008). Volociximab, a chimeric integrin alpha5beta1 antibody, inhibits the growth of VX2 tumors in rabbits. Invest New Drugs *26*, 7-12.

Bissell, M.J., and Hines, W.C. (2011). Why don't we get more cancer? A proposed role of the microenvironment in restraining cancer progression. Nat Med *17*, 320-329.

Bledzka, K., Smyth, S.S., and Plow, E.F. (2013). Integrin αIIbβ3: From Discovery to Efficacious Therapeutic Target. Circ Res *112*, 1189-1200.

Borges, E., Jan, Y., and Ruoslahti, E. (2000). Platelet-derived growth factor receptor beta and vascular endothelial growth factor receptor 2 bind to the beta 3 integrin through its extracellular domain. J Biol Chem *275*, 39867-39873.

Borsig, L., Wong, R., Hynes, R.O., Varki, N.M., and Varki, A. (2002). Synergistic effects of L- and P-selectin in facilitating tumor metastasis can involve non-mucin ligands and implicate leukocytes as enhancers of metastasis. Proc Natl Acad Sci USA *99*, 2193-2198.

Bouillet, P., and Strasser, A. (2002). BH3-only proteins - evolutionarily conserved proapoptotic Bcl-2 family members essential for initiating programmed cell death. J Cell Sci *115*, 1567-1574.

Bradstock, K.F., and Gottlieb, D.J. (1995). Interaction of acute leukemia cells with the bone marrow microenvironment: implications for control of minimal residual disease. Leuk Lymphoma *18*, 1-16.

Brooks, P.C. (1996). Cell adhesion molecules in angiogenesis. Cancer Metastasis Rev *15*, 187-194.

Brooks, P.C., Montgomery, A.M., Rosenfeld, M., Reisfeld, R.A., Hu, T., Klier, G., and Cheresh, D.A. (1994). Integrin alpha v beta 3 antagonists promote tumor regression by inducing apoptosis of angiogenic blood vessels. Cell *79*, 1157-1164.

Brooks, P.C., Stromblad, S., Klemke, R., Visscher, D., Sarkar, F.H., and Cheresh, D.A. (1995). Antiintegrin alpha v beta 3 blocks human breast cancer growth and angiogenesis in human skin. J Clin Invest *96*, 1815-1822.

Burger, S.R., Zutter, M.M., Sturgill-Koszycki, S., and Santoro, S.A. (1992). Induced cell surface expression of functional alpha 2 beta 1 integrin during

megakaryocytic differentiation of K562 leukemic cells. In Exp Cell Res (United States), pp. 28-35.

Burridge, K., and Connell, L. (1983). Talin: a cytoskeletal component concentrated in adhesion plaques and other sites of actin-membrane interaction. Cell Motil *3*, 405-417.

Butler, T.M., Ziemiecki, A., and Friis, R.R. (1990). Megakaryocytic differentiation of K562 cells is associated with changes in the cytoskeletal organization and the pattern of chromatographically distinct forms of phosphotyrosyl-specific protein phosphatases. Cancer Res *50*, 6323-6329.

Byzova, T.V., Kim, W., Midura, R.J., and Plow, E.F. (2000). Activation of integrin alpha(V)beta(3) regulates cell adhesion and migration to bone sialoprotein. Exp Cell Res *254*, 299-308.

Bönig, H., and Kim, Y.-M. (2015). VLA4 in Acute Lymphoblastic Leukemia. In Targeted Therapy of Acute Myeloid Leukemia (Springer), pp. 637-654.

Calderwood, D.A. (1999). The talin head domain binds to integrin [beta] subunit cytoplasmic tails and regulates integrin activation. J Biol Chem *274*, 28071-28074.

Carmeliet, P. (2003). Angiogenesis in health and disease. Nat Med *9*, 653-660.
Carmeliet, P., and Jain, R.K. (2000). Angiogenesis in cancer and other diseases. Nature *407*, 249-257.

Carmeliet, P., and Jain, R.K. (2011). Principles and mechanisms of vessel normalization for cancer and other angiogenic diseases. Nat Rev Drug Discov *10*, 417-427.

Carter, P.J. (2006). Potent antibody therapeutics by design. Nat Rev Immunol *6*, 343-357.

Casalou, C., Fragoso, R., Nunes, J.F.M., and Dias, S. (2007). VEGF/PLGF induces leukemia cell migration via P38/ERK1/2 kinase pathway, resulting in Rho GTPases activation and caveolae formation. Leukemia *21*, 1590.

Chambers, A.F., Groom, A.C., and MacDonald, I.C. (2002). Dissemination and growth of cancer cells in metastatic sites. Nat Rev Cancer *2*, 563-572.

Chatterjee, S., Brite, K.H., and Matsumura, A. (2001). Induction of apoptosis of integrin-expressing human prostate cancer cells by cyclic Arg-Gly-Asp peptides. Clin Cancer Res *7*, 3006-3011.

Chen, J., Alexander, J.S., and Orr, A.W. (2012). Integrins and their extracellular matrix ligands in lymphangiogenesis and lymph node metastasis. Int J Cell Biol *2012*, 853703.

Cheng, E.H., Wei, M.C., Weiler, S., Flavell, R.A., Mak, T.W., Lindsten, T., and Korsmeyer, S.J. (2001). BCL-2, BCL-X(L) sequester BH3 domain-only molecules preventing BAX- and BAK-mediated mitochondrial apoptosis. Mol Cell *8*, 705-711.

Cheng, T., Wang, Y., and Dai, W. (1994). Transcription factor egr-1 is involved in phorbol 12-myristate 13-acetate-induced megakaryocytic differentiation of K562 cells. J Biol Chem *269*, 30848-30853.

Cheng, W., Feng, F., Ma, C., and Wang, H. (2016). The effect of antagonizing RGD-binding integrin activity in papillary thyroid cancer cell lines. Onco Targets Ther *9*, 1415-1423.

Cho, P., Schneider, G.B., Kellogg, B., Zaharias, R., and Keller, J.C. (2006). Effect of glucocorticoid-induced osteoporotic-like conditions on osteoblast cell attachment to implant surface microtopographies. Implant Dent *15*, 377-385.

Christenheit, A., Heffeter, P., and Selzer, E. (2016). A Novel Small-Molecule Integrin Antagonist Inhibits Cells Adhesion Followed By Anoikis in Endothelial Cells-A Comparative Analysis with Cilengitide. Glob J Cancer Ther *2,* 9-18.

Cirkel, G.A., Kerklaan, B.M., Vanhoutte, F., Van der Aa, A., Lorenzon, G., Namour, F., Pujuguet, P., Darquenne, S., de Vos, F.Y., Snijders, T.J.*, et al.* (2016). A dose escalating phase I study of GLPG0187, a broad spectrum integrin receptor antagonist, in adult patients with progressive high-grade glioma and other advanced solid malignancies. Invest New Drugs *34*, 184-192.

Cohen, S.A., Trikha, M., and Mascelli, M.A. (2000). Potential future clinical applications for the GPIIb/IIIa antagonist, abciximab in thrombosis, vascular and oncological indications. Pathol Oncol Res *6*, 163-174.

Coller, B.S., and Shattil, S.J. (2008). The GPIIb/IIIa (integrin alphaIIbbeta3) odyssey: a technology-driven saga of a receptor with twists, turns, and even a bend. Blood *112*, 3011-3025.

Conran, N., and Hemming, F.W. (1998). The effect of PMA-induced differentiation on the surface expression of integrins on CHRF 288-11 megakaryoblastic cells in culture. Platelets *9*, 103-108.

Cooper, C.R., Chay, C.H., and Pienta, K.J. (2002). The role of alpha(v)beta(3) in prostate cancer progression. Neoplasia *4*, 191-194.

Cosset, E., Ilmjarv, S., Dutoit, V., Elliott, K., von Schalscha, T., Camargo, M.F., Reiss, A., Moroishi, T., Seguin, L., Gomez, G.*, et al.* (2017). Glut3 Addiction Is a Druggable Vulnerability for a Molecularly Defined Subpopulation of Glioblastoma. Cancer Cell *32*, 856-868.

Cox, D., Brennan, M., and Moran, N. (2010). Integrins as therapeutic targets: lessons and opportunities. Nat Rev Drug Discov *9*, 804-820.

Currier, N.V., Ackerman, S.E., Kintzing, J.R., Chen, R., Filsinger Interrante, M., Steiner, A., Sato, A.K., and Cochran, J.R. (2016). Targeted Drug Delivery with an Integrin-Binding Knottin-Fc-MMAF Conjugate Produced by Cell-Free Protein Synthesis. Mol Cancer Ther *15*, 1291-1300.

Davis, G.E. (1992). Affinity of integrins for damaged extracellular matrix: alpha v beta 3 binds to denatured collagen type I through RGD sites. Biochem Biophys Res Commun *182*, 1025-1031.

Dayam, R., Aiello, F., Deng, J., Wu, Y., Garofalo, A., Chen, X., and Neamati, N. (2006). Discovery of small molecule integrin alphavbeta3 antagonists as novel anticancer agents. J Med Chem *49*, 4526-4534.

Desgrosellier, J.S., and Cheresh, D.A. (2010). Integrins in cancer: biological implications and therapeutic opportunities. Nat Rev Cancer *10*, 9-22.

Dome, B., Raso, E., Dobos, J., Meszaros, L., Varga, N., Puskas, L.G., Feher, L.Z., Lorincz, T., Ladanyi, A., Trikha, M.*, et al.* (2005). Parallel expression of alphaIIbbeta3 and alphavbeta3 integrins in human melanoma cells upregulates bFGF expression and promotes their angiogenic phenotype. Int J Cancer *116*, 27-35.

Dutta, A., Sen, T., and Chatterjee, A. (2010). Culture of K562 human myeloid leukemia cells in presence of fibronectin expresses and secretes MMP-9 in serum-free culture medium. Int J Clin Exp Pathol *3*, 288-302.

Edlund, M., Miyamoto, T., Sikes, R.A., Ogle, R., Laurie, G.W., Farach-Carson, M.C., Otey, C.A., Zhau, H.E., and Chung, L.W. (2001). Integrin expression and usage by prostate cancer cell lines on laminin substrata. Cell Growth Differ *12*, 99-107.

Edmondson, R., Broglie, J.J., Adcock, A.F., and Yang, L. (2014). Three-dimensional cell culture systems and their applications in drug discovery and cell-based biosensors. Assay Drug Dev Technol *12*, 207-218.

Elgavish, A., Prince, C., Chang, P.L., Lloyd, K., Lindsey, R., and Reed, R. (1998). Osteopontin stimulates a subpopulation of quiescent human prostate epithelial cells with high proliferative potential to divide in vitro. Prostate *35*, 83-94.

Eliceiri, B.P., Puente, X.S., Hood, J.D., Stupack, D.G., Schlaepfer, D.D., Huang, X.Z., Sheppard, D., and Cheresh, D.A. (2002). Src-mediated coupling of focal adhesion kinase to integrin alpha(v)beta5 in vascular endothelial growth factor signaling. J Cell Biol *157*, 149-160.

Engebraaten, O., Trikha, M., Juell, S., Garman-Vik, S., and Fodstad, O. (2009). Inhibition of in vivo tumour growth by the blocking of host alpha(v)beta3 and alphaII(b)beta3 integrins. Anticancer Res *29*, 131-137.

Enns, A., Korb, T., Schluter, K., Gassmann, P., Spiegel, H.U., Senninger, N., Mitjans, F., and Haier, J. (2005). Alphavbeta5-integrins mediate early steps of metastasis formation. Eur J Cancer *41*, 1065-1072.

Felding-Habermann, B. (2001). Integrin activation controls metastasis in human breast cancer. Proc Natl Acad Sci USA *98*, 1853-1858.

Felding-Habermann, B., Fransvea, E., O'Toole, T.E., Manzuk, L., Faha, B., and Hensler, M. (2002). Involvement of tumor cell integrin alpha v beta 3 in hematogenous metastasis of human melanoma cells. Clin Exp Metastasis *19*, 427-436.

Felding-Habermann, B., O'Toole, T.E., Smith, J.W., Fransvea, E., Ruggeri, Z.M., Ginsberg, M.H., Hughes, P.E., Pampori, N., Shattil, S.J., Saven, A.*, et al.* (2001). Integrin activation controls metastasis in human breast cancer. Proc Natl Acad Sci U S A *98*, 1853-1858.

Feliciano, P. (2013). Integrin [beta]3 in MLL-AF9 leukemia. Nat Genet *45*, 851-851.

Fennema, E., Rivron, N., Rouwkema, J., van Blitterswijk, C., and de Boer, J. (2013). Spheroid culture as a tool for creating 3D complex tissues. Trends Biotechnol *31*, 108-115.

Fouad, Y.A., and Aanei, C. (2017). Revisiting the hallmarks of cancer. Am J Cancer Res *7*, 1016-1036.

Fragoso, R., Pereira, T., Wu, Y., Zhu, Z., Cabecadas, J., and Dias, S. (2006). VEGFR-1 (FLT-1) activation modulates acute lymphoblastic leukemia localization and survival within the bone marrow, determining the onset of extramedullary disease. Blood *107*, 1608-1616.

Friedl, P., and Wolf, K. (2003). Tumour-cell invasion and migration: diversity and escape mechanisms. Nat Rev Cancer *3*, 362-374.

Friedlander, M., Brooks, P.C., Shaffer, R.W., Kincaid, C.M., Varner, J.A., and Cheresh, D.A. (1995). Definition of two angiogenic pathways by distinct alpha v integrins. Science *270*, 1500-1502.

Friedrich, J., Seidel, C., Ebner, R., and Kunz-Schughart, L.A. (2009). Spheroid-based drug screen: considerations and practical approach. Nat Protoc *4*, 309-324.

Frisch, S.M., and Ruoslahti, E. (1997). Integrins and anoikis. Curr Opin Cell Biol *9*, 701-706.

Furger, K.A., Allan, A.L., Wilson, S.M., Hota, C., Vantyghem, S.A., Postenka, C.O., Al-Katib, W., Chambers, A.F., and Tuck, A.B. (2003). Beta(3) integrin expression increases breast carcinoma cell responsiveness to the malignancy-enhancing effects of osteopontin. Mol Cancer Res *1*, 810-819.

Galletti, P., Soldati, R., Pori, M., Durso, M., Tolomelli, A., Gentilucci, L., Dattoli, S.D., Baiula, M., Spampinato, S., and Giacomini, D. (2014). Targeting integrins

alphavbeta3 and alpha5beta1 with new beta-lactam derivatives. Eur J Med Chem *83*, 284-293.

Ganguly, K.K., Pal, S., Moulik, S., and Chatterjee, A. (2013). Integrins and metastasis. Cell Adh Migr *7*, 251-261.

Gay, L.J., and Felding-Habermann, B. (2011). Contribution of platelets to tumour metastasis. Nat Rev Cancer *11*, 123-134.

Geiger, B., Bershadsky, A., Pankov, R., and Yamada, K.M. (2001a). Transmembrane extracellular matrix-cytoskeleton crosstalk. Nat Rev Mol Cell Biol *2*, 793-805.

Geiger, B., Bershadsky, A., Pankov, R., and Yamada, K.M. (2001b). Transmembrane extracellular matrix-cytoskeleton crosstalk. Nature Reviews Molecular Cell Biology *2*, 793-805.

Glenn, H.L., Messner, J., and Meldrum, D.R. (2016). A simple non-perturbing cell migration assay insensitive to proliferation effects. Sci Rep *6*, 31694.

Gomes, N., Vassy, J., Lebos, C., Arbeille, B., Legrand, C., and Fauvel-Lafeve, F. (2004). Breast adenocarcinoma cell adhesion to the vascular subendothelium in whole blood and under flow conditions: effects of alphavbeta3 and alphaIIbbeta3 antagonists. Clin Exp Metastasis *21*, 553-561.

Goodman, S.L., Grote, H.J., and Wilm, C. (2012). Matched rabbit monoclonal antibodies against alphav-series integrins reveal a novel alphavbeta3-LIBS epitope, and permit routine staining of archival paraffin samples of human tumors. Biol Open *1*, 329-340.

Goodman, S.L., and Picard, M. (2012). Trends Pharmacol Sci. Trends in Pharmacological Sciences *33*, 405-412.

Gordon, J.A., Sodek, J., Hunter, G.K., and Goldberg, H.A. (2009). Bone sialoprotein stimulates focal adhesion-related signaling pathways: role in migration and survival of breast and prostate cancer cells. J Cell Biochem *107*, 1118-1128.

Gruber, G., Hess, J., Stiefel, C., Aebersold, D.M., Zimmer, Y., Greiner, R.H., Studer, U., Altermatt, H.J., Hlushchuk, R., and Djonov, V. (2005). Correlation between the tumoral expression of beta3-integrin and outcome in cervical cancer patients who had undergone radiotherapy Br J Cancer *92*, 41-46.

Gundem, G., Van Loo, P., Kremeyer, B., Alexandrov, L.B., Tubio, J.M., Papaemmanuil, E., Brewer, D.S., Kallio, H.M., Hognas, G., Annala, M.*, et al.* (2015). The evolutionary history of lethal metastatic prostate cancer. Nature *520*, 353-357.

Guo, W., and Giancotti, F.G. (2004). Integrin signalling during tumour progression. Nat Rev Mol Cell Biol *5*, 816-826.

Gupta, G.P., and Massague, J. (2006). Cancer metastasis: building a framework. Cell *127*, 679-695.

Gupta, G.P., Nguyen, D.X., Chiang, A.C., Bos, P.D., Kim, J.Y., Nadal, C., Gomis, R.R., Manova-Todorova, K., and Massague, J. (2007). Mediators of vascular remodelling co-opted for sequential steps in lung metastasis. Nature *446*, 765-770.

Hamidi, H., Pietila, M., and Ivaska, J. (2016). The complexity of integrins in cancer and new scopes for therapeutic targeting. Br J Cancer *115*, 1017-1023.

Hanahan, D., and Weinberg, R.A. (2011). Hallmarks of cancer: the next generation. Cell *144*, 646-674.

Hatley, R., Macdonald, S., Slack, R., Le, J., Ludbrook, S., and Lukey, P. (2017). An av-RGD integrin inhibitor toolbox: drug discovery insight, challenges and opportunities. Angew Chem Int Ed Engl *57*, 3298-3321.

Hauptmann, S., Denkert, C., Lohrke, H., Tietze, L., Ott, S., Klosterhalfen, B., and Mittermayer, C. (1995). Integrin expression on colorectal tumor cells growing as monolayers, as multicellular tumor spheroids, or in nude mice. Int J Cancer *61*, 819-825.

Havaki, S., Kouloukoussa, M., Amawi, K., Drosos, Y., Arvanitis, L.D., Goutas, N., Vlachodimitropoulos, D., Vassilaros, S.D., Katsantoni, E.Z., Voloudakis-Baltatzis, I.*, et al.* (2007). Altered expression pattern of integrin alphavbeta3 correlates with actin cytoskeleton in primary cultures of human breast cancer. Cancer Cell Int *7*, 16.

He, H., Davidson, A.J., Wu, D., Marshall, F.F., Chung, L.W., Zhau, H.E., He, D., and Wang, R. (2010). Phorbol ester phorbol-12-myristate-13-acetate induces epithelial to mesenchymal transition in human prostate cancer ARCaPE cells. Prostate *70*, 1119-1126.

Hehlgans, S., Haase, M., and Cordes, N. (2007). Signalling via integrins: implications for cell survival and anticancer strategies. Biochim Biophys Acta *1775*, 163-180.

Hersey, P., Sosman, J., O'Day, S., Richards, J., Bedikian, A., Gonzalez, R., Sharfman, W., Weber, R., Logan, T., Buzoianu, M.*, et al.* (2010). A randomized phase 2 study of etaracizumab, a monoclonal antibody against integrin alpha(v)beta(3), + or - dacarbazine in patients with stage IV metastatic melanoma. Cancer *116*, 1526-1534.

Heß, K., Böger, C., Behrens, H.-M., and Röcken, C. (2014). Correlation between the expression of integrins in prostate cancer and clinical outcome in 1284 patients. Ann Diagn Pathol *18*, 343-50.

Hieken, T.J., Farolan, M., Ronan, S.G., Shilkaitis, A., Wild, L., and Das Gupta, T.K. (1996). β3 Integrin Expression in Melanoma Predicts Subsequent Metastasis. Journal of Surgical Research *63*, 169-173.

Hiratsuka, S., Duda, D.G., Huang, Y., Goel, S., Sugiyama, T., Nagasawa, T., Fukumura, D., and Jain, R.K. (2011). C-X-C receptor type 4 promotes metastasis by activating p38 mitogen-activated protein kinase in myeloid differentiation antigen (Gr-1)-positive cells. Proc Natl Acad Sci U S A *108*, 302-307.

Hirohashi, S., and Kanai, Y. (2003). Cell adhesion system and human cancer morphogenesis. Cancer Sci *94*, 575-581.

Hook, B., and Schagat, T. (2012). Profiling compound effects on cell health in a time course using a multiplexed same-well assay. (Promega Corporation.http://www.promega.co.uk/resources/pubhub/profiling-compound-effects-on-cell-health-in-a-time-course-using-a-multiplexed-same-well-assay/. Accessed 08 Feb 2018.).

Horton, E.R., Byron, A., Askari, J.A., Ng, D.H.J., Millon-Fremillon, A., Robertson, J., Koper, E.J., Paul, N.R., Warwood, S., Knight, D.*, et al.* (2015). Definition of a consensus integrin adhesome and its dynamics during adhesion complex assembly and disassembly. Nat Cell Biol *17*, 1577-1587.

Hu, Z., and Slayton, W.B. (2014). Integrin VLA-5 and FAK are Good Targets to Improve Treatment Response in the Philadelphia Chromosome Positive Acute Lymphoblastic Leukemia. Front Oncol *4*, 112.

Huang, C.Y., Yu, H.S., Lai, T.Y., Yeh, Y.L., Su, C.C., Hsu, H.H., Tsai, F.J., Tsai, C.H., Wu, H.C., and Tang, C.H. (2011). Leptin increases motility and integrin up-regulation in human prostate cancer cells. J Cell Physiol *226*, 1274-1282.

Huang, R., Zhao, L., Chen, H., Yin, R.H., Li, C.Y., Zhan, Y.Q., Zhang, J.H., Ge, C.H., Yu, M., and Yang, X.M. (2014). Megakaryocytic differentiation of K562 cells induced by PMA reduced the activity of respiratory chain complex IV. PLoS One *9*, 96246.

Huang, S., and Ingber, D.E. (1999). The structural and mechanical complexity of cell-growth control. Nat Cell Biol *1*, E131-138.

Huang, Y., Song, N., Ding, Y., Yuan, S., Li, X., Cai, H., Shi, H., and Luo, Y. (2009). Pulmonary vascular destabilization in the premetastatic phase facilitates lung metastasis. Cancer Res *69*, 7529-7537.

Humphries, J.D., Byron, A., and Humphries, M.J. (2006). Integrin ligands at a glance. J Cell Sci *119*, 3901-3903.

Humphries, J.D., Paul, N.R., Humphries, M.J., and Morgan, M.R. (2015). Emerging properties of adhesion complexes: what are they and what do they do? Trends Cell Biol *25*, 388-397.

Humphries, M.J. (2000). Integrin structure. Biochem Soc Trans *28*, 311-339.

Huo, X.F., Yu, J., Peng, H., Du, Z.W., Liu, X.L., Ma, Y.N., Zhang, X., Zhang, Y., Zhao, H.L., and Zhang, J.W. (2006). Differential expression changes in K562 cells during the hemin-induced erythroid differentiation and the phorbol myristate acetate (PMA)-induced megakaryocytic differentiation. Mol Cell Biochem *292*, 155-167.

Hussong, J.W., Rodgers, G.M., and Shami, P.J. (2000). Evidence of increased angiogenesis in patients with acute myeloid leukemia. Blood *95*, 309-313.

Huttenlocher, A., and Horwitz, A.R. (2011). Integrins in cell migration. Cold Spring Harb Perspect Biol *3*,5074.

Hynes, R.O. (1992). Integrins: versatility, modulation, and signaling in cell adhesion. Cell *69*, 11-25.

Hynes, R.O. (2002a). A reevaluation of integrins as regulators of angiogenesis. Nature Med *8*, 918-921.

Hynes, R.O. (2002b). Integrins: bidirectional, allosteric signaling machines. Cell *110*, 673-687.

Hynes, R.O. (2002c). Integrins: bidirectional, allosteric signaling machines. Cell *110*, 673-687.

Hynes, R.O. (2003). Metastatic potential: generic predisposition of the primary tumor or rare, metastatic variants [mdash] or both? Cell *113*, 821-823.

Ishikawa, F., Yoshida, S., Saito, Y., Hijikata, A., Kitamura, H., Tanaka, S., Nakamura, R., Tanaka, T., Tomiyama, H., Saito, N.*, et al.* (2007). Chemotherapy-resistant human AML stem cells home to and engraft within the bone-marrow endosteal region. Nat Biotechnol *25*, 1315-1321.

Jalagadugula, G., Dhanasekaran, D.N., and Rao, A.K. (2008). Phorbol 12-myristate 13-acetate (PMA) responsive sequence in Galphaq promoter during megakaryocytic differentiation. Regulation by EGR-1 and MAP kinase pathway. Thromb Haemost *100*, 821-828.

Jarvinen, M., Ylanne, J., and Virtanen, I. (1993). The effect of differentiation inducers on the integrin expression of K562 erythroleukemia cells. Cell Biol Int *17*, 399-407.

Jenson, H.B., Grant, G.M., Ench, Y., Heard, P., Thomas, C.A., Hilsenbeck, S.G., and Moyer, M.P. (1998). Immunofluorescence microscopy and flow cytometry characterization of chemical induction of latent Epstein-Barr virus. Clin Diagn Lab Immunol *5*, 91-97.

Jia, D., Entersz, I., Butler, C., and Foty, R.A. (2012). Fibronectin matrix-mediated cohesion suppresses invasion of prostate cancer cells. BMC Cancer *12*, 94.

Jiang, Y., Dai, J., Yao, Z., Shelley, G., and Keller, E.T. (2017). Abituzumab Targeting of alphaV-Class Integrins Inhibits Prostate Cancer Progression. Mol Cancer Res *15*, 875-883.

Jin, H., and Varner, J. (2004). Integrins: roles in cancer development and as treatment targets. Br J Cancer *90*, 561-565.

Jin, J.K., Dayyani, F., and Gallick, G.E. (2011). Steps in prostate cancer progression that lead to bone metastasis. Int J Cancer *128*, 2545-2561.

Johansen, S., Brenner, A.K., Bartaula-Brevik, S., Reikvam, H., and Bruserud, O. (2018). The Possible Importance of beta3 Integrins for Leukemogenesis and Chemoresistance in Acute Myeloid Leukemia. Int J Mol Sci *19*.

Joyce, J.A., and Pollard, J.W. (2009). Microenvironmental regulation of metastasis. Nat Rev Cancer *9*, 239-252.

Justus, C.R., Leffler, N., Ruiz-Echevarria, M., and Yang, L.V. (2014). In vitro cell migration and invasion assays J Vis Exp. 1, 88.

Kapp, T.G., Rechenmacher, F., Neubauer, S., Maltsev, O.V., Cavalcanti-Adam, E.A., Zarka, R., Reuning, U., Notni, J., Wester, H.J., Mas-Moruno, C*., et al.* (2017). A Comprehensive Evaluation of the Activity and Selectivity Profile of Ligands for RGD-binding Integrins. Sci Rep *7*, 39805.

Katrancha, E.D., and Gonzalez, L.S., 3rd (2014). Trauma-induced coagulopathy. Crit Care Nurse *34*, 54-63.

Katt, M.E., Placone, A.L., Wong, A.D., Xu, Z.S., and Searson, P.C. (2016). In Vitro Tumor Models: Advantages, Disadvantages, Variables, and Selecting the Right Platform. Front Bioeng Biotechnol 12, 4-12.

Khalili, A.A., and Ahmad, M.R. (2015). A Review of Cell Adhesion Studies for Biomedical and Biological Applications. Int J Mol Sci *16*, 18149-18184.

Kim, C., Ye, F., and Ginsberg, M.H. (2011). Regulation of integrin activation. Annu Rev Cell Dev Biol *27*, 321-345.

Kim, S., Bell, K., Mousa, S.A., and Varner, J.A. (2000). Regulation of angiogenesis in vivo by ligation of integrin alpha5beta1 with the central cell-binding domain of fibronectin. Am J Pathol *156*, 1345-1362.

Kononczuk, J., Surazynski, A., Czyzewska, U., Prokop, I., Tomczyk, M., Palka, J., and Miltyk, W. (2015). alphaIIbbeta3-integrin Ligands: Abciximab and Eptifibatide as Proapoptotic Factors in MCF-7 Human Breast Cancer Cells. Curr Drug Targets *16*, 1429-1437.

Kumar, C. (2003). Integrin alpha v beta 3 as a therapeutic target for blocking tumor-induced angiogenesis. Curr Drug Targets *4*, 123-131.

Lasky, L.A., Singer, M.S., Dowbenko, D., Imai, Y., Henzel, W.J., Grimley, C., Fennie, C., Gillett, N., Watson, S.R., and Rosen, S.D. (1992). An endothelial ligand for L-selectin is a novel mucin-like molecule. Cell *69*, 927-938.

Lau, T.L., Kim, C., Ginsberg, M.H., and Ulmer, T.S. (2009). The structure of the integrin αIIbβ3 transmembrane complex explains integrin transmembrane signalling. EMBO J *28*, 1351-1361.

Le Gall, M., Chambard, J.C., Breittmayer, J.P., Grall, D., Pouyssegur, J., and Van Obberghen-Schilling, E. (2000). The p42/p44 MAP kinase pathway prevents apoptosis induced by anchorage and serum removal. Mol Biol Cell *11*, 1103-1112.

Legate, K.Rz., Wickstrom, S.A., and Fassler, R. (2009). Genetic and cell biological analysis of integrin outside-in signaling. Genes Dev *23*, 397-418.

Li, C.L., Tian, T., Nan, K.J., Zhao, N., Guo, Y.H., Cui, J., Wang, J., and Zhang, W.G. (2008). Survival advantages of multicellular spheroids vs. monolayers of HepG2 cells in vitro. Oncol Rep *20*, 1465-1471.

Li, R., Maminishkis, A., Zahn, G., Vossmeyer, D., and Miller, S.S. (2009). Integrin alpha5beta1 mediates attachment, migration, and proliferation in

human retinal pigment epithelium: relevance for proliferative retinal disease. Invest Ophthalmol Vis Sci *50*, 5988-5996.

Li, X., Regezi, J., Ross, F.P., Blystone, S., Ilic, D., Leong, S.P., and Ramos, D.M. (2001). Integrin alphavbeta3 mediates K1735 murine melanoma cell motility in vivo and in vitro. J Cell Sci *114*, 2665-2672.

Li, Y., Drabsch, Y., Pujuguet, P., Ren, J., van Laar, T., Zhang, L., van Dam, H., Clement-Lacroix, P., and Ten Dijke, P. (2015). Genetic depletion and pharmacological targeting of alphav integrin in breast cancer cells impairs metastasis in zebrafish and mouse xenograft models. Breast Cancer Res *17*, 28.

Liddington, R.C. (2014). Structural aspects of integrins. Adv Exp Med Biol *819*, 111-126.

Lipscomb, E.A., and Mercurio, A.M. (2005). Mobilization and activation of a signaling competent alpha6beta4integrin underlies its contribution to carcinoma progression. Cancer Metastasis Rev *24*, 413-423.

Liu, Y., Zhao, F., Gu, W., Yang, H., Meng, Q., Zhang, Y., and Duan, Q. (2009). The roles of platelet GPIIb/IIIa and alphavbeta3 integrins during HeLa cells adhesion, migration, and invasion to monolayer endothelium under static and dynamic shear flow. J Biomed Biotechnol *2009*, 829243.

Liu, Z., Wang, F., and Chen, X. (2008). Integrin alpha(v)beta(3)-Targeted Cancer Therapy. Drug Dev Res *69*, 329-339.

Lonsdorf, A.S., Kramer, B.F., Fahrleitner, M., Schonberger, T., Gnerlich, S., Ring, S., Gehring, S., Schneider, S.W., Kruhlak, M.J., Meuth, S.G.*, et al.* (2012). Engagement of alphaIIbbeta3 (GPIIb/IIIa) with alphavbeta3 integrin mediates interaction of melanoma cells with platelets: a connection to hematogenous metastasis. J Biol Chem *287*, 2168-2178.

Luo, B.H., and Springer, T.A. (2006). Integrin structures and conformational signaling. Curr Opin Cell Biol *18*, 579-586.

Madrazo, E., Conde, A.C., and Redondo-Munoz, J. (2017). Inside the Cell: Integrins as New Governors of Nuclear Alterations? Cancers (Basel) 6, 9.

Mahabeleshwar, G.H., Feng, W., Phillips, D.R., and Byzova, T.V. (2006). Integrin signaling is critical for pathological angiogenesis. Journal of Experimental Medicine *203*, 2495-2507.

Marthick, J.R., and Dickinson, J.L. (2012). Emerging putative biomarkers: the role of alpha 2 and 6 integrins in susceptibility, treatment, and prognosis. Prostate Cancer *2012*, 298732.

Martin, S.S., and Vuori, K. (2004). Regulation of Bcl-2 proteins during anoikis and amorphosis. Biochim Biophys Acta *1692*, 145-157.

Martin, T., Ye, L., Aj, S., Lane, J., and Jiang, W. (2013). Cancer Invasion and Metastasis: Molecular and Cellular perspective.

Maruyama, R., Toyooka, S., Toyooka, K.O., Virmani, A.K., Zochbauer-Muller, S., Farinas, A.J., Minna, J.D., McConnell, J., Frenkel, E.P., and Gazdar, A.F. (2002). Aberrant promoter methylation profile of prostate cancers and its relationship to clinicopathological features. Clin Cancer Res *8*, 514-519.

Massague, J., and Obenauf, A.C. (2016). Metastatic colonization by circulating tumour cells. Nature *529*, 298-306.

McAllister, S.S., Gifford, A.M., Greiner, A.L., Kelleher, S.P., Saelzler, M.P., Ince, T.A., Reinhardt, F., Harris, L.N., Hylander, B.L., Repasky, E.A.*, et al.* (2008). Systemic endocrine instigation of indolent tumor growth requires osteopontin. Cell *133*, 994-1005.

McCabe, N.P., De, S., Vasanji, A., Brainard, J., and Byzova, T.V. (2007). Prostate cancer specific integrin alphavbeta3 modulates bone metastatic growth and tissue remodeling. Oncogene *26*, 6238-6243.

McCarty, O.J., Zhao, Y., Andrew, N., Machesky, L.M., Staunton, D., Frampton, J., and Watson, S.P. (2004). Evaluation of the role of platelet integrins in fibronectin-dependent spreading and adhesion. J Thromb Haemost *2*, 1823-1833.

McNeel, D.G., Eickhoff, J., Lee, F.T., King, D.M., Alberti, D., Thomas, J.P., Friedl, A., Kolesar, J., Marnocha, R., Volkman, J.*, et al.* (2005). Phase I trial of a monoclonal antibody specific for alphavbeta3 integrin (MEDI-522) in patients with advanced malignancies, including an assessment of effect on tumor perfusion. Clin Cancer Res *11*, 7851-7860.

Meyer, T., Marshall, J.F., and Hart, I.R. (1998). Expression of alphav integrins and vitronectin receptor identity in breast cancer cells. Br J Cancer *77*, 530-536.
Millard, M., Odde, S., and Neamati, N. (2011). Integrin targeted therapeutics. Theranostics *1*, 154-188.

Miller, P.G., Al-Shahrour, F., Hartwell, K.A., Chu, L.P., Jaras, M., Puram, R.V., Puissant, A., Callahan, K.P., Ashton, J., McConkey, M.E.*, et al.* (2013). In Vivo RNAi screening identifies a leukemia-specific dependence on integrin beta 3 signaling. Cancer Cell *24*, 45-58.

Minn, A.J., Kang, Y., Serganova, I., Gupta, G.P., Giri, D.D., Doubrovin, M., Ponomarev, V., Gerald, W.L., Blasberg, R., and Massague, J. (2005). Distinct organ-specific metastatic potential of individual breast cancer cells and primary tumors. J Clin Invest *115*, 44-55.

Missirlis, D., Haraszti, T., Scheele, C., Wiegand, T., Diaz, C., Neubauer, S., Rechenmacher, F., Kessler, H., and Spatz, J.P. (2016). Substrate engagement of integrins alpha5beta1 and alphavbeta3 is necessary, but not sufficient, for high directional persistence in migration on fibronectin. Sci Rep *6*, 23258.

Mitra, S.K., and Schlaepfer, D.D. (2006). Integrin-regulated FAK-Src signaling in normal and cancer cells. Curr Opin Cell Biol *18*, 516-523.

Morgan, M.R., Byron, A., Humphries, M.J., and Bass, M.D. (2009). Giving off mixed signals--distinct functions of alpha5beta1 and alphavbeta3 integrins in regulating cell behaviour. IUBMB Life *61*, 731-738.

Mould, A.P., Askari, J.A., Byron, A., Takada, Y., Jowitt, T.A., and Humphries, M.J. (2016). Ligand-induced Epitope Masking: Dissociation of integrin alpha beta 1-fibronectin complexes only by monoclonal antibodies with an allosteric mode of action. J Biol Chem *291*, 20993-21007.

Mould, A.P., Craig, S.E., Byron, S.K., Humphries, M.J., and Jowitt, T.A. (2014). Disruption of integrin-fibronectin complexes by allosteric but not ligand-mimetic inhibitors. Biochem J *464*, 301-313.

Nasulewicz-Goldeman, A., Uszczynska, B., Szczaurska-Nowak, K., and Wietrzyk, J. (2012). siRNA-mediated silencing of integrin beta3 expression inhibits the metastatic potential of B16 melanoma cells. Oncol Rep *28*, 1567-1573.

Nieberler, M., Reuning, U., Reichart, F., Notni, J., Wester, H.J., Schwaiger, M., Weinmuller, M., Rader, A., Steiger, K., and Kessler, H. (2017). Exploring the Role of RGD-Recognizing Integrins in Cancer. Cancers (Basel) *4*, 9.

Nolan, J.P., and Sklar, L.A. (1998). The emergence of flow cytometry for sensitive, real-time measurements of molecular interactions. Nat Biotech *16*, 633-638.

Nussenbaum, F., and Herman, I.M. (2010). Tumor angiogenesis: insights and innovations. J Oncol 132641, 24.

Okegawa, T., Pong, R.C., Li, Y., and Hsieh, J.T. (2004). The role of cell adhesion molecule in cancer progression and its application in cancer therapy. Acta Biochim Pol *51*, 445-457.

Oleksowicz, L., Mrowiec, Z., Schwartz, E., Khorshidi, M., Dutcher, J.P., and Puszkin, E. (1995). Characterization of tumor-induced platelet aggregation: the role of immunorelated GPIb and GPIIb/IIIa expression by MCF-7 breast cancer cells. Thromb Res *79*, 261-274.

Oliveira-Ferrer, L., Hauschild, J., Fiedler, W., Bokemeyer, C., Nippgen, J., Celik, I., and Schuch, G. (2008). Cilengitide induces cellular detachment and apoptosis in endothelial and glioma cells mediated by inhibition of FAK/src/AKT pathway. J Exp Clin Cancer Res *27*, 86.

Padua, D., Zhang, X.H., Wang, Q., Nadal, C., Gerald, W.L., Gomis, R.R., and Massague, J. (2008). TGFbeta primes breast tumors for lung metastasis seeding through angiopoietin-like 4. Cell *133*, 66-77.

Paoli, P., Giannoni, E., and Chiarugi, P. (2013). Anoikis molecular pathways and its role in cancer progression. Biochimica et Biophysica Acta (BBA) - Molecular Cell Research *1833*, 3481-3498.

Park, I.C., Park, M.J., Rhee, C.H., Lee, J.I., Choe, T.B., Jang, J.J., Lee, S.H., and Hong, S.I. (2001). Protein kinase C activation by PMA rapidly induces apoptosis through caspase-3/CPP32 and serine protease(s) in a gastric cancer cell line. Int J Oncol *18*, 1077-1083.

Pecheur, I., Peyruchaud, O., Serre, C.-M., Guglielmi, J., Voland, C., Bourre, F., Margue, C., Cohen-Solal, M., Buffet, A., and Kieffer, N. (2002). Integrin αvβ3 expression confers on tumor cells a greater propensity to metastasize to bone. The FASEB Journal *16*, 1266-1268.

Perez-Atayde, A.R., Sallan, S.E., Tedrow, U., Connors, S., Allred, E., and Folkman, J. (1997). Spectrum of tumor angiogenesis in the bone marrow of children with acute lymphoblastic leukemia. Am J Pathol *150*, 815-821.

Perinpanayagam, H., Zaharias, R., Stanford, C., Brand, R., Keller, J., and Schneider, G. (2001). Early cell adhesion events differ between osteoporotic and non-osteoporotic osteoblasts. J Orthop Res *19*, 993-1000.

Pickarski, M., Gleason, A., Bednar, B., and Duong, L.T. (2015). Orally active alphavbeta3 integrin inhibitor MK-0429 reduces melanoma metastasis. Oncol Rep *33*, 2737-2745.

Plow, E.F., Haas, T.A., Zhang, L., Loftus, J., and Smith, J.W. (2000). Ligand binding to integrins. J Biol Chem *275*, 21785-21788.

Pontes-Junior, J., Reis, S.T., de Oliveira, L.C., Sant'anna, A.C., Dall'oglio, M.F., Antunes, A.A., Ribeiro-Filho, L.A., Carvalho, P.A., Cury, J., Srougi, M.*, et al.* (2010). Association between integrin expression and prognosis in localized prostate cancer. Prostate *70*, 1189-1195.

Psaila, B., and Lyden, D. (2009). The metastatic niche: adapting the foreign soil. Nat Rev Cancer *9*, 285-293.

Qi, X.J., Wildey, G.M., and Howe, P.H. (2006). Evidence that Ser87 of BimEL is phosphorylated by Akt and regulates BimEL apoptotic function. J Biol Chem *281*, 813-823.

Qian, B.Z., Li, J., Zhang, H., Kitamura, T., Zhang, J., Campion, L.R., Kaiser, E.A., Snyder, L.A., and Pollard, J.W. (2011). CCL2 recruits inflammatory monocytes to facilitate breast-tumour metastasis. Nature *475*, 222-225.

Quinn, M.J., Byzova, T.V., Qin, J., Topol, E.J., and Plow, E.F. (2003). Integrin alphaIIbbeta3 and its antagonism. Arterioscler Thromb Vasc Biol *23*, 945-952.

Raab-Westphal, S., Marshall, J.F., and Goodman, S.L. (2017). Integrins as therapeutic targets: successes and cancers. Cancers *9*, 110.

Ramakrishnan, V., Bhaskar, V., Law, D.A., Wong, M.H., DuBridge, R.B., Breinberg, D., O'Hara, C., Powers, D.B., Liu, G., Grove, J.*, et al.* (2006). Preclinical evaluation of an anti-alpha5beta1 integrin antibody as a novel anti-angiogenic agent. J Exp Ther Oncol *5*, 273-286.

Ramos, O.H., Kauskot, A., Cominetti, M.R., Bechyne, I., Salla Pontes, C.L., Chareyre, F., Manent, J., Vassy, R., Giovannini, M., Legrand, C.*, et al.* (2008). A novel alpha(v)beta (3)-blocking disintegrin containing the RGD motive, DisBa-01, inhibits bFGF-induced angiogenesis and melanoma metastasis. Clin Exp Metastasis *25*, 53-64.

Ray, A.M., Schaffner, F., Janouskova, H., Noulet, F., Rognan, D., Lelong-Rebel, I., Choulier, L., Blandin, A.F., Lehmann, M., Martin, S.*, et al.* (2014). Single cell tracking assay reveals an opposite effect of selective small non-peptidic alpha5beta1 or alphavbeta3/beta5 integrin antagonists in U87MG glioma cells. Biochim Biophys Acta. 9, 2978-87.

Reardon, D.A., Fink, K.L., Mikkelsen, T., Cloughesy, T.F., O'Neill, A., Plotkin, S., Glantz, M., Ravin, P., Raizer, J.J., Rich, K.M.*, et al.* (2008). Randomized phase II study of cilengitide, an integrin-targeting arginine-glycine-aspartic acid peptide, in recurrent glioblastoma multiforme. J Clin Oncol *26*, 5610-5617.

Reeves, K.J., Hurrell, J.E., Cecchini, M., van der Pluijm, G., Down, J.M., Eaton, C.L., Hamdy, F., Clement-Lacroix, P., and Brown, N.J. (2015). Prostate cancer cells home to bone using a novel in vivo model: modulation by the integrin antagonist GLPG0187. Int J Cancer *136*, 1731-1740.

Reymond, N., d'Agua, B.B., and Ridley, A.J. (2013). Crossing the endothelial barrier during metastasis. Nat Rev Cancer *13*, 858-870.

Ricart, A.D., Tolcher, A.W., Liu, G., Holen, K., Schwartz, G., Albertini, M., Weiss, G., Yazji, S., Ng, C., and Wilding, G. (2008). Volociximab, a chimeric monoclonal antibody that specifically binds alpha5beta1 integrin: a phase I,

pharmacokinetic, and biological correlative study. Clin Cancer Res *14*, 7924-7929.

Ridley, A.J., Schwartz, M.A., Burridge, K., Firtel, R.A., Ginsberg, M.H., Borisy, G., Parsons, J.T., and Horwitz, A.R. (2003). Cell Migration: Integrating Signals from Front to Back. Science *302*, 1704-1709.

Roselova, P., Obr, A., Holoubek, A., Grebenova, D., and Kuzelova, K. (2017). Adhesion structures in leukemia cells and their regulation by Src family kinases. Cell Adh Migr, 5, 1-13.

Rosenthal, M.A., Davidson, P., Rolland, F., Campone, M., Xue, L., Han, T.H., Mehta, A., Berd, Y., He, W., and Lombardi, A. (2010). Evaluation of the safety, pharmacokinetics and treatment effects of an alpha(nu)beta(3) integrin inhibitor on bone turnover and disease activity in men with hormone-refractory prostate cancer and bone metastases. Asia Pac J Clin Oncol *6*, 42-48.

Ross, F.P., Chappel, J., Alvarez, J.I., Sander, D., Butler, W.T., Farach-Carson, M.C., Mintz, K.A., Robey, P.G., Teitelbaum, S.L., and Cheresh, D.A. (1993). Interactions between the bone matrix proteins osteopontin and bone sialoprotein and the osteoclast integrin alpha v beta 3 potentiate bone resorption. J Biol Chem *268*, 9901-9907.

Russo, M.A., Paolillo, M., Sanchez-Hernandez, Y., Curti, D., Ciusani, E., Serra, M., Colombo, L., and Schinelli, S. (2013). A small-molecule RGD-integrin antagonist inhibits cell adhesion, cell migration and induces anoikis in glioblastoma cells. Int J Oncol *42*, 83-92.

Schaller, M.D. (2010). Cellular functions of FAK kinases: insight into molecular mechanisms and novel functions. J Cell Sci *123*, 1007-1013.

Schittenhelm, J., Klein, A., Tatagiba, M.S., Meyermann, R., Fend, F., Goodman, S.L., and Sipos, B. (2013). Comparing the expression of integrins alphavbeta3, alphavbeta5, alphavbeta6, alphavbeta8, fibronectin and fibrinogen in human

brain metastases and their corresponding primary tumors. Int J Clin Exp Pathol *6*, 2719-2732.

Schneller, M., Vuori, K., and Ruoslahti, E. (1997). [alpha]v[beta]3 integrin associates with activated insulin and PDGF[beta] receptors and potentiates the biological activity of PDGF. EMBO J *16*, 5600-5607.

Schnerch, D., Yalcintepe, J., Schmidts, A., Becker, H., Follo, M., Engelhardt, M., and Wasch, R. (2012). Cell cycle control in acute myeloid leukemia. Am J Cancer Res *2*, 508-528.

Schwarz, M., Meade, G., Stoll, P., Ylanne, J., Bassler, N., Chen, Y.C., Hagemeyer, C.E., Ahrens, I., Moran, N., Kenny, D.*, et al.* (2006). Conformation-specific blockade of the integrin GPIIb/IIIa: a novel antiplatelet strategy that selectively targets activated platelets. Circ Res *99*, 25-33.

Serhan, C.N., and Savill, J. (2005). Resolution of inflammation: the beginning programs the end. Nat Immunol *6*, 1191-1197.

Serini, G., Valdembri, D., and Bussolino, F. (2006). Integrins and angiogenesis: a sticky business. Exp Cell Res *312*, 651-658.

Shan, D., Li, J., Cai, P., Prasad, P., Liu, F., Rauth, A.M., and Wu, X.Y. (2015). RGD-conjugated solid lipid nanoparticles inhibit adhesion and invasion of alphavbeta3 integrin-overexpressing breast cancer cells. Drug Deliv Transl Res *5*, 15-26.

Shattil, S.J., and Newman, P.J. (2004). Integrins: dynamic scaffolds for adhesion and signaling in platelets. Blood *104*, 1606-1615.

Sheldrake, H.M., and Patterson, L.H. (2009). Function and antagonism of beta3 integrins in the development of cancer therapy. Curr Cancer Drug Targets *9*, 519-540.

Sheldrake, H.M., and Patterson, L.H. (2014). Strategies To Inhibit Tumor Associated Integrin Receptors: Rationale for Dual and Multi-Antagonists. J Med Chem. 57, 6301-15

Shelly, C., Petruzzelli, L., and Herrera, R. (2000). K562 cells resistant to phorbol 12-myristate 13-acetate-induced growth arrest: dissociation of mitogen-activated protein kinase activation and Egr-1 expression from megakaryocyte differentiation. Cell Growth Differ *11*, 501-506.

Shimaoka, M., Takagi, J., and Springer, T.A. (2002). Conformational regulation of integrin structure and function. Annu Rev Biophys Biomol Struct *31*, 485-516.

Simon, S.I., and Green, C.E. (2005). Molecular mechanics and dynamics of leukocyte recruitment during inflammation. Annu Rev Biomed Eng *7*, 151-185.

Soldi, R., Mitola, S., Strasly, M., Defilippi, P., Tarone, G., and Bussolino, F. (1999). Role of αvβ3 integrin in the activation of vascular endothelial growth factor receptor-2. EMBO J *18*, 882-892.

Soloviev, D., Pluskota, E., and Plow, E. (2007). Cell Adhesion and Migration Assays. In Cardiovascular Disease, Q. Wang, ed. (Humana Press), pp. 267-278.

Sonoshita, M., Aoki, M., Fuwa, H., Aoki, K., Hosogi, H., Sakai, Y., Hashida, H., Takabayashi, A., Sasaki, M., Robine, S.*, et al.* (2011). Suppression of colon cancer metastasis by Aes through inhibition of Notch signaling. Cancer Cell *19*, 125-137.

Stachurska, A., Elbanowski, J., and Kowalczynska, H.M. (2012). Role of alpha5beta1 and alphavbeta3 integrins in relation to adhesion and spreading dynamics of prostate cancer cells interacting with fibronectin under in vitro conditions. Cell Biol Int *36*, 883-892.

Stewart, J.R., and O'Brian, C.A. (2005). Protein kinase C-{alpha} mediates epidermal growth factor receptor transactivation in human prostate cancer cells. Mol Cancer Ther *4*, 726-732.

Stott, S.L., Hsu, C.H., Tsukrov, D.I., Yu, M., Miyamoto, D.T., Waltman, B.A., Rothenberg, S.M., Shah, A.M., Smas, M.E., Korir, G.K.*, et al.* (2010). Isolation of circulating tumor cells using a microvortex-generating herringbone-chip. Proc Natl Acad Sci U S A *107*, 18392-18397.

Strazielle, N., Creidy, R., Malcus, C., Boucraut, J., and Ghersi-Egea, J.F. (2016). T-Lymphocytes Traffic into the Brain across the Blood-CSF Barrier: Evidence Using a Reconstituted Choroid Plexus Epithelium. PLoS One *11*, e0150945.

Stupp, R., Hegi, M.E., Gorlia, T., Erridge, S.C., Perry, J., Hong, Y.-K., Aldape, K.D., Lhermitte, B., Pietsch, T., Grujicic, D.*, et al.* (2014). Cilengitide combined with standard treatment for patients with newly diagnosed glioblastoma with methylated MGMT promoter (CENTRIC EORTC 26071-22072 study): a multicentre, randomised, open-label, phase 3 trial. Lancet Oncol. *15*, 1100-1108.

Stupp, R., Hegi, M.E., Neyns, B., Goldbrunner, R., Schlegel, U., Clement, P.M., Grabenbauer, G.G., Ochsenbein, A.F., Simon, M., Dietrich, P.Y.*, et al.* (2010). Phase I/IIa study of cilengitide and temozolomide with concomitant radiotherapy followed by cilengitide and temozolomide maintenance therapy in patients with newly diagnosed glioblastoma. J Clin Oncol *28*, 2712-2718.

Sutherland, M., Gordon, A., Shnyder, S.D., Patterson, L.H., and Sheldrake, H.M. (2012). RGD-Binding Integrins in Prostate Cancer: Expression Patterns and Therapeutic Prospects against Bone Metastasis. Cancers (Basel) *4*, 1106-1145.

Suyin, P.C., Joanne Louise, D., and Adele Frances, H. (2013). Integrins in Prostate Cancer Invasion and Metastasis. Intech *10*, 5772-5384.

Szekanecz, Z., and Koch, A.E. (2000). Cell-cell interactions in synovitis. Endothelial cells and immune cell migration. Arthritis Res *2*, 368-373.

Taga, T., Suzuki, A., Gonzalez-Gomez, I., Gilles, F.H., Stins, M., Shimada, H., Barsky, L., Weinberg, K.I., and Laug, W.E. (2002). alpha v-Integrin antagonist EMD 121974 induces apoptosis in brain tumor cells growing on vitronectin and tenascin. Int J Cancer *98*, 690-697.

Taherian, A., Li, X., Liu, Y., and Haas, T.A. (2011). Differences in integrin expression and signaling within human breast cancer cells. BMC Cancer *11*, 293.

Takagi, J. (2007). Structural basis for ligand recognition by integrins. Curr Opin Cell Biol *19*, 557-564.

Tavernier-Tardy, E., Cornillon, J., Campos, L., Flandrin, P., Duval, A., Nadal, N., and Guyotat, D. (2009). Prognostic value of CXCR4 and FAK expression in acute myelogenous leukemia. Leuk Res *33*, 764-768.

Taylor, R.C., Cullen, S.P., and Martin, S.J. (2008). Apoptosis: controlled demolition at the cellular level. Nat Rev Mol Cell Biol *9*, 231-241.

Taylor, R.M., Severns, V., Brown, D.C., Bisoffi, M., and Sillerud, L.O. (2012). Prostate cancer targeting motifs: expression of alphav beta3, neurotensin receptor 1, prostate specific membrane antigen, and prostate stem cell antigen in human prostate cancer cell lines and xenografts. Prostate *72*, 523-532.

Tentori, L., Dorio, A.S., Muzi, A., Lacal, P.M., Ruffini, F., Navarra, P., and Graziani, G. (2008). The integrin antagonist cilengitide increases the antitumor activity of temozolomide against malignant melanoma. Oncol Rep *19*, 1039-1043.

Terry, S.Y., Abiraj, K., Frielink, C., van Dijk, L.K., Bussink, J., Oyen, W.J., and Boerman, O.C. (2014). Imaging integrin alphavbeta3 on blood vessels with 111In-RGD2 in head and neck tumor xenografts. J Nucl Med *55*, 281-286.

Teti, A., Migliaccio, S., and Baron, R. (2002). The role of the alphaVbeta3 integrin in the development of osteolytic bone metastases: a pharmacological target for alternative therapy? Calcif Tissue Int *71*, 293-299.

Tiede, C., Tang, A.A., Deacon, S.E., Mandal, U., Nettleship, J.E., Owen, R.L., George, S.E., Harrison, D.J., Owens, R.J., Tomlinson, D.C.*, et al.* (2014). Adhiron: a stable and versatile peptide display scaffold for molecular recognition applications. Protein Eng Des Sel *27*, 145-155.

Tilghman, R.W., and Parsons, J.T. (2008). Focal adhesion kinase as a regulator of cell tension in the progression of cancer. Semin Cancer Biol *18*, 45-52.

Tohyama, Y., Tohyama, K., Tsubokawa, M., Asahi, M., Yoshida, Y., and Yamamura, H. (1998). Outside-In signaling of soluble and solid-phase fibrinogen through integrin alphaIIbbeta3 is different and cooperative with each other in a megakaryoblastic leukemia cell line, CMK. Blood *92*, 1277-1286.

Tomiyama, Y. (2000). Glanzmann thrombasthenia: integrin alpha IIb beta 3 deficiency. Int J Hematol *72*, 448-454.

Trendowski, M. (2015). The inherent metastasis of leukaemia and its exploitation by sonodynamic therapy. Critical Reviews in Oncology/Hematology *94*, 149-163.

Trikha, M., Raso, E., Cai, Y., Fazakas, Z., Paku, S., Porter, A.T., Timar, J., and Honn, K.V. (1998). Role of αIIbβ3 integrin in prostate cancer metastasis. The Prostate *35*, 185-192.

Trikha, M., Timar, J., Lundy, S.K., Szekeres, K., Tang, K., Grignon, D., Porter, A.T., and Honn, K.V. (1996). Human prostate carcinoma cells express functional alphaIIb(beta)3 integrin. Cancer Res *56*, 5071-5078.

Trikha, M., Timar, J., Zacharek, A., Nemeth, J.A., Cai, Y., Dome, B., Somlai, B., Raso, E., Ladanyi, A., and Honn, K.V. (2002a). Role for beta3 integrins in human melanoma growth and survival. Int J Cancer *101*, 156-167.

Trikha, M., Zhou, Z., Timar, J., Raso, E., Kennel, M., Emmell, E., and Nakada, M.T. (2002b). Multiple roles for platelet GPIIb/IIIa and alphavbeta3 integrins in tumor growth, angiogenesis, and metastasis. Cancer Res *62*, 2824-2833.

Tuck, A.B., Arsenault, D.M., O'Malley, F.P., Hota, C., Ling, M.C., Wilson, S.M., and Chambers, A.F. (1999). Osteopontin induces increased invasiveness and plasminogen activator expression of human mammary epithelial cells. Oncogene *18*, 4237-4246.

Tuck, A.B., Elliott, B.E., Hota, C., Tremblay, E., and Chambers, A.F. (2000). Osteopontin-induced, integrin-dependent migration of human mammary epithelial cells involves activation of the hepatocyte growth factor receptor (Met). J Cell Biochem *78*, 465-475.

Tuck, A.B., Hota, C., and Chambers, A.F. (2001). Osteopontin(OPN)-induced increase in human mammary epithelial cell invasiveness is urokinase (uPA)-dependent. Breast Cancer Res Treat *70*, 197-204.

Vacca, A., Ria, R., Presta, M., Ribatti, D., Iurlaro, M., Merchionne, F., Tanghetti, E., and Dammacco, F. (2001). alpha(v)beta(3) integrin engagement modulates cell adhesion, proliferation, and protease secretion in human lymphoid tumor cells. Exp Hematol *29*, 993-1003.

Valastyan, S., and Weinberg, R.A. (2011). Tumor metastasis: molecular insights and evolving paradigms. Cell *147*, 275-292.

van der Horst, G., van den Hoogen, C., Buijs, J.T., Cheung, H., Bloys, H., Pelger, R.C., Lorenzon, G., Heckmann, B., Feyen, J., Pujuguet, P.*, et al.* (2011). Targeting of alpha(v)-integrins in stem/progenitor cells and supportive

microenvironment impairs bone metastasis in human prostate cancer. Neoplasia *13*, 516-525.

Vincent, A.M., Cawley, J.C., and Burthem, J. (1996). Integrin function in chronic lymphocytic leukemia. Blood *87*, 4780-4788.

Vugmeyster, Y., Xu, X., Theil, F.P., Khawli, L.A., and Leach, M.W. (2012). Pharmacokinetics and toxicology of therapeutic proteins: Advances and challenges. World J Biol Chem *3*, 73-92.

Wang, W., Goswami, S., Lapidus, K., Wells, A.L., Wyckoff, J.B., Sahai, E., Singer, R.H., Segall, J.E., and Condeelis, J.S. (2004). Identification and testing of a gene expression signature of invasive carcinoma cells within primary mammary tumors. Cancer Res *64*, 8585-8594.

Weber, M.R., Zuka, M., Lorger, M., Tschan, M., Torbett, B.E., Zijlstra, A., Quigley, J.P., Staflin, K., Eliceiri, B.P., Krueger, J.S.*, et al.* (2016). Activated tumor cell integrin alphavbeta3 cooperates with platelets to promote extravasation and metastasis from the blood stream. Thromb Res *140 Suppl 1*, S27-36.

Wei, J., Wunderlich, M., Fox, C., Alvarez, S., Cigudosa, J.C., Wilhelm, J.S., Zheng, Y., Cancelas, J.A., Gu, Y., Jansen, M.*, et al.* (2008). Microenvironment determines lineage fate in a human model of MLL-AF9 leukemia. Cancer Cell *13*, 483-495.

Weis, S., Cui, J., Barnes, L., and Cheresh, D. (2004). Endothelial barrier disruption by VEGF-mediated Src activity potentiates tumor cell extravasation and metastasis. J Cell Biol *167*, 223-229.

Weis, S.M., and Cheresh, D.A. (2011). alphaV integrins in angiogenesis and cancer. Cold Spring Harb Perspect Med *1*,6478.

Whalen, A.M., Galasinski, S.C., Shapiro, P.S., Nahreini, T.S., and Ahn, N.G. (1997). Megakaryocytic differentiation induced by constitutive activation of mitogen-activated protein kinase kinase. Mol Cell Biol *17*, 1947-1958.

Wichmann, G., Cedra, S., Schlegel, D., Kolb, M., Wiegand, S., Boehm, A., Hofer, M., and Dietz, A. (2017). Cilengitide and Cetuximab Reduce Cytokine Production and Colony Formation of Head and Neck Squamous Cell Carcinoma Cells Ex Vivo. Anticancer Res *37*, 521-527.

Wilder, R.L. (2002). Integrin alpha V beta 3 as a target for treatment of rheumatoid arthritis and related rheumatic diseases. Ann Rheum Dis 2, 96-99.

Wirth, M., Heidenreich, A., Gschwend, J.E., Gil, T., Zastrow, S., Laniado, M., Gerloff, J., Zuhlsdorf, M., Mordenti, G., Uhl, W.*, et al.* (2014). A multicenter phase 1 study of EMD 525797 (DI17E6), a novel humanized monoclonal antibody targeting alphav integrins, in progressive castration-resistant prostate cancer with bone metastases after chemotherapy. Eur Urol *65*, 897-904.

Witkowski, C.M., Rabinovitz, I., Nagle, R.B., Affinito, K.S., and Cress, A.E. (1993). Characterization of integrin subunits, cellular adhesion and tumorgenicity of four human prostate cell lines. J Cancer Res Clin Oncol *119*, 637-644.

Witz, I.P. (2008). The selectin–selectin ligand axis in tumor progression. Cancer Metastasis Rev. *27*, 19-30.

Wong, C.W., Lee, A., Shientag, L., Yu, J., Dong, Y., Kao, G., Al-Mehdi, A.B., Bernhard, E.J., and Muschel, R.J. (2001). Apoptosis: an early event in metastatic inefficiency. Cancer Res *61*, 333-338.

Wong, P.P., Demircioglu, F., Ghazaly, E., Alrawashdeh, W., Stratford, M.R., Scudamore, C.L., Cereser, B., Crnogorac-Jurcevic, T., McDonald, S., Elia, G.,

et al. (2015). Dual-action combination therapy enhances angiogenesis while reducing tumor growth and spread. Cancer Cell *27*, 123-137.

Wyckoff, J.B., Wang, Y., Lin, E.Y., Li, J.F., Goswami, S., Stanley, E.R., Segall, J.E., Pollard, J.W., and Condeelis, J. (2007). Direct visualization of macrophage-assisted tumor cell intravasation in mammary tumors. Cancer Res *67*, 2649-2656.

Xie, J.J., Guo, J.C., Wu, Z.Y., Xu, X.E., Wu, J.Y., Chen, B., Ran, L.Q., Liao, L.D., Li, E.M., and Xu, L.Y. (2016). Integrin alpha5 promotes tumor progression and is an independent unfavorable prognostic factor in esophageal squamous cell carcinoma. Hum Pathol *48*, 69-75.

Xiong, J.P. (2002). Crystal structure of the extracellular segment of integrin [alpha]V[beta]3 in complex with an Arg-Gly-Asp ligand. Science *296*, 151-155.

Yacobovich, S., Tuchinsky, L., Kirby, M., Kardash, T., Agranyoni, O., Nesher, E., Redko, B., Gellerman, G., Tobi, D., Gurova, K.*, et al.* (2016). Novel synthetic cyclic integrin alphavbeta3 binding peptide ALOS4: Antitumor activity in mouse melanoma models. Oncotarget *7*, 63549-63560.

Yi, H., Zeng, D., Shen, Z., Liao, J., Wang, X., Liu, Y., Zhang, X., and Kong, P. (2016). Integrin alphavbeta3 enhances beta-catenin signaling in acute myeloid leukemia harboring Fms-like tyrosine kinase-3 internal tandem duplication mutations: implications for microenvironment influence on sorafenib sensitivity. Oncotarget *7*, 40387-40397.

Ylanne, J., Cheresh, D.A., and Virtanen, I. (1990). Localization of beta 1, beta 3, alpha 5, alpha v, and alpha IIb subunits of the integrin family in spreading human erythroleukemia cells. Blood *76*, 570-577.

Yoon, S.-H., and Mofrad, M.R.K. (2011). Cell adhesion and detachment on gold surfaces modified with a thiol-functionalized RGD peptide. Biomaterials *32*, 7286-7296.

Zanyk, M.J., Banerjee, D., and McFarlane, D.L. (1988). Flow cytometric analysis of the phenotypic changes in tumour cell lines following TPA induction. Cytometry *9*, 374-379.

Zeisig, Bernd B., and So, Chi Wai E. (2013). Linking MLL Leukemia with Integrin Signaling. Cancer Cell *24*, 5-7.

Zent, R., Pozzi, Ambra (2010). Cell-Extracellular Matrix Interactions in Cancer, Vol XII (Springer New York), pp. 1-17.

Zhai, J., Wang, Y., Xu, C., Zheng, L., Wang, M., Feng, W., Gao, L., Zhao, L., Liu, R., Gao, F.*, et al.* (2015). Facile approach to observe and quantify the alpha(IIb)beta3 integrin on a single-cell. Anal Chem *87*, 2546-2549.

Zhang, K., and Chen, J. (2012). The regulation of integrin function by divalent cations. Cell Adh Migr *6*, 20-29.

Zhang, X.H., Wang, Q., Gerald, W., Hudis, C.A., Norton, L., Smid, M., Foekens, J.A., and Massague, J. (2009). Latent bone metastasis in breast cancer tied to Src-dependent survival signals. Cancer Cell *16*, 67-78.

Zhao, Y., and Adjei, A.A. (2015). Targeting Angiogenesis in Cancer Therapy: Moving Beyond Vascular Endothelial Growth Factor. Oncologist *20*, 660-673.

Zhao, Y., Bachelier, R., Treilleux, I., Pujuguet, P., Peyruchaud, O., Baron, R., Clement-Lacroix, P., and Clezardin, P. (2007). Tumor alphavbeta3 integrin is a therapeutic target for breast cancer bone metastases. Cancer Res *67*, 5821-5830.

Zhao, Y.Z., Lin, Q., Wong, H.L., Shen, X.T., Yang, W., Xu, H.L., Mao, K.L., Tian, F.R., Yang, J.J., Xu, J.*, et al.* (2016). Glioma-targeted therapy using Cilengitide nanoparticles combined with UTMD enhanced delivery. J Control Release *224*, 112-125.

Zheng, D.Q., Woodard, A.S., Fornaro, M., Tallini, G., and Languino, L.R. (1999). Prostatic carcinoma cell migration via alpha(v)beta3 integrin is modulated by a focal adhesion kinase pathway. Cancer Res *59*, 1655-1664.

Zheng, D.Q., Woodard, A.S., Tallini, G., and Languino, L.R. (2000). Substrate specificity of alpha(v)beta(3) integrin-mediated cell migration and phosphatidylinositol 3-kinase/AKT pathway activation. J Biol Chem *275*, 24565-24574.

Zhou, X., Seto, S.W., Chang, D., Kiat, H., Razmovski-Naumovski, V., Chan, K., and Bensoussan, A. (2016a). Synergistic Effects of Chinese Herbal Medicine: A Comprehensive Review of Methodology and Current Research. Front Pharmacol *7*, 201.

Zhou, Z.L., Ma, J., Tong, M.H., Chan, B.P., Wong, A.S., and Ngan, A.H. (2016b). Nanomechanical measurement of adhesion and migration of leukemia cells with phorbol 12-myristate 13-acetate treatment. Int J Nanomedicine *11*, 6533-6545.

Appendices

Appendix I: Cytotoxicity effect of dimethyl sulfoxide (DMSO).

The MTT assay was used to assess the cytotoxicity of DMSO against K562 (±PMA) and MCF-7 cells over a range of different concentrations (0.01, 0.1, 1, 10 & 100 µM) for 96 hours.

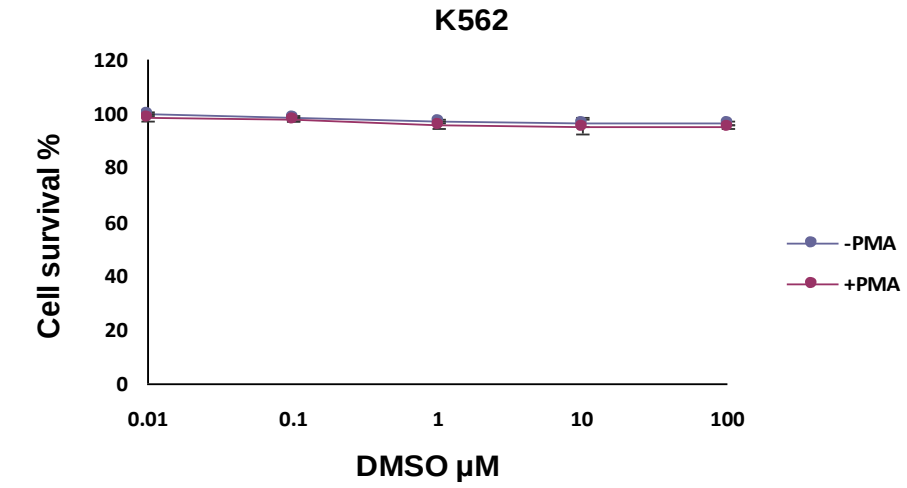

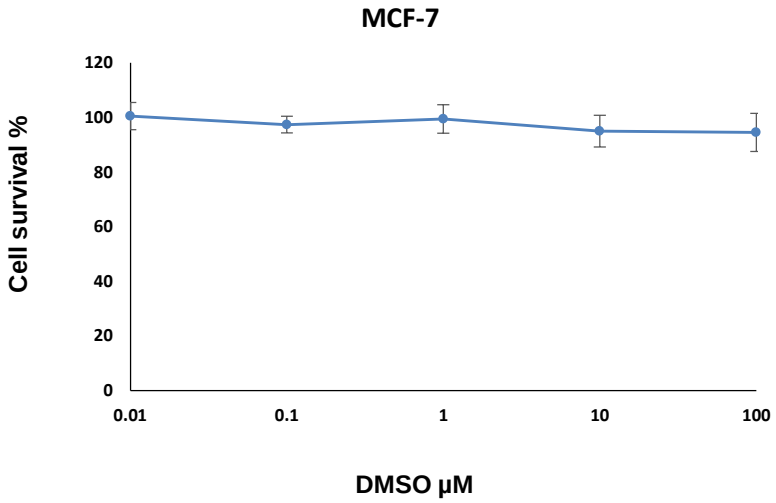

Appendix II: Analysis of Scratch assay of MCF-7

Migration of MCF-7 cell lines was assessed by the scratch assay. 1x105 cells/ml were seeded into 24-well plates and incubated at 37 °C for 24 hours. After 24, 48 and 72 hours, the appearance of the monolayer was examined visually. The scratch was not healed after 72 hours due to slow wound closure, meaning MCF-7 could not be used in this migration assay.

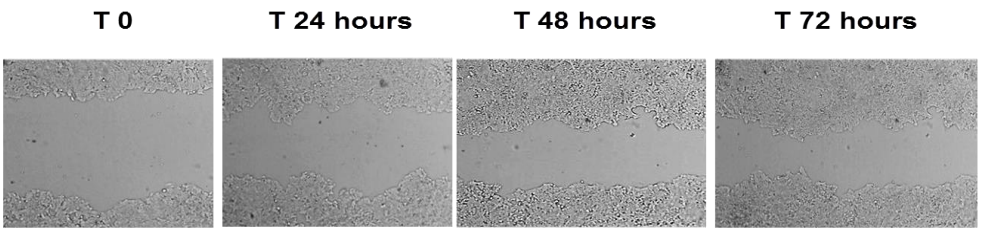

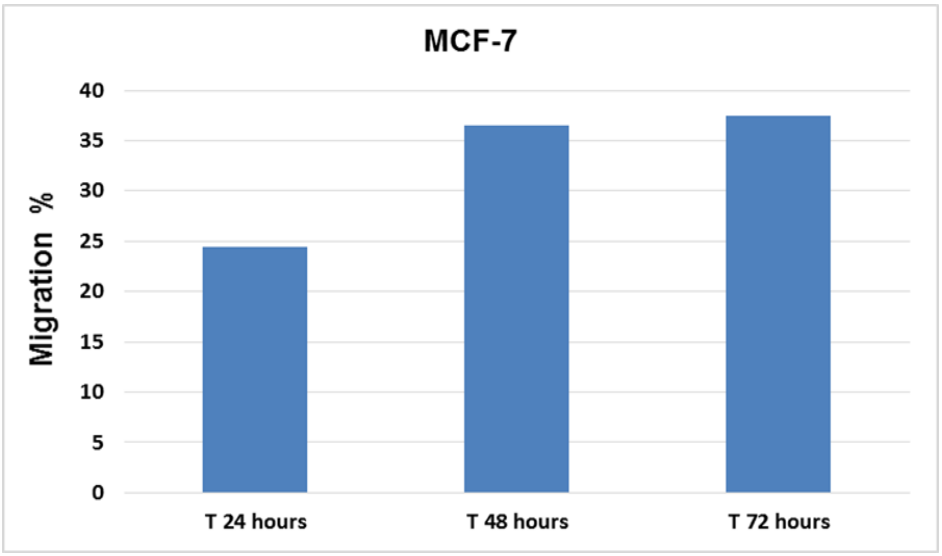

Appendix III: Histogram analysis of αv, αIIb, α5, β3 and β5 integrin subunit expression (coloured histograms) compared to negative control cells (purple histograms) in K562, DU145, PC-3, LNCap and MCF-7 cells using FACS.

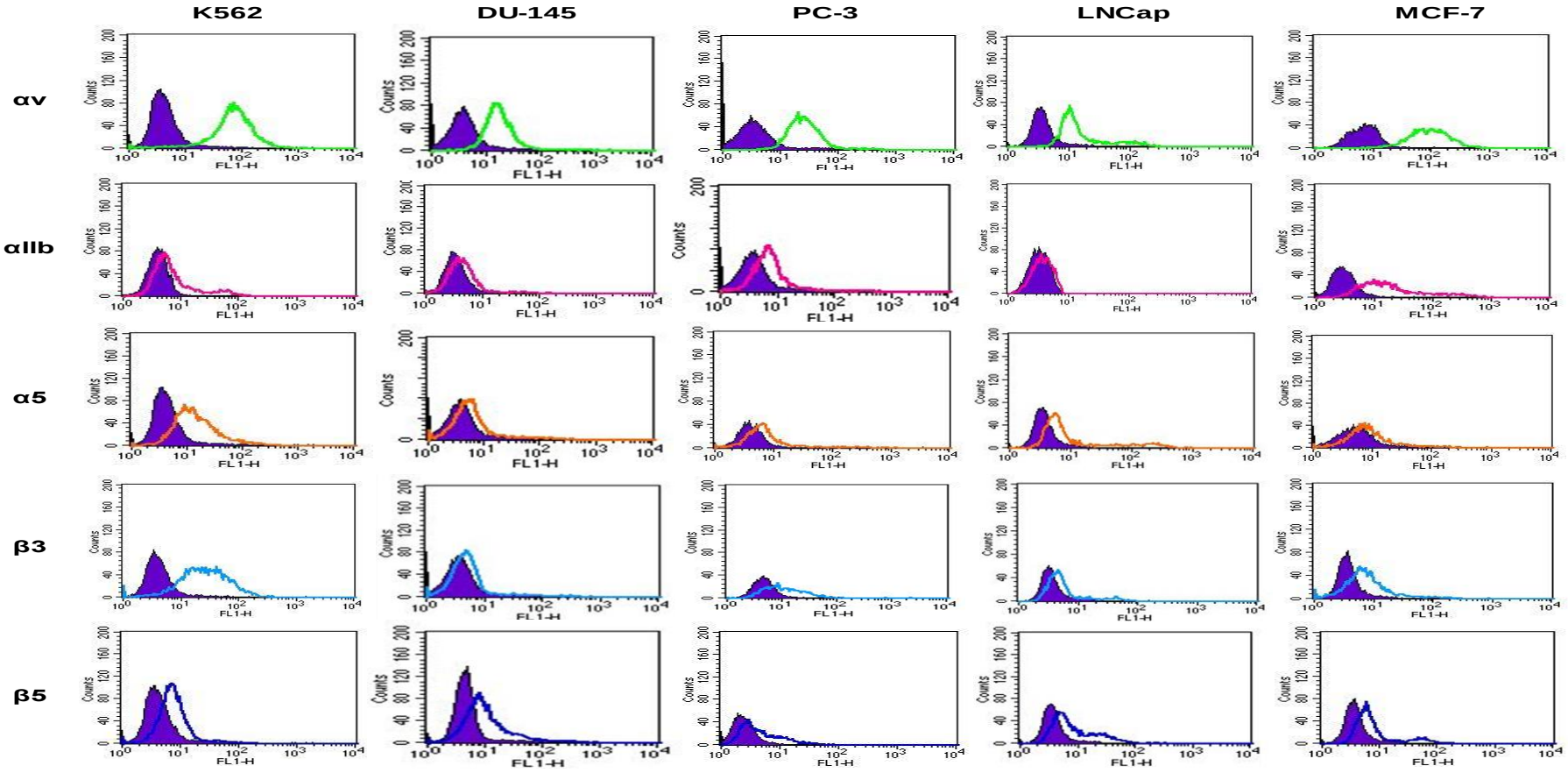

Appendix IV: Histogram analysis of αIIb and β3 integrin subunit expression (green histograms) compared to negative control cells (purple histograms) in M14, MeWo, UACC-62 and HT-29 cells using FACS.

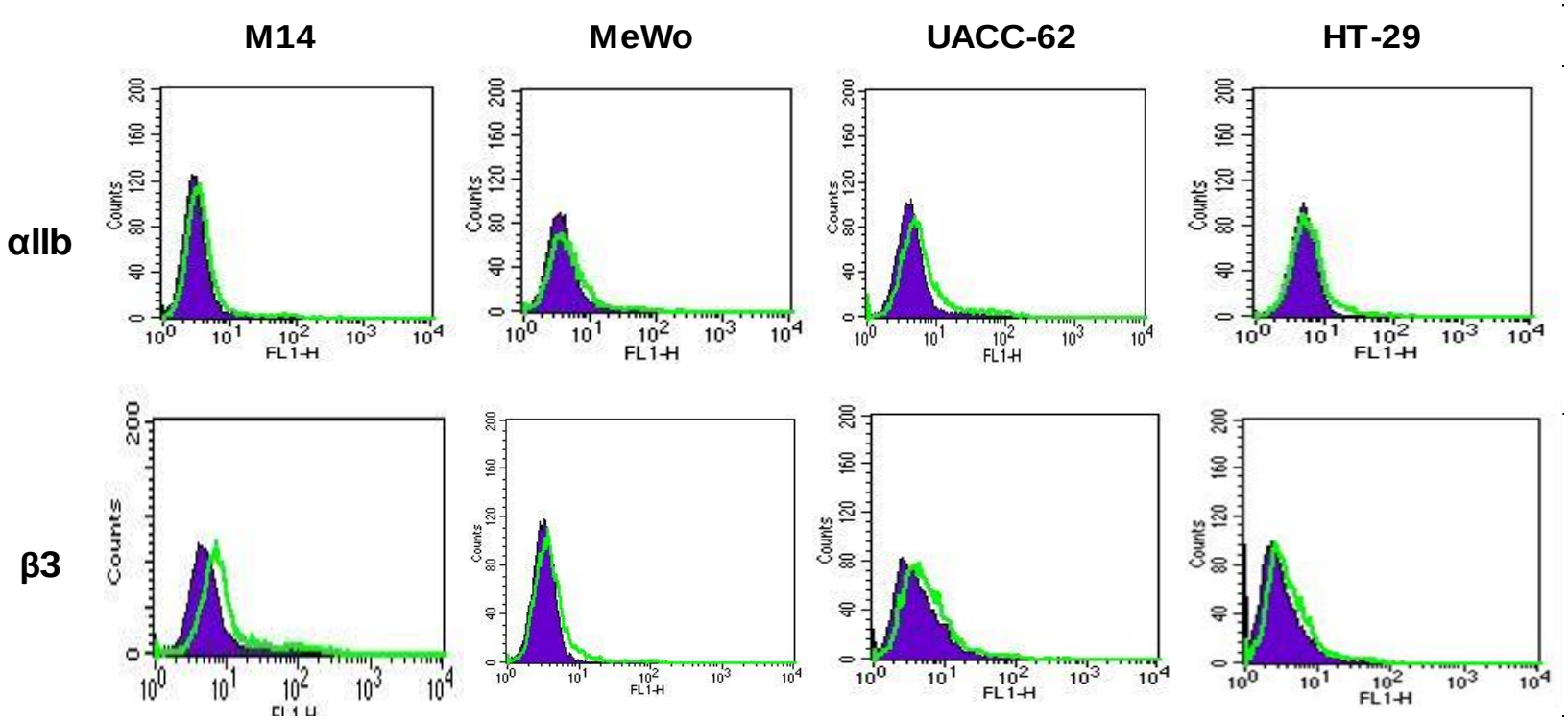

Appendix V: Histograms analysis of effect of PMA concentration on expression of αv in K562 cells

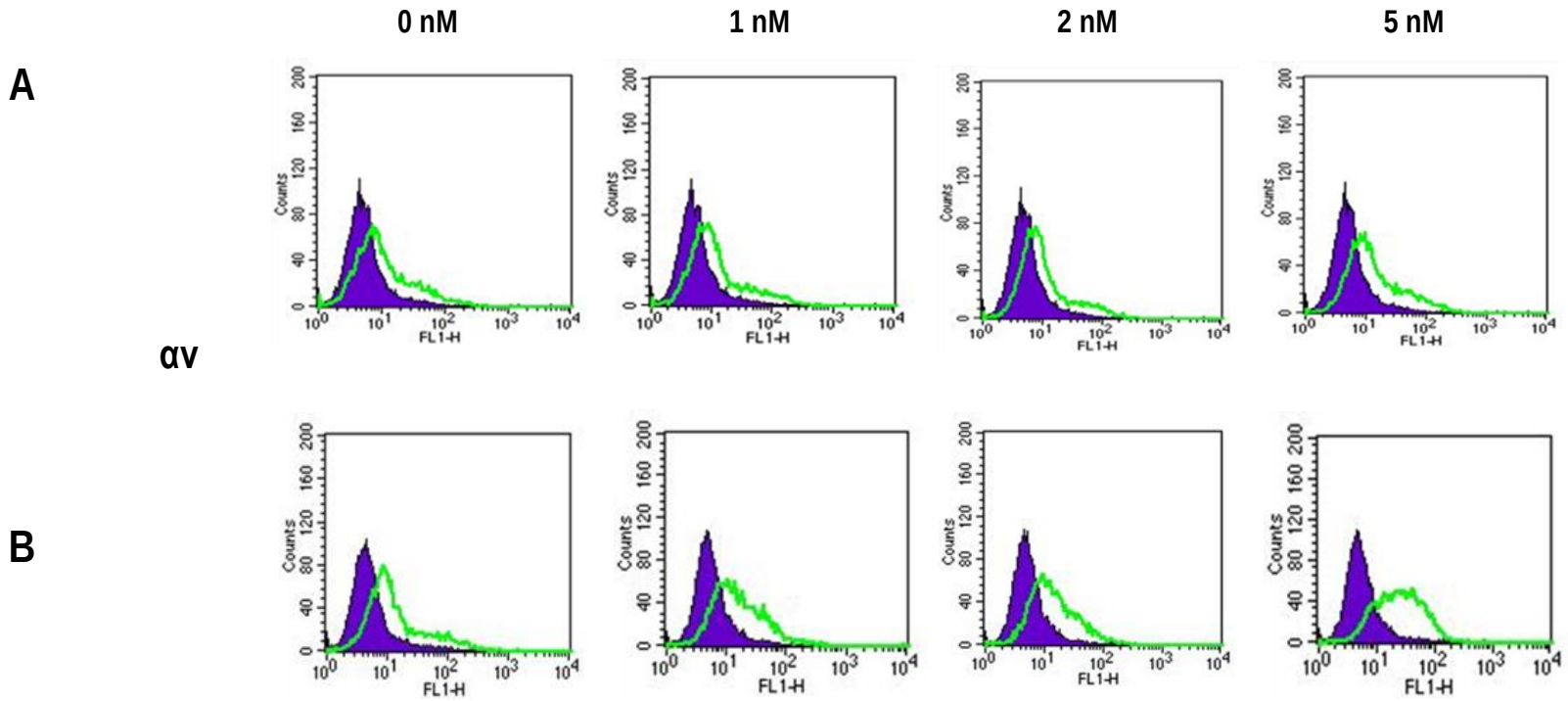

Appendix VI: Histograms analysis of effect of PMA concentration on expression of αIIb in K562 cells

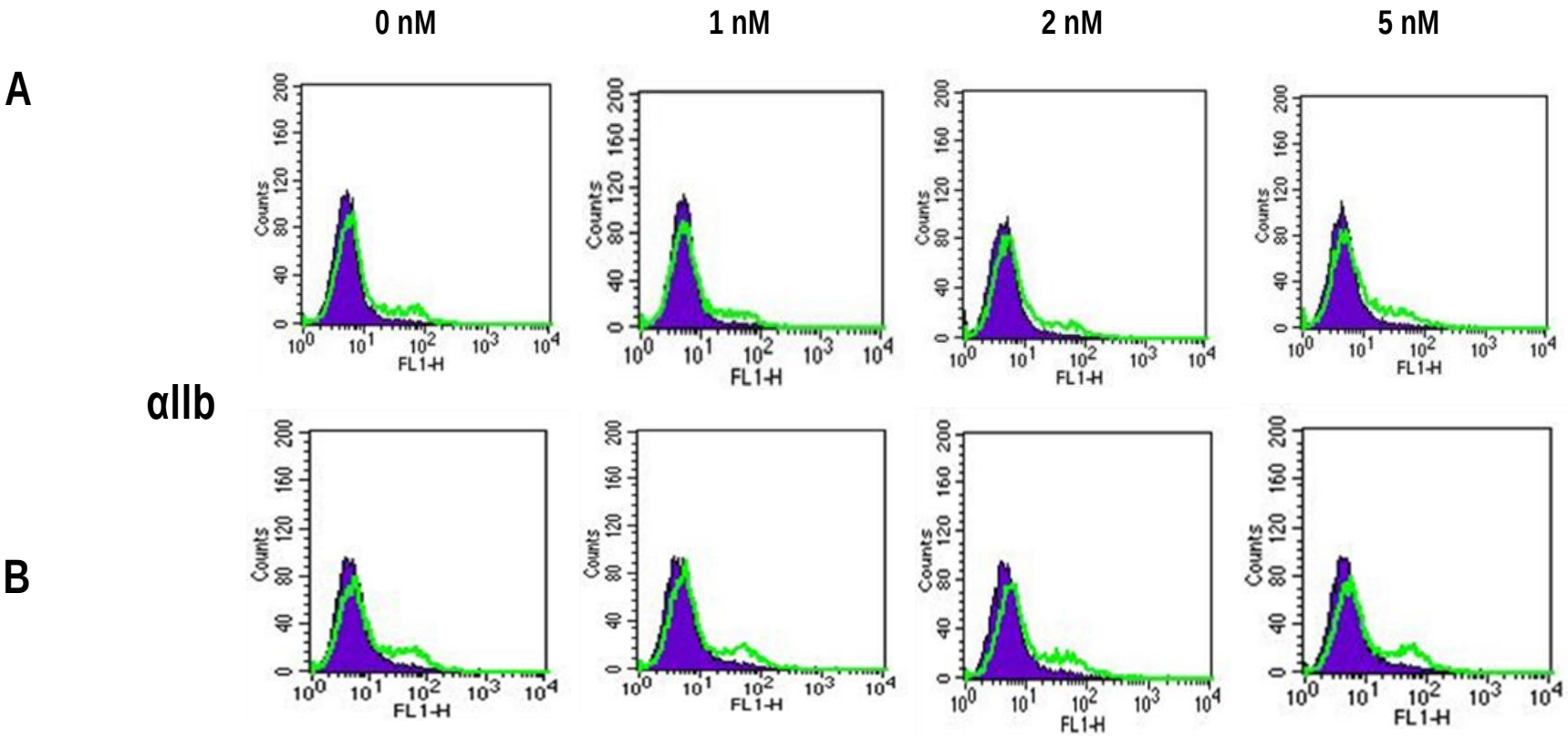

Appendix VII: Histograms of αv and αIIb integrin subunit expression in K562 induced by three concentrations (0.5 µM 1 µM, 2 µM of PMA) for 24h (A), 48 h (B), and 72h (C).

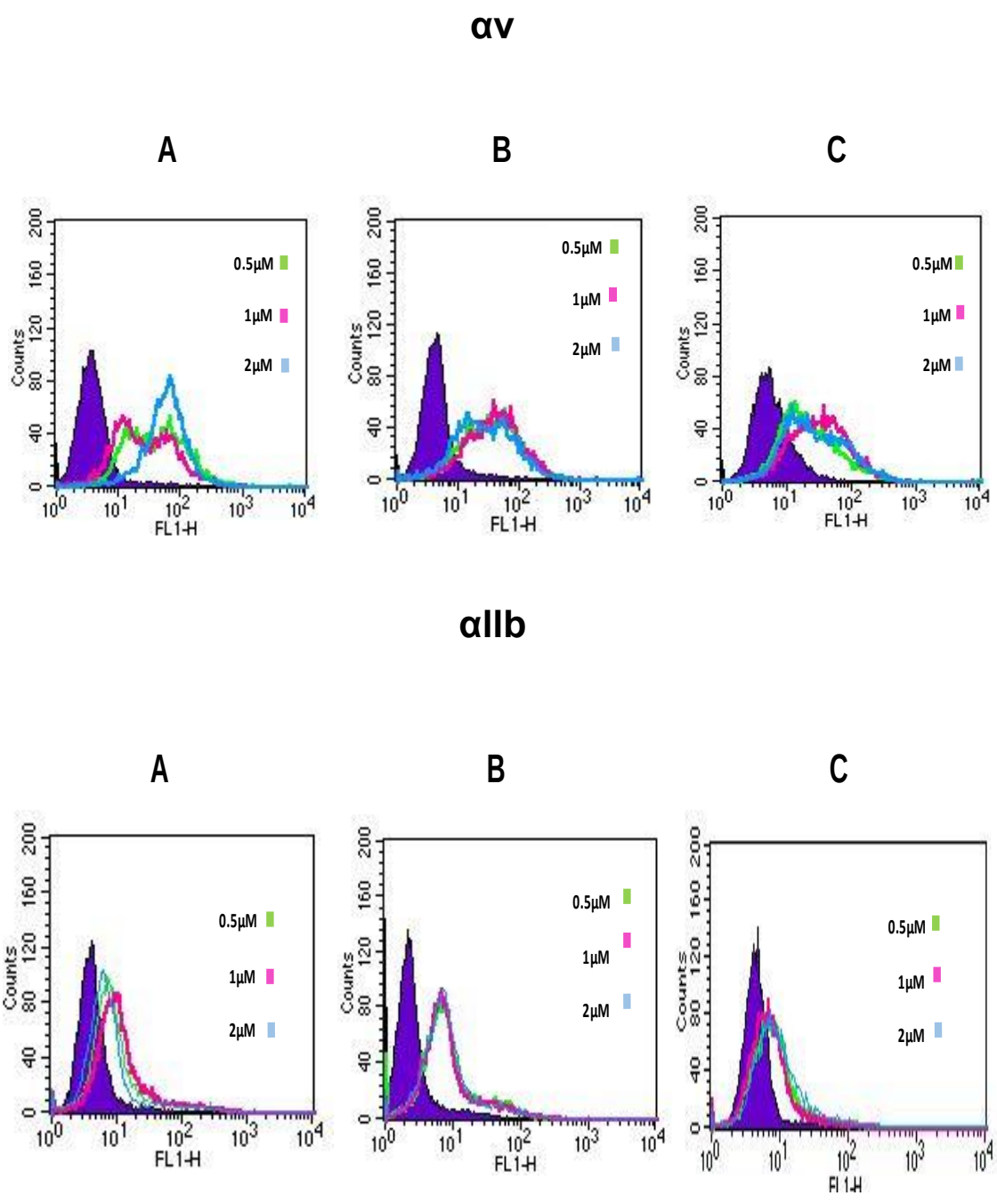

Appendix VIII: Histograms of αv and αIIb integrin subunit expression. in DU145 induced by three concentrations (0.5 μM 1 μM, 2 μM of PMA) for 24h (A), 48 h (B), and 72h (C).

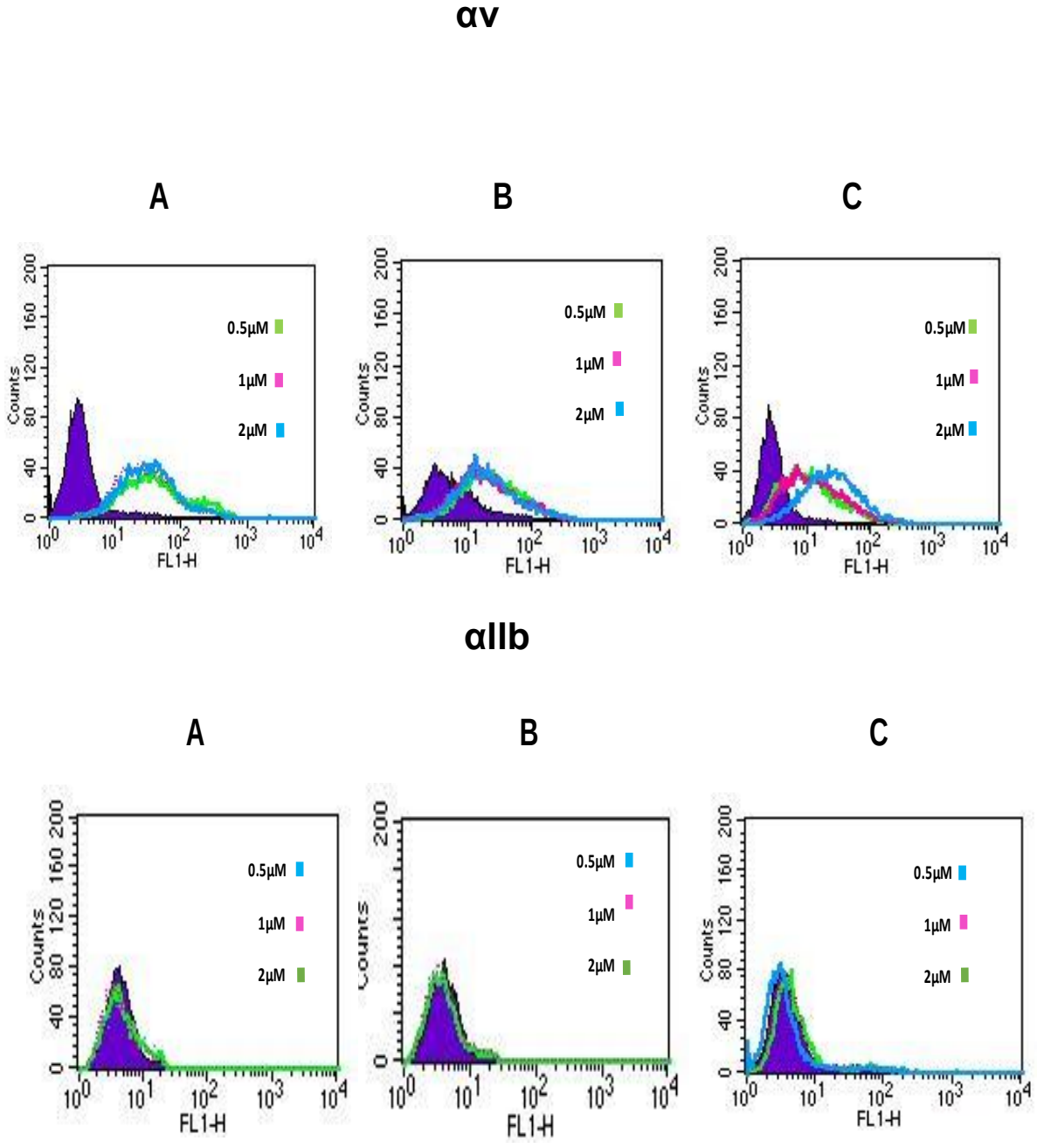

Appendix IX: Histograms of αv, αIIb, α5, β3 and β5 subunits expression in PMA (0.1μM) stimulated K562 cells.

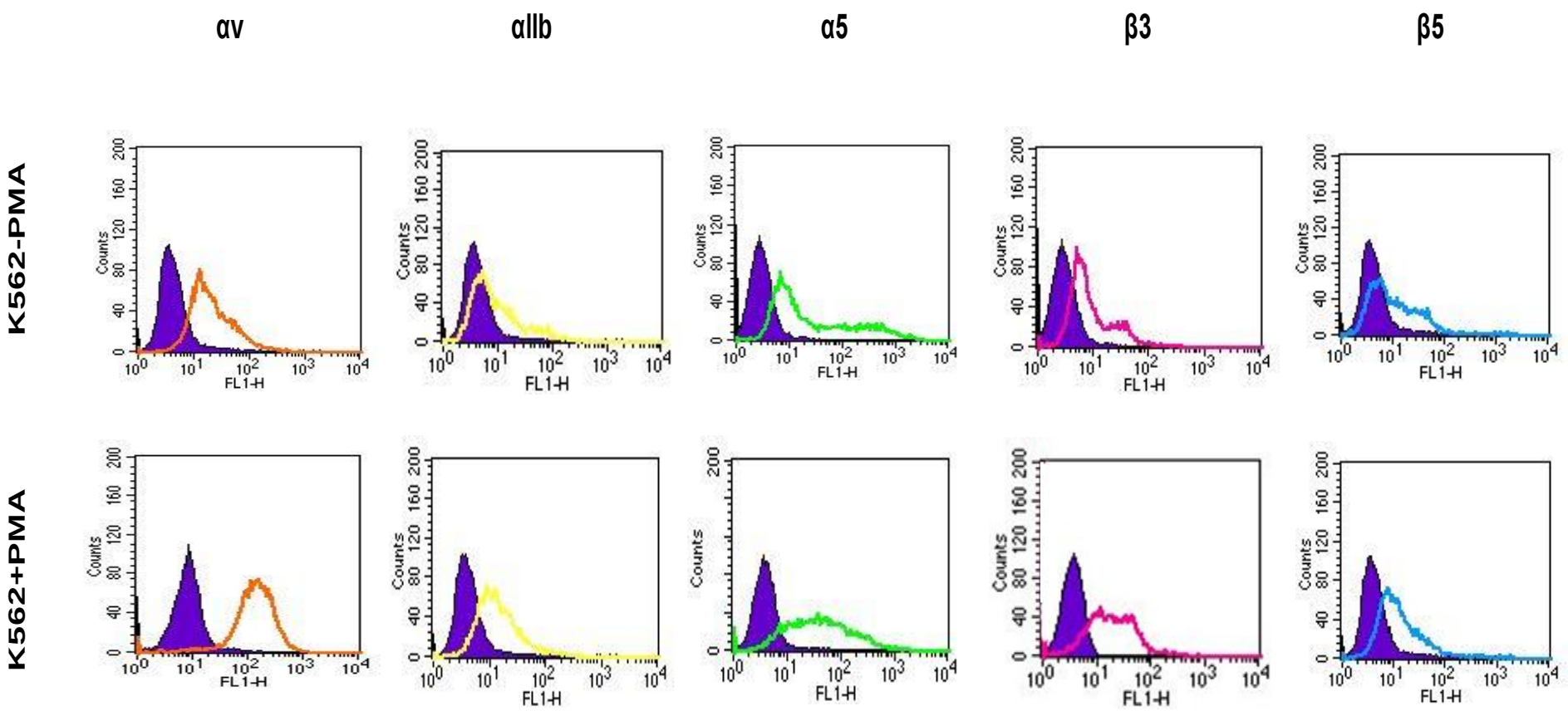

Appendix X: Histograms of αv, αIIb, α5, β3 and β5 subunits expression in PMA (2 μM) stimulated K562 cells

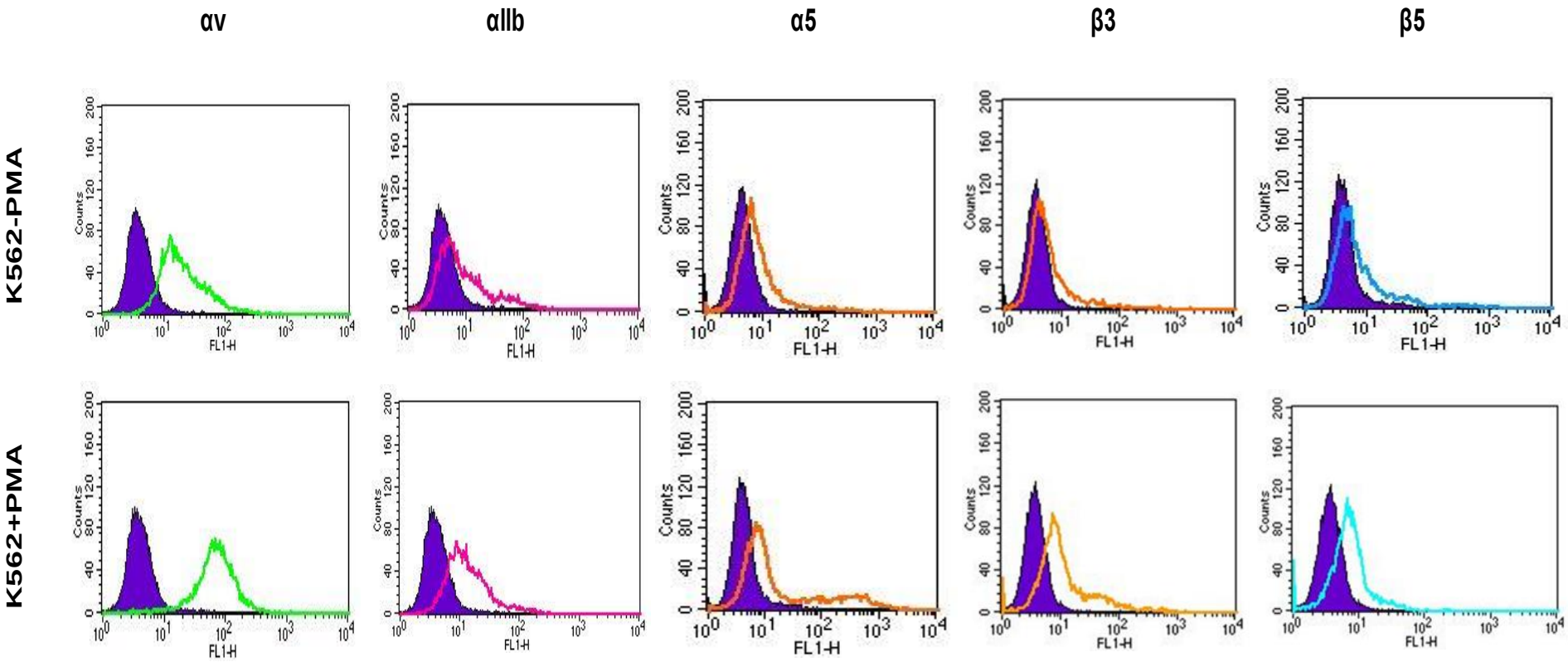

Appendix XI: Histograms of αv, αIIb, α5, β3 and β5 subunits expression in PMA (0.5μM) stimulated Du145 cells

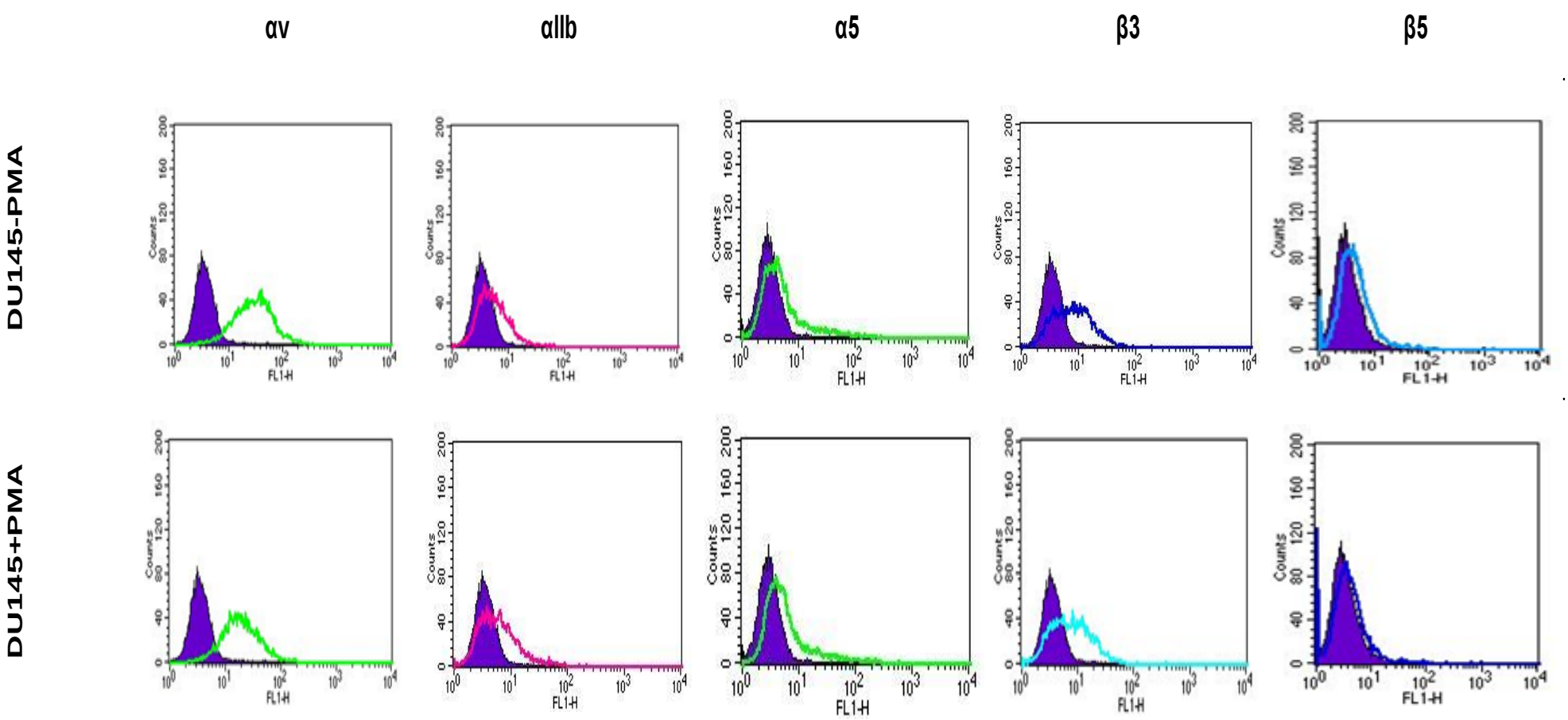

Appendix XII; Histograms analysis of αIIb expression in K562 treated with 0.04 µM PMA for different times

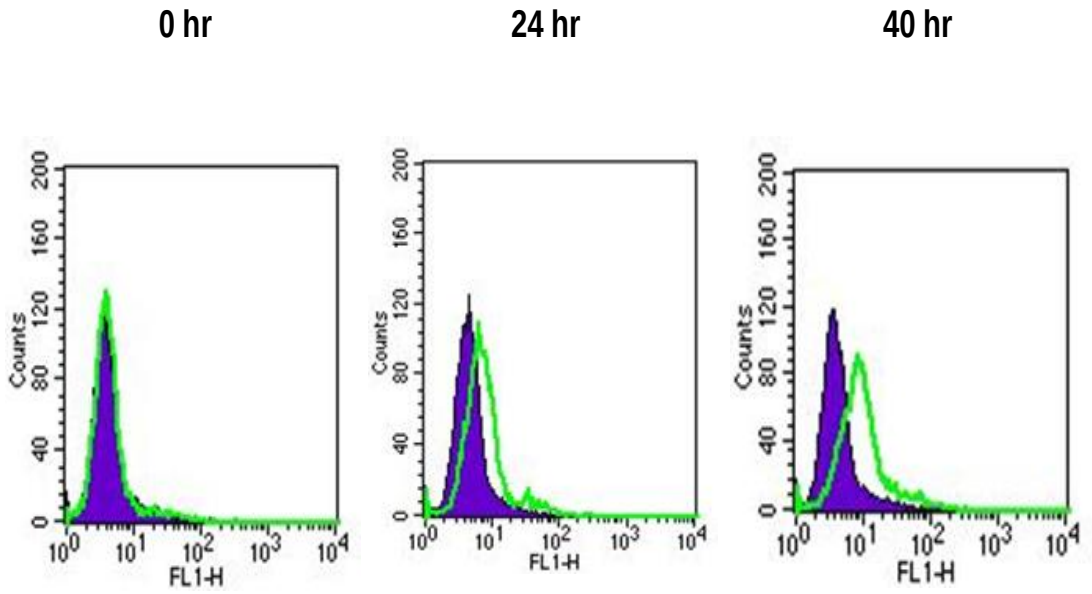

Appendix XIII: Table 14: Summary of the effect of ICT compounds on the functional assays. NT: Not Tested

		K562 -PMA						K562 +PMA						MCF-7					
The compound	Concentration	Percentage of the effect			Level of significance			Percentage of the effect			Level of significance			Percentage of the effect			Level of significance		
		Adhesion	Detachment	Migration	Adhesion	Detachment	Migration	Adhesion	Detachment	Migration	Adhesion	Detachment	Migration	Adhesion	Detachment	Migration	Adhesion	Detachment	Migration
ICT9001	0.1µM 1 µM 10 µM 100 µM	9 ± 0.3 28 ± 6 34 ± 6.9 44 ± 3.4	NT	NT	P<0.05 P<0.01 P<0.01 P<0.01	NT	NT	16 ± 4.8 30 ± 3.0 38 ± 4.7 53 ± 6.4	NT	NT	P<0.05 P<0.01 P<0.01 P<0.01	NT	NT	15 ± 4.9 20 ± 2.9 32 ± 5.0	NT	NT	P<0.05 P<0.01 P<0.01	NT	NT
ICT9025	0.1 µM 1 µM 10 µM	16% ± 7 22 ± 6.4 29 ± 3.3	NT	NT	P>0.05 P>0.05 P<0.05	NT	NT	21 ± 10 27 ± 8.2 36 ± 5.9	NT	NT	P=0.05 P<0.05 P<0.01	NT	NT	15 ± 5.3 20 + 2.6 25 + 5.4	NT	NT	P<0.05 P<0.01 P<0.05	NT	NT
ICT9026	0.1 µM 1 µM 10 µM 100 µM	15 ± 8.4 20 ± 8.9 26 ± 8.0	NT	NT	P>0.05 P>0.05 P<0.05	NT	NT	19 ± 2.0 28 ± 6.2 40 ± 12.3	NT	NT	P<0.1 P<0.05 P<0.05	NT	NT	18 ± 5.6 26 ± 3.0 31 ± 1.6.8 33 ± 6.5	NT	NT	P<0.05 P<0.01 P<0.05 P<0.05	NT	NT
ICT9055	0.01 µM 0.1 µM 1 µM 10 µM 100 µM	25 ± 4.4 31 ± 1.6 51 ± 1.0 57 ± 2.9	42% ± 3.2 53% ± 3.0 67% ± 2.8	26 ± 4.0 41 ± 4.5 53 ± 1.3 69 ± 6.5	P<0.05 P<0.001 P<0.001 P<0.001	P<0.01 P<0.01 P<0.01	P<0.01 P<0.01 P<0.001 P<0.01	33 ± 3.7 51 ± 1.2 65 ± 2.2 77 ± 4.2	54 ± 3.5 70 ± 2.5 81 ±1.5	NT	P<0.01 P<0.001 P<0.001 P<0.001	P<0.01 P<0.01 P<0.01	NT	31 ± 8.0 45 ± 4.4 58 ± 5.0 68 ± 6.3	42 ± 2.0 48 ± 4.0 68 ± 2.4	36 ± 10.5 54 ± 5.0 70 ± 5.8	P<0.05 P<0.01 P<0.01 P<0.01	P<0.05 P<0.05 P<0.05	P<0.05 P<0.01 P<0.01
ICT9066	0.1 µM 1 µM 10 µM 100 µM	18 ± 6.4 23 + 9.6 30 + 9.7 33 + 5.9	NT	NT	P<0.05 P=0.05 P<0.05 P=0.01	NT	NT	21 ± 4.6 29 ± 3.9 34 ± 2.2 39 + 5.7	NT	NT	P<0.05 P<0.01 P<0.01 P<0.01	NT	NT	16 ± 7.6 24 ± 3.0 38 + 9.9	NT	NT	P>0.05 P<0.01 P<0.05	NT	NT
ICT9085	0.1 µM 1 µM 10 µM 100 µM	14 ± 3.0 19 ± 4.5 25 ± 2.8 31 ± 2.3	NT	NT	P>0.05 P<0.05 P<0.01 P<0.001	NT	NT	23 ± 11.4 28 ± 11.9 38 ± 10 46 +13	NT	NT	P>0.05 P= 0.05 P<0.05 P<0.05	NT	NT	18 ± 4.8 21 ± 6.4 37 ± 8.3	NT	NT	P>0.05 P>0.05 P>0.05	NT	NT
ICT9072	0.01 µM 0.1 µM 1 µM 10 µM 100 µM	16 ± 3.7 27 ± 2.2 38 ± 4.4 55 ± 4.9	34 + 1.6 43 ± 3.7 51 ± 1.4	20 ± 4.8 34 ± 2.8 45 ± 3 57 ± 1.5	P<0.05 P<0.01 P<0.01 P<0.01	P<0.05 P<0.05 P<0.05	P<0.05 P<0.01 P<0.01 P<0.001	28 ± 2.7 45 ± 4 52 ± 2.7 63 ±3.9	41 ± 2.8 64 ± 3.5 74 ± 4.5	NT	P<0.01 P<0.01 P<0.001 P<0.01	P<0.05 P<0.05 P>0.05	NT	27 ± 6.0 40 ± 2.0 56 ± 4.0	17 ± 1.8 24 ± 2.4 44 ± 2.3	25 ± 8.8 47 ± 8.6 63 ± 5.0	P<0.05 P<0.001 P<0.01	P<0.001 P<0.001 P<0.05	P<0.05 P<0.01 P<0.01
ICT9073	0.01 µM 0.1 µM 1 µM 10 µM 100 µM	10 ± 5 16 ± 3.7 34 ± 3.5 50± 1.3	27 ± 1.7 34 ± 4.8 46 ± 10	18 ± 3.6 32 ± 2.5 43 ± 4.7 51 ± 0.6	P>0.05 P<0.05 P<0.01 P<0.001	P<0.05 P<0.05 P>0.05	P>0.05 P<0.01 P<0.01 P<0.0001	20 ± 1.6 35 ± 5 50 ± 1.8 59 ± 1.9	33 ± 2.4 44 ± 5 59 ± 3	NT	P<0.01 P<0.01 P<0.001 P<0.001	P<0.05 P<0.05 P<0.05	NT	22 ±3.3 33 ± 3.6 50 ± 4.5	28 ± 2.5 48 ± 2.0 61 ± 8.3	18 ± 8.5 32 ± 5.0 53 ± 2.0	P<0.1 P<0.05 P<0.05	P<0.001 P<0.001 P<0.001	P>0.05 P<0.01 P<0.001
ICT9094	0.1 µM 1 µM 10 µM	9 ± 6.8 21 ± 1.9 31 ± 5.2	NT	NT	P>0.05 P<0.01 P<0.01	NT	NT	18 ± 4.8 30 ± 3.9 42 ± 6.9	NT	NT	P<0.05 P<0.01 P<0.01	NT	NT	26 ± 5.5 33 ± 2.9	NT	NT	P<0.05 P<0.05	NT	NT
ICT9099	0.1 µM 1 µM 10 µM	18 ± 1.6 34 ± 2.5 51 ± 4	27 ± 2.7 35 ± 4 51 ± 3.5	NT	P<0.01 P<0.01 P<0.01	P<0.001 P<0.01 P<0.01	NT	18 ± 1.6 34 ± 2.5 51 ± 4	37 ±3.8 48 ± 1.5 63 ± 4	NT	P>0.05 P<0.01 P<0.01	P>0.01 P<0.001 P<0.01	NT	32 ± 2.0 42 ± 4.6 58 ± 5.8	19 ± 4.3 32 ± 5.2 42 ± 3.4	NT	P<0.05 P<0.05 P<0.05	P<0.05 P<0.05 P<0.05	NT
ICT9101	0.1 µM 1 µM 10 µM 100 µM	11 ± 1.8 17 ± 5.7 28 ± 7	NT	NT	P<0.01 P<0.05 P<0.05	NT	NT	17 ± 3.9 34 ± 7.9 42 ± 10.5	NT	NT	P<0.05 P<0.05 P<0.05	NT	NT	8 ± 4.5 20 ± 2.8 26 ± 6.6 30 ± 9.7	NT	NT	P>0.05 P>0.05 P>0.05 P>0.05	NT	NT
ICT9103A	0.1 µM 1 µM 10 µM	14 ± 6.9 24 ± 7.5 34 ± 5.9	NT	NT	P>0.05 P<0.05 P<0.01	NT	NT	23 ± 6.9 38 ± 3 50 ± 5	NT	NT	P<0.05 P<0.01 P<0.01	NT	NT	13 ± 3.7 26 ± 2.8 37 ± 3.3	NT	NT	P<0.05 P<0.05 P<0.05	NT	NT